Temporal Variation in the Radio Environment

by

Roger Lewenz B.Sc(Eng), M.Sc, C Eng, MBCS

A thesis submitted to the
University of Durham
for the degree of Doctor of Philosophy

2005

School of Engineering
University of Durham
Durham, England

ABSTRACT

Modern digital radio systems using high symbol rates are more susceptible to multipath interference than traditional systems. These systems need to adapt to the propagation environment in order to minimise transmission errors while minimising transmitted power and interference between systems. Mobile terminals will experience variations in the propagation environment as they move. Both fixed and mobile terminals will experience variations in the propagation environment as the environment changes with time. The extent and speed of environmental changes are necessary inputs to the design process for new radio systems.

Previous reported measurements aimed at characterising the radio environment have been made over short durations of a few tens of milliseconds. In this thesis measurements over periods of up to 15 seconds are described and the results analysed to quantify longer term variations. The channel sounder developed at UMIST was used for the measurements and the environment was sampled over a number of paths in Manchester and Durham.

The data from each 15 second measurement was split into two ensembles, one from the first 7.5 seconds and one from the remaining 7.5 seconds so that statistics from different times could be compared. The number of multipath components, the mean delay and the RMS delay spread were extracted for each 20 msec interval of each measurement.

Cumulative Distribution Functions formed from the data from the two ensembles of each measurement showed differences between the ensembles. The results from Kolmogorov-Smirnof tests confirmed the differences for all three statistics. Attempts to model the variation of the statistics by fitting Normal and Weibull distributions to the data failed in most cases. PDFs of the RMS delay spread were multimodal suggesting that insufficient data was available.

It has been concluded that there is temporal variation in the radio environment but that more measurement data will be needed for the variation to be characterised.

DECLARATION

No part of the work described in this thesis has been submitted in support of an application for another degree or qualification to this or any other university or institute of learning.

ACKNOWLEDGEMENTS

I would like to express my gratitude to my supervisor Professor S. Salous for the guidance she gave me during the work leading to this thesis. I would also like to thank my fellow students Dr Pantelis Filippidis, Stuart Feeney, Mustafa Abdalla and Nima Razavi for their help in making the measurements and some useful ideas for enhancing the channel sounder. Dr Hulya Gokalp and Phillipa Pardue have been a constant source of encouragement, particularly during the writing up phase of the project. Finally I thank my children for their understanding and acceptance of my absence from home during my studies.

I would like to acknowledge the support of the Engineering and Physical Research Council whose award of a research studentship allowed me to carry out this work.

I would also like to acknowledge the financial support given by BT Exact under their Virtual University Research Initiative. This removed some of the uncertainties caused by lack of funding for new components and test equipment.

DEDICATION

I would like to dedicate this thesis to the students who will come after me in the hope that at least one of them will be inspired to continue the work.

ABBREVIATIONS

ADC	Analogue to Digital Converter
BER	Bit Error Ratio
BFWA	Broadband Fixed Wireless Access
CDF	Cumulative Distribution Function
CIO	Carrier Insertion Oscillator
CW	Continuous Wave, a carrier without modulation.
DECT	Digitally Enhanced Cordless Telephone
DFT	Discrete Fourier Transform
EIRP	Effective Isotropic Radiated Power
FDM	Frequency Division Multiplex
GSM	A French abbreviation describing the European TDMA, FDM mobile telephone standard (now also available in other parts of the world.
HF	High Frequency, indicating the frequency bands form 3 MHz to 30 MHz.
IR	Impulse Response
LO	Local Oscillator.
MIMO	Multiple Input Multiple Output
PC	Personal Computer, a computer using the IBM architecture with a processor using the Intel x86 architecture.
PCB	Printed Circuit Board
PDF	Probability Distribution Function
PDP	Power Delay Profile
RCS	Radar Cross Section
RF	Radio Frequency
RMS	Root Mean Square
SHF	Super High Frequency, indicating the frequency bands between 3 GHz and 30 GHz.
TDMA	Time Division Multiple Access
TTL	Transistor Transistor Logic.

UHF	Ultra High Frequency, indicating the frequency bands between 300 MHz and 3 GHz.
UMTS	Universal Mobile Telephone System

CONTENTS

CHAPTER 1 INTRODUCTION

1.1 Background

Digital radio systems have been used routinely since the middle of the 20th century. The early systems (mostly telegraphs) relied on mechanical senders and receivers so the symbol rate was limited to 50 or 75 Baud. At these symbol rates the occupied bandwidth of the transmitted signal was small enough for frequency selective fading in the radio channel to have negligible impact. To achieve the intercontinental ranges to which radio was most suited the HF bands were used and transmission impairments were caused by ionospheric phenomena.

Today digital radio systems are used to provide mobility, local access to telephone networks, high data rate short range connectivity and trunk network links in addition to traditional uses. These newer systems provide users with data rates from 512 kbits/sec to hundreds of Mbits/sec over paths which seldom exceed 30 km in length. They operate in the UHF and SHF bands since there is not sufficient spectrum bandwidth in the lower frequency bands. Unlike traditional long range systems and excluding trunk network links, the newer systems are required to operate in environments with various types of obstacles which may block a line of sight between terminals. This type of environment may cause multipath propagation which can distort transmissions between terminals with the distortions having greater impact on link quality as symbols rates increase. Mobile terminals will experience a propagation environment which changes as they move. The environment may also move about fixed terminals (moving road traffic, wind induced vegetation movement) so fixed terminal systems may also experience a propagation environment which changes with time. To maintain reliable links modern communications systems must be able to adapt to the changing environment and their designers will need some knowledge of the environment and its variation with time. Measuring the characteristics of the radio environment is an expensive activity. In addition to changing with time there may be differences between the characteristics in one frequency band and those in another

band. If it is possible to relate the characteristics in the different bands a reduced measurement activity would satisfy the requirements of designers.

1.2 Motivation

Variation of the radio channel characteristics with time has two main effects on the use of digital radio systems. The first effect is on the radio systems themselves, particularly on those parts which seek to adapt to the radio environment. The second effect concerns the installation and maintenance of radio systems with fixed terminals.

Multipath propagation can cause intersymbol interference. A symbol which reaches the receiving terminal by two or more different routes through the environment will suffer different delays over the different routes. When a high symbol rate is used a delayed symbol can be confused with the succeeding symbol and unless the receiver can differentiate between a delayed symbol and the succeeding symbol the system Bit Error Ratio (BER) will be degraded. Receivers are designed to combat the degradation of the signal using a RAKE receiver architecture, equaliser or combination of the two. Both of these techniques require the receiver to adapt to the time varying channel characteristics. To design such systems it is necessary to know how the radio channel varies with time.

Another method of combating multipath propagation for systems with mobile terminals is to use highly directional antenna systems at the fixed terminal and steer the beams of these antennas. These smart antenna systems also need to adapt to the environment so as to minimise the impact of multipath propagation, maximise the carrier to interference ratio for signals from the mobile terminal and minimise interference to and from other terminals.

Digital radio systems are also used to provide access to telephone or data networks where there is no fixed infrastructure (copper wires or optical fibres) or there is insufficient capacity in the fixed network. There are a number of situations where an operator will choose radio rather than copper or fibre. In remote rural areas the cost of installing fixed infrastructure may not be recoverable from the revenue from the service provided within the timescales demanded by shareholders. In this case radio may be

cheaper to install and facilitate the maintenance of an acceptable service. Some operators have an obligation to provide a basic telephone service and limitations on the price that can be charged to the customer. In urban areas, particularly centres of business activity, there may be a requirement to provide a service requiring network capacity in excess of that which can be supported by the fixed network infrastructure. Local planning restrictions may limit the operator's ability to increase fixed network capacity (digging up the roads to put in new ducts is only allowed after consultation and this imposes time delays). In this case the operator may choose to install a radio link until the fixed network can be enhanced. Unlike trunk network radio links, which are mounted in uncluttered locations on high towers over paths which are carefully surveyed before installation, local access radio links must be installed quickly and have terminals mounted on existing buildings. If such a link is installed and made to work on a day when propagation conditions are benign it is possible that the link will fail if propagation conditions degrade. When the link is installed a system which can tolerate the multipath environment must be selected and a margin must be allowed for degradation of the radio channel. The system type and margin can only be deduced from a knowledge of the time variant behaviour of the radio channel.

This thesis describes work done to measure the temporal variation of a number of radio channel statistics. A wideband chirp channel sounder was used for making measurements over longer timescales than have been reported in the literature. A significant amount of preliminary work was necessary to ensure that the sounder was suitable for the measurement task and to ascertain its characteristics and limitations. Measurements were made over a number of paths in Manchester and Durham and the data from these measurements processed to extract number of multipath components, mean delay and RMS delay spread.

1.3 Structure of the Thesis

After this introductory chapter, chapter 2 considers the radio propagation channel and the mechanisms which give rise to temporal variations. In chapter 3 previous work is reviewed after a study of the current literature.

The method of making wideband channel measurements is described in chapter 4 while chapters 5 and 6 cover the testing and calibration of the wideband channel sounder. A new data acquisition system developed during the project is described in Chapter 7. Results from the measurements and subsequent analysis of the data are presented in chapter 8. Chapter 9 contains conclusions and recommendations for further work. The software developed for this project is contained in the CDROM enclosed at the back of this thesis with a listing of the CDROM contents in appendix 5.

1.4 References

All the documents used as references and other documents which were found useful are listed in the bibliography at the end of this thesis. A reference is cited by including a number in square brackets in the text thus: [1]. The number in the brackets is the item number in the bibliography.

CHAPTER 2 THE RADIO PROPAGATION CHANNEL

2.1 INTRODUCTION

Radio communication systems exist to serve people. The greatest density of people are found in urban environments and this is where most radio basestations and terminals will be found. This environment will contain obstacles such as buildings, trees and other items of infrastructure. In such an environment radio frequency (RF) energy may travel between basestation and terminal by a number of routes and be subject to a number of propagation mechanisms. The overall effect of the various mechanisms is that the received RF energy is less than that transmitted, the electric and magnetic fields which support the energy transmission will suffer phase changes relative to the transmitted fields and the symbols which carry the transmitted information will be delayed. Because the RF energy may travel by a number of different routes a terminal will receive the sum of the RF energy from a number of components, one from each different propagation path. Thus if we denote the electric field contribution from the ith component by $c_i(E,\phi)$ having field strength E and phase ϕ, then the combined field is given by :

$$E_r(E,\phi) = \sum_{i=1}^{N} c_i(E,\phi)$$

Noting that this is a vector sum and assumes that all field interactions are in the far field and that the characteristic impedance of the medium is constant.

2.2 PROPAGATION MECHANISMS

It has been assumed that at a frequency of 2 GHz the effects of rain attenuation and depolarisation and gaseous absorption are negligible [1]. This leaves five propagation mechanisms to consider:

1. The basic transmission loss over a line-of-sight path.
2. Reflection, either specular or diffuse, from the surface of an obstacle.
3. Transmission through an obstacle.
4. Diffraction round or over and obstacle.
5. Clear air effects, particularly, refraction.

The physics of basic transmission loss, reflection and diffraction are well known and are not described in detail here. Transmission through obstacles is discussed later with minimal theoretical description. Transmission theory can only be applied to real situations if the morphology of the obstacle is known and parameters such as the conductivity, relative permitivity and relative permeability of the materials have been determined (strictly speaking this is also true for reflection and diffraction).
For this project the most important characteristic to be known about each of the propagation mechanisms is its susceptibility to time variation.

2.3 Basic Transmission Loss

The basic transmission loss occurs because RF energy transmitted from a practical antenna system does not travel as a single ray from one terminal to another. By design the RF energy transmitted from a basestation spreads out so that it can be received by any customer terminal in a designated service area. If the case of P_t Watts of power transmitted from an isotropic antenna is considered:
The energy propagates equally in all directions and at a distance d metres from the antenna will pass through the surface of a sphere of radius d so the power flux density will be $\frac{P_t}{4\pi d^2}$ Watts per square metre.
At this distance an antenna of aperture A square metres will absorb $\frac{AP_t}{4\pi d^2}$ Watts if it is properly terminated.
Denoting the received power by P_r allows the basic transmission loss to be calculated as $\frac{P_t}{P_r} = \frac{4\pi d^2}{A}$.
In the case of a transmitting antenna with directivity (and hence gain) this calculation is modified by the antenna radiation pattern which is fixed by the antenna design and dimensions. The aperture of the receiving antenna is fixed by its physical dimensions and will not change with time. The basic transmission loss is dependent on the distance between terminals and if this distance changes with time so too will the basic transmission loss. If one of

the terminals is mobile then the distance between it and the basestation and hence the basic transmission loss will change with time.

2.4 DIFFRACTION

Whenever a radiowave encounters the corner of a building some of the energy will be diffracted into the shadow region where the building blocks the line of sight to the transmitter. Any other obstacle which has corners or edges will similarly cause diffraction. The field strength after diffraction relative to that from a line of sight path may be deduced from the Huygens-Fresnel theory and the geometry of the diffracting obstacle.

Diffraction may also occur around obstacles which are curved but for deciding whether diffraction effects can vary with time only the simple case of diffraction at a sharp edge will be considered. The edge is modelled as the limit of a perfectly absorbing screen. Figure 1 shows the geometry most commonly used for the calculation of the diffraction loss. The transmitter is marked as **TX** and the point at which the field is to be sampled (the receiver) is marked as **P**. The distance from the line of sight path to the diffraction edge is **h**, the distance of the diffraction edge to the transmitter is **d1** and the distance between the diffraction edge and the sample point is **d2**.

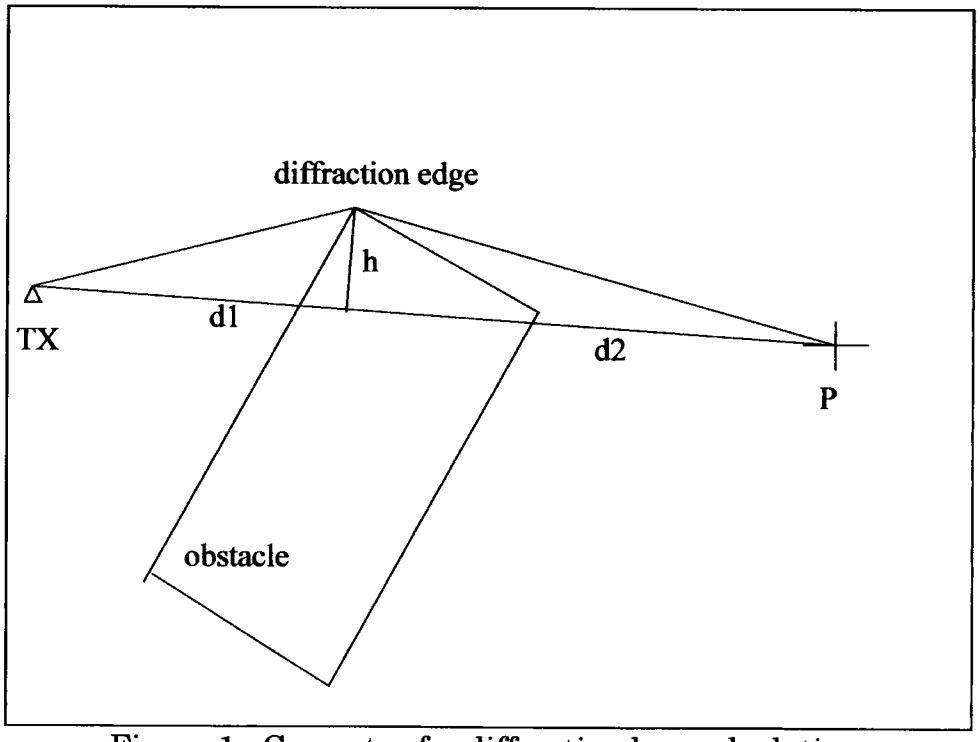

Figure 1. Geometry for diffraction loss calculation.

An approximate solution to the problem of calculating the diffraction loss is as follows. This solution provides accurate results only when the distances from the edge to the transmitter and the sample point are very much greater than the distance of the edge from the line of sight. If this constraint is not met the theory involved in the approximation breaks down. A dimensionless parameter v is first calculated as:

$$v = h\sqrt{\frac{2(d1+d2)}{\lambda d1 d2}}$$

The gain after diffraction over a knife edge as compared with the line of sight case is calculated as follows:

$$G_K = 20.0\log_{10}\left|\frac{(0.5 - C(v)) - j(0.5 - S(v))}{1.0 - j1.0}\right|$$

where:

G_K is the gain over the knife edge in dB relative to the line of sight case.

v is the dimensionless parameter previously stated.

C(v) and S(v) are the cosine and sine Fresnel integrals of the argument v. The Fresnel integrals are usually computed numerically [2].

Since G_k is the gain over the diffracted path compared with a line of sight path, the additional loss due to diffraction is $-G_k$.

Since the diffraction loss depends on the distances d1, d2 and h if the obstacle moves relative to either the basestation or the customer terminal there will be a change in the diffraction loss. Hence if the customer terminal moves with time then the diffraction loss will change with time. Also if the obstacle moves with time (for example a moving vehicle) the diffraction loss will change with time.

If there are a number of obstacles causing diffraction the situation becomes more complicated. There are methods for calculating diffraction losses due to more than one obstacle [3][4][5] but these methods all take the geometry of the situation into account, so do not change the assertion that moving

time. If there are a large number of moving obstacles it is to be expected that the overall change of diffraction loss with time will be less than if there is a single dominant obstacle and it will be difficult to identify the character of changes to individual components.

2.5 REFLECTION

A radiowave encountering the surface of an obstacle will be partly reflected and partly refracted into the substance of the building.

Consider figure 2 showing a radiowave encountering an obstacle (shaded rectangle) at an oblique angle. Snell's Law of reflection states that the reflected wave will leave the obstacle making an angle θ_r with a normal to the surface of the obstacle which is equal to the angle θ_i that the incident wave makes with the same normal. Hence if the obstacle is rotated the reflected wave will change direction by an angle which is twice the angle through which the obstacle rotates. If the obstacle orientation varies with time then the direction of the reflected wave will vary with time and this will lead to changes in the later interactions with the environment.

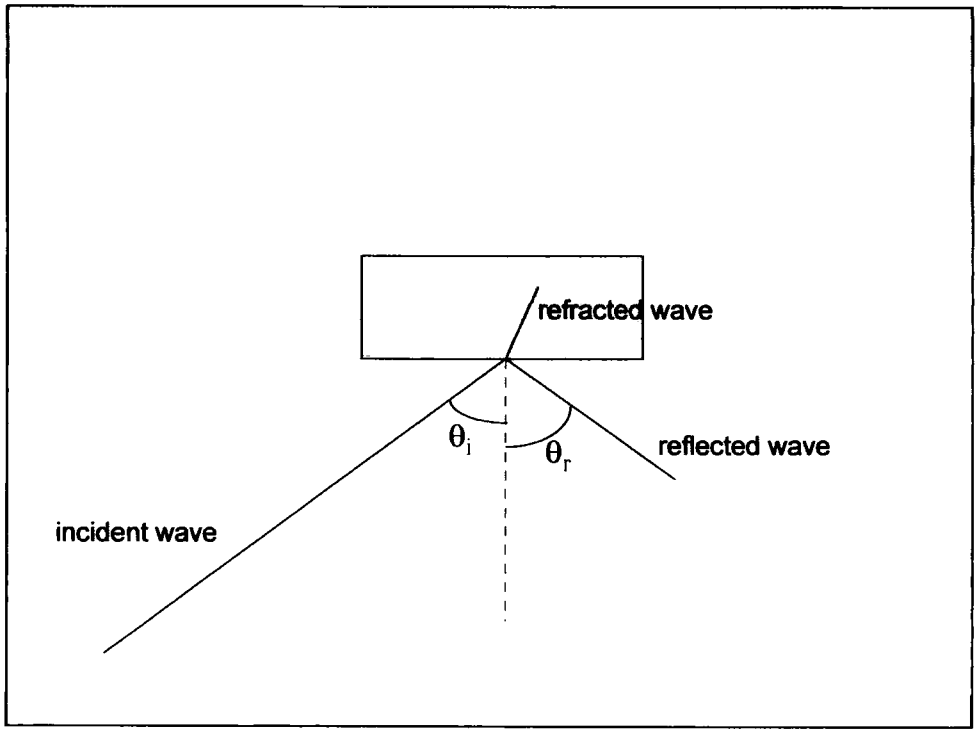

Figure 2. Reflection from an obstacle

The radiowave energy which is not reflected from an obstacle is refracted and is transmitted through the substance of the obstacle. It may emerge after a further refraction and continue to interact with the environment. Another effect which occurs when a radiowave is reflected is a change in the plane of polarisation. This has been recognised by cellular telephone operators who have utilised the effect to give a degree of diversity on the uplink (mobile to basestation transmission). Basestation antenna systems include pairs elements with each member of the pair having polarisation orthogonal to that of the other member.

2.6 THE MOVEMENT OF OBSTACLES

It is assumed that buildings in the environment do not move. Although some tall slender buildings deform slightly under the influence of wind this is not considered to be a significant factor in the variation of radio channel characteristics.

Motor vehicles, trains and aircraft do move and these can be a significant factor in the variation of the radio channel characteristics with time. Trains and aircraft tend to move according to predefined schedules and are hence to some extent predictable. Road traffic is highly variable both in density and in radar cross section and its influence on radio channel characteristics can only be described statistically. The density at a particular time will vary depending on the degree of urbanisation and the class of road upon which it is travelling. The density will also vary with time of day and to some extent on the weather and season. The radar cross section is the area of a plane pefectly reflecting surface which would reflect the same fraction of the illuminating power as the vehicle and this will depend on the size, construction and orientation of the vehicle.

In addition to buildings and vehicles of various types there may be vegetation in the environment. Trees are known to diffract, absorb and reflect radiowaves [6]. Trees are also stimulated into movement by the wind so their influence on radiowaves will vary with time. This movement can cause rapid changes in received signal level at a fixed station [7] but it is not clear whether this variation is caused by changes in diffraction losses or by multipath effects.

2.7 SLOW CHANGES

Although buildings do not move it is possible that the weather will cause changes in the properties of the materials from which they are constructed. Since the reflection coefficient depends on the conductance, relative permitivity and relative permeability of the media at the reflecting surface it is possible that a building may change its reflection characteristics as the weather changes. There was not time within this project to consider or measure the influence of the weather on the reflections from buildings. Variations in pathloss due to changes in the refractive index of the atmosphere have been observed by the author [8]. These changes occur over timescales of several hours and can result in either a reduction or an increase in the path loss. The observations were made on two fixed paths with lengths of 11 km and 4 km. There were obstacles on both paths. The path loss on these paths was measured at 2240 MHz using a CW signal for a period of three years and the effect occurred several times, usually in June when weather conditions were conducive to atmospheric stratification.

The Earth's atmosphere refracts radio waves in the tropospheric region. This effect arises because the density of the air reduces as altitude increases. The propagation velocity of electromagnetic waves increases as air density reduces. A radiowave emitted parallel to the Earth's surface will travel faster at higher altitudes than at lower altitudes hence the wavefront will be rotated towards the Earth's surface.

The degree to which a radiowave is refracted depends on the relative permittivity ε_r of the air and how this changes with altitude. The index of refraction is more often used when describing refraction and this is denoted by **n** and is defined as:

$$n = \sqrt{\varepsilon_r}$$

n can be evaluated either in terms of the air density or in terms of the air pressure [49].

In terms of air density:

$$n = 1 + \frac{\chi\rho}{\rho_{SL}} + humidity\_term$$

where:

ρ is the air density at the altitide of interest

ρ_{SL} is the air density at sea level

χ is the Gladstone-Dale constant with approximate value 0.00029.

In terms of air pressure:

$$n = \frac{77.6}{T}\left(p + \frac{4810e}{T}\right)10^{-6} + 1$$

where

T is the air temperature in degrees Kelvin

p is the air pressure in millibars

e is the partial pressure of water vapour in millibars.

In a tropospheric region where the air is well mixed (no stratification) the pressure and the density of the air and hence the refractive index will reduce with increasing altitude. The effect of water vapour will be ignored for now.

Under certain weather conditions temperature and pressure variation with altitude departs from the well mixed troposphere case. It is possible for there to exist a region of high refractive index some distance above the Earth's surface. When this condition exists a radiowave emitted parallel to the Earth's surface may follow the curvature of the Earth at a fixed altitude for a considerable distance.

It is also possible that a radiowave is refracted more strongly than is necessary to follow the Earth's surface. In this case the apparent line of sight path may be lifted to clear obstacles which would normally obstruct it. A receiver encountering such a refracted radiowave at the same time as radiowaves reflected from or diffracted around obstacles would experience multipath propagation which varied with atmospheric conditions and thus with time. Changes in the atmosphere tend to happen over a period of

hours rather than seconds so it would be necessary to make measurements over long periods of time in order to detect them.

2.8 EFFECT OF ENVIRONMENTAL MOVEMENT

The overall effect of the movement of obstacles in the environment is to cause the multipath characteristics to change with time. Thus a radio terminal will receive signals with various delays and of various strengths, the number of delayed signals, the strength of the delayed signals and the magnitude of the delays changing with time. Unless the radio terminal has a line of sight path to the basestation the dominant signal component may appear from different directions as time progresses. In the case of a mobile terminal a small movement of the terminal may result in an enhanced or degraded radio channel. The change of position may expose the terminal to multipath components to which the terminal is better able to adapt. In the case of a fixed terminal the temporal variation of the radio channel cannot be ignored. The limits of the expected variation must be taken into account when the location of the terminal is decided and it may be necessary to choose terminal equipment which employs diversity techniques.

CHAPTER 3 PREVIOUS WORK

3.1 General Review of the Literature

There appear to have been few workers who have reported on the variation of the radio channel statistics with time other than as an informal observation based on data collected for other purposes.

A number of researchers consider such channel parameters as coherence time but there are few reports of long term variations in the channel statistics. It is possible that this aspect of the radio channel has not been the subject of detailed measurements however it is equally likely that measurements have not yet been reported. Telecom operators are currently designing and installing wideband networks (UMTS and Broadband Fixed Wireless Access (BFWA)) and each may consider the publication of measurements would give other operators a commercial advantage.

3.2 Variation of Channel Parameters with Time

A good introduction to the radio channel and the challenges it poses for the radio system designer is the short monograph by Prof Roland King [9]. In this document the major channel parameters are described and their variation with time presented in an intuitive manner. It is not the purpose of the monograph to present measurement results but to provide a basic understanding of the propagation mechanisms.

A description of the radio channel inside a room is presented by Sharma et al [10] with the assertion that a deterministic channel model is to be preferred in these circumstances. Sharma also highlights the differences between the indoor and the outdoor radio channel and the differences to be expected in the temporal behaviour. No measurements are reported but a model for estimating the channel impulse response is presented.

Measurement presented by Allen et al [11] are analysed to yield channel parameters for indoor, urban and rural situations. Short term time variation will have been masked by the averaging over 16 snapshots (6.4ms) used to reduce the effects of uncorrelated noise. The measurements at each location were limited to a single period of 10 seconds so it will not have been possible to detect variations in channel parameters over a longer timescale.

The results presented show the range of channel parameters measured over the limited measurement period.

A comprehensive mathematical treatment of the radio channel characteristics and their interrelationships has been presented by Bello [12] and models have been proposed by Zollinger [13], Rappaport [14, 15], Turkmani et al [16], Saleh and Valenzuela [17] and others. The models examined have been statistical in nature with parameters derived from measurements but have only considered variations of the channel within timescales of a few milliseconds or less. Thus, estimates of channel coherence time have been obtained but further work is required to examine the variation of channel parameters over longer timescales.

Other reports of wideband measurements and approaches to modelling the radio channel [18, 19, 20, 21] recognise that there will be long term variation of the channel parameters with time. It appears, however, that priority has been given to investigating the channel parameters at different locations, using both static and moving measurement terminals and this has not allowed time for the study of long term effects. Included in these reports are discussions of what are the channel parameters which will be useful to manufacturers designing equipment and to operators designing and deploying networks. These discussions have not yet considered any parameter which might be a useful indicator of the effects that long term time variations will have on a radio communications system.

Marinier [22] has reported medium term time variations in the parameters of the radio channel but the investigation was limited to the indoor environment. In this study the effects of people moving in an office building containing both transmitter and receiver were reported however, the experiments were conducted at a frequency of 30GHz and the results may not be representative of the situation outdoors and at lower frequencies.

Measurements conducted by McNamara et al [26] aimed at evaluating MIMO systems were limited to indoor scenarios. Temporal variations over periods of a few seconds in the 5.2 GHz band were observed. These results were obtained from a limited set of data and it was concluded that further

Kivinen et al [28] made measurements which were limited to indoor scenarios and the 5.2 GHz band. They report that measurements could be made continuously but variations of the channel statistics were either not investigated or not reported.

Bultitude et al [29] made wideband measurements and presented some CDFs of multipath delay spread. Their measurements were limited to the 28 GHz band and although there was probably enough data collected variations in channel statistics with time were not reported.

Thoma et al [30] limited their measurements to an indoor industrial scenario and the 5.2 GHz band. Much of the paper was concerned with describing the equipment used and only example results were presented.

Kermoal et al [31] made measurements in the 2 GHz band but these were limited to an indoor environment. These measurements were aimed at evaluating the MIMO architecture and used moving antennas to form a synthetic aperture at the receiver. The interval between collection of successive PDPs is not reported so it is not possible to deduce whether an analysis of the time variation of the channel statistics was possible.

Hampicke et al [32] reported measurements made at 5.2 GHz in a small courtyard. The channel sampling rate was fast enough to capture time variations but none were reported.

The Applied Signal Technology and Blind Equalisation Research Group at Cornell University [33] have reported measurements made in order to construct part of a propagation database for future research. Some time variation in the channel statistics are reported in the paper but only example results presented.

Byoung-Jo et al [34] describe an experimental broadband link which has been operational for a year. The link is partially instrumented and it is possible to extract path loss variation with time. It is not reported whether any other channel statistics are available.

Overall the published literature lacks reports of temporal variations in the wideband characteristics of the radio channel. It is clear that many workers in the field recognise that there will be long term variations but there is no significant body of experimental evidence from which the variations can be

concentrated on the indoor environment. This is understandable if it is assumed that most broadband systems will be deployed to serve single organisations and that the greatest capacity will be required within single or small groups of buildings. In the case of a telecom operator wishing to offer a public broadband service to many customers in buildings distributed over an urban microcell it is necessary to determine how temporal variations in the environment will affect the service. It is particularly important to know the extent of the variations and how they are distributed about some easily measurable value since a lack of this knowledge may result in fixed access infrastructure ceasing to work shortly after it is installed.

CHAPTER 4. MEASUREMENTS

4.1 Introduction

This project has involved an extensive measurement campaign. The conduct of these measurements and the processing of the resultant data are described in this chapter. Procedures for making measurements and calibrating the sounder were developed and these are also described.
The next section describes the general idea, the equipment, limitations on the measurements and the supporting activities in outline. Further sections describe the procedures and supporting activities in detail.

4.2 General Idea

There are two ways in which time variation can occur in the characteristics of the radio channel between two terminals. If one or both of the terminals moves the propagation path(s) between them will change. The propagation channel after movement will be different from that before movement. To isolate the time variation of the characteristics of the environment from that due to terminal movement it was important that both terminals should be static while measurements were being made.
In the absence of any a priori knowledge about the limits and rates of change of the channel characteristics, measurements over extended periods are desirable. Results from measurements over periods of a few hundred milliseconds have been reported in the recent literature. At least one series of measurements over longer periods has been made but at the time computing resources were inadequate to process the measurement data.
For this study measurements have been made over periods of 10 or 15 seconds in a number of different environments. The data from these measurements have been processed to extract the variation in the number of multipath components, the mean delay, the RMS delay spread and the coherence time of the channel among other characteristics. The RMS delay spread is a good indicator of the capacity of the channel while the coherence time indicates the rate of change.
The measurement campaign was conducted in collaboration with other students since a team of two or three persons was needed to handle and

system was to be used so measurements were made with two types of antenna systems. One was an array of six directional antennas plus an omnidirectional antenna. The directional antennas each had an azimuth beamwidth of 60° and their boresight directions were distributed at 60° intervals to cover a complete circle in the azimuth plane. The second antenna system had eight directional elements each with an azimuth beamwidth of 45° and with boresight directions distributed at 45° intervals to cover a complete circle.

4.3 Equipment

The Radio Systems Research Group has constructed a wideband channel sounder. This sounder uses the chirp technique and is capable of sweeping a bandwidth of 90 MHz around a centre frequency between 1950 MHz and 2145 MHz. The transmitter can transmit a sweep in two bands simultaneously so the differences in channel behaviour at different frequencies can be investigated. The receiver has eight channels so an eight element antenna array can be connected to facilitate the measurement of the directions of arrival of multipath components. Figures 4.1, 4.2 and 4.3 show the functionality of the sounder as it was configured for the measurements during this project.

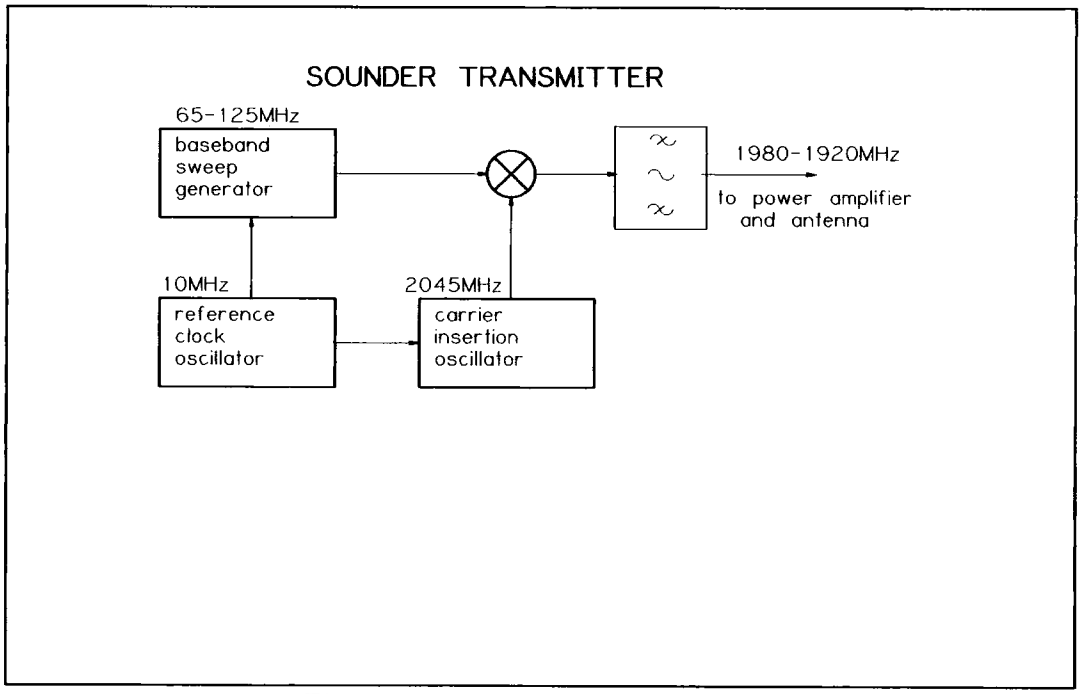

Figure 4.1. The sounder transmitter

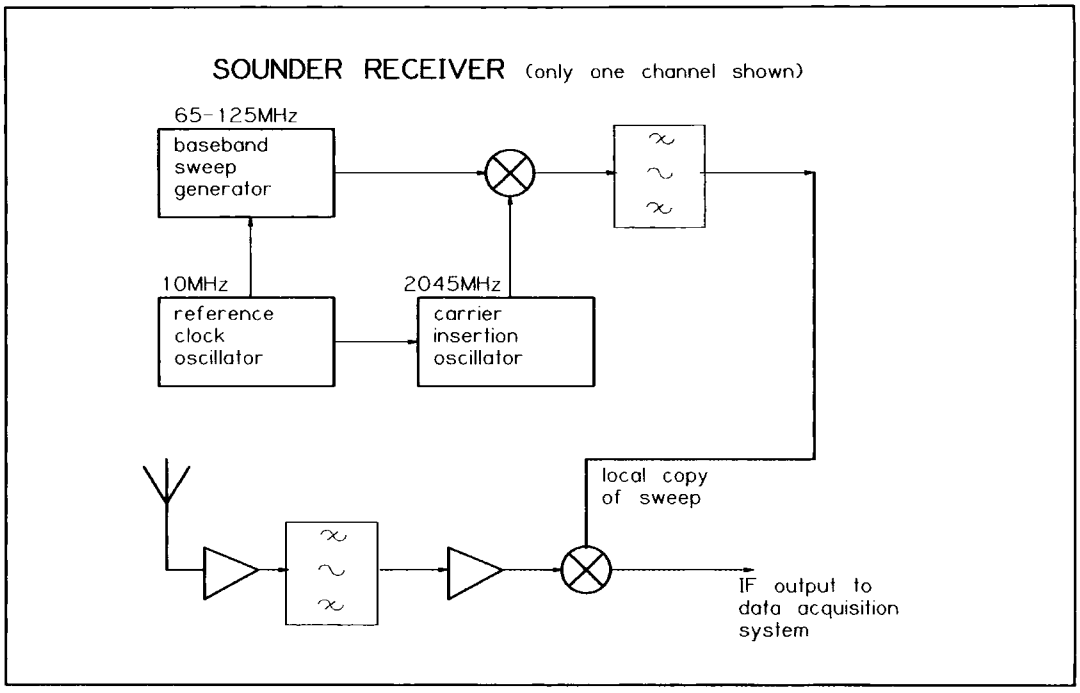

Figure 4.2. Sounder receiver (RF part)

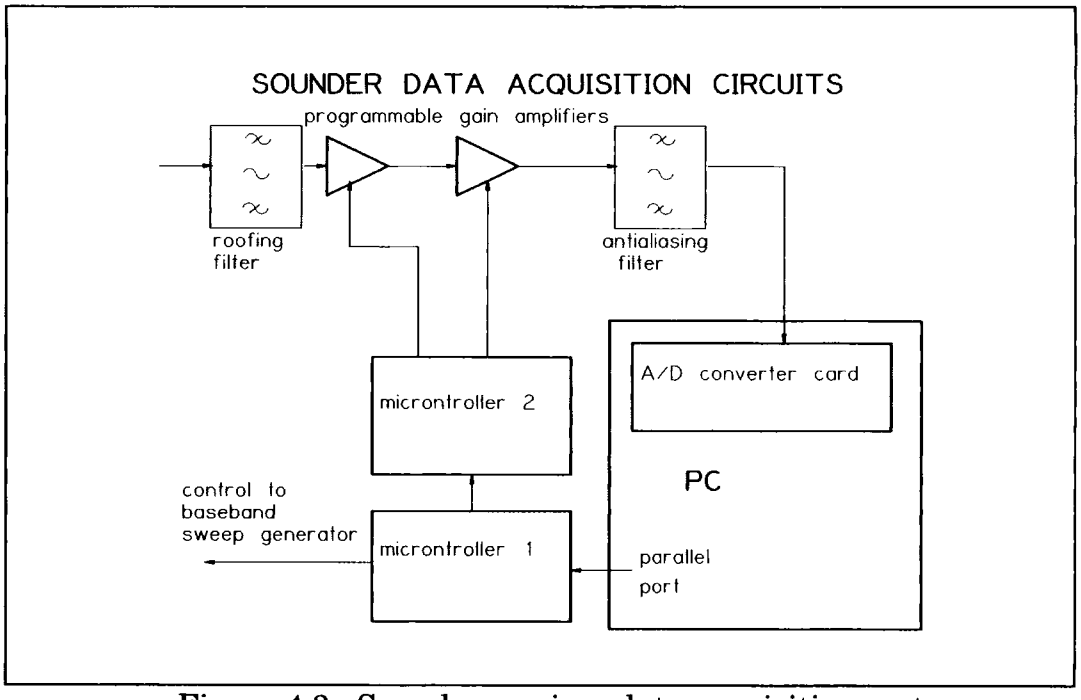

Figure 4.3. Sounder receiver data acquisition system

Both transmitter and receiver derive timing signals from stable atomic reference clock oscillators. The transmitter generates a baseband sweep whose parameters are programmable from a front panel keypad. The baseband sweep is mixed with the output of a carrier insertion oscillator and a filter selects the upconverted sweep signal. A power amplifier (not shown) raises the signal level so that the EIRP is approximately 0.5 W.

In the receiver, circuits identical to those in the transmitter generate a local upconverted sweep signal. The signal from each antenna is filtered and amplified before being mixed with the local copy of the upconverted sweep. There is a programmable attenuator for each channel which allow the input to the mixer to be adjusted to ensure that the mixer is operating over the linear part of its characteristic. These attenuators are controlled by the data acquisition PC. The output from the mixer contains the beat notes due to the various delayed components received from the channel.
The output from the mixer is passed to the receiver data acquisition system. A roofing filter removes wideband noise and out of band signals so that the amplifier stages are not overloaded by unwanted signals. The signals are then amplified before being filtered to a bandwidth which does not exceed the Nyquist limit of the Analogue to Digital Converter (ADC). The gain of the amplifiers is programmable and controlled by the data acquisition system to ensure that the signal to be sampled is always well within the voltage range of the ADCs.
Once the receiver has been synchronised with the transmitter the reference clock oscillators ensure that both will remain in step for several hours. Both transmitter and receiver may be powered from 230V ac mains or from 24V dc from batteries. To facilitate measurements remote from the university both transmitter and receiver are trolley mounted and installation in a vehicle is possible. Data acquisition at the receiver is via an eight channel data acquisition card installed in a PC. The sounder has been described in detail by Filippidis [41].

4.4 Data acquisition and control software

The data acquisition PC runs a program which controls some of the sounder characteristics and the ADC card used to capture the measurement data. Communication between PC and sounder is via the PC parallel port. Within the sounder is a microntroller which handles the sounder end of the communications protocol. This microcontroller also controls the sounder timing functions which affect data acquisition and communicates with a second microntroller. The second microntroller controls the signal conditioning functions such as the gain of the amplifiers.

The data acquisition program allows the user to automatically adjust the sounder attenuators and amplifiers to suit the received signal levels and to capture data over a specified number of frequency sweeps. The results from a single sweep may be displayed on the computer screen either in the time domain or in the frequency domain. The program also implements a number of other functions, some of which have been tested and others ignored. The most useful of these functions allows the gains of the signal conditioning amplifiers to be adjusted manually. The automatic adjustment facility of the program sometimes sets the amplifier gains too high so the ADC range is exceeded. If the ADC range is exceeded the captured data will exhibit limiting in the time domain and various harmonics of the principal beat note will be observed in the frequency domain. It is therefore useful to be able to reduce the gain slightly after the program has performed its automatic adjustment procedures.

The data acquisition program also allows one of two ADC sampling rates to be selected. The default rate is 1 Msample/sec and 500 ksample/sec is allowed. Unfortunately the number of sweeps and the number of samples per sweep reported in the data file header is incorrect when the 500 ksample/sec sampling rate is selected. The data file must be edited to double the number of sweeps recorded and to halve the number of samples per sweep.

4.5 Procedures

Procedures for making measurements with the sounder have been passed from student to student largely by word of mouth. The following sections are an attempt to document the procedures used for this measurement campaign

4.5.1 Setting up the sounder

The sounder transmitter was located on the roof of the UMIST main building for measurements in Manchester. For measurements in Durham it was located on the roof of the School of Engineering of the University of Durham. In both cases power was derived from 230 V mains. An omnidirectional antenna with a gain of 2.2 dBi was used in both cases.

The transmitter was not switched on until the receiver is ready so as to minimises interference to other users. The transmitter was never switched on without an antenna or dummy load connected to the output connector since this would have caused damage to the power amplifiers.
The receiver was mounted on a trolley. This trolley was designed to be light and to be able to mount kerbs easily. This trolley is only stable when all equipment and batteries are loaded on to it so care needs to be taken when loading equipment
The sounder was programmed using the front panel keypad. The sweep width, centre frequency and number of sweeps per second were programmed into the digital programmer using the following sequence of keys:

60 E

96 E

250 E.

The START button was then pressed to start sweep generation. This sequence was used at both transmitter and receiver and set the sweep width to 60 MHZ about a centre frequency of 95 MHz with 250 sweeps per second. An inconsistency in the digital programmer necessitated the keying of 96 rather than 95 for the centre frequency. The Carrier Insertion Oscillator (CIO) frequency was set to 2045 MHz so that two sweep sidebands were produced as a result of mixing the baseband sweep with the output from the CIO. These sidebands were separated by filters. Once the atomic clocks had stabilised the start of sweep at transmitter and receiver was synchronised and measurements then began. Perfect synchronisation of the start of sweep at the transmitter and receiver was not possible since the additional delays programmed into the receiver to delay the start of sweep have a finite step size. Also: perfect synchronisation is not desirable since it would require that the signal conditioning circuits work down to DC. All that is required is that the difference frequencies (beat notes) between the transmitter sweep and the receiver sweep for all delays of interest should fall inside the passband of the signal conditioning subsystem. A difference frequency of approximately 40 kHz for the time of flight delay of a line of

sight signal was found to be a good target and allowed components with excess delays of up to 15 microseconds to be identified.
When the receiver was at the desired measurement location the data acquisition software was used to automatically adjust the RF attenuation and the signal conditioning gains. If any further adjustment was required this was achieved manually using the facilities of the data acquisition software. A run of 2500 or 3750 sweeps were then sampled. Using P Filippidis' data acquisition software required more than one hour to save the data to disk. Since the battery endurance was 2 hours it was only possible to make one measurement before returning to the university for a change of batteries..

4.6 Environments

Measurements have been made in central Manchester and around Durham. The Manchester environment is characterised by wide streets with six storey buildings on either side and an occasional higher building. There are few mature trees in central Manchester and the terrain is either flat or gently sloping. Durham is a small old city built on a number of hills. The streets are narrow with buildings seldom higher than three stories. Outside the city centre there are many mature trees arranged sparsely in parks or densely in woods. Durham also has a large cathedral built on one of the hills which dominates the city.

4.7 Limitations of the Measurement Campaign

Apart from time there are two main limitations of the measurement campaign. There are limitations in the sounder's capabilities and there are limitations imposed by the environment.

4.7.1 Sounder Limitations

The data acquisition card used to capture the data from the receiver stores the samples from the receiver output in its on-board memory. This memory is limited to 128Mbyte which is sufficient to store 131 million samples. At a sampling rate of 1MHz with 8 channels this is 16 seconds of measuring time. The software which the PC uses to control the data acquisition card has been written using Microsoft Visual Basic which appears to be

15 seconds of measurement takes more than one hour. It is therefore impossible to measure continuously and the best that can be achieved is 15 seconds each hour. When running from batteries the receiver may be run for two hours before it is necessary to stop and recharge the batteries so it was only possible to record one 15 second measurement run between recharges. The original data acquisition program took 20 minutes to save data from a 1 second measurement run. While at UMIST the program was modified to reduce the save time for a 1 second run to 4 minutes. After the move to Durham the Microsoft Visual Basic 5 development environment was not available so further development of the program was impossible. Work to develop a new data acquisition system using commercial data acquisition cards and newer development software was started at UMIST and continued at Durham. During this work a number of unadvertised limitations of the new data acquisition cards were discovered and the work was stopped to allow time for making measurements. Chapter 7 describes the new data acquisition system at the point at which work was stopped.

4.7.2 Environmental Limitation

The sounder transmitter emits approximately 0.5 W of RF power. There is therefore a limit on the separation between transmitter and receiver which depends on the environment. In built-up areas such as central Manchester it is possible to separate transmitter and receiver by 1.5 km. In flat rural areas with few trees it is possible to make measurements with transmitter - and receiver separated by up to 4 km.

There are other users of the radio spectrum. When measurements first started the bands allocated to UMTS were unoccupied and could be used. Now that the UMTS network is being rolled out it is not possible to use the UMTS downlink band because there is a high level of interference from UMTS basestations. Measurements have therefore been confined to the UMTS uplink band (1920 to 1980 MHz) which is still mostly unoccupied. Measurements at other frequencies are possible but will require new filters to be acquired for the 2 GHz band and frequency converters to be constructed for other bands.

4.8 Preparation

Before any measurements were attempted the sounder was tested and calibrated. Sounder testing is described in chapter 5 and sounder calibration in chapter 6.

A number of modifications were implemented to rectify shortcomings found during testing. These are described in chapter 5.

A new data acquisition system was implemented to reduce the time taken to save measurement data to disk. This is described in chapter 7.

4.9 Processing

4.9.1 Number of Bins with Multipath Components

The first examination of the data from the measurements was to see how the number of multipath components varied with time at various locations. Where directional antennas were available at the receiver the differences between the signals received from different directions was also noted

At each measurement location the received signal was recorded for 10 or 15 seconds with both transmitter and receiver stationary. The data was split into separate files for each sounder channel. The data from each sweep was subject to a Discrete Fourier Transform (DFT) to extract the spectral components and yield an Impulse Response (IR). The average of the IRs for each 5 sweeps was taken to produce a Power Delay Profile (PDP) for each 20 msec of the measurement run. The averaging of the IRs enhances the signal to noise ratio of the PDP since the IR from each sweep contain significant noise. It was established experimentally that taking an average over 5 sweeps provides an acceptable signal to noise ratio and averaging over more than 5 sweeps does not yield any significant improvement. The output from this process is a number of delay bins each containing the power in the multipath components at that particular delay.

The PDPs from each measurement run were examined to determine which delay bins contain multipath components. To do this a threshold value was set so that only the most significant components were detected. For each PDP the power in the most powerful component was determined and the threshold value was subtracted from this power value to give a threshold

power value. Only components with power greater than this threshold were considered to be significant. Over the duration of the measurement run the number of bins containing multipath components was plotted. To see if a particular delay bin contained more than one component a further DFT was performed over all the IR power values for that delay bin. This yielded the component Doppler frequencies allowing different components to be identified.

Figure 4.4 below shows a typical PDP for the first 5 sweeps of a measurement in Durham. The power values in this PDP have been normalised with respect to the most powerful component.

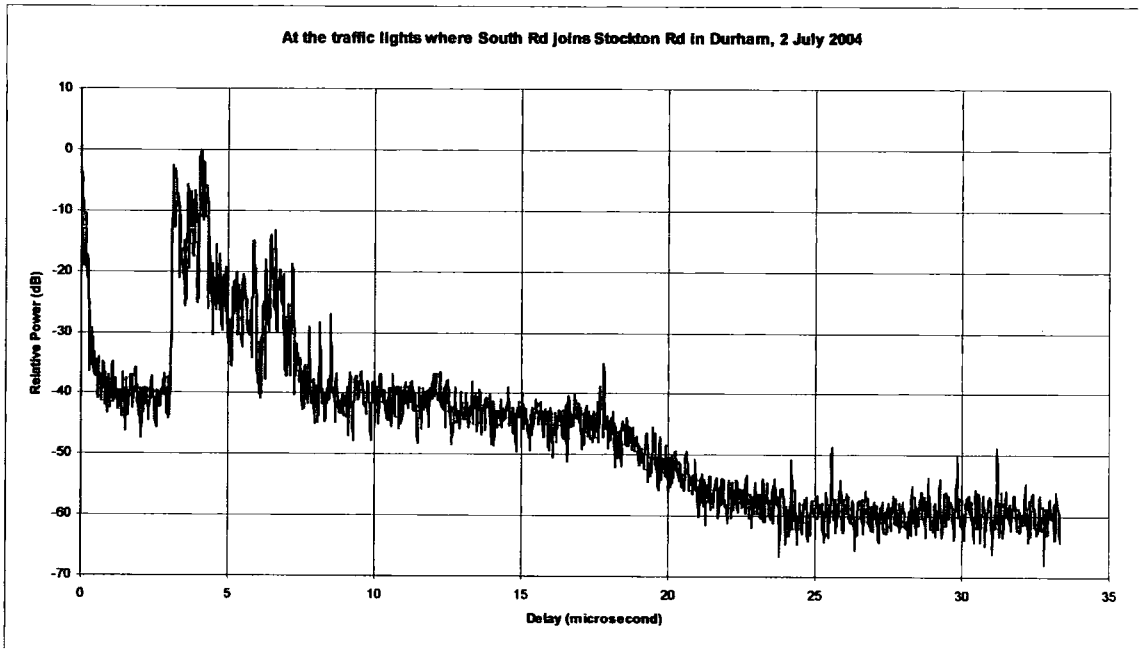

Figure 4.4. typical power delay profile

From figure 4.4 it can be seen that there may be a large number of components in the PDP. Radio systems have a limited ability to deal with multipath components so it does not make sense to characterise all of them. For the processing of these measurements a threshold was set which was 6 dB less than the power of the most powerful component.

Figure 4.5 below shows a typical Doppler plot for a single delay bin. The Doppler frequency axis has been scaled to indicate the speed in mph of the scatterer causing the multipath component. The response at zero speed comes from local clutter which is not moving.

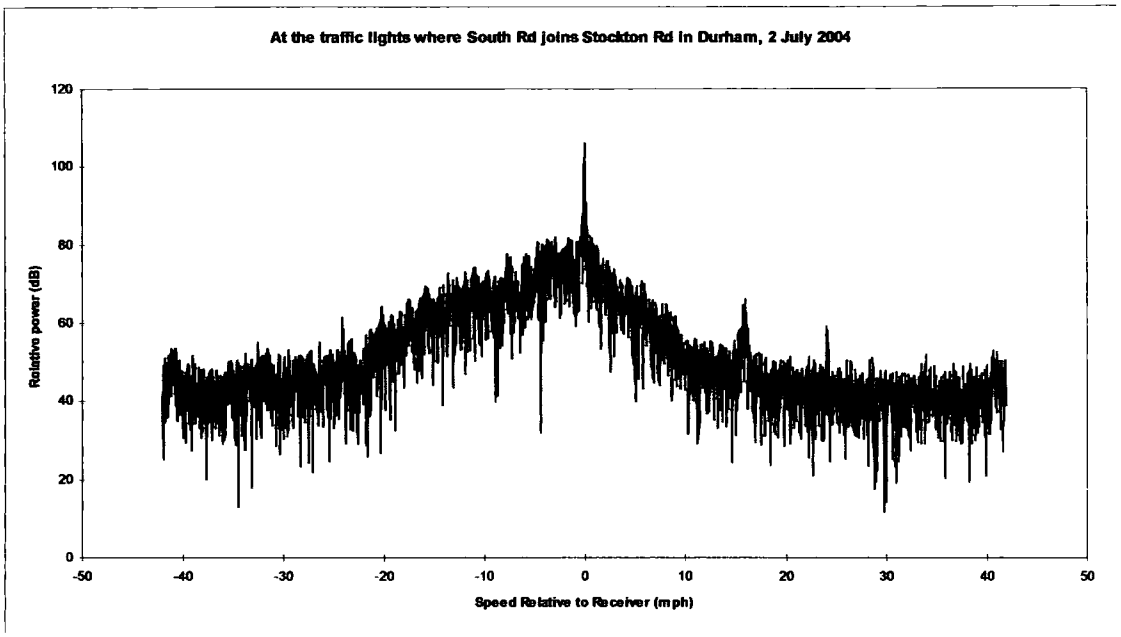

Figure 4.5. Typical Doppler plot for a single delay bin.

From figure 4.5 it can be seen that there may be more than one Doppler responses for a single delay bin indicating more than one scatterer. In this case power in a single delay bin does not uniquely identify a single multipath component, the Doppler information is also required. The location at which the measurement was taken had a clear view of the motor vehicles moving along the Stockton and South Roads. Two vehicles can be seen, both moving towards the receiver with relative radial speeds of 16 mph and 23 mph. The relative powers in these responses indicate that the vehicles had a smaller Radar Cross Section (RCS) than the local clutter. Time did not permit each delay bin to be examined to see how many multipath components there were with that delay. In chapter 8 all references to multipath components should be taken to mean delay bins with multipath components.

The method of identifying delay bins with significant multipath components had to take into account the leakage from bin to bin which occurs because a finite time series of measurements was analysed. Before extracting the spectral components with a DFT the time series data was modified with a Hamming window. This window tends to reduce the leakage from bin to bin at the expense of broadening the spectral peaks. The PDP is scanned and when the bin with the greatest power is found it is counted as having a multipath component provided that the power is greater than the threshold.

This component is removed by subtracting the power found in the bin from the bin in which it was found and subtracting 0.6 of this power from the adjacent bins. This procedure has been found to work and takes into account that the delay of a particular component is unlikely to be equal to the delay at the centre of any bin so the component power is spread over two or more bins. The factor of 0.6 was determined experimentally, factors between 0.1 and 0.9 did not strongly affect the number of components detected. A factor of 0.6 was used for processing all the measurements.

4.9.2 Mean Delay

Although the sounder could not measure absolute delay it was possible to analyse the data to determine the mean delay with reference to an arbitrary datum and hence the temporal variation of the mean delay. The time series data were subjected to a DFT and averaging over 5 sweeps as for the detection of multipath components. Considering only those delay bins whose power exceeded the threshold for each bin a product was formed of the power in the bin and the delay of the bin. The sum of these products was divided by the sum of the powers in the bins considered to yield the mean delay.

i.e.

$$mean\_delay = \frac{\sum_{i=1}^{n} d_i P_i}{\sum_{i=1}^{n} P_i} \text{ for all } i \text{ where } P_i > P_{thresh} \text{ where}$$

n is the number of components found

d_i is the delay of the ith bin

P_i is the power in the ith bin and

P_{thresh} is the threshold power value.

Cumulative distribution functions (CDF) were plotted for the mean delay at each measurement location.

4.9.3 RMS Delay Spread

The RMS delay spread was calculated by:

squaring the result to form a positive quantity

forming the product of the power in the bin and the squared delay difference

summing the power delay products

dividing the square root of the power delay products by the total power in the bins containing significant components.

i.e.

$$RMS\_delay\_spread = \frac{\sqrt{\sum_{i=1}^{n}(d_i - d_m)(d_i - d_m)P_i}}{\sum_{i=1}^{b} P_i} \text{ for all } i \text{ where } P_i > P_{thresh}$$

and where

d_m is the mean delay and

all other sysmbols are as for calculating the mean delay.

CHAPTER 5 SOUNDER TESTING AND MODIFICATION

5.1 Introduction

The sounder was developed and constructed by previous students, first in single channel form and more recently in eight channel form. The single channel sounder was tested by Gokalp [42] before making measurements. The eight channel sounder was tested by Philippidis [41] only as far as was necessary to demonstrate that it was possible to construct a functioning two band eight channel sounder.

Before any serious measurement activity could be contemplated the sounder had to be thoroughly tested to characterise its functionality and limitations. Where faults or limitations were found either the sounder was repaired or modified or procedures were developed to ensure that valid measurements of the environment could be performed. A number of multi-element antenna arrays could be used with the eight channel sounder so that directional information could be gained. These antenna arrays needed to be characterised. Antenna design and characterisation are the subject of another project and will be described in detail by Abdalla [43]. The outline procedure is described and the results for the antenna used for this project presented.

This chapter describes the testing performed on the sounder, the faults and limitations found and the remedial work performed to make the sounder suitable for the proposed measurement programme. Some work on a new data acquisition system and proposals for sounder modification are documented as a basis for future work. The additional hardware and software developed for sounder and antenna calibration are also described.

5.2 The Purposes of the Testing

In order to make an extended series of field measurements the sounder had to be shown to be reliable and to make repeatable measurements. In order to make useful deductions from the experimental data the characteristics and limitations of the sounder needed to be known. Where sounder

limitations placed constraints on measurement procedures the constraints needed to be documented and observed.

The tests performed were designed to evaluate the sounder performance in terms of resolution, dynamic range, repeatability and flexibility.

5.3 Resolution

The theoretical resolution of the sounder is inversely proportional to the swept bandwidth. Using a sweep width of 60 MHz the theoretical time resolution is 16.67 nsec which equates to a path length resolution of 5 m. The sweep width of 60 MHz allowed the use of the UMTS bands which were unoccupied at the start of the measurements. During the processing of the measurement data a Fourier Transform is used in estimating the spectral components. Since the finite length of the data would cause leakage of energy between components a Hamming Window is used to weight the time series data. One of the side effects of using such a window is a widening of the spectral components in the frequency domain and a consequent degradation of the resolution. For the Hamming Window a spectral component is increased in width by a factor of 1.30 [44] leading to a practical time resolution of 21.67 nsec, a distance resolution of 6.5 m. Further explanation of the sounder resolution is in Appendix 3.

A further complication arises because the analogue time series data has been digitised to facilitate storage and subsequent processing. The data are thus allocated to bins and after the Fourier Transform the spectral components are allocated to bins in the frequency domain. If a spectral component does not have a frequency that exactly matches one of the available bins it will be spread over two bins.

The tests performed to evaluate the sounder resolution were a CW test, a single tone back to back test and a two tone back to back test.

5.3.1 CW Test

The CW test is the most basic test of resolution and is also used to determine the differential channel gains for calibration purposes.

Two cavity oscillators were used, each phase locked to a crystal oscillator. The output frequencies of these oscillators were 2134.500 MHz and 2134.540 MHz. These frequencies are well within the operational frequency range of the sounder and, when mixed together, yield a difference frequency of 40 kHz which is well within the passband of the sounder signal conditioning system. These oscillators had phase noise less than - 50 dBc at 100 Hz offset from the carrier so the component represented by the difference frequency should span no more than two frequency bins. If the result from a CW test showed a component spanning significantly more than two bins this would have indicated a degraded resolution when compared with the theoretical value.

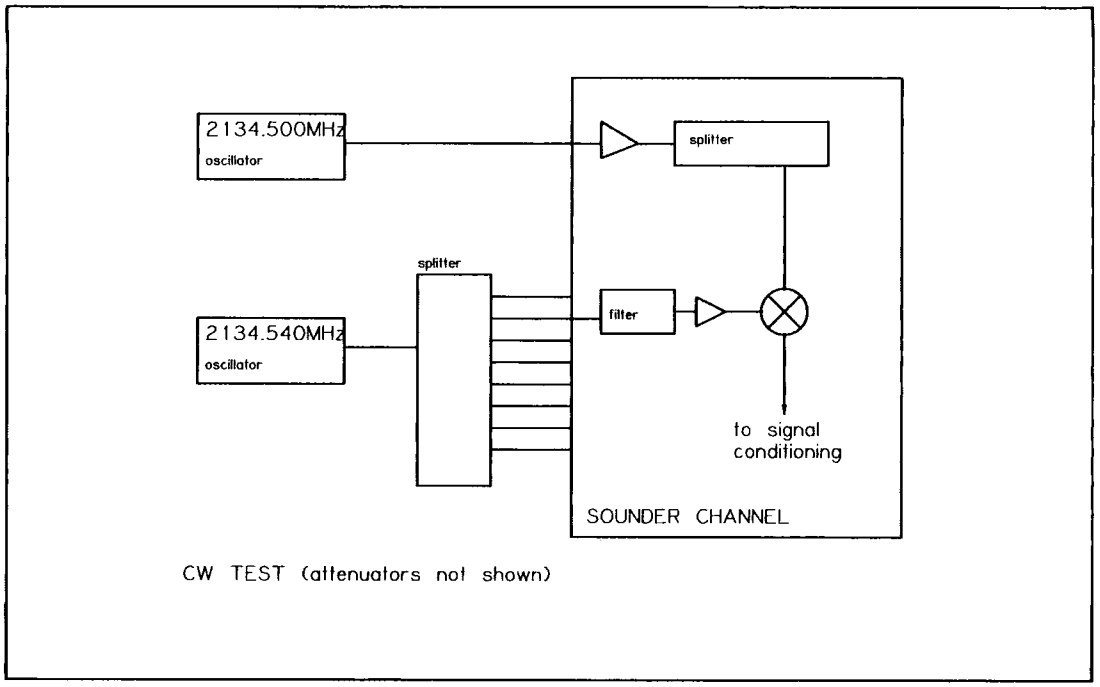

Figure 5.1 Arrangement for CW Test.

To perform this test one of the oscillators was used as local oscillator and was connected to the input of the receiver local oscillator amplifier/splitter subunit. Attenuator pads were inserted to adjust the LO input to the mixers to the specified - 10 dBm level. The other oscillator was used as RF input for all eight channels. The output of this oscillator was attenuated to provide an input level at each antenna connector of - 80 dBm which was well within the dynamic range of the RF front end circuits. Figure 5.1

above shows the arrangement used for the CW test. For the CW test the sounder does not sweep. The part of the sounder which generates the sweep was diabled. It was found necessary to separate the sounder from the test oscillators by a distance of 5 m to prevent signals propagating from the oscillators to the sounder other than via the connecting cables.

The data acquisition circuits and software were used in the usual way to automatically adjust the signal conditioning gains and to sample and store data over 500 sweeps. The normal postprocessing software was used to split the data into single channel files and to perform the spectral analysis using a Discrete Fourier Transform. A typical output from this test is shown in figures 5.2 and 5.3 below. Figure 5.2 shows the complete frequency spectrum, scaled for delay, while figure 5.3 shows how the dominant component is spread over frequency bins. This was a severe test since 500 sweeps are taken over 2 seconds and any drift in the frequency determining components of the sounder would have been revealed. Instability of the rubidium reference oscillator or timing jitter in the data acquisition circuits would have resulted in a widening of the dominant component.

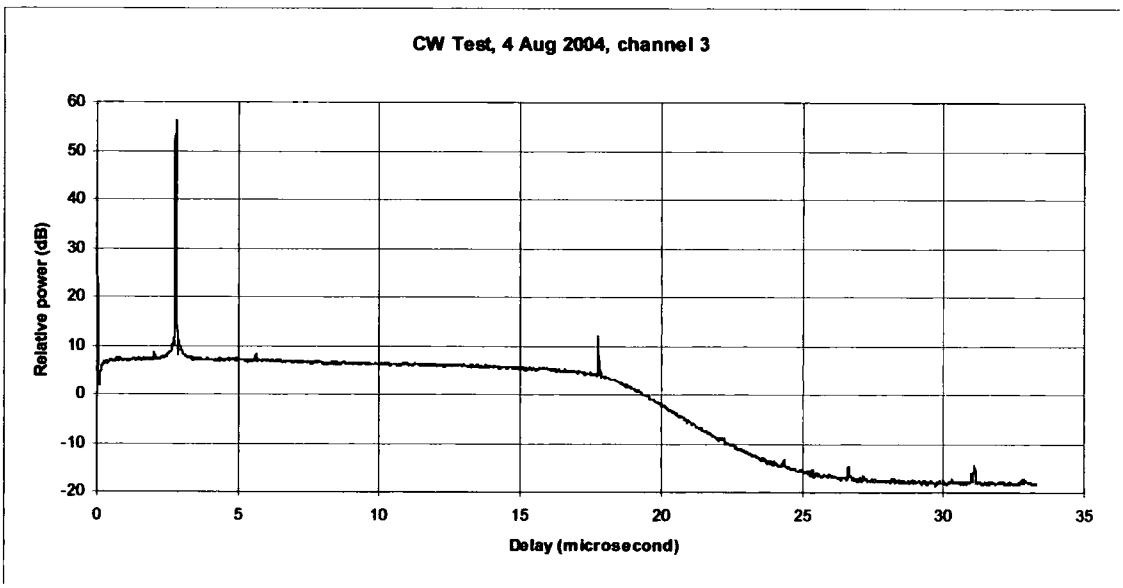

Figure 5.2 Result of typical CW Test, complete spectrum

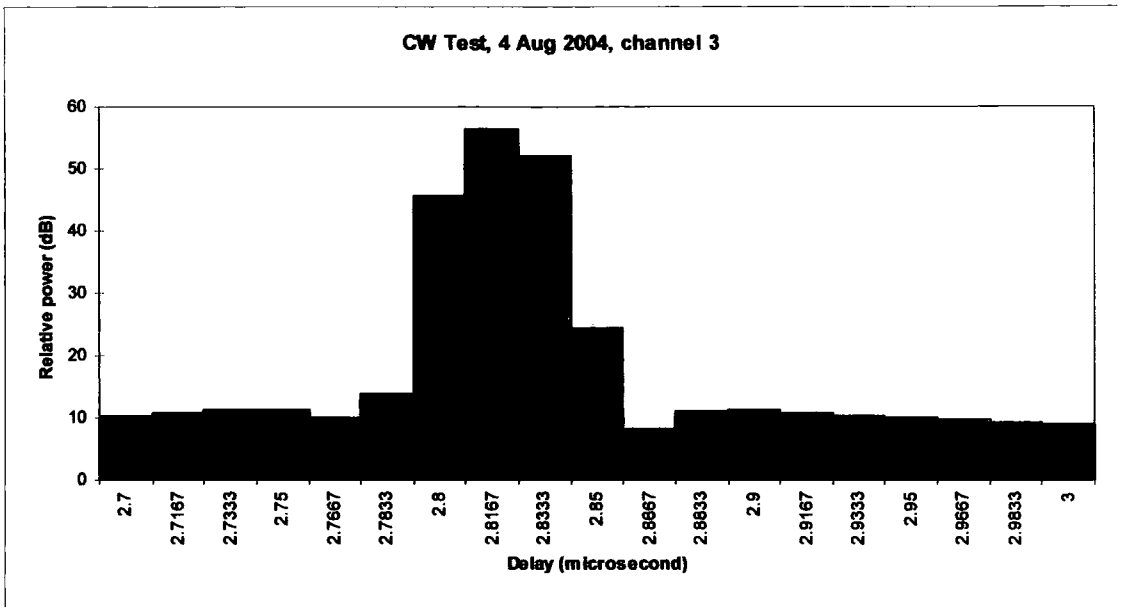

Figure 5.3 Result of typical CW Test, detail about dominant component.

Figure 5.2 shows the dominant component and a small spurious component at a delay of approximately 18 microseconds. The spurious component was probably due to contamination by power supply ripple from one of the switched mode power supplies and was not considered to be important since it was 43 dB below the peak of the dominant component. The anti-aliasing filter characteristic is clearly visible in figure 5.2. Figure 5.3 shows the dominant component spread over 3 bins. Although this is not perfect it was considered acceptable for the measurements proposed. The other channels showed similar performance except for some spurious components which were investigated as described elsewhere in this chapter.

The CW tests were also used to determine whether the gain of the sounder receiver varied with time. A series of tests were made starting 5 minutes after switch-on and repeated every 15 minutes for 2 hours. It was found that the sounder gain did change significantly between the first and second tests but that after 20 minutes remained constant.

5.3.2 Single Tone Back to Back Test

For single tone back to back tests the sounder transmitter was connected to the receiver via a cable, attenuators and a splitter. As for the CW tests the transmitter and receiver had to be separated by at least 5 m. A combination

at the receiver to be adjusted so as to prevent overloading and to conduct tests at various input levels. The data acquisition system was used as normal for making measurements.

The single tone back to back test can highlight deficiencies in both transmitter and receiver, particularly frequency instability and spurious signals. Figure 5.4 shows the result from a back to back test made on 6 August 2004.

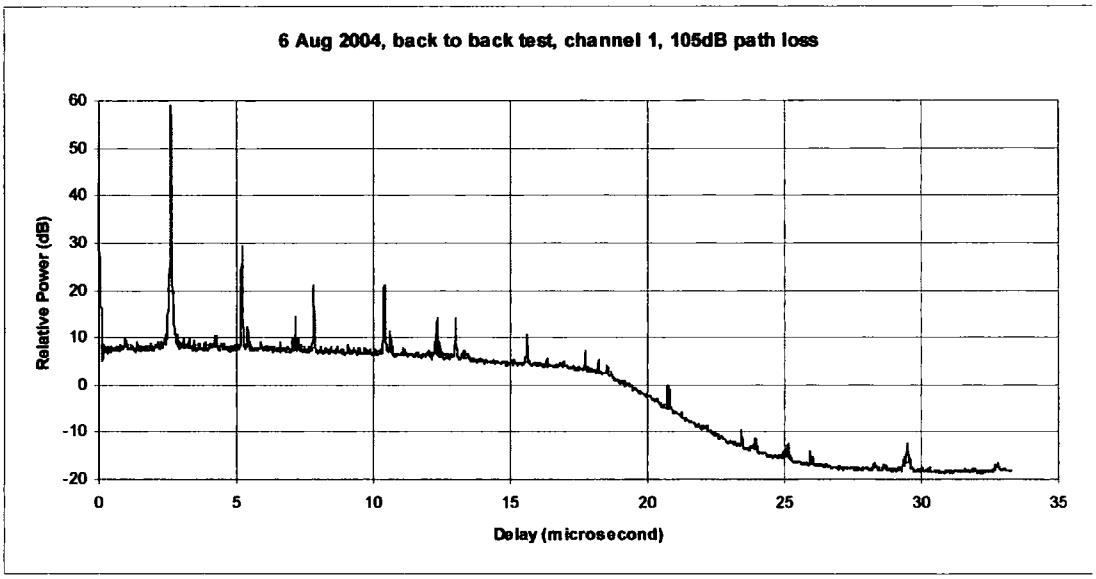

Figure 5.4 Results of back to back test on 6 August 2004 for channel 1.

This result shows a number of spurious components, some of which are harmonically related to the principal component and have levels only 29 dB less than that of the principal component. A detailed view of the principal component is shown in figure 5.5 below.

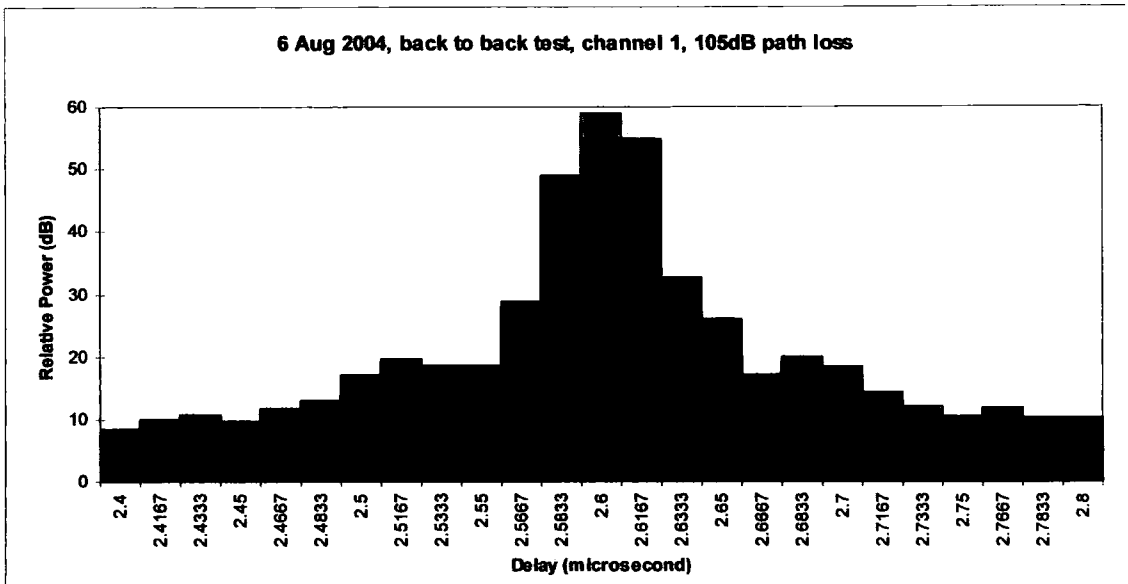

Figure 5.5 Detail of the principal component shown in figure 5.4.

Despite the spurious components the principal component may be seen to occupy 3 bins as is the case for the CW tests. These results are for channel 1 and need to be compared with the result for channel 3 which is shown in figure 5.6 below.

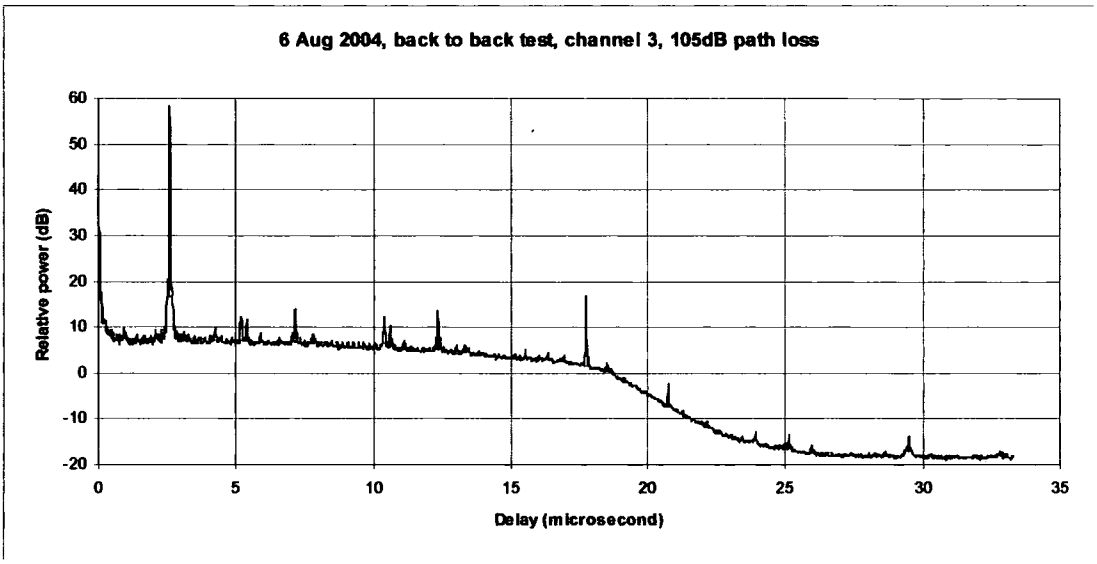

Figure 5.6 Result from back to back test on 6 August 2004 for channel 3.

Although figure 5.6 shows some spurious components, all are at levels 42 dB less than the level of the principal component. Examination of the results from other channels showed that channels 1, 2, 7 and 8 exhibit strong spurious responses while channels 4, 5 and 6 are similar to channel 3.

The signal conditioning unit contains two PCBs on which are mounted the channel amplifiers and anti-aliasing filters. The circuits for channels 1, 2, 7 and 8 are one PCB and the circuits for channels 3, 4, 5 and 6 are on the other PCB. A close visual examination of the PCB containing channels 1, 2, 7 and 8 revealed a cracked track in the feedback path of one of the operational amplifiers. This had the effect of disturbing the DC operating conditions of the amplifier to the extent that limiting occurred. Limiting in this situation turns a sinusoidal signal into something approaching a rectangular waveform and hence generates harmonics of the sinusoidal components of the input waveform. It was the harmonics generated by this fault which appeared as spurious components in the results of the back to back test for channel 1 on 6 August.

The track was repaired and testing continued. During the post repair testing the harmonically spurious components were found to have disappeared but the sounder noise floor was considered to be higher than it should have been. The output from the mixers in the RF front end circuits was connected directly to the programmable gain amplifiers in the signal conditioning unit. Since the mixer output could contain sum components and wideband noise in addition to the wanted difference components it was considered that some form of filtering was desirable.
A roofing filter was interposed between the mixer output and the programmable gain amplifier input. This was an elliptic lowpass filter designed for a cutoff frequency of 600 kHz and stopband attenuation of 40 dB. The elliptic form was chosen since this gives a sharp cutoff at the band edge and reasonable stopband attenuation with few components. The cutoff frequency was chosen to give minimal group delay distortion over the 250 kHz band of interest.

A schematic of the roofing filter is shown at figure 5.7 below. The design of this filter followed standard practice as described by Williams [45] and Zverev [46] from which references were taken the normalised element

frequency gave capacitor values which could be closely approximated by combinations of two preferred values. The inductors were wound on ferrite torroidal cores readily available from Farnell and the measured values were within 5 percent of those calculated. Since this filter does not define the bandwidth of the signal conditioning subsystem the approximations of the component values are acceptable. The measured performance of the filter showed a cutoff frequency slightly higher than that calculated, a maximum attenuation of 80 dB at 800 kHz and attenuation greater than 40 dB in the stopband. Eight of these filters were constructed on stripboard and incorporated into the re-engineered signal conditioning units. This modification resulted in a lowering of the sounder noise floor by at least 5 dB on all channels.

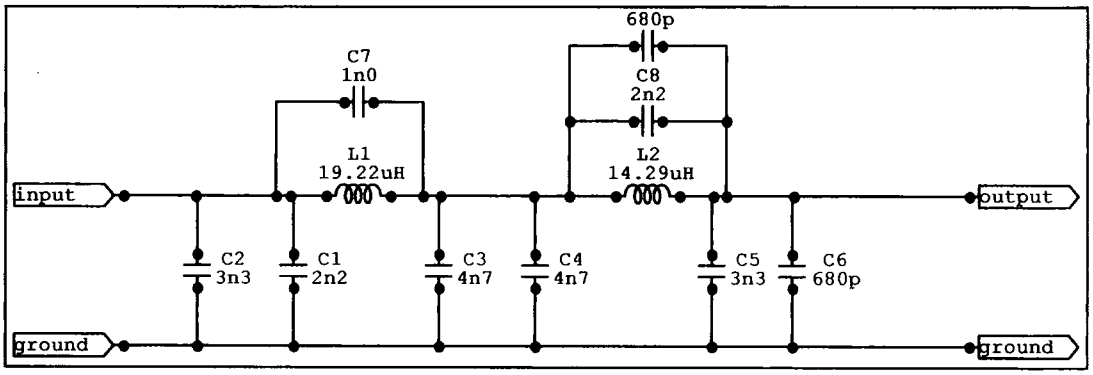

Figure 5.7. Signal Conditioning Roofing Filter

During testing of the signal conditioning unit a number of spurious signals were detected. The strongest of these was at a frequency well above the cutoff frequency of the antialiasing filters. With the signal conditioning unit removed from the sounder the frequency of this spurious signal varied from 1.8 MHz to 900 kHz as a hand was brought near to the unit.

An examination of the signal conditioning system showed that for each channel there is a programmable gain amplifier followed by one of two active filters which serve as anti-aliasing filters. The inputs to the two filters are connected in parallel to the output of the programmable gain amplifier. The output from one or other of the filters is selected under

active filters, each with three stages, having cutoff frequencies of 165 kHz for indoor measurements and 250 kHz for outdoor measurements. When the 250 kHz filter output was selected the 165 kHz filter was oscillating at a high enough level to leak into the selected filter circuitry and contaminate the wanted signal.

Since this study requires outdoor measurements it was decided to disable the indoor filter. This was achieved by removing all reactive components and connecting the amplifier inputs to ground. Since switching between filters is no longer required the analogue switches and associated cabling were removed. This modification has removed the most troublesome spurious signals generated within the signal conditioning subsystem.

There was also a suspicion of oscillation on some channels with certain gain settings. The outputs from the signal conditioning subsystem are connected to the data acquisition system by coaxial cables approximately 1 m in length. It is possible that the oscillations were caused by the signal conditioning output amplifiers having to drive capacitive loads for which they were not designed. To minimise the probability of these oscillations occurring in future a 150 ohm resistor was interposed between the output of the signal conditioning amplifier and the cable to the data acquisition system. The data acquisition system presents a high impedance at the input so the resistor does not significantly affect the sensitivity. The resistor and the capacitance of the cables form a low pass filter pole at a frequency which is approximately six times the cutoff frequency of the signal conditioning filter and so does not affect the overall performance.
To allow the modification to the signal conditioning circuits some mechanical re-engineering was required. Appendix 4 gives more details of the modifications to the signal conditioning unit.
To confirm that the sounder performance was acceptable another single tone back to back test was performed. Some of the results of this test are shown in the following figures.

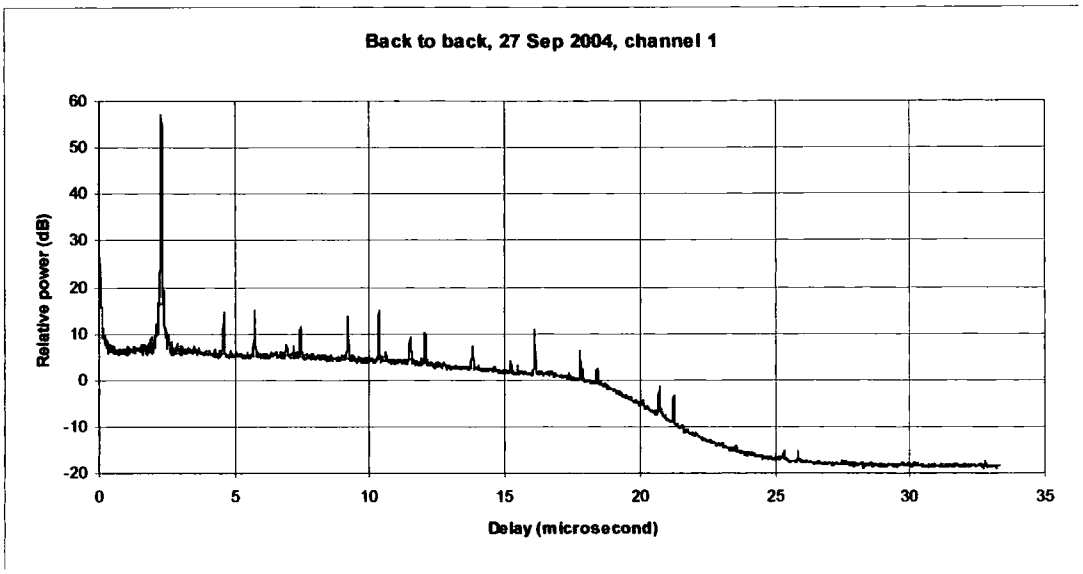

Figure 5.8. Single tone back to back test after modification, channel 1.

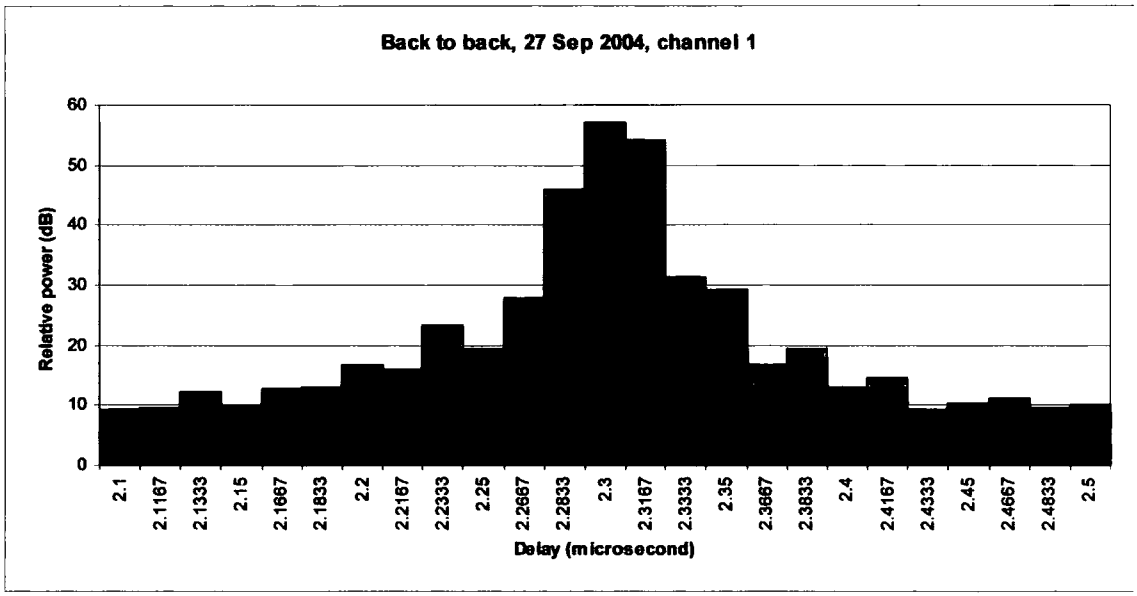

Figure 5.9. Single tone back to back test, detail from figure 4.8.

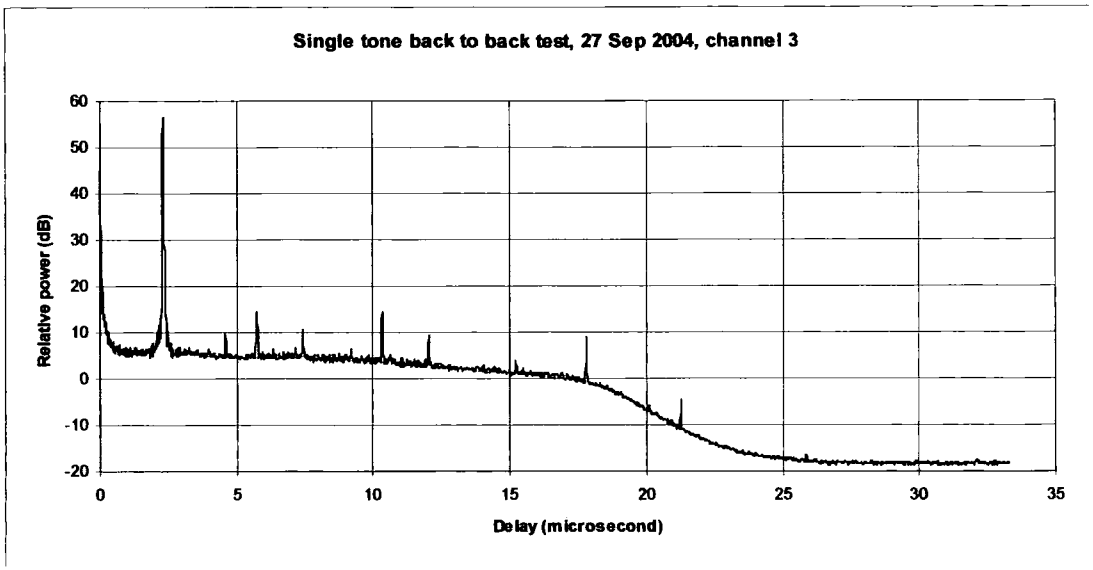

Figure 5.10. Single tone back to back test after modification, channel 3.

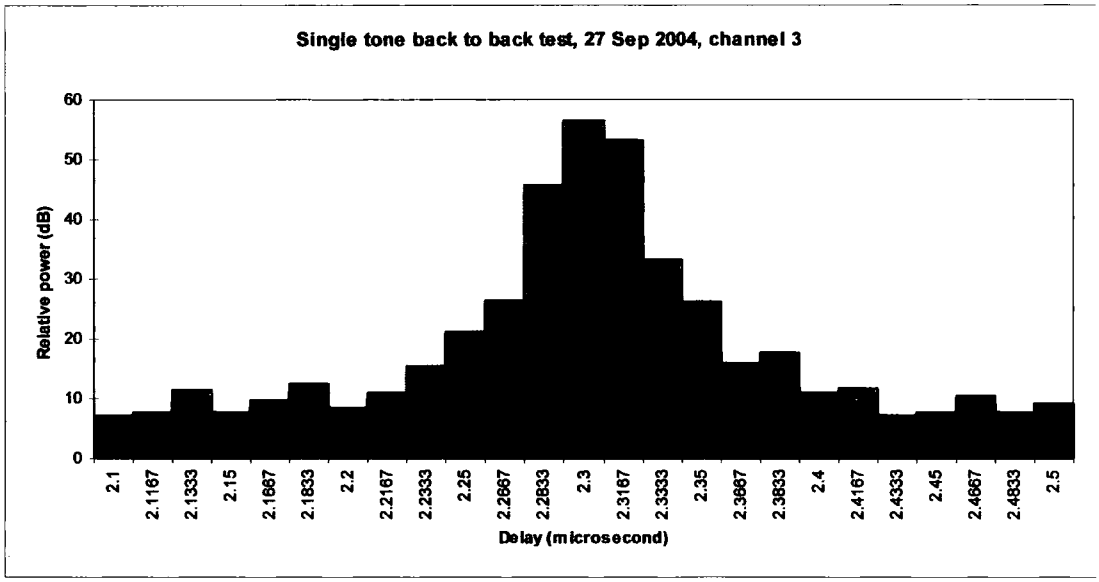

Figure 5.11. Single tone back to back test, detail from figure 4.10

Figures 5.8 to 5.11 show the difference in level between the peak of the principal component and the strongest spurious component (the dynamic range) to be 42 dB or more. This is the dynamic range to be expected from an 8 bit analogue to digital converter (ADC) when the input is adjusted so that the maximum peak-to-peak voltage is 0.7 of the ADC input range. The principal component can be seen to occupy no more than 3 bins when levels more than 20 dB below the peak are ignored. The sounder performance measured by single tone back to back tests was considered acceptable for progression to two tone back to back tests.

5.3.3 Two Tone Back to Back Tests

Two tone back to back tests were conducted to determine the sounder's ability to distinguish between components with similar, but not identical, delays. For these tests the sounder transmitter was connected to the sounder receiver by cables. Instead of using a single cable, the output from the transmitter is split and two cables carry the split outputs. At the receiver the two cables are connected to a combiner whose sum port connects to an 8 way splitter as for single tone tests. Figure 5.12 shows the arrangement. By using cables of different lengths between the transmit splitter and the combiner, components with different delays can be made to reach the receiver.

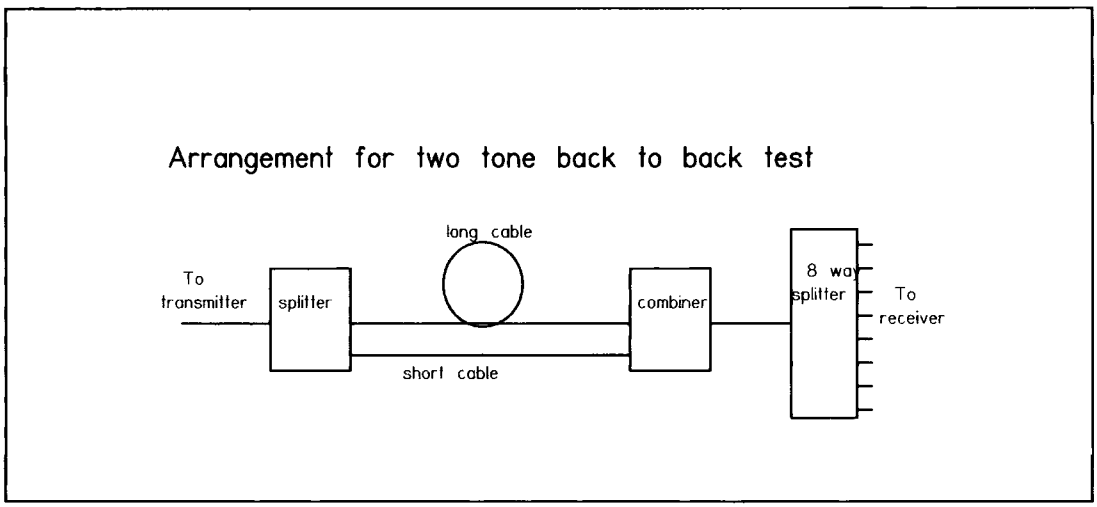

Figure 5.12. The arrangement used for two tone back to back tests.

Figures 5.13 and 5.14 show the result of a two tone back to back test using a short cable 300 mm long and a long cable 100 m long.

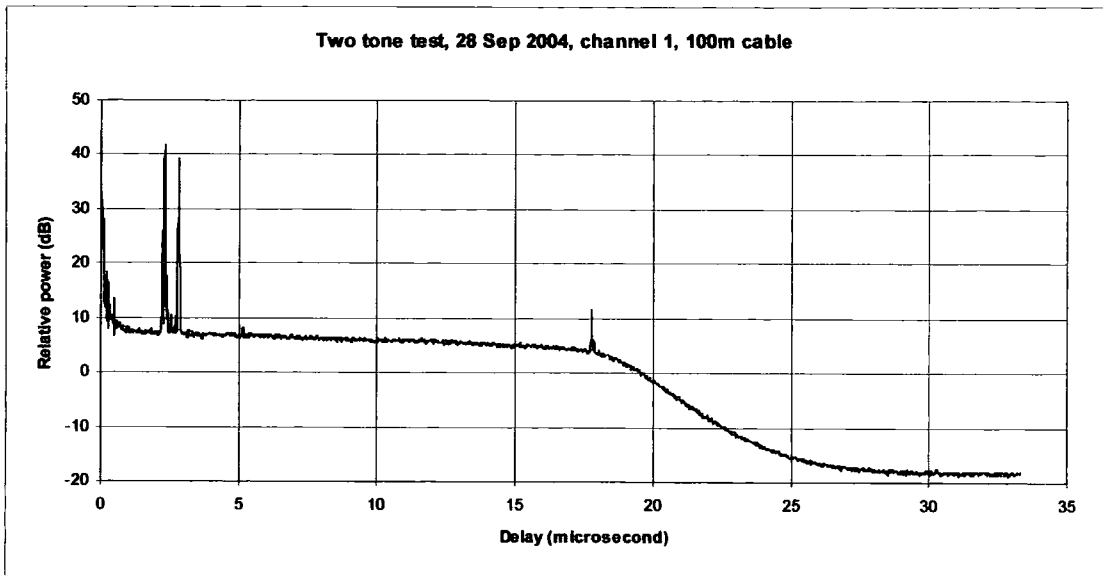

Figure 5.13. Two tone back to back test with 100 m cable.

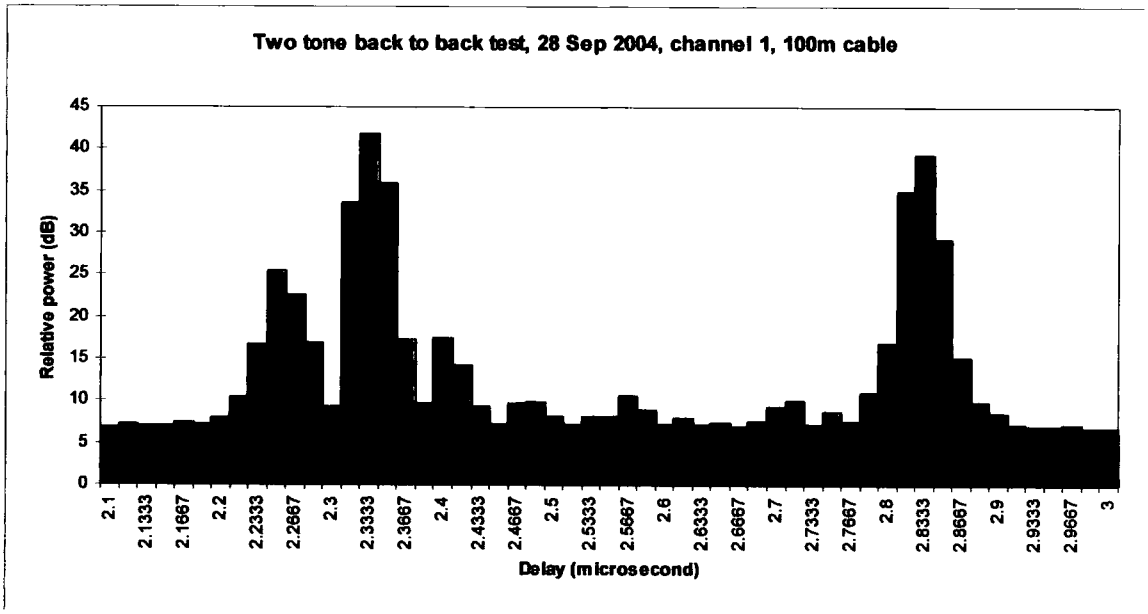

Figure 5.14. Two tone back to back test, detail from figure 4.13.

Figure 5.13 clearly shows two components with different delays. Figure 5.14 shows the difference in delay to be 500 nsec. The cable used had a velocity factor of 0.67 hence 100 m of cable equates to 150 m propagation in free space. Taking the velocity of propagation to be 300,000 km/sec the propagation delay over 150 m is 499 nsec which is equal to what is shown in figure 5.14 if the resolution of the sounder is taken into account.

Figures 5.15, 5.16 and 5.17 show the detail around the principal component for results of two tone back to back tests with the 100 m cable replaced by cables of 8 m, 6 m and 4 m.

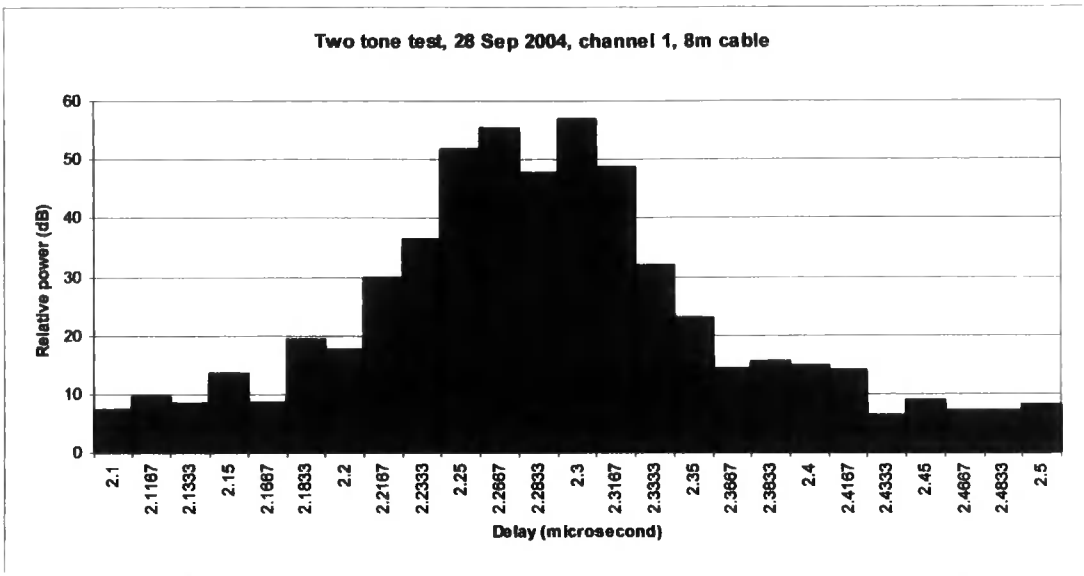

Figure 5.15. Result from two tone back to back test with 8 m cable.

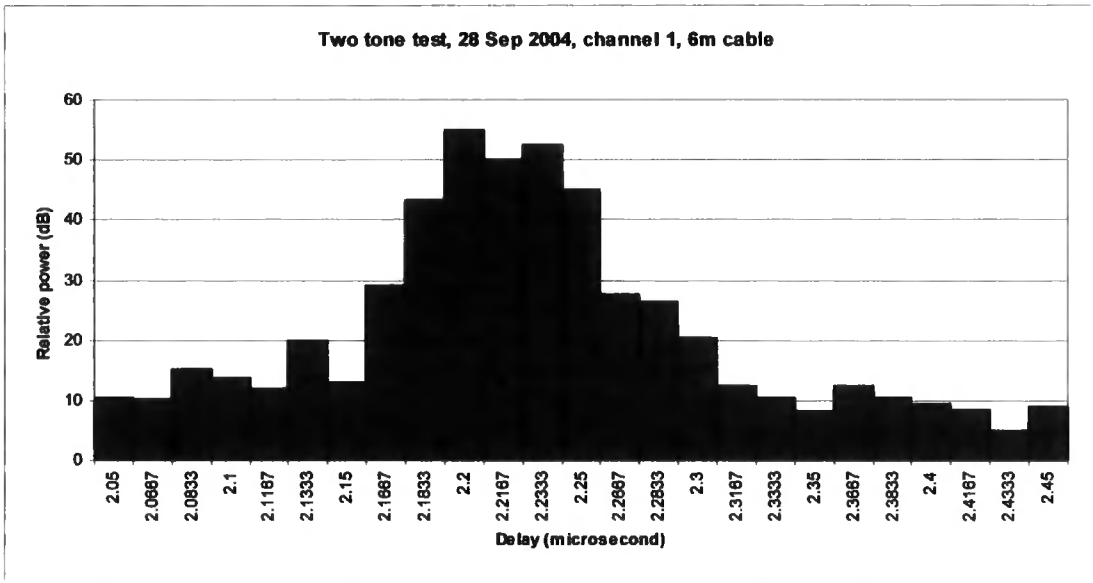

Figure 5.16. Results from two tone back to back test with 6 m cable.

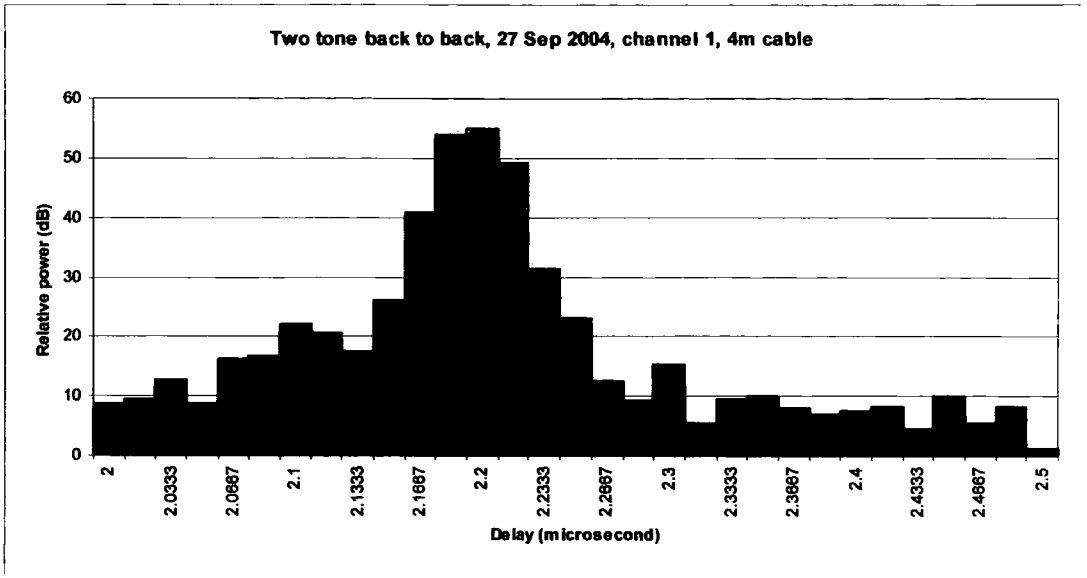

Figure 5.17. Results from two tone back to back test with 4 m cable.

As the long cable length is reduced the separation between components is also reduced until in figure 5.17 there is only a widening of the component rather than two distinct components. Even with the 4 m cable it is possible to detect that a second component is present. Allowing for the propagation factor of the cable the sounder may detect two components with path lengths which differ by 6 m and this is consistent with the predicted resolution.

5.4 Testing the Sounder Functions

After completing the modifications to the signal conditioning unit the sounder and data acquisition system was thoroughly tested to ensure that the functions needed for the proposed measurements worked and that there was no significant variation of performance with time. Not all of the data acquisition functions were tested and no attempt was made to investigate the undocumented features of the digital programmer.

A number of tests of the data acquisition system were also performed to discover which functions were reliable. One problem found during these tests was that Microsoft Windows does not always detect and process event messages generated by the application software. Although this is inconvenient it is usually possible to generate another windows event (by pressing a button for example) which stimulates Windows to process the

event messages in the queue. Another limitation of the data acquisition software is the inability to correctly report the number of sweeps and the number of samples per sweep when sampling at 500 ksamples/sec. The default sampling rate is 1 Msample/sec and the user interface appears to offer a rate of 500 ksamples/sec also. Selecting the 500 ksamples/sec sample rate appears to change the sample rate for the display but not the sample rate when saving data to file. In fact when the 500 ksample/sec rate is used for samples stored in the file the number of sweeps reported in the file header is half what it should be and the number of samples per sweep is double what it should be. The total number of samples in the file is correct but the incorrect header can lead to confusion when postprocessing the results. To avoid confusion the 1 Msample/sec rate was used for all the measurements.

5.5 Sounder Limitations Not Corrected

During the testing of the sounder, particularly at low input signal levels, some spurious signals were noticed at the output from the mixers in the RF units. These spurious signals are the same on all channels and take the form of a negative spike which starts 40 nsec after the start of sweep signal and lasts 280 nsec. The amplitude of this spike is typically 8 mV. Since the wanted output from the mixers under low signal conditions is typically 2 mV and the signal conditioning gain needs to be high, the spike can momentarily paralyse the signal conditioning amplifiers. These spikes could be gated out in the signal conditioning circuits. This would require major modification of the signal conditioning unit and time did not permit this. The spikes are probably caused by the reactive components in the mixers reacting to the rapid change of frequency at the start of each sweep. Because of the limitation imposed by the data acquisition system new data acquisition cards were purchased and it was intended to write new software that would allow continuous measurement with the data being streamed to disk. A large part of the new software has been written but in the course of testing it a number of shortcomings in the sounder hardware were exposed. Time has not permitted the completion of the new software since a number of modifications to the hardware were made to rectify the shortcomings

found during software testing. Modification of the hardware and completion of the software would not have allowed time for measurements. Chapter 7 describes the new data acquisition system at the time of writing.

CHAPTER 6 SOUNDER AND ANTENNA CHARACTERISATION

6.1 Introduction

Before using the sounder it was necessary to measure some of its characteristics in the configuration which was to be used for the measurements. Although it was not necessary to calibrate the sensitivity or frequency accuracy against national standards, it was necessary to measure the relative gains of the eight channels. It was also necessary to characterise the array of antennas which was to be used for the measurements.

6.2 Channel Gain Measurement

The gain of each of the sounder channels is dependent on the setting of the RF attenuator for the channel and on the setting of the programmable gain amplifier in the signal conditioning unit. Manufacturing tolerances will allow small differences between the actual attenuation of each of the RF attenuators for a given attenuation setting. The signal conditioning programmable gain amplifiers are not capable of providing all possible gains. This is due to the topology of the variable gain blocks each of which consisted of an operational amplifier with a digitally programmable resistor in the feedback path. The desired gain is set using the data acquisition program and the nearest possible gain which does not exceed the desired gain is programmed. The gain programmed in response to a desired gain will be different for the different channels. The relative gains of the sounder channels were therefore measured shortly after measurements had been made, when the attenuation and gain settings were known.

The relative gains were measured by inputting equal power signals to the eight antenna connectors and recording the channel outputs using the data acquisition system. In this way the whole of each sounder channel was subject to measurement and the errors and tolerances of all parts of the sounder could be taken into account. Figure 6.1 shows the arrangement used for these relative gain measurements.

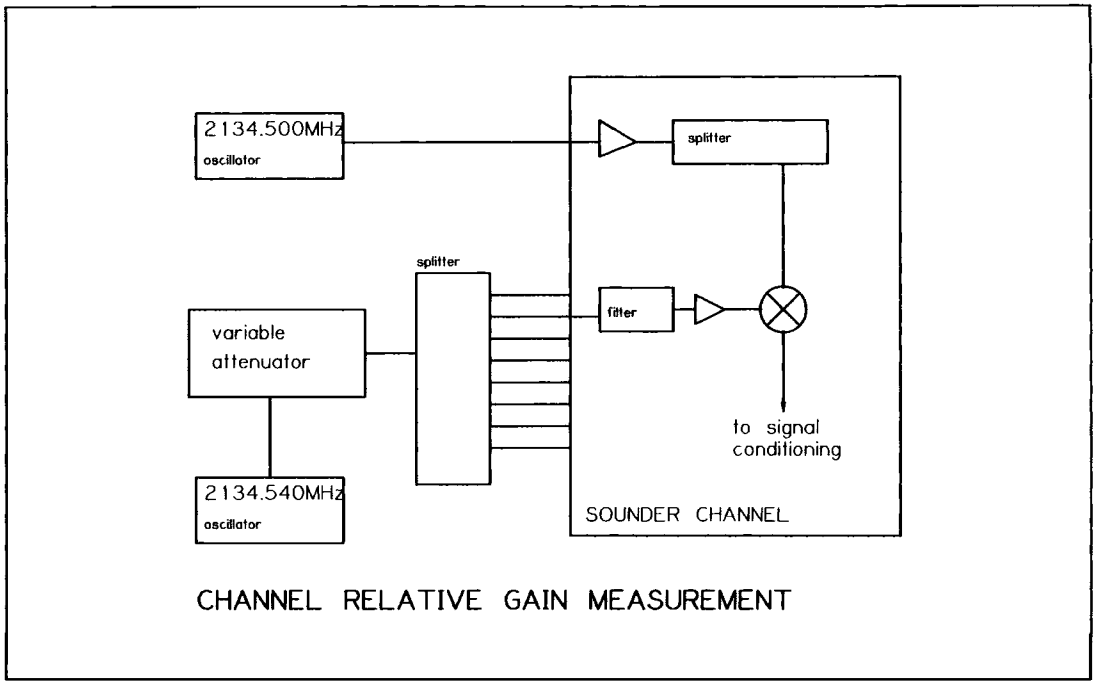

Figure 6.1 Arrangement used for channel relative gain measurements.

As shown in figure 6.1, two oscillators are used, one as local oscillator and the other as RF signal source. These oscillators were commercial phase locked cavity oscillators with crystal controlled reference. They were tuned to frequencies that were well within the sounder operating bandwidth and differed by a frequency which was well within the passband of the signal conditioning filters. They had phase noise of -60 dBc at 100 Hz separation from carrier and their use was unlikely to result in spurious signals which upset the gain measurements.

The sounder was set up as in figure 6.1 and the data acquisition software used first to autoadjust the channel gains and then to set the gains and RF attenuation manually. The RF attenuation and gains to be set were extracted from the header of the field measurements file (see Appendix 1). The variable attenuator was adjusted so that the voltages from the signal conditioning unit were within the input range of the data acquisition system. The analogue to digital converters (ADC) in the data acquisition system have an input range of +/- 1.25 V. Allowing a small margin for noise, the variable attenuator was adjusted until the signal level from the channel with the strongest signal did not exceed +/- 1.0 V. The data

analysed to extract the envelopes of the recorded signals. From the envelopes the mean peak to peak voltage from each channel was estimated. Since all channels had the same signal level at their inputs the channel gain was directly proportional to the peak to peak voltage output. The software used to estimate the channel gains from the recorded data normalises the gains using the minimum gain as datum and writes the result to a file which may be used when postprocessing the data from the field measurements.

6.3 Antenna Characterisation

Although estimating the direction of arrival of the various multipath components was not an objective of this project the eight channel sounder provided the opportunity to compare the multipath components arriving from different directions when using a multi-element antenna system. A system consisting of a circular array of six directional antennas and an omnidirectional antenna was constructed early in the project and this was used for measurements in Manchester. Later an array of eight directional elements became available. Since any attempt to measure arrivals from different directions would depend on a knowledge of the radiation pattern of the antenna in use it was necessary to characterise each antenna array. An antenna test range would normally be used for this purpose but no suitable range was available. A portable antenna characterisation rig was designed and constructed.

6.3.1 Antenna Characterisation Rig

The objective of building the antenna characterisation rig was to produce a device which could be easily transported to a large open space or to a rooftop and be used to rotate an antenna system in a controlled manner. It was not expected that the accuracy or resolution of a professional test range could be achieved and with very little money available to buy parts a somewhat relaxed specification was decided. Initially the test rig was to be able to rotate a small antenna array through a complete circle in 5 degree steps and using simple receivers record the response of up to eight elements.

The dynamic range was to be 50 dB and the minimum detectable signal to be –60 dBm. Only the amplitude response was to be recorded. The operating frequency of the rig was to be limited to the 2 GHz band.

Using parts recovered from other projects it was possible to build eight logarithmic receivers which had 55 dB dynamic range and a minimum detectable signal of -65 dBm.

The turntable on which the antenna system to be measured was mounted was made from a wheel hub from a scrapped motor. The fixed part of the hub was machined so that it had a flat surface perpendicular to the axis of rotation and this part was bolted to a 6 mm light alloy plate which formed the baseplate of the unit. The rotating part of the hub was machined so that a collar could be fitted and a collar was manufactured from an offcut of 12 mm light alloy plate. Various spur gears were available from the authors junk box and a reduction gearbox was constructed using these. A small stepper motor and drive electronics were purchased and used to drive the turntable via the reduction gearbox. The gear ratio was such that 159 steps of the stepper motor rotated the turntable through 5°. A rectangular sheet aluminium box was fabricated and mounted on the turntable for housing for the receivers. The antenna array was mounted on the top of the box.

An old PC and data acquisition card were used to control the turntable and record the output from the receivers. The moment of inertia of the turntable with the antenna system mounted was significant and had to be taken into account when writing the turntable control software. The maximum stepping rate was determined experimentally by varying the programmed delay between stepping pulses. Since the overall structure was not perfectly rigid and anti-backlash gearing was not used in the gearbox some time had to be allowed for it to stabilise after a rotation and before making a measurement. High speed data acquisition was therefore unnecessary so a

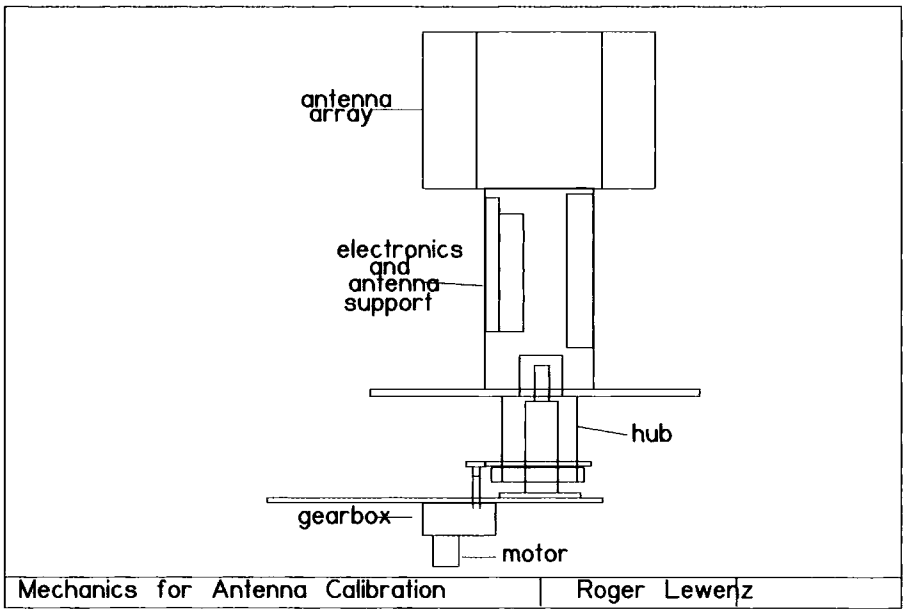

Figure 6.2 The mechanical arrangement of the calibration rig turntable

Figure 6.2 shows the mechanical arrangement of the calibration rig turntable. The baseplate consisted of a 300 mm square, 6 mm thick aluminium plate and this was bolted to a speedframe stand 2 m high. The whole rig weighs approximately 20 kg and may be carried by one person. By removing the turntable and disassembling the stand the rig may be stowed in a medium sized motor car for transport.

The electronics of the calibration rig consists of eight receivers and the stepper motor controller. Figure 6.3 shows a block diagram of the receivers.

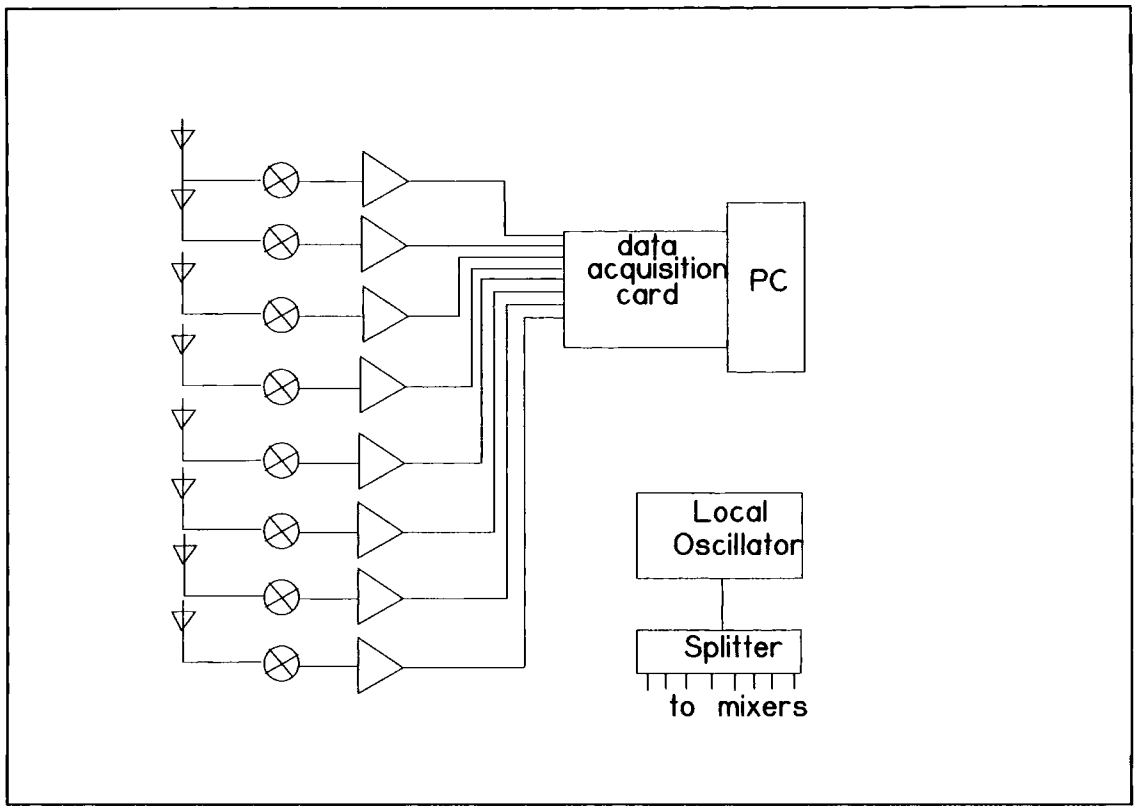

Figure 6.3 Block diagram of the calibration rig receivers

Each receiver channel consists of a mixer and logarithmic IF amplifier. Pre-mixer amplification was not considered necessary since the antenna array under test would be illuminated by a transmitter close by. The local oscillator consisted of a 2 GHz phase locked loop, identical to those used in the sounder, and an amplifier. The phase locked loop was locked to a 10 MHz crystal oscillator. The output from the amplifier was split eight ways to provide +7 dBm for each mixer. The mixers, amplifier and splitter were connectorised parts so that rapid reconfiguration could be accomplished if necessary. The local oscillator frequency was offset by 70 MHz from that of the illuminating transmitter. Both local oscillator and transmitter frequencies could be programmed by switches to cover frequencies from 1.9 GHz to 2.8 GHz in 10 MHz steps so that radiation patterns at different frequencies could be recorded. The logarithmic amplifiers were made in-house using Plessey SL523 integrated circuits. These amplifiers were of the successive detection type and produced a DC voltage proportional to the logarithm of the input power. (The successive detection type of amplifier has a number of stages, each with an RF input, an RF output and a detected output. The detected output is a dc current

which is approximately proportional to the logarithm of the RF input. The amplifier is designed to operate in both the linear and the saturated mode. Using a number of stages the amplifier stages are allowed to saturate as the RF input increases and the sum of the detected output from all stages is summed.) Figure 6.4 shows the circuit diagram of the logarithmic amplifiers which were constructed on printed circuit boards and housed in individual tin plate boxes. (Note that the inputs marked "–" are bias points, not real inputs and need not be connected except for the first stage. The unconnected output from the final stage is the RF output and is not required.

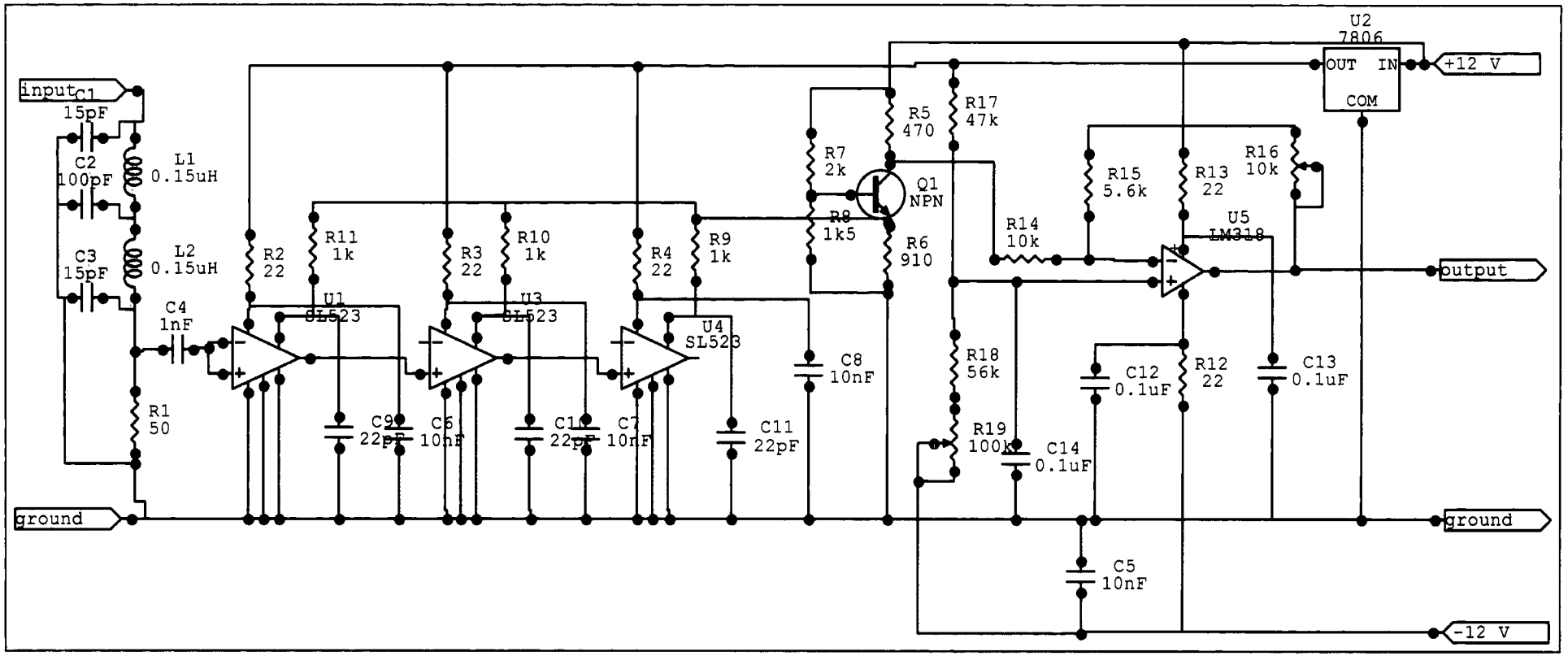

Figure 6.4 Circuit diagram of one of the logarithmic amplifiers.

The transmitter used to illuminate the antenna array under test consisted of a phase locked loop with 10 MHz reference oscillator as in the receiver and a power amplifier. The power amplifier could produce up to +26 dBm at the input of the illuminating antenna. Both the transmitter and the illuminating antenna were mounted on a tripod so that the antenna was 2 m above the ground. The illuminating antenna was positioned 3 m from the test rig to ensure that all interactions with the antennas were in their far fields (The far field was assumed to start at 10 wavelengths from the antenna phase centre. At 2 GHz the wavelength is 0.15 m.)

Both transmitter and calibration rig were powered from 24 V DC so that mains power was not required. Four 85 Ah lead-acid batteries were used and allowed more than 8 hours of continuous operation.

A PC was used for control of the turntable rotation and datalogging. A data acquisition card was fitted into the PC. This data acquisition card had eight analogue input channels, each with 12 bit resolution. The eight channels are implemented using a single analogue to digital converter and switches. This means that the eight channels are sampled in rotation rather than concurrently. The analogue to digital converter is capable of performing one conversion every 5 microseconds so all eight channels are sampled in 40 microseconds. Since the antenna under test is held stationary while the receiver outputs are sampled the small time difference was not considered important.

In addition to the eight analogue input channels the data acquisition card had 24 digital input/output lines, each capable of driving a standard TTL load. The stepper motor which rotated the turntable was driven by a matching controller. This controller required two high level logic inputs, one to control the direction of the motor and the other to cause the motor to rotate by one step. A level converter was constructed from open collector TTL logic to translate the TTL outputs from the data acquisition card into high level logic levels required by the motor controller. The digital

stepper motor rotate the turntable through 360 degrees in 5 degree increments. After each increment a short delay was allowed for the moving parts to stabilise and the eight receiver channels were sampled.

The eight receivers were calibrated using the illuminating test transmitter and attenuators to provide known input power levels to the receivers and recording the receiver output using the data acquisition card in the PC. A table showing the receiver output for input power levels from -80 dBm to -5 dBm for each receiver was generated and written to a calibration file. This calibration file was read by the program used for antenna characterisation.

6.3.2 Datalogging and Software

The basic routines performed by the data logging software are as follows:

- Read the calibration file.
- Set the list of channels to be sampled.
- Set the direction digital output (left rotation or right rotation).
- Do 72 times (72 steps of 5 degrees):

    Do 159 times (for a 5 degree rotation):

        Set the step digital output.

        Delay to allow the motor to respond.

        Reset the step digital output.

        Delay to allow the motor to respond.

    Delay to allow the moving parts to stabilise.

    Do 21 times:

        Sample each channel and store the result.

    Find the median value of the samples for each channel.

    Using the calibration data convert each channel median value into dBm

- Open the output file.
- Write the 8 channel values for each step to the output file.
- Close the output file.
- Terminate.

The data acquisition card did not have any drivers but did have a manual which described the architecture. It was therefore decided that the software would address the data acquisition card hardware direct. This placed constraints on the operating system which could be used since most of the 32 bit systems did not allow direct access to hardware. The first versions of the programs were written in C under MS-DOS and compiled with the Zortech version 1 C compiler. These programs were run on a 80286 based PC and proved that software control and data acquisition were possible. Later versions were written and compiled using Borland Delphi version 1 (16 bit version) to provide a Windows user interface. These programs were run on a 100 MHz Pentium PC running Windows 95. Windows 95 allows direct access to the hardware while providing a Windows user interface and proved to be satisfactory platform with two exceptions which could be worked around. The first problem concerns power saving modes. When power saving was enabled Windows was likely to switch the PC into power saving mode during the rotation of the turntable and the data acquisition software would be suspended. Power saving had to be disabled. The second problem concerns the processing of Windows messages. It was found that Windows 95 did not regularly process all of the messages in the queue and this could cause a program to hang. To work around this it was only necessary to generate another message and this could be done by clicking a mouse button to cause a change of state of the desktop.

6.3.3 Characterising an Antenna

To characterise an antenna it was necessary to find a location where there would not be any spurious signals which might be interpreted as part of the antenna pattern. The most likely source of interfering signals was reflections from objects near to the calibration rig or the illuminating transmitter. Figure 6.5 shows a worst case scenario in which there is a large perfectly reflecting object 200 m from the calibration rig. In this scenario the direct path from the illuminating transmitter to the calibration rig has a path loss of 48 dB. A signal reflected from the object will have a path length of 400 m and a path loss of 90.5 dB. The reflected signal will be 42.5 dB weaker than the direct signal and should not contaminate the

measured radiation pattern. In practice reflecting objects will have reflection coefficients much less than unity. The illuminating transmitter had a directional antenna with a beamwidth of 60° in both azimuth and elevation and a front to back ratio of 20 dB. It was only necessary to ensure that there were no reflecting objects within 30° of the boresight direction of the illuminating antenna.

In Manchester antenna calibration was conducted on the roof of the UMIST Main Building. With the illuminating antenna pointing East there were no reflecting objects within 200 m. In Durham antenna calibration was conducted on the roof of the School of Engineering with the illuminating antenna pointing North. With this arrangement there were no reflecting objects within 500 m.

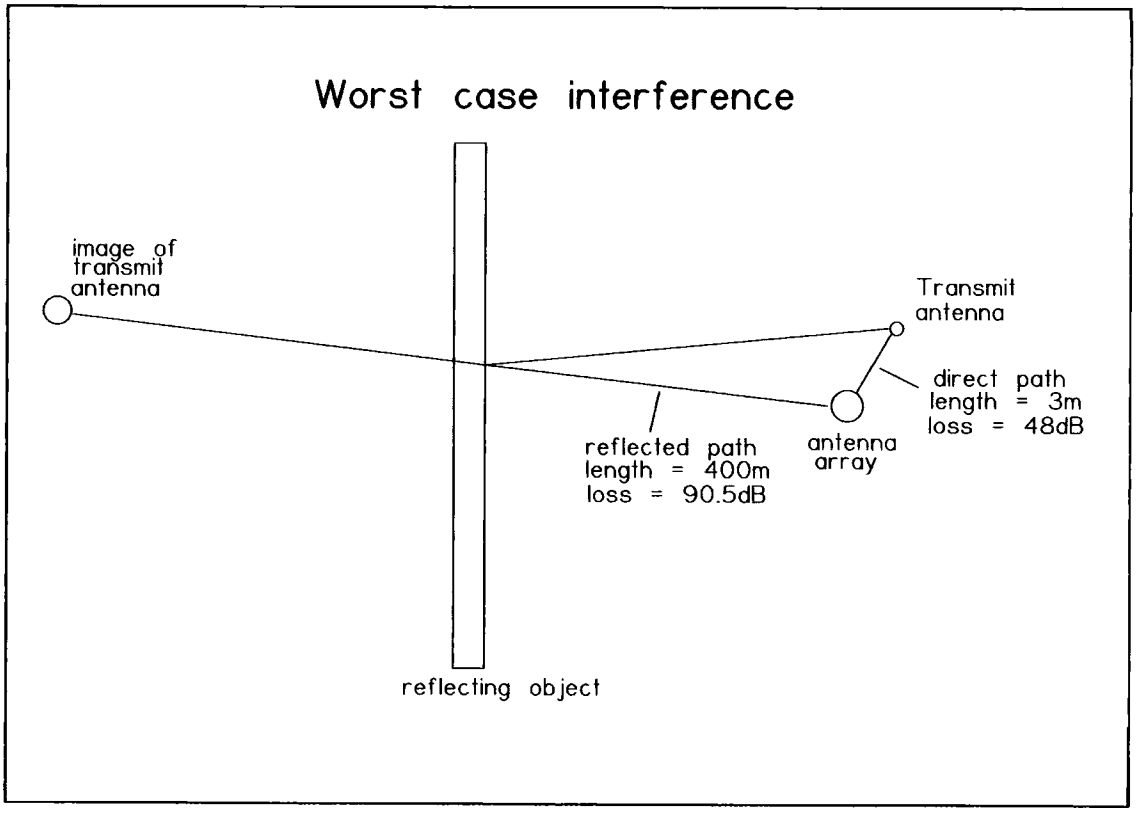

Figure 6.5. Worst case interference

The results from characterising the antennas used for the measurements are described in M Abdalla's thesis [43].

CHAPTER 7 SOUNDER DATA ACQUISITION

7.1 INTRODUCTION

At the start of the project the data acquisition system consisted of a Personal Computer (PC) in which was installed an eight channel data acquisition card. The data acquisition card was developed and constructed by Dr I Hawkins of the Solid State Systems Group at UMIST. This card had a separate 8 bit Analogue to digital converter for each channel, 128 Mbytes of memory and some timing and control logic. The timing and control logic ensured that the correct number of samples were taken for each sweep at the correct sampling rate and that sampling started at the beginning of each sweep. The timing and control logic was implemented in field programmable logic devices and the card was constructed on a PC ISA bus prototype card using the wire-wrap technique.

A data acquisition program was written by Dr P Philippidis [41] who was a student at the time. This program controls a number of sounder functions, sets up the data acquisition card, initiates the sampling of the data and saves the sampled data to a file on disk. The format of the file on disk is described in Appendix 1. The program was written in Microsoft Visual Basic 5 under Windows 95 and used a number of OCX controls. A separate program written by Dr I Hawkins provided the functions of a card driver thus allowing the data acquisition program to communicate with the card. Communication with the sounder was via the parallel port of the PC using a protocol which is described as far as is possible in Appendix 2.

7.2 SHORTCOMINGS

There are a number of shortcomings of the current data acquisition system, some concerning performance and some concerning future development.

7.2.1 Performance

The current data acquisition system will reliably sample sounder data at 1 Msample/sec for up to 15 seconds. There is a limit on the duration of the sampling time which is imposed by the size of the memory on the data acquisition card. Two sampling rates appear to be possible: 1 Msample/sec

and 500 ksample/sec. When the samples are written to file a file header records the number of sweeps recorded and the number of samples per sweep. When the 1 Msample/sec rate is used the header is correct but when the 500 ksample/sec rate is used the header records half of the number of sweeps recorded and twice the number of samples per sweep. It is therefore impossible to determine from the header which sampling rate was used. Although when using the 500 ksample/sec rate it would be possible to sample for 30 seconds this sampling rate was never used due to the unreliability of the file header.

The second performance issue concerns the time taken to save the sampled data to file. The program took more than one hour to save the samples from a 15 second measurement. A number of modifications to the data acquisition program were tried but it proved impossible to reduce the save time. It appears that the slow transfer rate from card memory to disk is a feature of Visual Basic running under Windows 95.

7.2.2 Development

After the move of the work from UMIST to University of Durham further development of the data acquisition program became impossible. Microsoft have stopped supporting Visual Basic 5 and this software is no longer available. University of Durham has Visual Basic 6 but this has no support for OCX controls. Any further development using the current data acquisition card would require a complete redesign and implementation of the data acquisition software. Since the data acquisition card is a prototype and without support reliance on this card in the long term would be inadvisable.

7.3 NEW DATA ACQUISITION SYSTEM

Rather than relying on in-house developed data acquisition hardware it was decided to purchase commercial data acquisition cards which would come with support.

implementing a consistent programming interface for all Measurement Computing cards. Each of these cards has 4 analogue input channels, two analogue output channels and 24 lines of digital I/O. Each analogue input channel has a 12 bit analogue to digital converter with a maximum sampling rate of 20 Msamples/sec. The card has a first-in-first-out (FIFO) memory which buffers the data between card and PC memory. A number of clock options are provided including an internal clock, external clock input and external clock gating input. An installation and configuration program: INSTACAL is provided and this allows assignment of clock inputs to pins and connectors.

Physically the card is a 2/3 length card which plugs into the PC's PCI bus. On the back panel are 5 BNC sockets of which four are the analogue inputs. The fifth socket may be assigned to external clock input or external clock gating input. At the forward end of the card is a 40 pin header providing connection to the digital I/O lines, the analogue outputs and a number of timing functions.

The Universal Library provides functions to configure the card. The analogue input range can be set. The digital I/O lines can be configured as input or output and a number of timing functions can be configured. The Universal Library also provides functions to sample analogue data and to send or receive data via the digital I/O lines. Using the Universal Library there is never any need to address the card hardware directly.

7.3.2 Operating System and Programming Environment

While using the current data acquisition system it has been found that the program becomes unresponsive sometimes. This appears to be caused by Windows 95 failing to process its message queue at appropriate times. Since Windows 95 is no longer supported it was decided to use Windows NT4 as an operating system. Previous experience with Windows 95 also suggests that an artificial limit is placed on the amount of memory that can be dynamically allocated. This limit is not present with Windows NT4. There is no reason to suppose that the card and software will not work with

Windows 2000 or Windows XP but these operating systems have been rejected in the first instance because both run many processes which are not required and which are difficult to disable. The PC on which the software has been developed has a Pentium 3 processor running at a clock speed of 750MHz and 1 Gbyte of memory.

Rather than continuing to use Microsoft Visual Basic with its known shortcomings it was decided to use Borland Delphi for programming. This is a 32 bit programming environment which will run under any of the 32 bit Microsoft operating systems. It also has the advantage that there is a version: KYLIX which runs under Linux thus providing some portability of code if it were decided not to use a Microsoft operating system. A further advantage of Delphi is that it has a ready made chart object so that programming to display results is minimal. The language underlying Delphi is Pascal with extensions to make Object Oriented Programming possible. Borland C++ Builder was considered but this product does not have the chart object and so would have required additional programming.

7.3.3 Limitations Discovered During Development

The new data acquisition software causes the card to take samples of the analogue inputs and store these in PC memory. When a large number of samples is to be taken at high sample rates it is necessary to allocate a block of contiguous memory in which to store the samples. The INSTACAL program allows the allocation of contiguous memory and reports the number of samples it is possible to store. It was found that there was a limit on the size of contiguous memory that INSTACAL will allocate. This limit was 64 Mbytes irrespective of how much real memory was installed in the PC. If an attempt was made to allocate more than 64 Mbyte the size of contiguous memory was silently reduced to zero. This appears to be an undocumented feature of INSTACAL as supplied with the Universal Library Version 5.24. When notified of this problem Measurement Computing supplied Universal Library Version 5.56b with a later version of INSTACAL. With this version of the Universal Library it was found possible to allocate more memory but there was still a limit of approximately 120 Mbytes, the exact limit being

different on different PCs. Having successfully allocated contiguous memory INSTACAL reports the number of samples that may be stored. The number of samples reported is actually twice the number of samples that can be stored and any attempt to store more than half the reported number of samples results in a runtime error.

When sampling four channels using an external clock, one channel is sampled on each clock pulse. It is therefore necessary to provide a clock which is four times the sampling rate required for sampling all four channels. This also means that channels will be sampled at slightly different times.

7.3.4 Limitations Imposed by the Sounder

It was discovered late in the data acquisition system development that there is not an integral number of clock pulses output by the sounder between each Start of Sweep (SRF) pulse. The use of the SRF pulse to gate the clock from the sounder was therefore abandoned. The sounder produces a REAL CLOCK output in which the correct number of clock pulses between SRF pulses is output. Unfortunately this output assumes simultaneous sampling of all channels at each clock pulse so it is incompatible with the new data acquisition cards. It was therefore decided to develop additional logic which would meter the correct number of clock pulses between SRF pulses to the data acquisition card external clock inputs.

7.4 NEW DATA ACQUISITION SYSTEM

7.4.1 General Idea

The new data acquisition system will consist of some additional logic and a program to run on the PC which controls both the sounder, the additional logic and the data acquisition cards. It was intended that two of the new data acquisition cards should be used to provide eight channels of data acquisition. Using the functions in the Universal Library it is possible to use two cards simultaneously provided that at least one of them runs in the background. If an external clock is used this is feasible since both cards can be set up and armed and acquisition will start when the external clock

delivered to both cards starting at a start of sweep pulse so both cards sample in synchronism.

7.4.2 Limitations

According to the technical manual which was supplied with the cards each 12 bit sample is stored in a 16 bit word in memory. If 120 Mbytes of contiguous memory is allocated there should be space for 60,000,000 samples. When using eight channels there should be space for 7,500,000 samples per channel. In practice it was found that only half this number i.e. (3,750,000) samples per channel could be saved. At a sampling rate of 1.25 Msamples/sec this allows measurement for 3 seconds. At a sample rate of 625,000 samples/sec measurements for 6 seconds would be possible.

7.4.3 The Additional Logic

A functional diagram of the additional logic is shown in figure 7.1.
The 74161 counter divides the 10 MHz input clock to 5 MHz for a 1.25 MHz sampling rate, 2 MHz for a 500 kHz sampling rate or 1 MHz for a 250 kHz sampling rate. A 10 MHz clock is produced by gating the 10 MHz input round the 74161 counter.

This clock is used to drive a set of 4 74191 down counters which are programmed to reset after the appropriate number of samples depending on the sampling rate.

The SRF input initiates the sample counter and the terminal count from this counter inhibits further counting.

The programming values for the clock rate counter and the sample counter are latched by the 74573s. A 74138 is used as an address decoder so that the interface to this circuit is 8 data lines and 3 address lines. This will allow the circuit to be addressed either by the new data acquisition cards or via the parallel port in the traditional way. The addresses of the latches have been set to 12, 13 and 14 which are the three unused opcode values in the sounder control protocol. This additional logic could be integrated into the sounder to become an alternative REAL CLOCK source.

A switch will be installed on the front of the PC to provide an INHIBIT signal so that clock pulses will be inhibited while both cards are set up and armed.

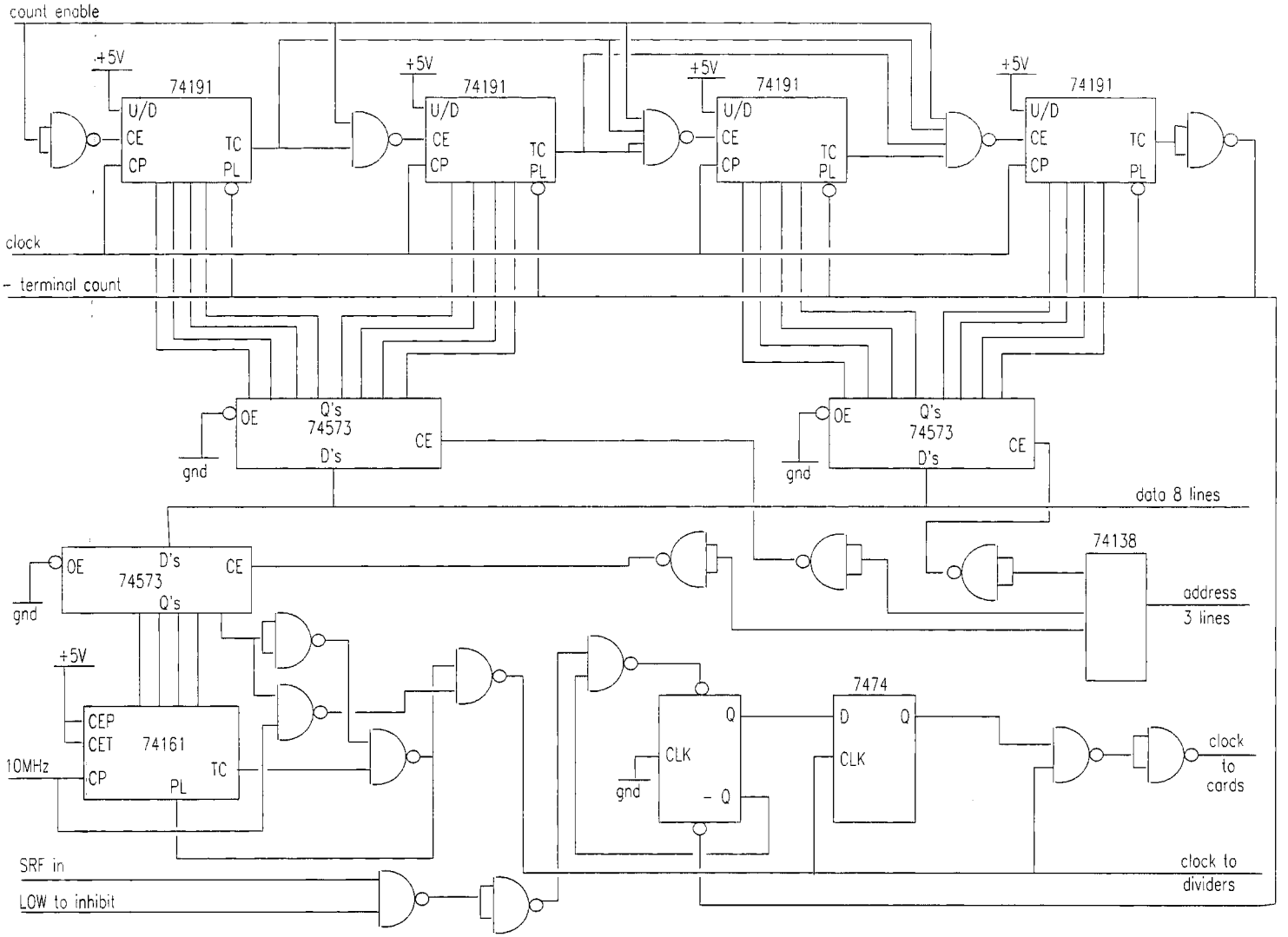

Figure 7.1.. Additional Logic for the New Data Acquisition System

The additional logic was constructed on strip board attached to an aluminium panel which fitted into a full length card slot on the PC. Power is derived from the data acquisition card which programs the latches. All of the devices used in the additional logic were from the 74HCT family since these will operate at the necessary speed while consuming less power than standard 74 series devices.

7.4.4 Testing

Because the discovery that there is not an integral number of clock pulses between SRF pulses came very late the additional logic had to be designed and constructed very quickly. If it had worked first time then it would have been adopted and now working. During testing it became clear that there was a fault, probably caused by trying to build it too quickly. Since any further testing and remedial work would leave an unacceptably short time for writing this thesis it was decided to abandon the new data acquisition in its eight channel form. A much simpler system using a single data acquisition card and providing three channel data acquisition was implemented.

7.5 SIMPLE DATA ACQUISITION

7.5.1 General Idea

Rather than metering the number of clock pulses the simple data acquisition system routes the SRF pulse to one channel on the data acquisition card and detects the start of sweep in software. Having detected the start of sweep the required number of samples are stored and any additional samples before the next start of sweep pulse discarded. The clock rate to the card is derived from a simple divide by 2 and divide by 4 circuit with the clock rate being selected by changing cables at the rear of the PC. The clock divider consists of a 74HCT74 dual D-type flip-flop and a 74HCT04 hex inverter as a buffer. The circuit has been constructed on strip board and fits into one card slot in the PC, deriving power from the data acquisition card.

This idea could be extended to use two data acquisition cards providing seven channels. Since each card needs to be armed separately it would be

necessary to have a manual switch to inhibit the external clock signal to the cards until both were armed.

7.5.2 Sounder Control

The present data acquisition system controls the sounder via the PC parallel port. This method of connecting the sounder to the PC has been in use for a long time and has worked well. Future PCs may not have a parallel port since printers are now usually provided with only a USB interface. It was decided to connect the sounder to the PC using the digital I/O lines of the data acquisition card. It is not necessary to mimic the parallel port exactly since the sounder only requires an interface with 8 data lines and 4 address lines. Using the digital I/O lines of a single data acquisition card and functions in the Universal Library it has been possible to implement the sounder control protocol. This protocol is described in Appendix 2.

7.5.3 The Data Acquisition Software

The sounder control part of the data acquisition software is not described here since it is straightforward and longwinded. The data acquisition functions are described in outline in the following figures. Since this is event driven software the top level diagram uses the Service Description Language (SDL) notation. The whole of the source code for the program is contained in the CDROM at the rear of this thesis.

The input events which cause a transition from the WAITING state represent the effect of clicking on the buttons of the screen presented by the program. Clicking a button causes the execution of a number of subroutines followed by a return to the WAITING state.

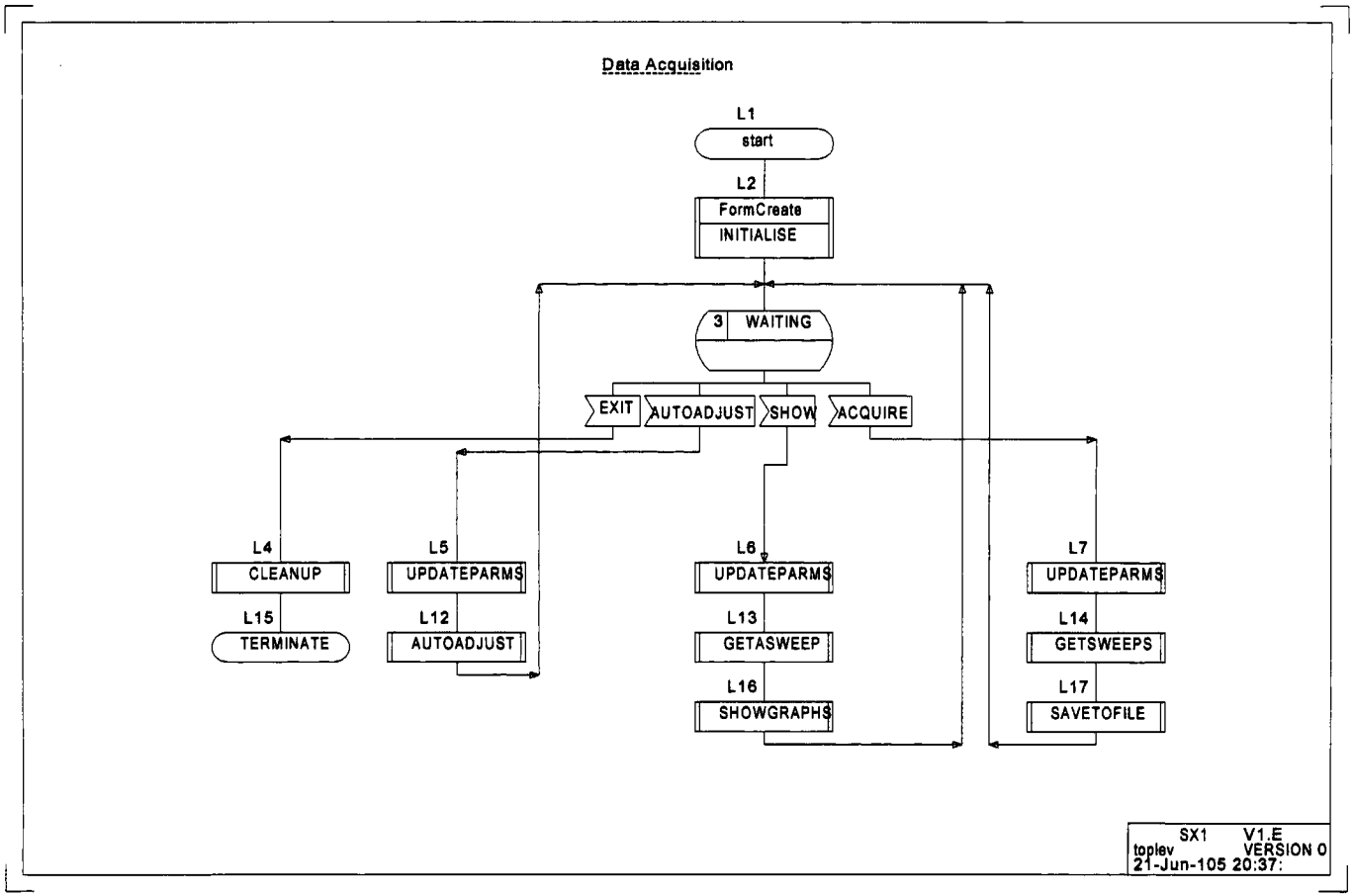

Figure 7.2. Top level Data Acquisition Program

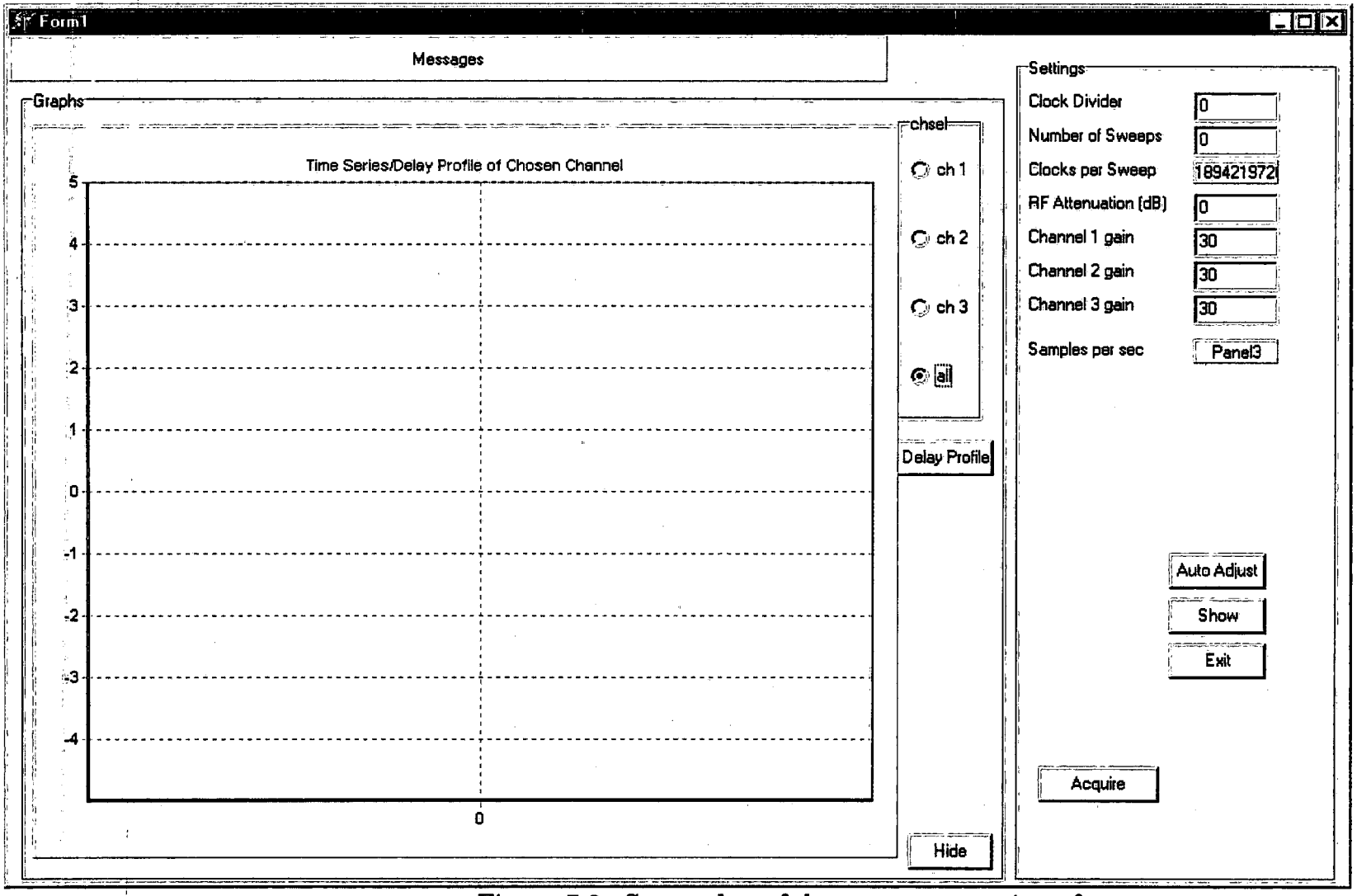

Figure 7.3. Screenshot of the program user interface.

The right hand part of the screen contains input boxes for the parameters used during data acquisition and four buttons which initiate the data acquisition functions.

The EXIT button causes termination of the program. If an output file is open it will be closed.

The SHOW button acquires data for one sweep and displays it on the right hand part of the screen. The parameters in the RF Attenuation and gain input boxes are used unchanged.

The AUTOADJUST button causes the RF attenuation and channel gains to be adjusted so that the signal to be sampled best fits the range of the data acquisition card. This is an iterative process with the new values of RF attenuation and gains shown in their respective input boxes.

The ACQUIRE button initiates the acquisition of the number of sweeps set in the "Number of sweeps" input box and the saving of the data to a file. The user is presented with a dialogue allowing specification of the location and name of the output file.

The left hand part of the screen allows display of the data and has buttons which control the display options. The small round buttons allow the user to specify which channels are displayed. The upper rectangular button switches between time series data and power delay profile.

The HIDE button does nothing at present.

Referring to figure 7.2 it can be seen that an UPDATEPARMS procedure is executed as part of the SHOW, AUTOADJUST and ACQUIRE functions. This procedure checks to see if the user has altered any of the parameters in the input boxes and updates the program internal data structures accordingly. The logic of this procedure is shown as a flowchart in Figure 7.4 below.

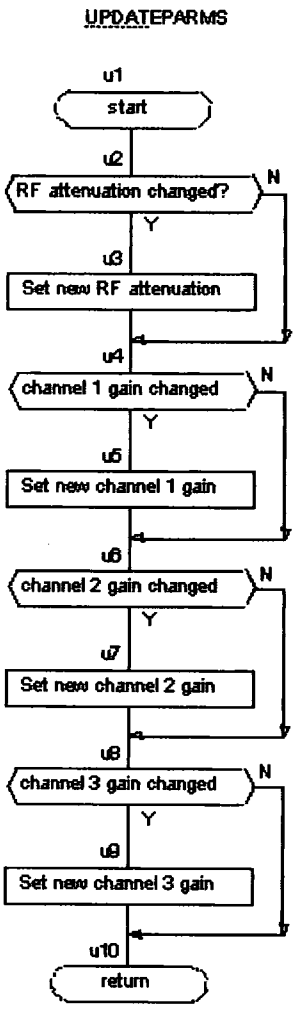

Figure 7.4. Logic of the UPDATEPARMS procedure.

The logic of the AUTOADJUST procedure is shown in figure 7.5 below.

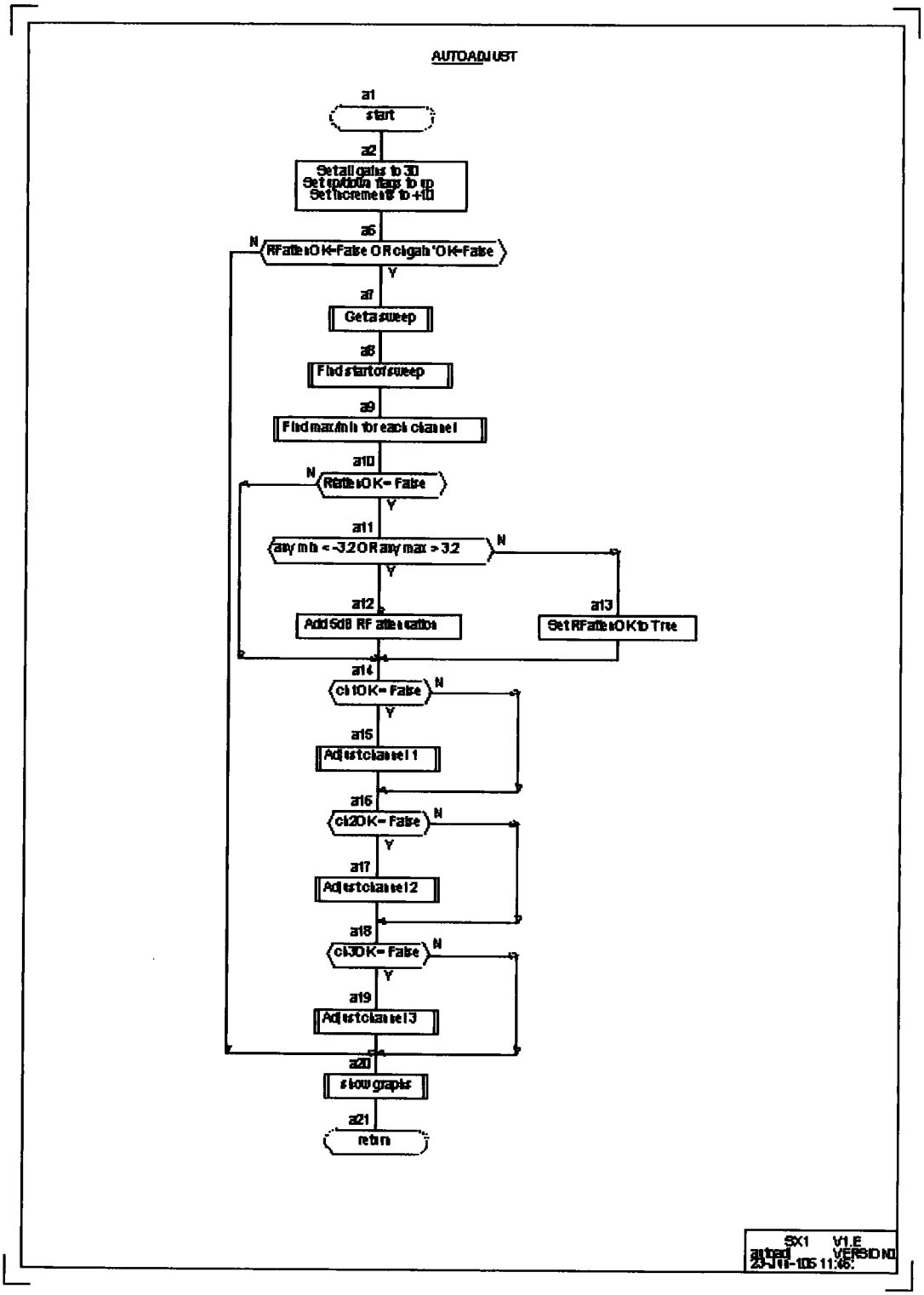

Figure 7.5. Logic of the AUTOADJUST procedure

The AUTOADJUST procedure sets flags, one for the RF attenuation and one for each channel gain, which are used to indicate whether further

adjustment is necessary. When all the flags indicate that no further adjustment is necessary the procedure is complete.

Initially all channel gains are set to a value of 30 which is at the low end of the useful range of values and the RF attenuation is set to 0dB. If the signal is too large RF attenuation is increased in 5dB steps until the signal amplitude is lower than the value which would cause overloading. No attempt is ever made to reduce the RF attenuation.

When the RF attenuation has been adjusted the channel gains are adjusted until each channel output is within the useful range of the data acquisition card.

The useful range of the data acquisition card and the overloading level are specified as follows. The analogue inputs of the data acquisition card are programmed to have a voltage range from -5V to +5V. Any voltage outside these limits would cause overloading of the A/D converters in the data acquisition card. The sounder signal conditioning circuits which include a programmable gain block and some active filters, have been built using the National Semiconductor CLC428 device. This is a high bandwidth low noise operational amplifier which operates with -5V and +5V power supplies. According o the CLC428 data sheet the amplifier is capable of producing an output swing between -3.8V and +3.8V when driving a high impedance load. This limited output voltage capability of the signal conditioning circuits means that the analogue inputs of the data acquisition card will never be overloaded. The load seen by the output of the signal conditioning circuits is the 1 MΩ input resistance of the data acquisition card plus approximately 100 pF capacitance imposed by the data acquisition card and the connecting cable. It was decided that any voltage outside the range -3.2 V to +3.2 V would be considered too large and adjustment would be required to reduce it. To make best use of the data acquisition card analogue input range the input voltage should be as large as possible without overloading. It was decided to make the minimum voltage target -0.8 V to +0.8 V.

There two other properties of the input voltage to take into account. There is a small negative DC bias on the input voltage so all comparisons of the input voltage with the target values consider only the negative going

have an amplitude much greater than the maximum amplitude for the remainder of the sweep. This appears to be caused by the combination of a very fast change of frequency at the Local Oscillator input to the RF mixers in the sounder and the inductive components of the mixers. So that these transients do not cause erroneous adjustment of the RF attenuation or gains, the first 100 samples of the sweep are ignored.

When adjusting the channel gains a direction flag indicates whether the gain has been increased or decreased. This flag is initially set to UP (gain to be increased). The increment by which the gain is changed is initially set to 10. If the direction of adjustment changes the size of the increment is halved so that the adjustment will converge when the increment has decreased to 1.

The channel gain is controlled by two digital potentiometers in the feedback path of the operational amplifiers which form the programmable gain block. The values to which these digital potentiometers should be set for a particular gain are derived from a lookup table produced when the signal conditioning circuits were calibrated by P Filippidis. The gain units are pseudo-logarithmic. True logarithmic units could not be achieved due to the programmable gain block circuitry. The logic of the gain adjustment routine for channel 1 is shown in figure 7.6 below. Similar routines are used for the other channels.

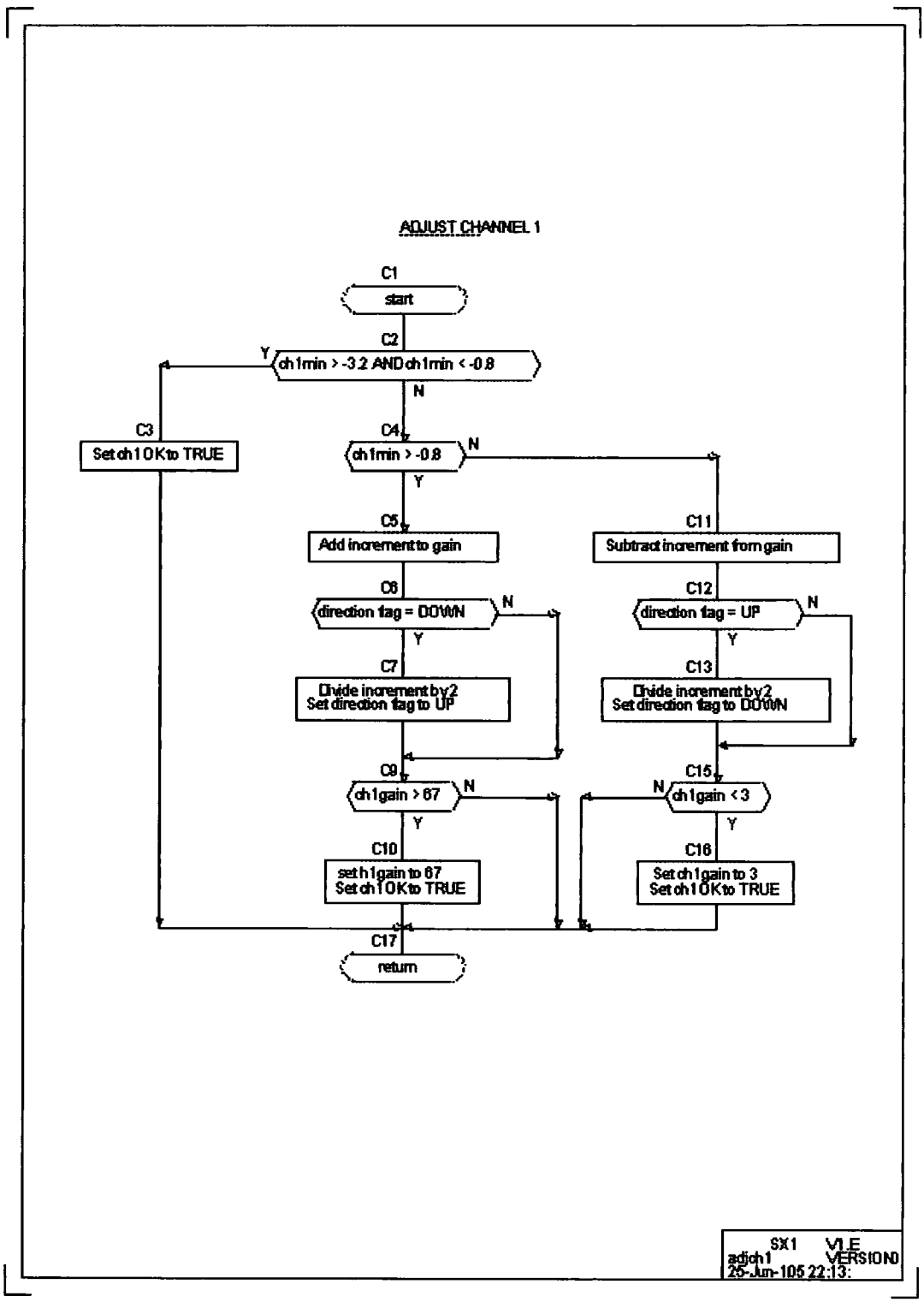

Figure 7.6. Logic of the channel gain adjustment routine.

Acquiring data in procedures GETASWEEP and GETSWEEPS is achieved by the following actions.

1. Calculate the amount of memory required to store all the samples to be collected.
2. Allocate the memory as a Windows buffer and lock the buffer to a pointer.
3. Set the number of samples and sample rate in program variables.
4. Arm the data acquisition card.
5. The card will sample the analogue input channels as soon as it is supplied with clock pulses and will continue until the specified number of samples has been taken. The card is operated in a foreground process so the program loses control and waits until the card has finished sampling.
6. At completion of sampling the sample data will be in the allocated memory and may be accessed by reference to the pointer to which the memory has been locked. The data may be used for display in the graphs, autoadjustment of the gains or saved to disk.
7. After the sample data has been used the memory is unlocked and de-allocated.

Because the sampling does not start at a start of sweep enough samples must be taken to ensure that, once the start of sweep has been detected, there will be enough succeeding samples from which a complete sweep can be extracted. When acquiring a single sweep (GETASWEEP) for display or autoadjustment, enough samples for two sweeps are collected. When acquiring samples to be saved to disk enough samples for 10 additional sweeps are collected.

The fourth analogue input to the data acquisition card is connected to the start of sweep pulse output from the sounder. This is a TTL signal and the transition from LOW to HIGH is detected by the program. The output values from the card take the value 0 for a -5 V input, 2048 for a 0 V input and 4095 for a +5 V input. For a TTL LOW input voltage of +0.8 V the card value will be 2375. For a TTL HIGH input of +2.4 V the card value will be 3031. The program uses a threshold value of 3000 to decide whether the start of sweep signal is LOW or HIGH. When accessing the sampled data by reference to the memory pointer the data may be considered to be

start of sweep signal first exceeds the 3000 threshold is considered to be the index of the first sample of the sweep data.

No logic diagrams of the procedures for acquiring data or detecting the start of sweep are presented since they are straightforward and may be understood from the program code.

7.5.4 Connections to data Acquisition

Figure 7.7 shows the data acquisition circuits as seen from the rear of the PC. Immediately to the left of the data acquisition card is a panel with two D type connectors. The 25 way connector is used instead of the PC parallel port for communications with the sounder. The pins of this connector are routed to the 40 pin header at the rear of the data acquisition card. The 9 way D type connector is not used.

To the left of the sounder connection panel is the clock divider. The 10 MHz clock from the sounder is connected to the SMC connector at the top of the panel. The two BNC connectors provide the divided clock for the data acquisition card. The EXT CLOCK input of the data acquisition card should be connected to the upper BNC connector on the clock divider for a 5 MHz clock rate (1.25 Msamples/sec). For a 2.5 MHz clock rate (625 ksamples/sec) the EXT CLOCK input of the data acquisition card is connected to the lower BNC connector on the clock divider.

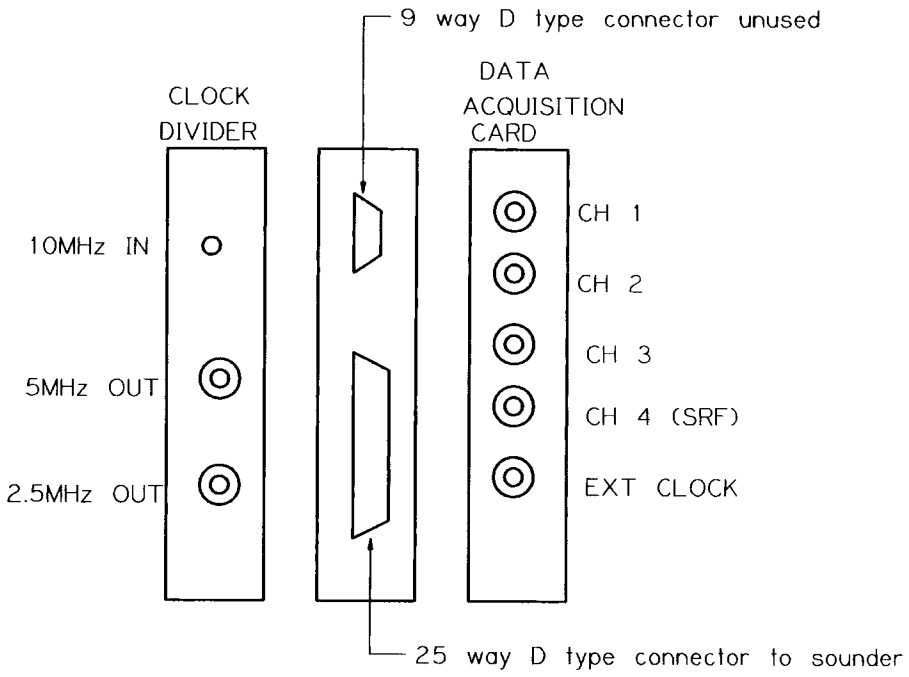

Figure 7.7. Data Acquisition card and Associated Connectors

CHAPTER 8. TEMPORAL VARIATIONS

8.1 INTRODUCTION

In this chapter the temporal variation of some of the statistics gained from the measurements are examined. The measurement data from the sounder consisted of time series data for 2500 or 3750 sweeps with 4000 samples per sweep. Measurements were made at various locations in Manchester and at various locations in Durham. The number of locations was limited by the need to share the sounder between four students, the time taken to save data and the weather. All the measurements, apart from those on 17 December 2002 in Manchester, were made using the frequency band 1920 MHz to 1980 MHz. On 17 December 2002 measurements were made in the bands 1920-1980 MHz and 2110-2170 MHz simultaneously. Only the measurements from the 1920-1980 MHz band are considered here since when later measurements were made there was severe interference in the 2110-2170 MHz band.

Because there was only one channel sounder and four students needing to make measurements there had to be some compromise as to the configuration of the sounder. At least two students were necessary for safe operation of the sounder and the resultant measurement data were shared. Some of the other students were primarily interested in extracting direction of arrival information from the measurement data so it was not always possible to use an omnidirectional antenna. Initially the data obtained from measurements with an omnidirectional antenna were analysed, later some of the data from measurements with directional antennas was also analysed. All the antennas were mounted at a height of 1.8 m and oriented for vertical polarisation.

The statistics examined were the number of multipath components, the mean delay and the RMS delay spread

components could be distinguished from the noise which is inevitably present in the data collected from the measurements. When setting this threshold the practical value of the results was considered. For the designer of equipment there will be a trade-off between performance and complexity. Although best possible performance will usually be desired, increasing complexity results in increasing cost of manufacture and testing. Taking a first generation UMTS receiver as an example, a RAKE architecture with 4 fingers is typical. Each RAKE finger can deal with one multipath component. UMTS uses soft handover when a mobile moves from one cell to another so the receiver must be capable of handling signals from at least 2 basestations. The receiver can then deal with only 2 multipath components from each basestation.

An initial examination of the data was made in order to decide on a suitable threshold for further analysis. Figure 8.1 shows the variation in the number of delay bins containing multipath components for three different thresholds over the duration of a 15 second measurement run. Figure 8.2 shows the CDF of the number of components for the whole 15 sec run. The threshold in each case has been set with reference to the power in the strongest multipath component.

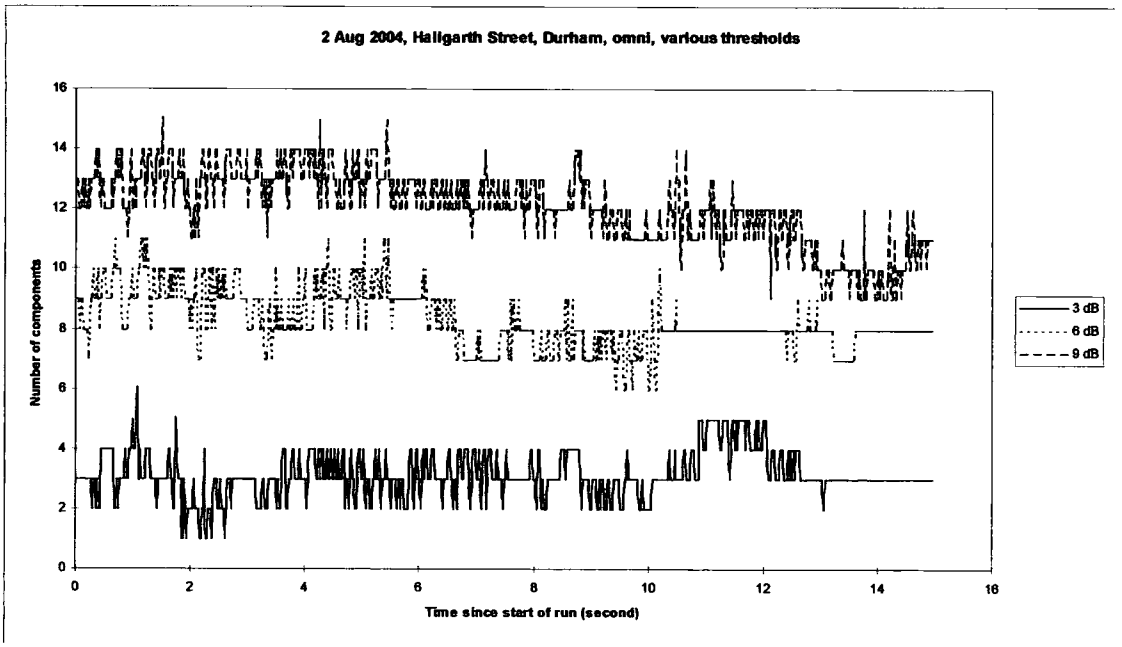

Figure 8.1. Variation of the number of components for three different thresholds in Hallgarth Street, Durham.

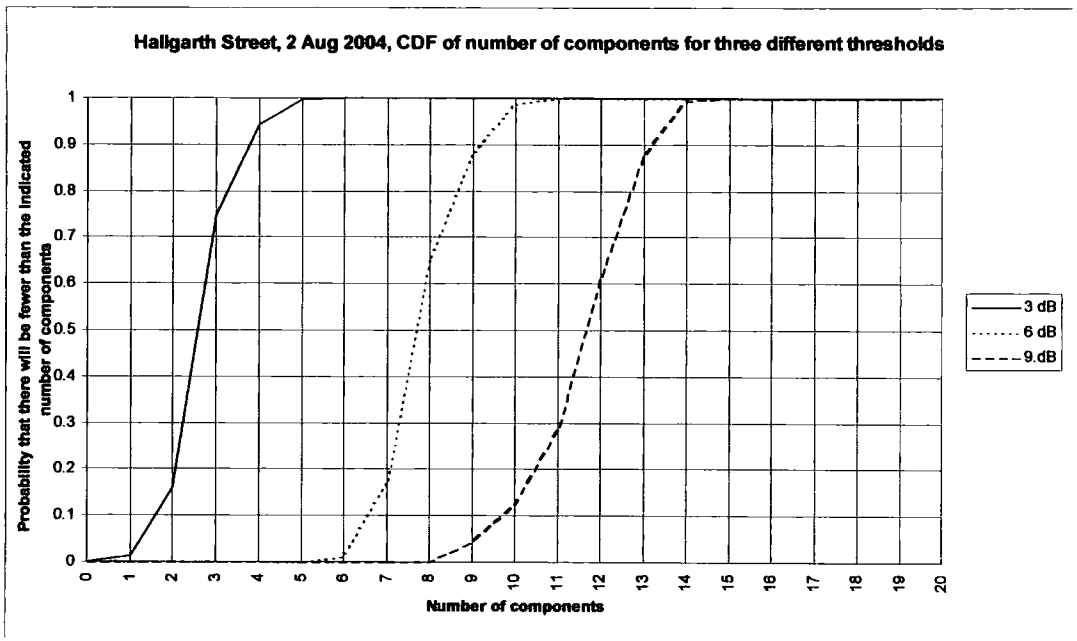

Figure 8.2. CDF of the number of components in Hallgarth street with various thresholds.

It can be seen from figure 8.1 that a threshold of 3 dB results in the detection of more multipath components than a four finger RAKE receiver can handle. The measurement was made in Hallgarth Street in Durham which is a quiet suburban street without a clear view of the cathedral and with little moving traffic. This represents a benign environment in which little change in the number of multipath components would be expected if they were due to vehicular traffic in the street.

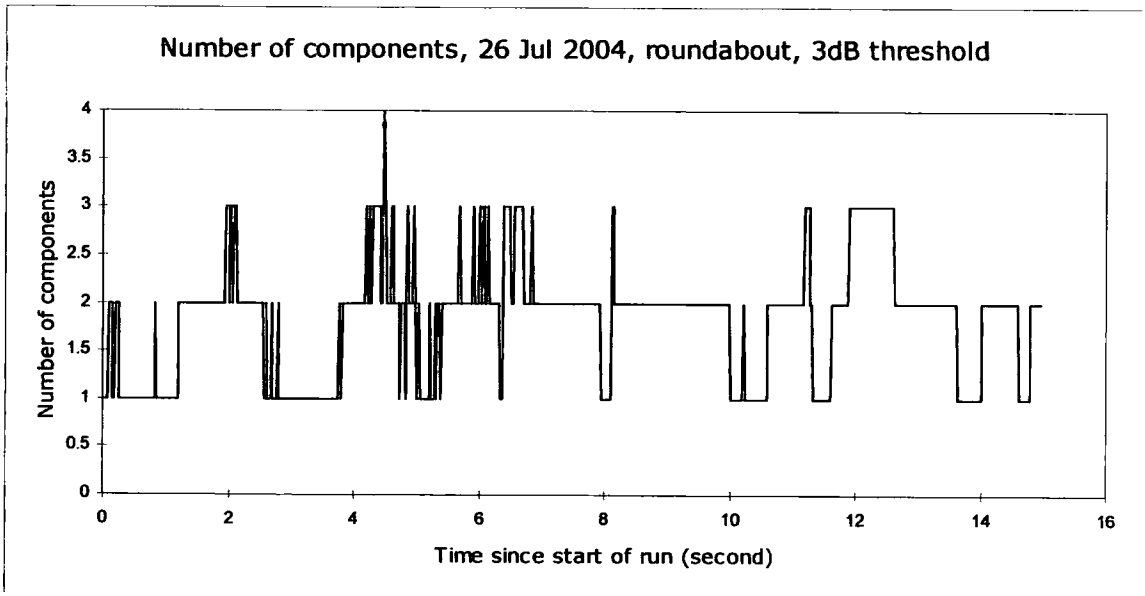

Figure 8.3 Variation in the number of components with a 3 dB threshold by the roundabout in Durham on 26 July 2004

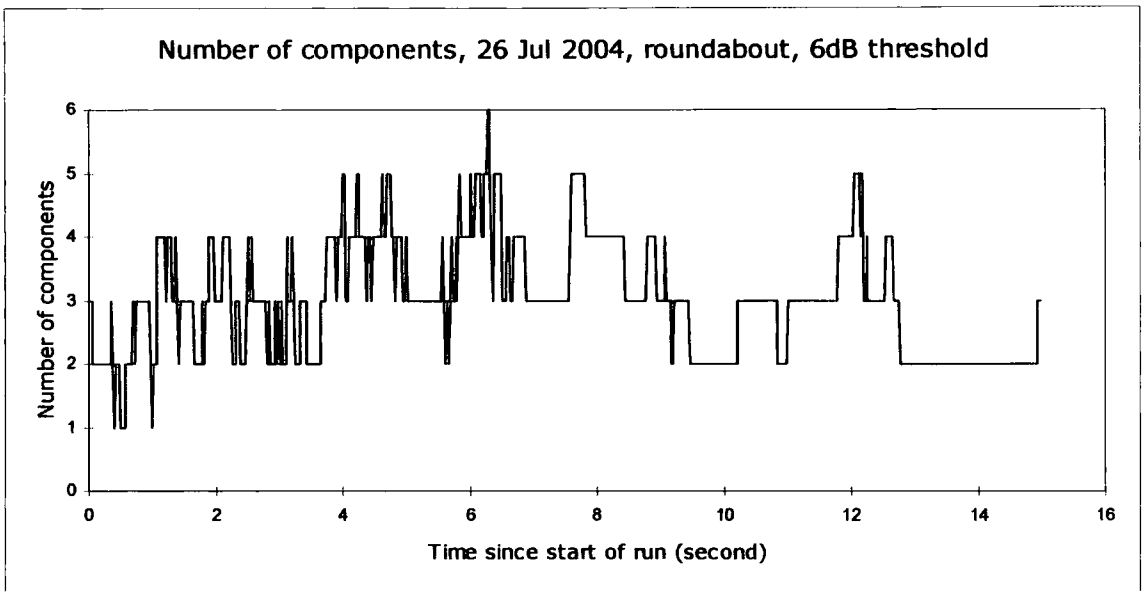

Figure 8.4 Variation in the number of components with a 6 dB threshold by the roundabout in Durham on 26 July 2004

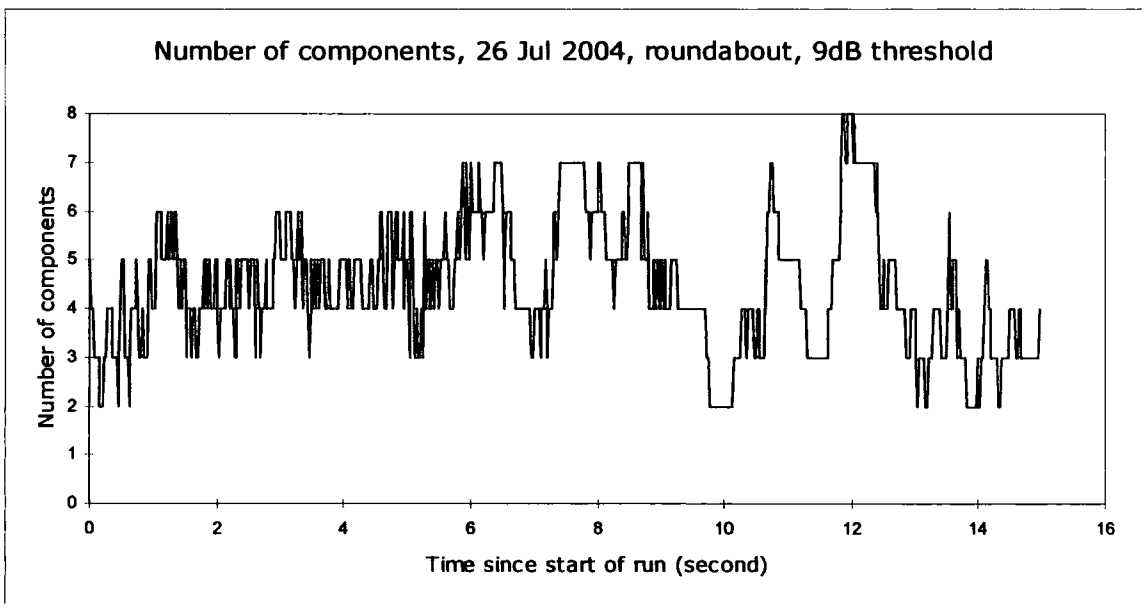

Figure 8.5 Variation in the number of components with a 9 dB threshold by the roundabout in Durham on 26 July 2004

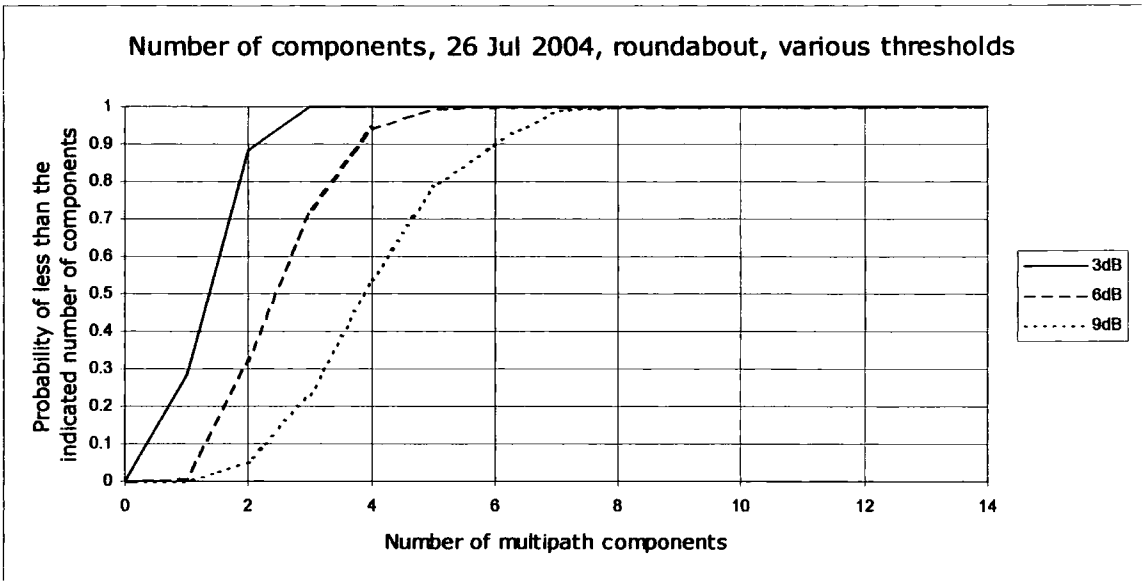

Figure 8.6. CDF of the number of components by the roundabout in Durham with various thresholds.

Figures 8.3, 8.4, 8.5 and 8.6 show the variation in the number of components near the roundabout in Durham on 26 July 2004. At this location there was a significant amount of moving traffic and in addition to there being more components found with the higher thresholds there was also more variation.

Examination of the measurements from Manchester showed fewer multipath components in streets with more traffic. In Manchester the surrounding buildings were higher than in Hallgarth Street and would more effectively obstruct multipath components from neighbouring streets. A threshold of 6 dB for the Manchester measurements resulted in the detection of a single component for most of the time in some locations, Figure 8.3 shows Whitworth Street as an example.

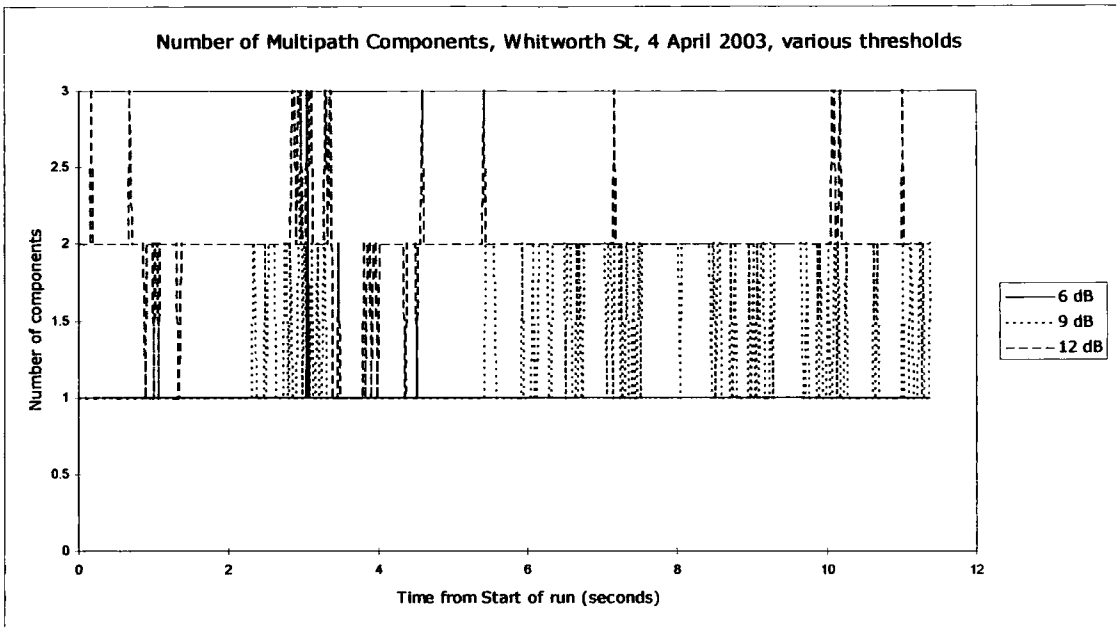

Figure 8.7 Variation in the number of multipath components for various thresholds in Whitworth Street, Manchester.

In Whitworth Street thresholds of 6 dB or less resulted in a single component being found. Thresholds of 9 dB and 12 dB allowed more components to be detected and taken into account when calculating the mean delay and the RMS delay spread. As more components are taken into account a more detailed view of the temporal variations in the radio channel emerges but to a designer of RAKE receivers with few fingers this may not be useful.

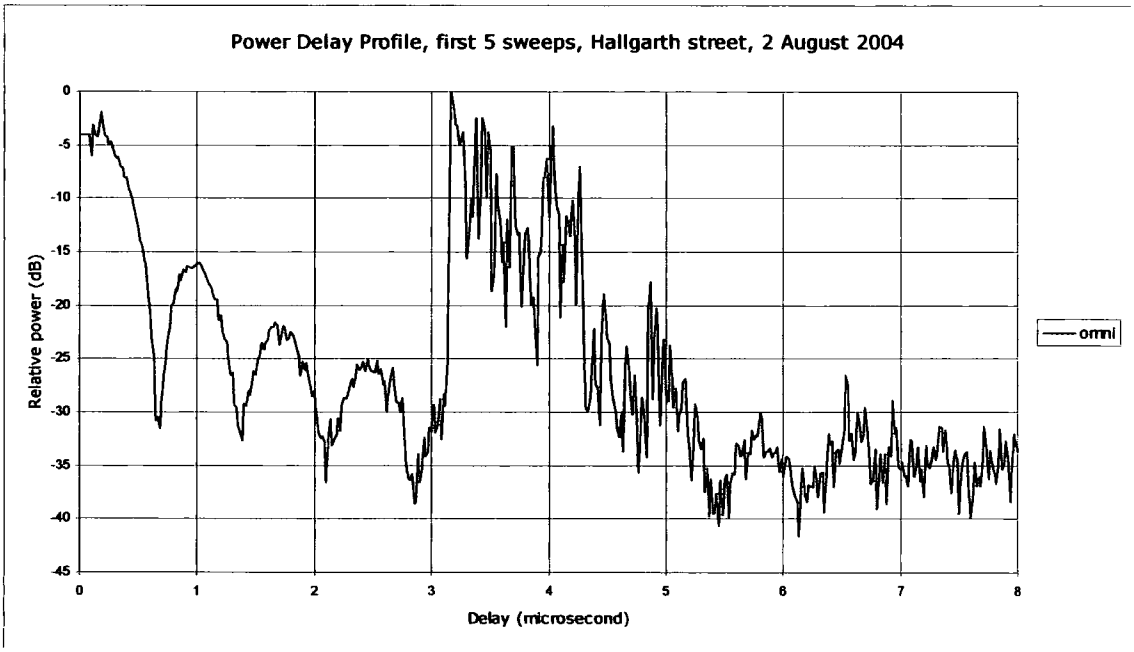

Figure 8.8 Power Delay Profile from Hallgarth Street, Durham on 2 August 2004.

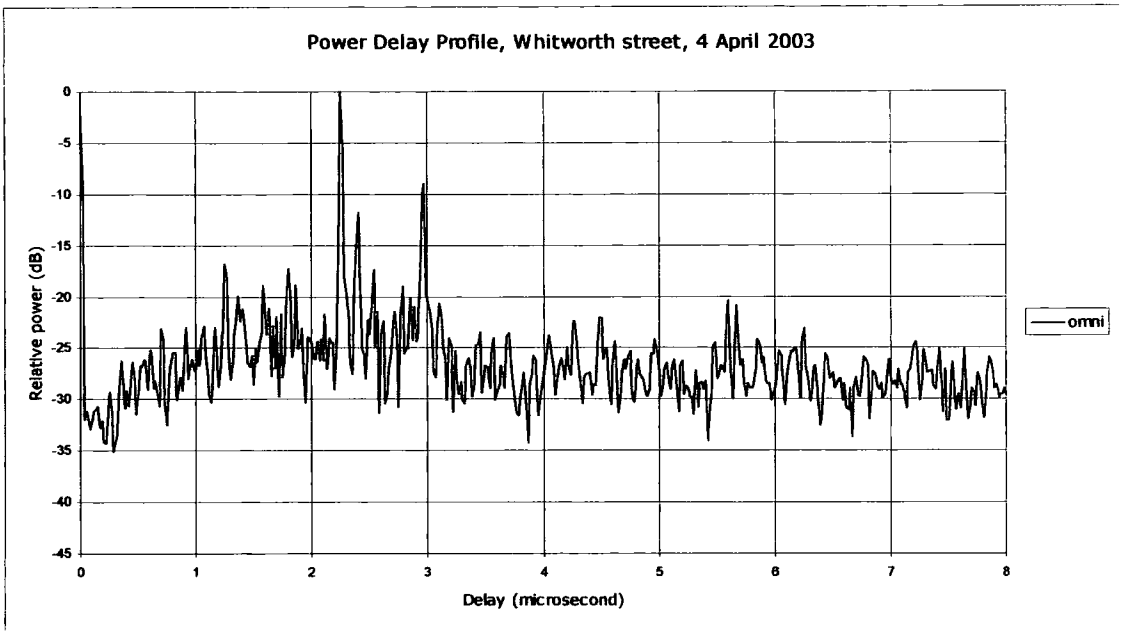

Figure 8.9 Power Delay Profile from Whitworth Street, Manchester on 3 April 2003.

As may be seen from the PDPs in figures 8.8 and 8.9 the number of components detected will vary with the threshold. More components will be detected with larger thresholds but notice that, in figure 8.9, a threshold of 20 dB would result in some of the noise being falsely detected as multipath components. In the Hallgarth Street measurement (figure 8.8) it would have been possible to use a threshold of 25 dB since a better signal to noise ratio was obtained. In both figures 8.8 and 8.9 it will be noticed that there are some spurious responses before the first multipath component (delay of 3.16 μsec in Hallgarth Street, 2.25 μsec in Whitworth Street). These are artefacts of the channel sounder and may be ignored. It was decided that the statistics of the radio channel would be extracted using thresholds of 6 dB and 12 dB. 6 dB may yield statistics useful for designers but in some locations there may not be enough components detected for computing meaningful statistics. A 12 dB threshold will be high enough to detect components where 6 dB is inadequate with little danger of interpreting noise as multipath components.

8.3 A SOUNDER LIMITATION

When considering the mean delay of the multipath components a limitation of the sounder became apparent. To determine if there were temporal variations in the radio signal it was necessary that the statistics should be extracted from measurements taken at the same location at two or more different times. Comparison of the mean delay statistic obtained at different times required that absolute delay times could be extracted from sounder measurement data. This was not possible because of the way the sounder receiver and transmitter were synchronised and the need to turn off the sounder for a battery change every 2 hours.

8.4 TAKING SAMPLES FROM THE MEASUREMENT DATA

Due to the sounder limitation mentioned at 8.3 above it was necessary to take samples from a single measurement run and form two ensembles of sample points. Since the time-series data from complete sweeps was required for the calculation of the statistics it was necessary to take a complete sweep as a sample. It was decided to split each run into two halves and take each half as an ensemble. An alternative scheme in which odd numbered sweeps formed one ensemble while even numbered sweeps formed a second ensemble yielded results almost indistinguishable from those obtained by considering data from the whole 15 second run. The ensembles formed from the first half and second half of the measurement run tended to highlight the longer term variations (over a number of seconds rather than msec). Since the first sample of the second ensemble was taken 7.5 seconds later than the first sample of the first ensemble it was possible to observe variations due to vehicles moving and wind induced vegetation movement. Figures 8.12 and 8.13 illustrate the difference between the two schemes for assigning samples to ensembles. Since the first half / second half scheme highlights the slower changes it has been used for all of the results except that shown in figure 8.13.

difficulty of moving the sounder receiver in the Durham environment with its narrow pavements and steep hills. Measurements were made in other locations using directional antennas. Figure 8.10 shows the area around the university with the measurement locations marked: **Tx** is the location of the transmitter on the roof of the School of Engineering, **T** is the traffic lights, **R** is the location at the roundabout and **P** is the post-box in Hallgarth Street.

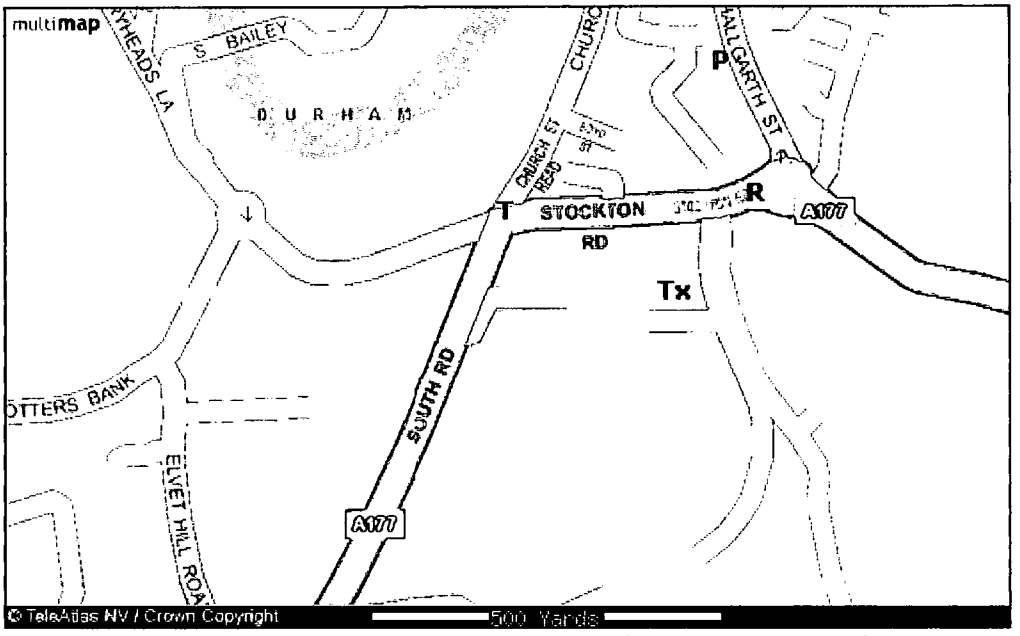

Figure 8.10 Measurement locations in Durham

Location T was near the university library at the traffic lights where South Road crosses Stockton Road. Both roads are busy during the morning and evening rush hours but quiet at other times. There is some heavy vehicle traffic. Near this cross-roads there are two storey buildings to the North and East, the university to the South and a wooded area to the West. There is a clear view of Durham Cathedral from this location. The separation between transmitter and receiver was 300 m.

Location R was on the West approach island to the roundabout near the university main entrance. There are two storey buildings and some trees on the North, East and West sides. To the South is the university. There is an obstructed view of the cathedral. The separation between transmitter and receiver was 250 m.

Location P was in Hallgarth Street by the post box. This is a quiet street with two and three storey buildings on both sides. The street runs in a North - South direction and the buildings prevent any view of the cathedral. The separation between transmitter and receiver was 500 m.

8.5.2 Manchester

The parts of Manchester accessible from UMIST within the sounder battery endurance were around the city centre. The streets were busy most of the time and surrounded by buildings of six storeys or more. The type of location at which measurements could be made was limited by safety concerns to areas where there was no moving road traffic and few pedestrians. Car parks were used since these were within a few metres of the street centre lines while affording protection from moving traffic. Figure 8.11 shows the locations: **Tx** is the transmitter location on the roof of the UMIST Main Building, **P** is Chorlton Street car park, **B** is Bloom Street car park and **W** is the location in Whitworth Street on the pavement by the Brazil Street car park.

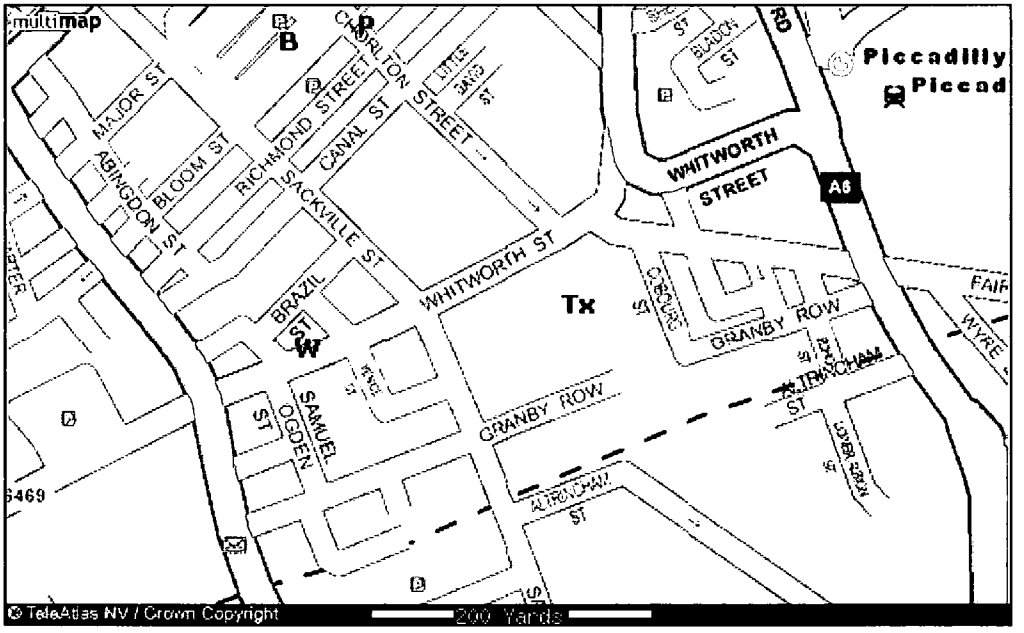

Figure 8.11 Measurement locations in Manchester.

Location P was in Chorlton Street car park. Chorlton Street was to the West of the car park. The East and North sides of the car park were enclosed by six storey buildings at a distance of 40 m. Separation between transmitter and receiver was 400 m.

Location W was near Whitworth Street car park. This location was just off the pavement of Whitworth Street which is a wide street with continuous motor traffic throughout the day. To the North was the car park which is a large open space. The separation between transmitter and receiver was 500 m and there was a line of sight path between them.

8.6 NUMBER OF MULTIPATH COMPONENTS

From figure 8.1 it can be seen that the number of multipath components detected over a 15 second interval at a particular location changes at random. The distribution of the numbers of multipath components at locations in Durham and Manchester using an omnidirectional receive antenna are shown as CDFs in the following figures. Separate figures are shown for 6 dB and 12 dB thresholds. In each figure CDFs are shown for the first and second halves of the measurement run.

8.6.1 Durham

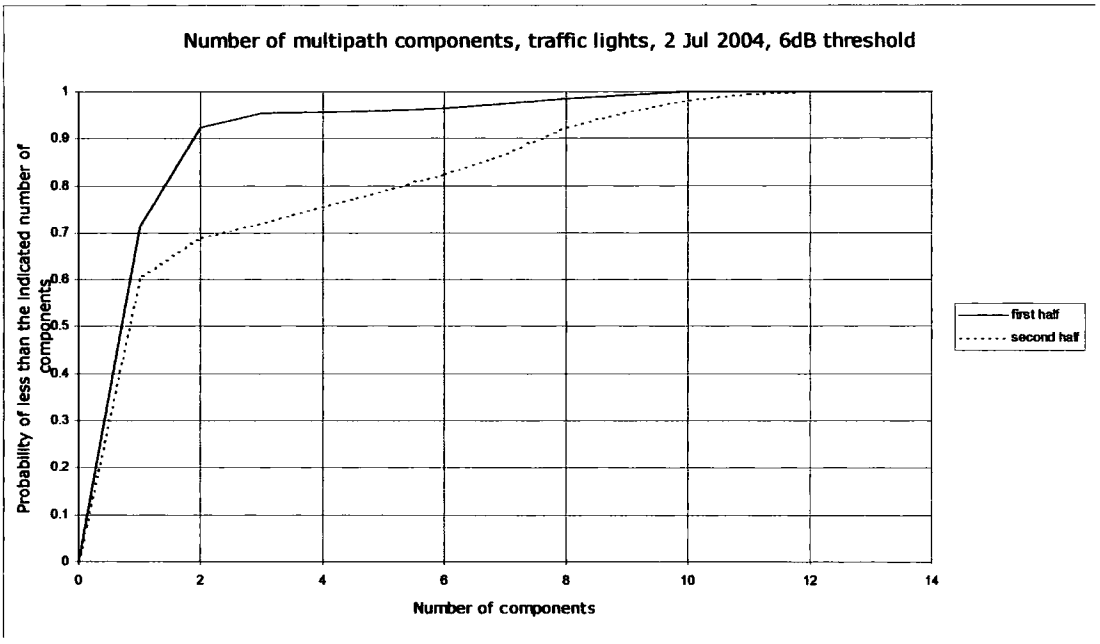

Figure 8.12 CDF of number of multipath components by the traffic lights in Durham on 2 July 2004.

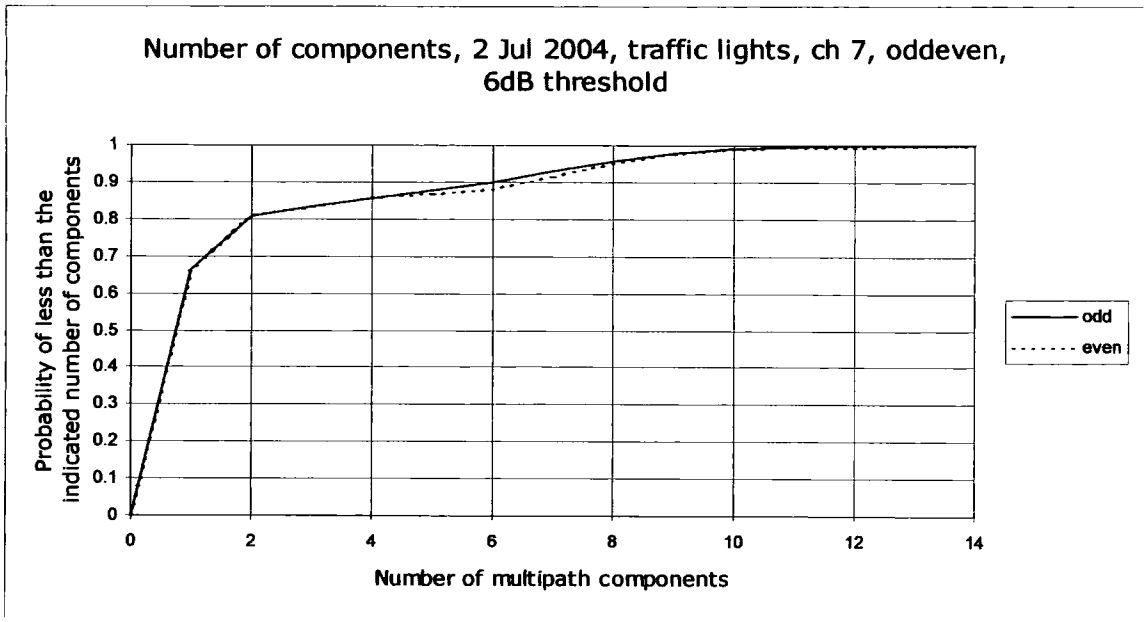

Figure 8.13 CDF of number of multipath components by the traffic lights in Durham on 2 July 2004 using the alternative method of creating ensembles.

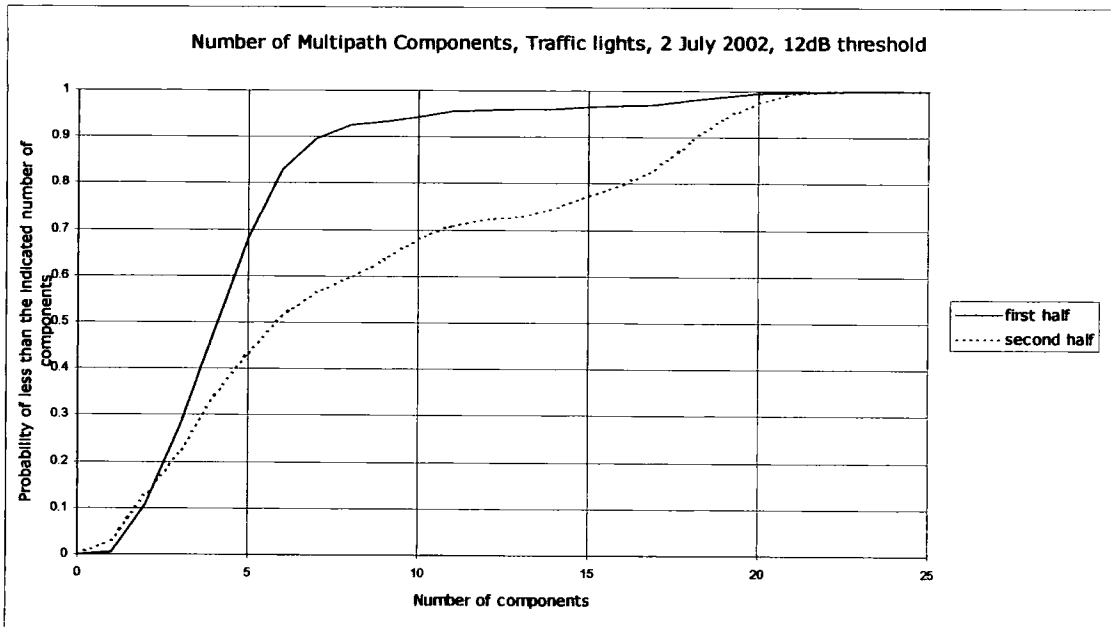

Figure 8.14 CDF of number of multipath components by the traffic lights in Durham on 2 July 2004 using a 12 dB threshold.

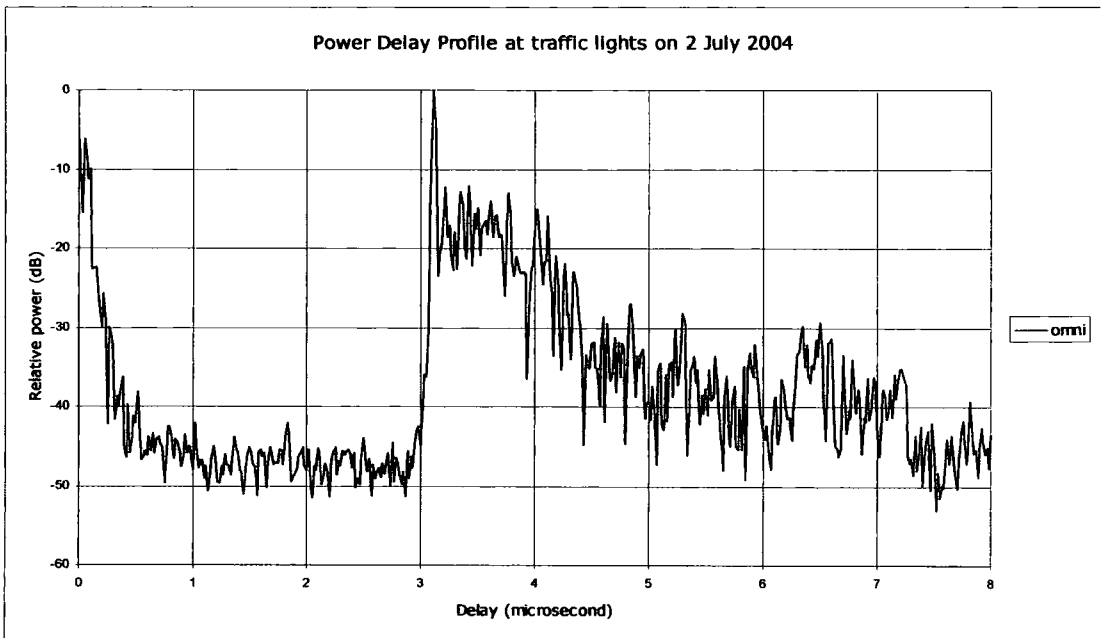

Figure 8.15 Power Delay Profile by the traffic lights in Durham on 2 July 2004.

The differences in the number of multipath components found with 6 dB and 12 dB thresholds (figures 8.12 and 8.14) are explained with reference to the PDP in figure 8.15. There were one or two strong components which were detected with a 6 dB threshold and many components which were detected with the 12 dB threshold. The measurement which yielded these results was made at the traffic lights outside the university where South Road crosses the Stockton Road. Both of these roads were busy at the time of the measurement. At this location there was a clear line of sight view of Durham Cathedral. There was no line of sight path to the transmitter. As might be expected there was a relatively high probability of seeing one multipath component and this was the signal reflected from the cathedral. The distribution has a long tail towards the higher numbers of components and this is different between the first and last halves of the measurement period. This indicates that some of the multipath components were interactions with moving vehicles, either reflections or obstruction of reflections from local clutter. A visual examination of the PDPs from 5 sweeps at a time showed that there was significant variation during the measurement run of both the relative power in the dominant component and the relative powers in the other components.

The following figures record the situation on the approach island to the roundabout near the main entrance to Durham University Science Laboratories (location R). Measurements were made on two days at this location. The exact locations of the receive antenna were likely to have been different by up to a wavelength since the location was recorded by a chalk mark on the road surface rather than by any more precise means. It was not possible to leave the antenna in place between the measurements on the two days.

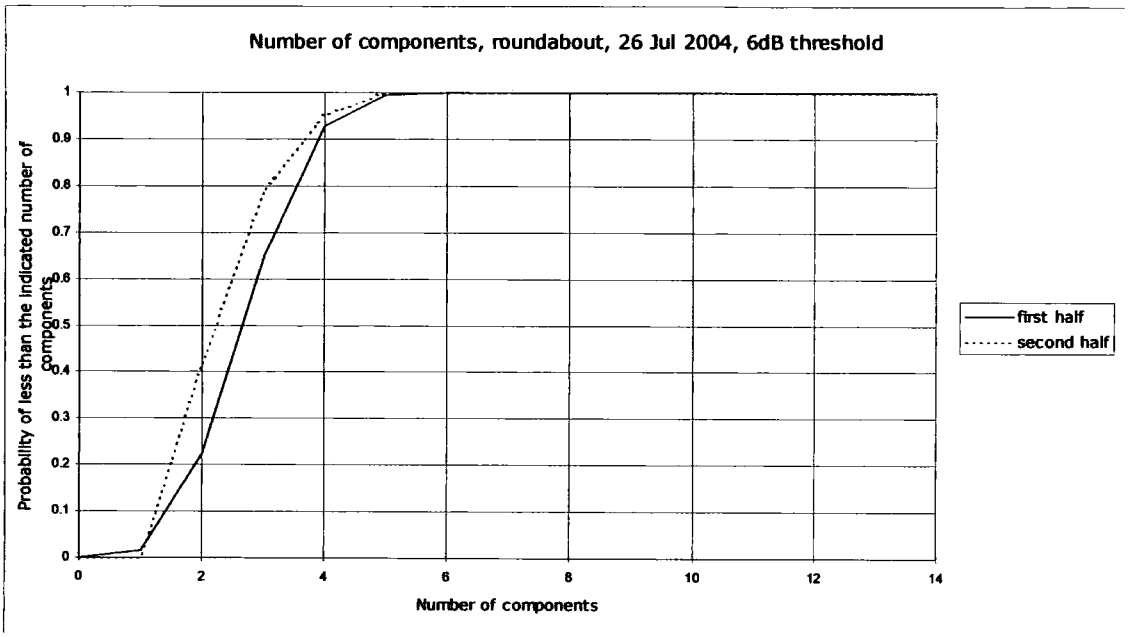

Figure 8.16 CDF of number of multipath components at the roundabout in Durham on 26 July 2004 with a 6 dB threshold.

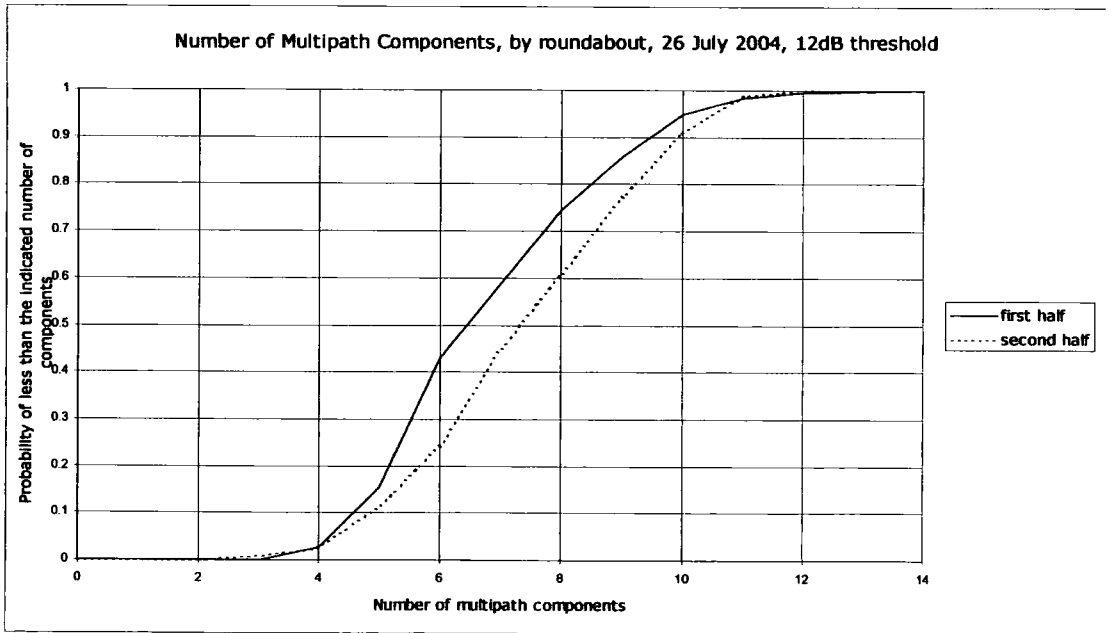

Figure 8.17 CDF of Number of Multipath Components at the roundabout in Durham on 26 July 2004 with a 12 dB threshold.

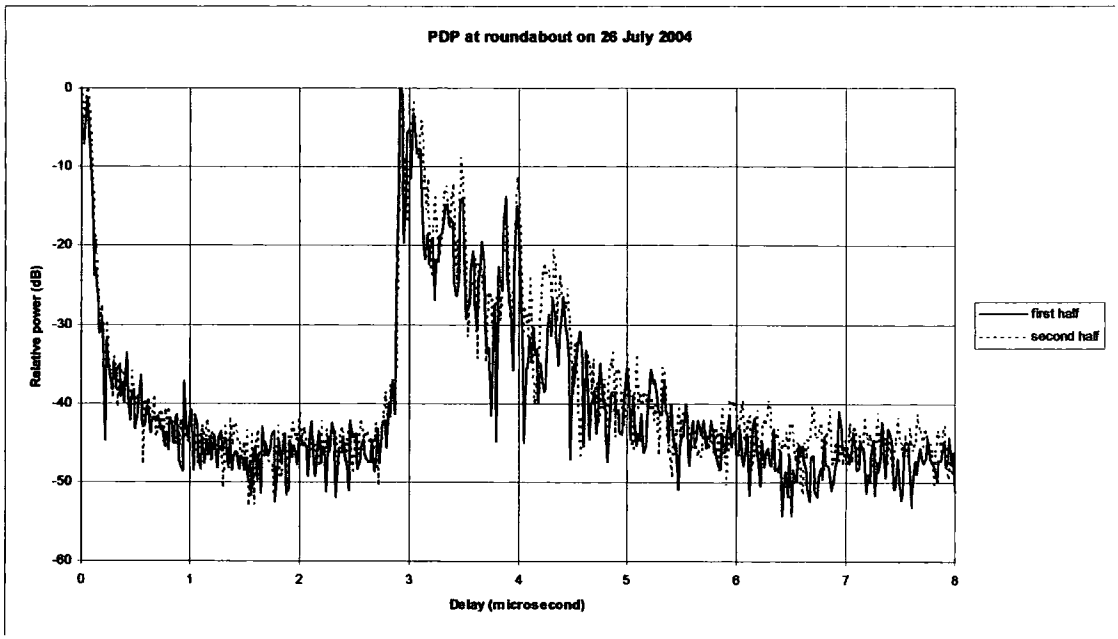

Figure 8.18 Power Delay Profile at the roundabout in Durham on 26 July 2004.

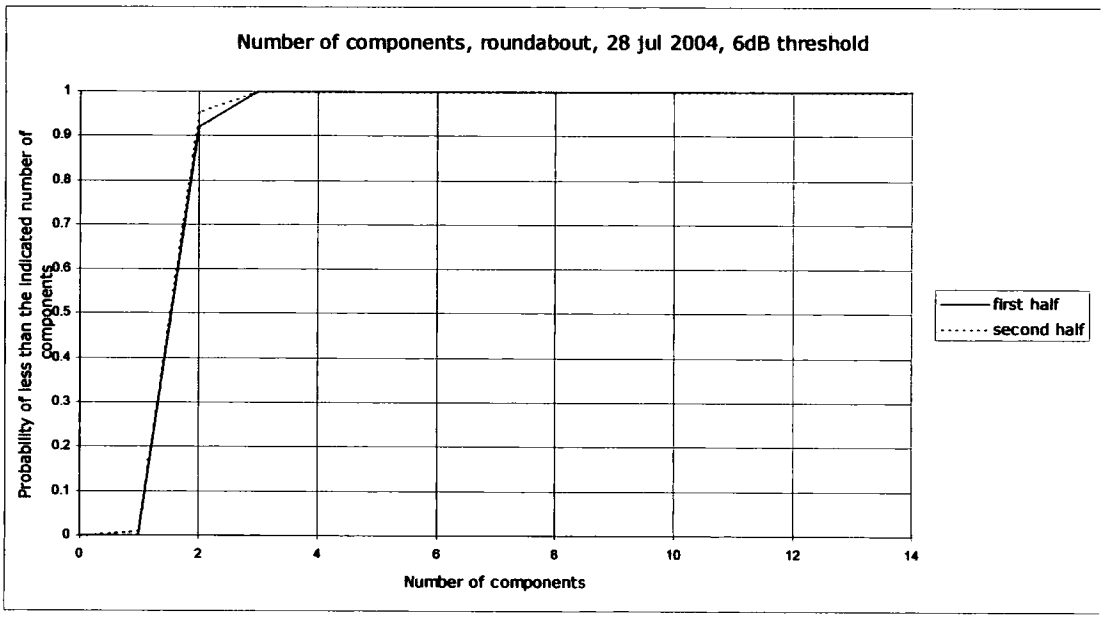

Figure 8.19 CDF of number of multipath components at the roundabout in Durham on 28 July 2004 with a 6 dB threshold.

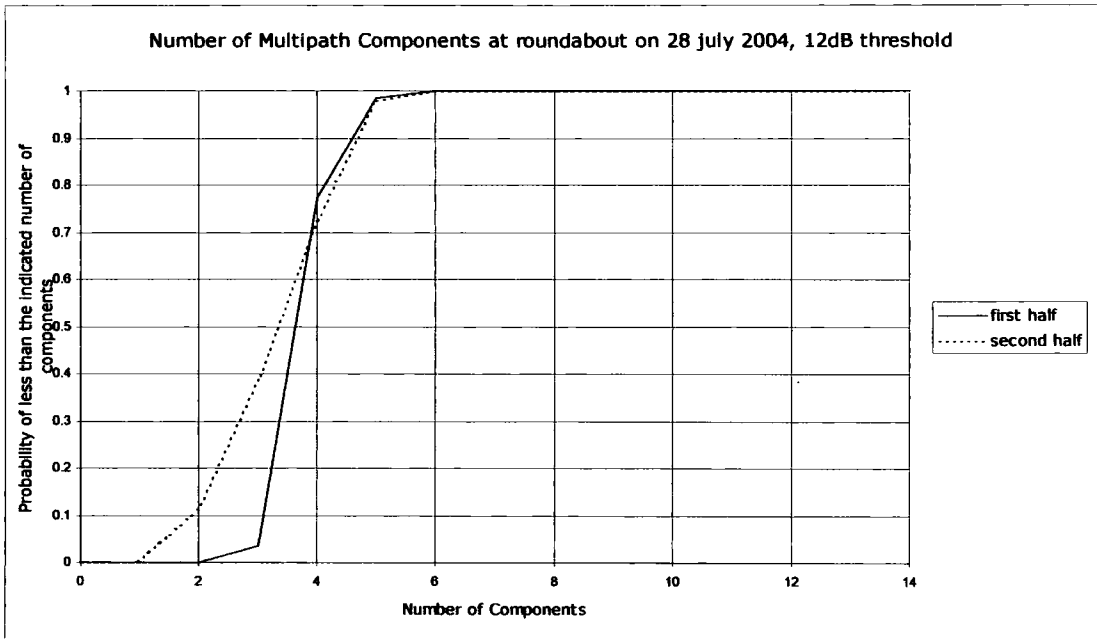

Figure 8.20 CDF of the Number of Multipath Components at the roundabout in Durham on 28 July 2004 with a 12 dB threshold.

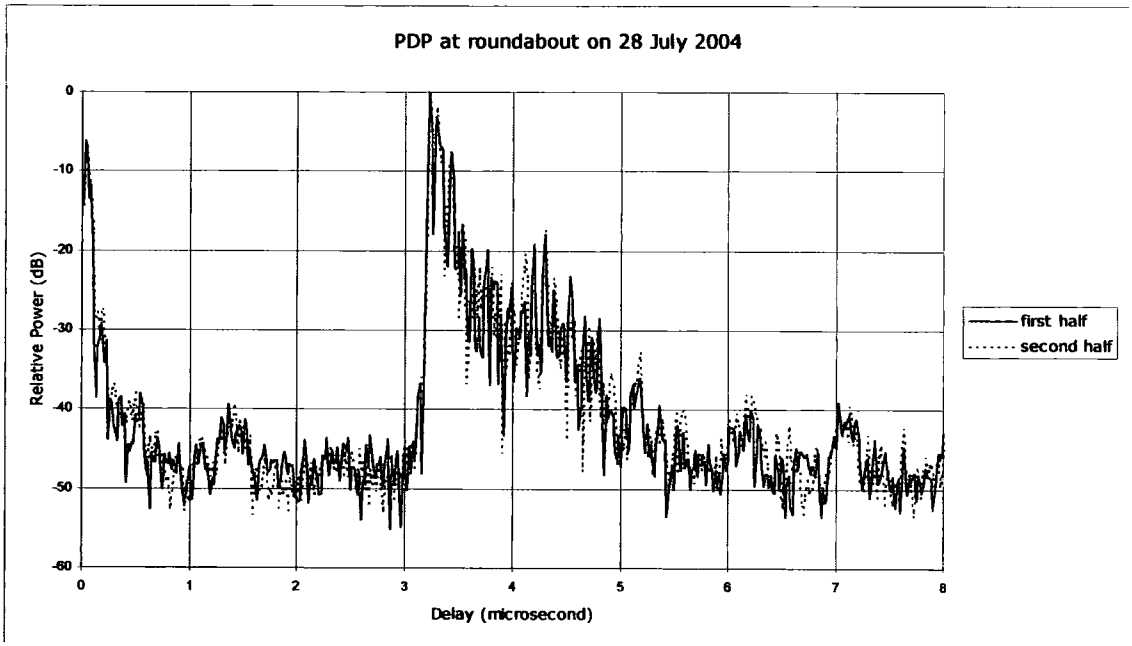

Figure 8.21 Power Delay Profile at the roundabout in Durham on 28 July 2004.

Figures 8.16 and 8.17 show CDFs of the number of components at the roundabout next to the main entrance of Durham University Science Laboratories on 26 July 2004. Figures 8.19 and 8.20 show the situation on 28 July 2004. On 26 July 2004 the measurement was made late in the afternoon when there was a moderate amount of traffic moving along the Stockton Road. On 28 July 2004 the measurement was made in the middle of the morning when there was little traffic. The result from 28 July shows

little difference between the first half and the second half of the measurement run when using a 6 dB threshold and indicates a single component which was probably the result of a reflection from a substantial building on the North side of the Stockton Road. The result from 26 July shows more variation, indicating that there were reflections from the passing traffic but little difference between first half and second half of the measurement run indicating a near constant rate of passing vehicular traffic.

Using a 12 dB threshold admitted many more components than the 6 dB case on 26 July 2004 whereas there was only a small increase on 28 July 2004. This tends to confirm that most of the components were reflections from road traffic.

The PDPs (figures 8.18 and 8.21) were similar in structure on the two days as would be expected from measurements at the same location. There were more components with small delays relative to the first peak on 26 July than on the 28 July confirming what is shown in the CDFs. There was also more variation between the first and second halves of the measurement run on 26 July.

Figures 8.22, 8.23 and 8.24 are from a measurement by the post-box in Hallgarth Street, Durham (location P). Hallgarth Street runs from the roundabout near the main entrance to the university science laboratories towards the city centre. The orientation of the street is such signals from the transmitter will tend to pass along the street to the receiver location rather than across streets as was the case for the measurement at the traffic lights. There are buildings along both sides of the street of 2, 3 and 4 storeys arranged so that there are a number of gable ends visible from the transmitter and receiver. Traffic on the roundabout can obstruct the Southern end of the street. There were cars parked along each side of the street but little moving traffic.

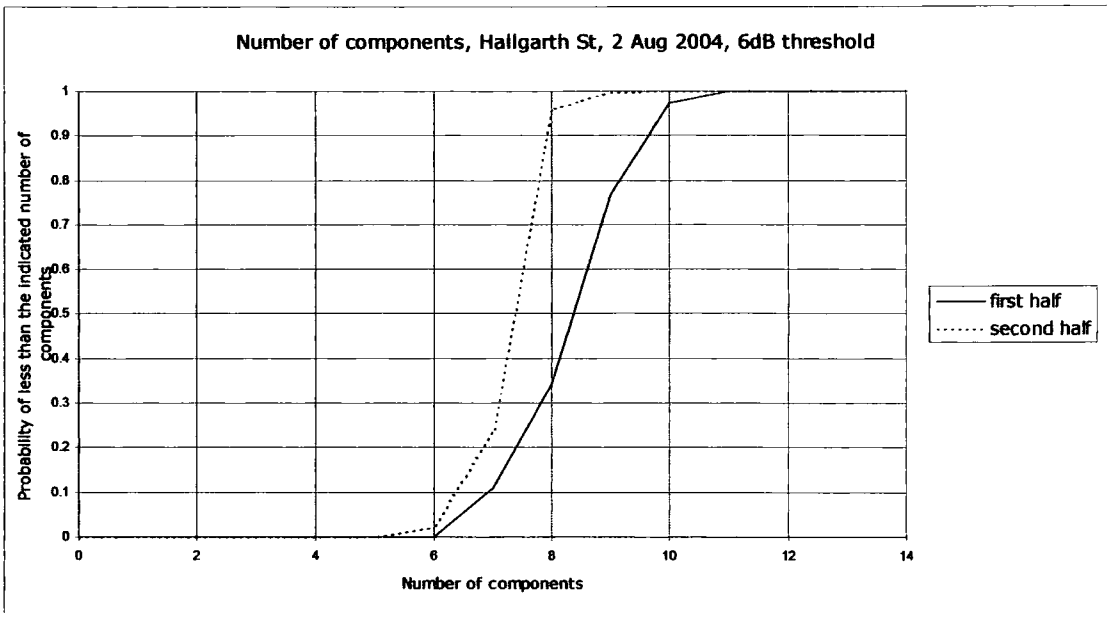

Figure 8.22 CDF of number of multipath components by the post-box in Hallgarth Street, Durham on 2 August 2004 with a 6 dB threshold

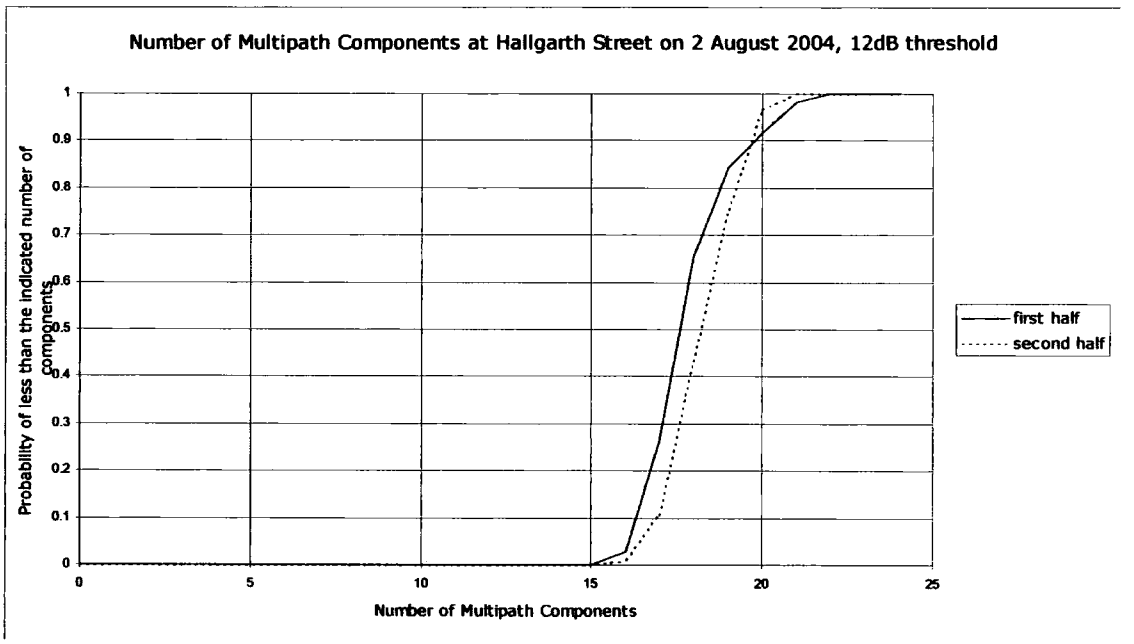

Figure 8.23 CDF of the Number of Multipath Components by the post-box in Hallgarth Street, Durham on 2 August 2004 with a 12 dB threshold.

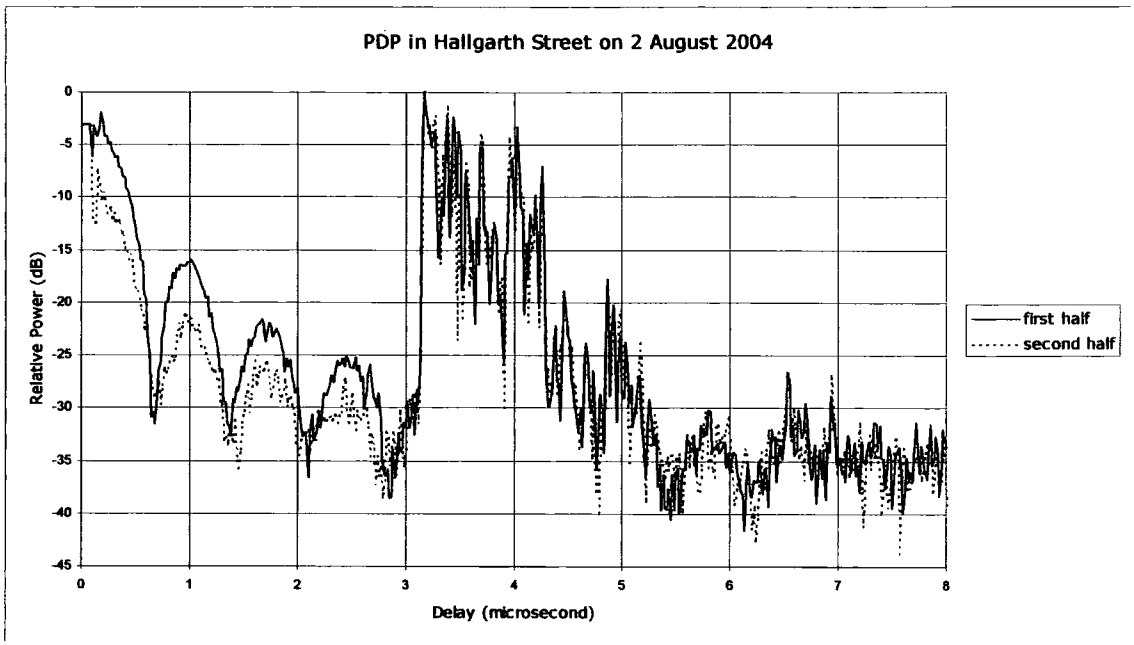

Figure 8.24 Power Delay Profile by the post-box in Hallgarth Street, Durham on 2 August 2004.

Figures 8.22 and 8.23 show the CDFs of the number of components in Hallgarth Street with thresholds of 6 dB and 12 dB respectively. The geometry of the situation suggests that the multipath components were probably caused by reflections from the buildings along each side of the street. There were more multipath components recorded in Hallgarth Street than at the other locations in Durham. The difference between the first and second halves of the measurement run suggests a variable degree of obstruction of the end of the street at the roundabout. This is an example of a situation in which variation of the channel in the street was caused by movement of objects in adjacent streets rather than in the street itself.

8.6.2 Manchester

Measurements were made in Chorlton Street car park in Manchester on three days. It was not possible to place the receive antenna at exactly the same location on each of the three days due to the parking pattern of the cars. Figures 8.25, 8.26, 8.28, 8.29, 8.31 and 8.32 are CDFs of the number of multipath components. Figures 8.27, 8.30 and 8.33 are PDPs recorded on each of the three days.

In Manchester the transmit antenna was mounted on the roof of the UMIST Main Building at a height of 45 m above ground level. The buildings

around the Main Building were of 5 or 6 storeys with heights of 30 m or less. There was a line of sight path from the transmit antenna to many of the buildings in the measurement area.

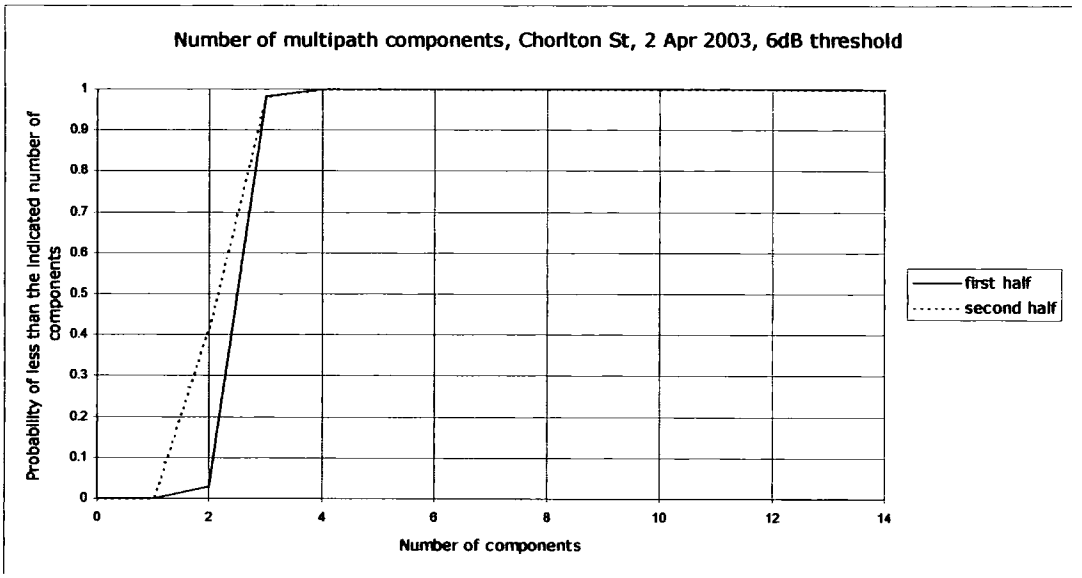

Figure 8.25 CDF of the number of multipath components at Chorlton Street car park, Manchester on 2 April 2003 with a 6 dB threshold.

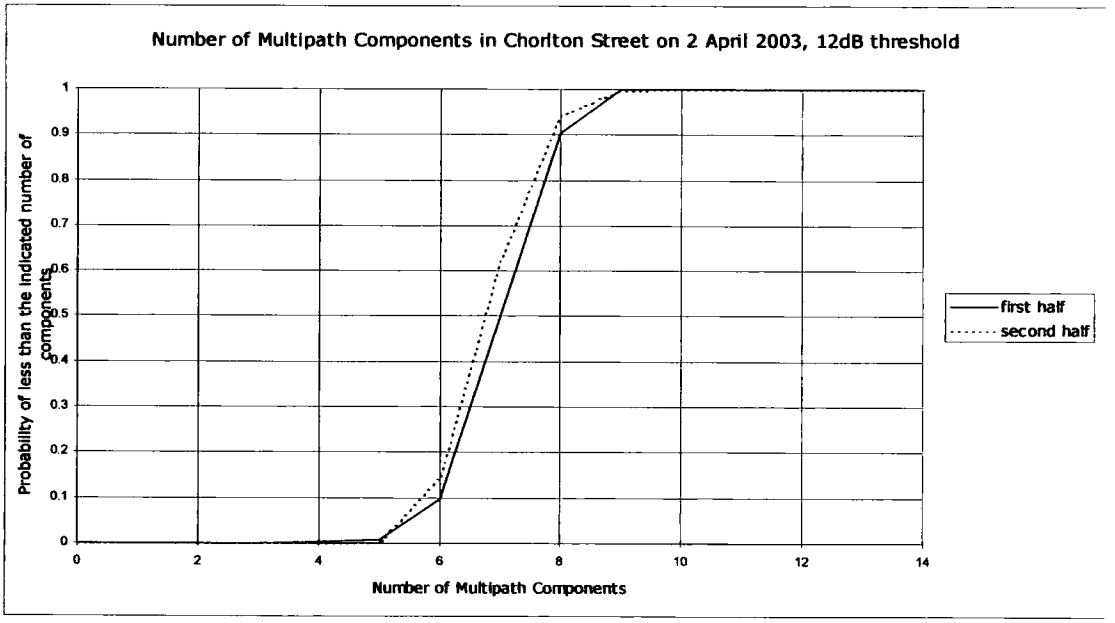

Figure 8.26 CDF of the Number of Multipath Components at Chorlton Street car park, Manchester on 2 April 2003 with a 12 dB threshold.

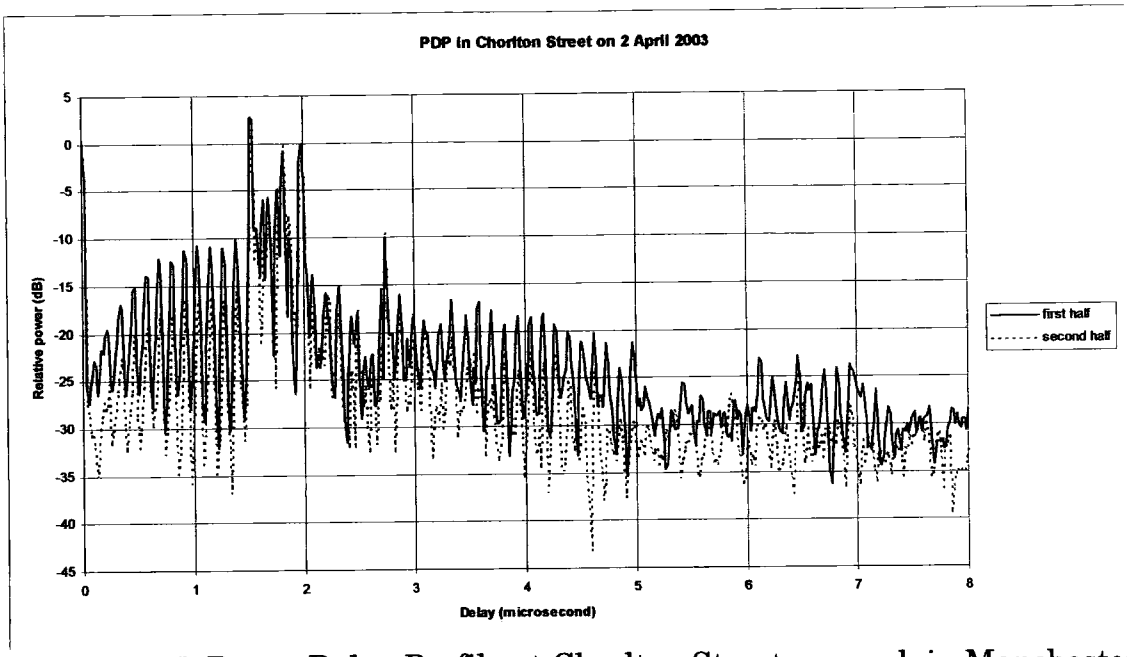

Figure 8.27 Power Delay Profile at Chorlton Street car park in Manchester on 2 April 2003.

Figures 8.25 and 8.26 show a CDFs of the number of components in Chorlton Street car park in Manchester on 2 April 2003. Although there was no line of sight path to the transmitter, the high transmitter location allowed a strong signal to reach the buildings to the West of the car park thereby ensuring that there was at least one component. The traffic moving along Chorlton Street, particularly buses, contributed to the additional components and to the difference between the first and second half of the measurement run. The small difference in the number of components was to be expected since only a short length of Chorlton Street was visible to the receiver and this could not accommodate more than one bus.

The PDP shows an oscillatory characteristic which suggests that there was interference present. UMTS antennas had recently appeared on one of the tall buildings near Piccadilly railway station and it is possible that a UMTS basestation was being tested during the measurement. A visual examination of the time series data from the sounder suggested interference but it was not possible to characterise it. The CDF using the 12 dB threshold must therefore be treated with caution.

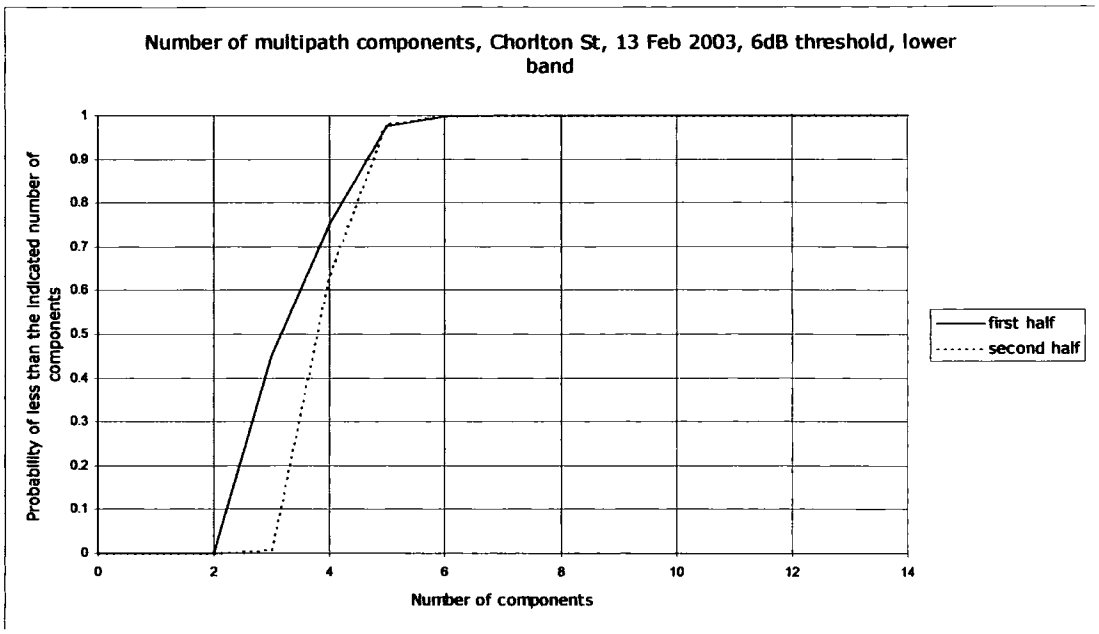

Figure 8.28 CDF of the number of multipath components in Chorlton Street car park, Manchester on 13 February 2003 with a 6 dB threshold.

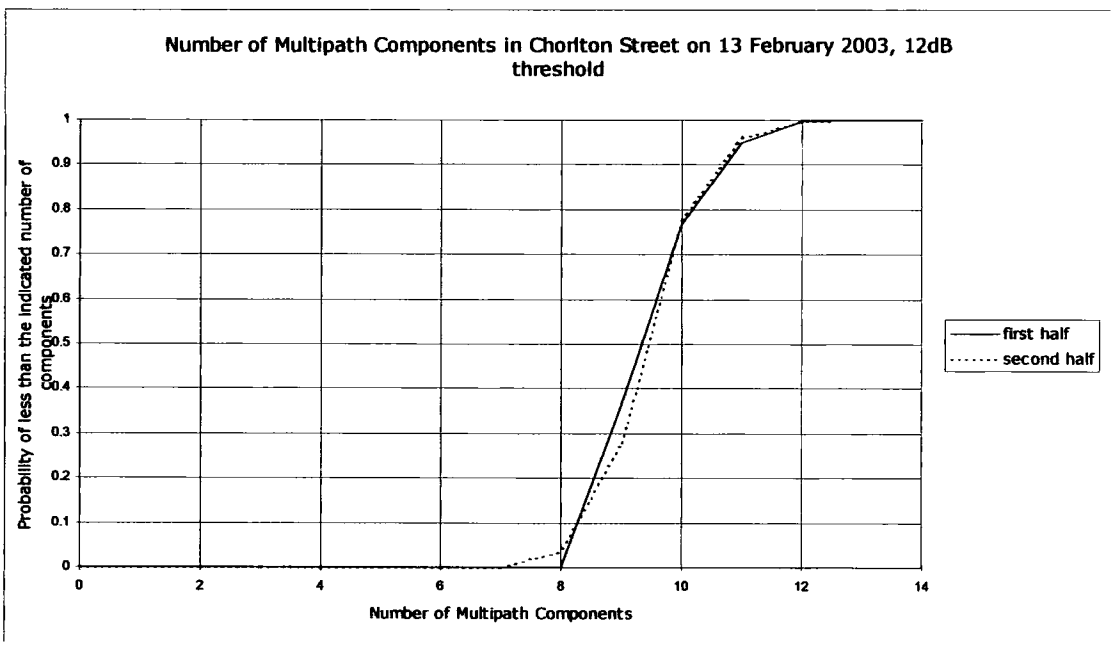

Figure 8.29 CDF of the Number of Multipath Components in Chorlton Street car park, Manchester on 13 February 2003 with a 12 dB threshold.

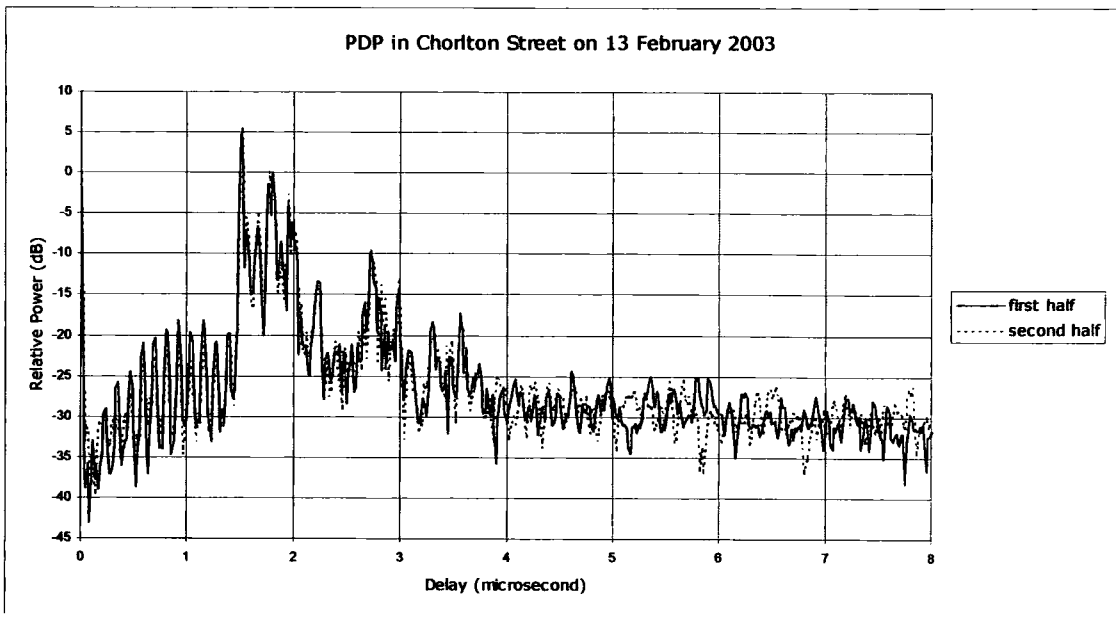

Figure 8.30 Power Delay Profile in Chorlton Street car park, Manchester on 13 February 2003.

Figures 8.28 and 8.29 show CDFs of multipath components in Chorlton Street car park on 13 February 2003. In this case the location was on the other side of the car park with more exposure to moving traffic than the case shown in figures 8.25 and 8.26. Here there are more components but the difference between the first and second half of the measurement run is similar.

There was also a suggestion of interference in the PDP (figure 8.30) which was reinforced by a visual examination of the time series data. The interference appears not to be as severe as it was on 2 April.

The larger number of components and the smaller difference between the first and second halves of the measurement run suggest that most components were reflections from buildings rather than from moving motor vehicles.

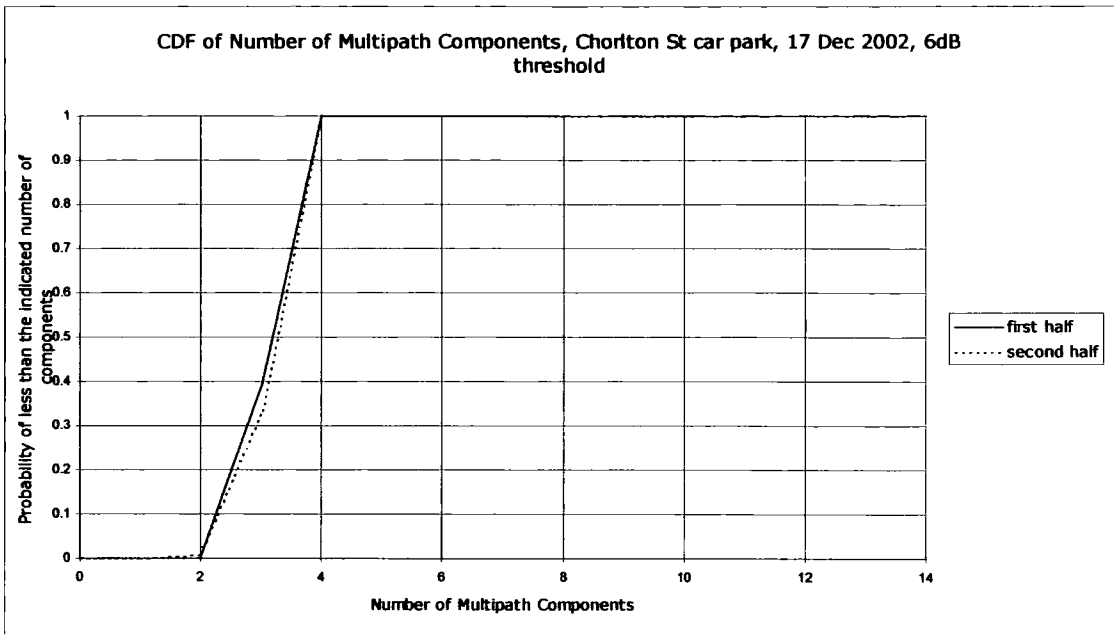

Figure 8.31 CDF of the number of multipath components in Chorlton Street car park, Manchester on 17 December 2002 with a 6 dB threshold.

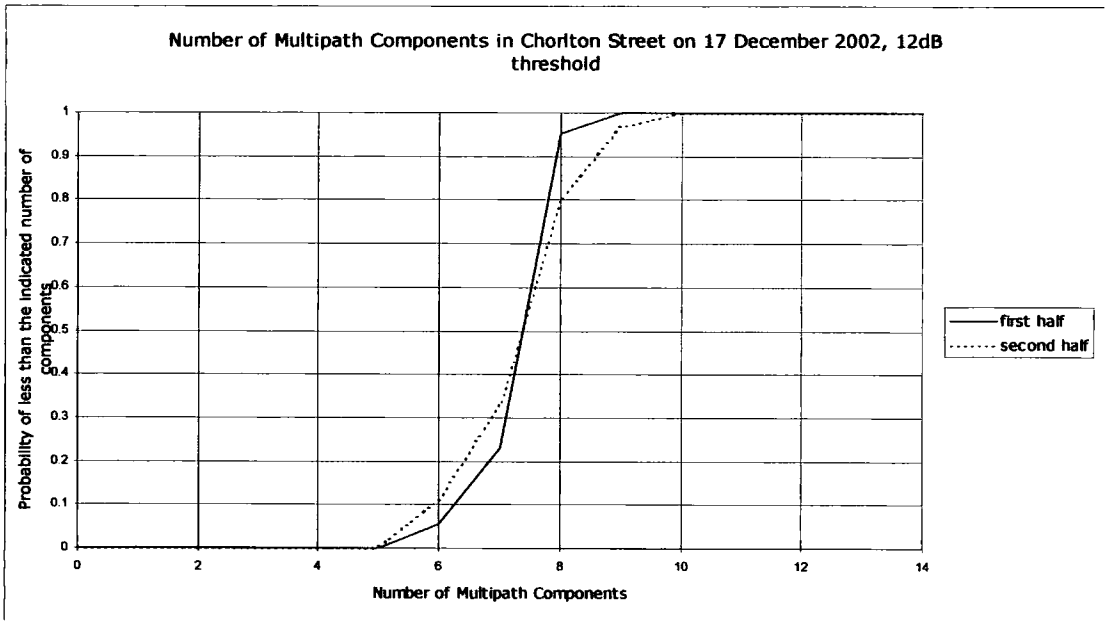

Figure 8.32 CDF of the Number of Multipath Components in Chorlton Street car park, Manchester on 17 December 2002 with a 12 dB threshold.

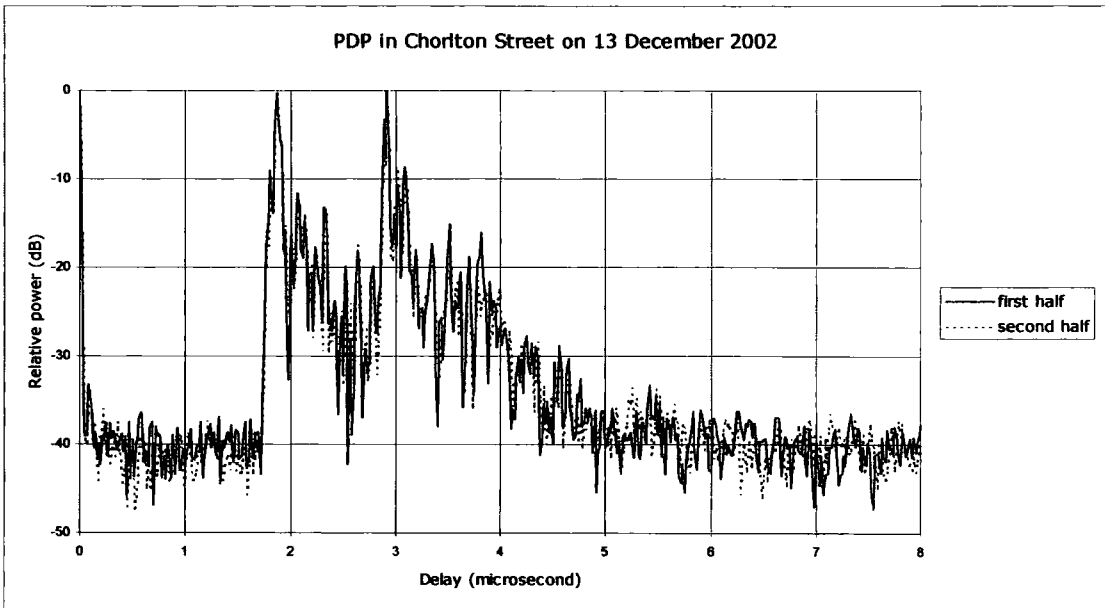

Figure 8.33 Power Delay Profile in Chorlton Street car park, Manchester on 17 December 2002.

Figures 8.31 and 8.32 show CDFs of the number of components in Chorlton Street car park on 17 December 2002. A different position from the February and April measurements was used. There was little difference between the first and second halves of the measurement run. The differences between the number of components detected on the three days shows how a small change of location can significantly affect the number of multipath components seen.

On this occasion no interference was detected. The PDP clearly shows two peaks containing the two components detected with a 6 dB threshold. A visual inspection of the PDPs of 5 sweeps at a time for the duration of the measurement run showed that each peak contained time varying components which exceeded the 6 dB threshold for some of the time. At this location the components appear to be a combination of reflections from buildings and interactions with moving motor vehicles.

Figures 8.31, 8.32 and 8.33 show the results from measurements in the lower band (1920 MHz to 1980 MHz). On 17 December 2002 the last set of measurements in the upper band (2110 MHz to 2170 MHz) were taken. A UMTS basestation became operational in 2003 which made further measurements in the upper band impossible. Figures 8.34, 8.35 and 8.36 show the upper band results.

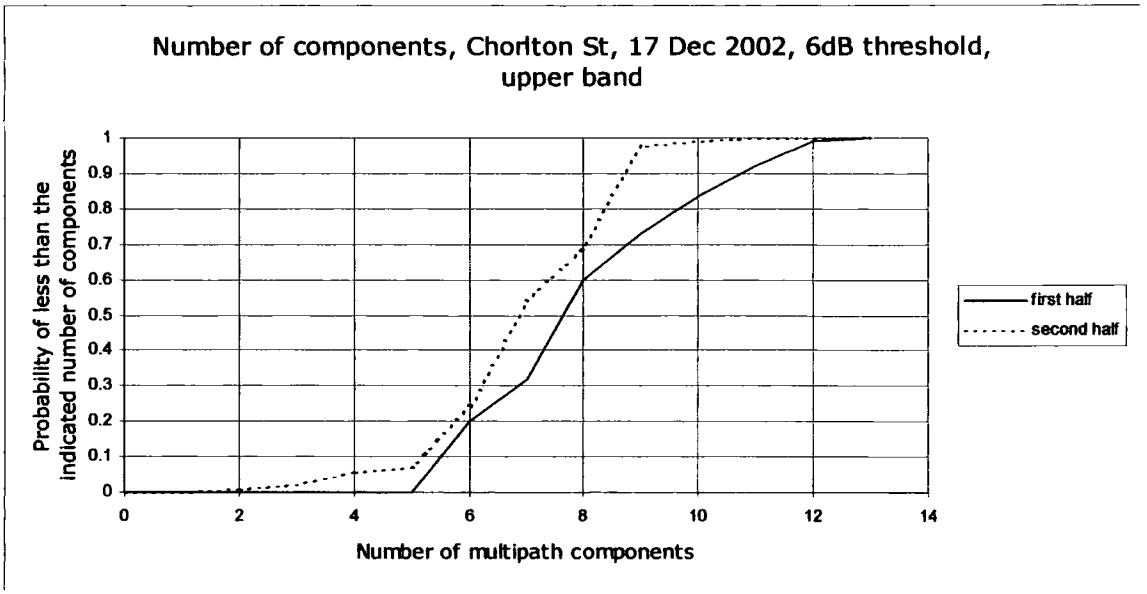

Figure 8.34 CDF of the number of multipath components in Chorlton Street car park, Manchester on 17 December 2002 with a 6 dB threshold, measurement in the upper band.

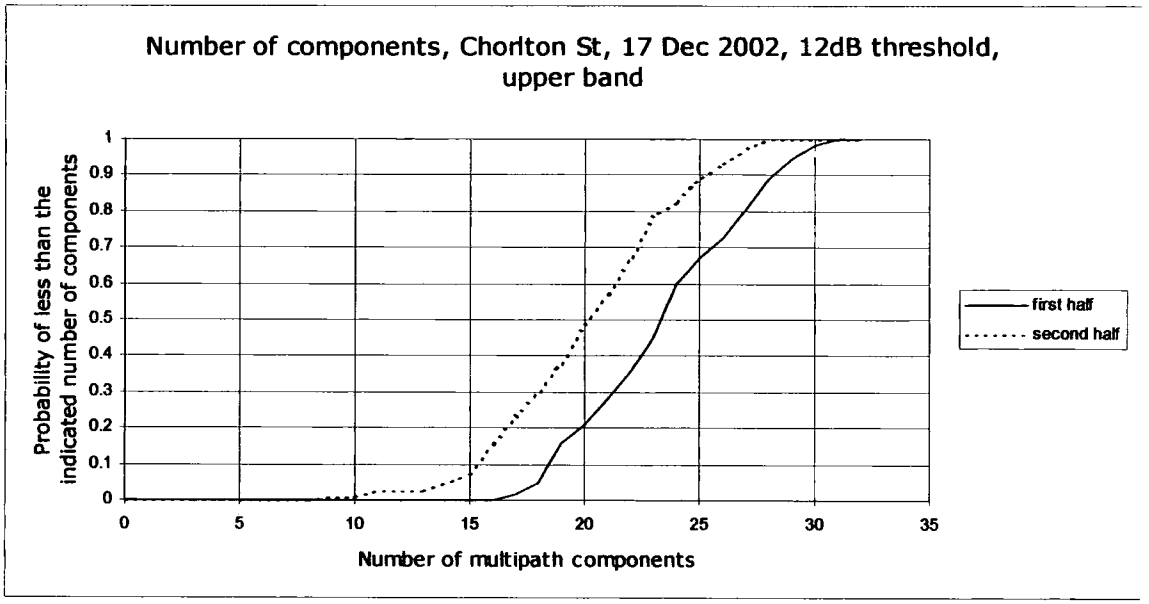

Figure 8.35 CDF of the Number of Multipath Components in Chorlton Street car park, Manchester on 17 December 2002 with a 12 dB threshold, measurement in the upper band.

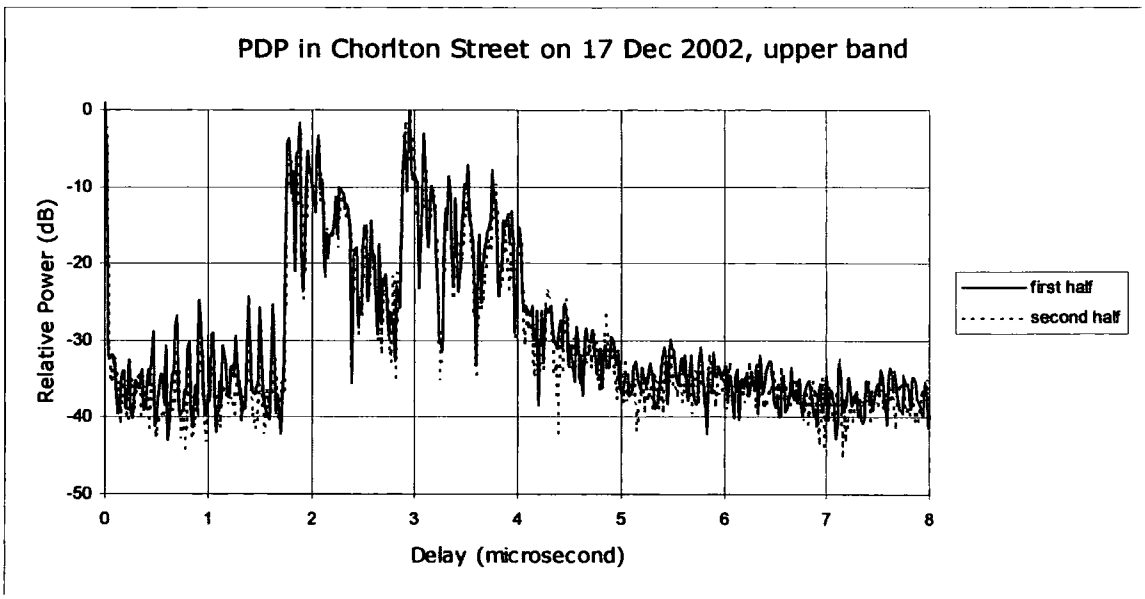

Figure 8.36 Power Delay Profile in Chorlton Street car park, Manchester on 17 December 2002, measurement in the upper band.

Examination of the PDP in figure 8.36 shows the same overall shape as that in figure 8.33 but in figure 8.36 there several components in a cluster with delays near to 2 microseconds whereas a single appears in figure 8.33. There is a similar cluster with delays near 3 microseonds. These clusters lead to the increased numbers of components detected and shown in figures 8.34 and 8.35. The reason for the difference in the results from the two bands is not clear. It is possible that the obstacles in the environment had different reflection coefficients at different frequencies.

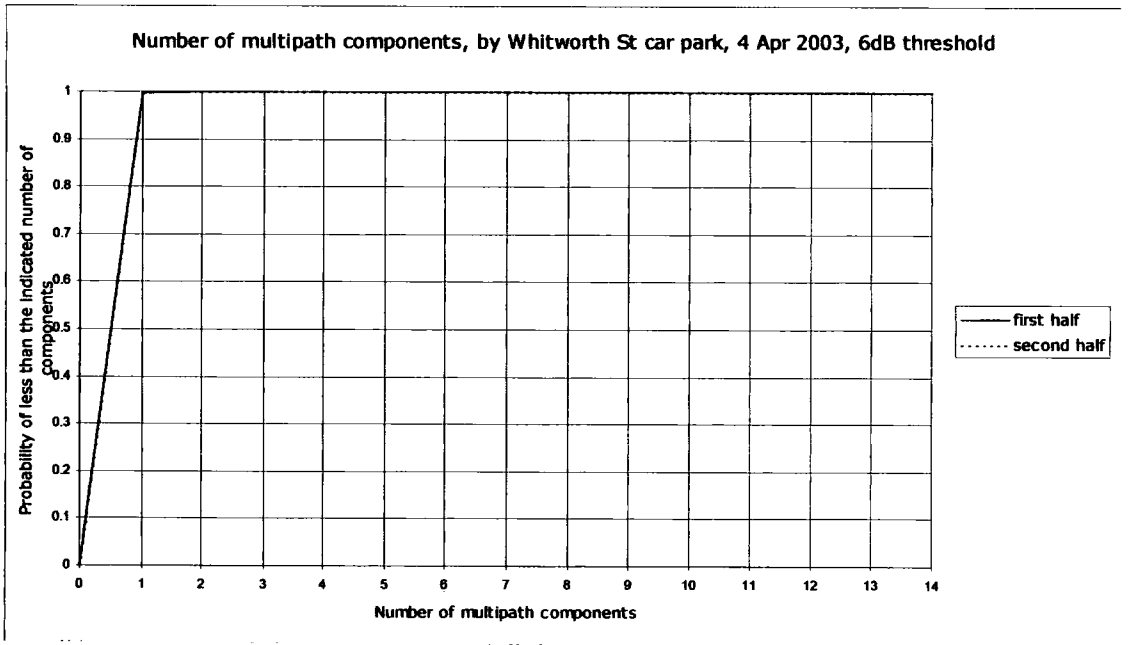

Figure 8.37 CDF of the Number of Multipath Components in Whitworth Street, Manchester on 4 April 2003 with a 6 dB threshold.

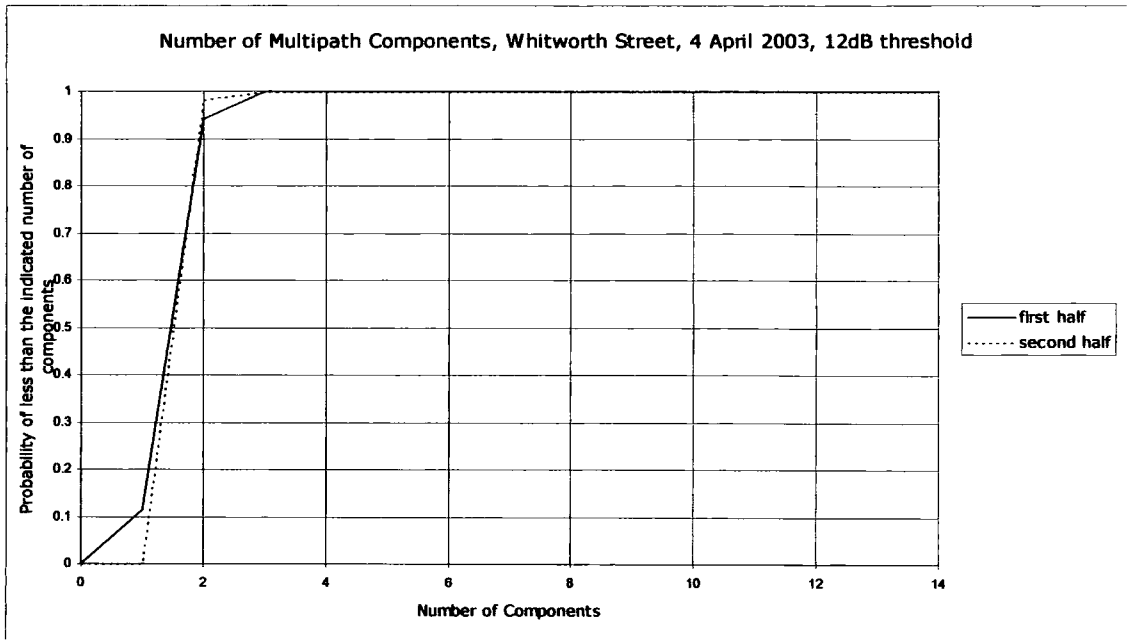

Figure 8.38 CDF of the Number of Multipath Components in Whitworth Street, Manchester on 4 April 2003 with a 12 dB threshold.

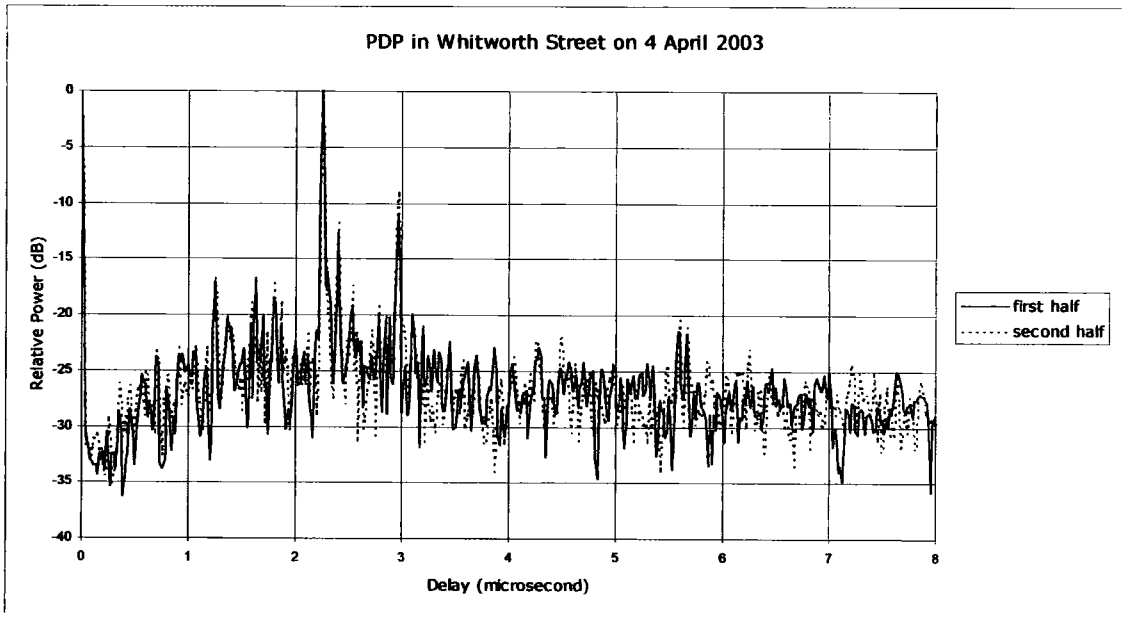

Figure 8.39 Power Delay Profile in Whitworth Street, Manchester on 4 April 2003.

Figures 8.37 and 8.38 shows CDFs of the number of components in Whitworth Street on 4 April 2003. Unfortunately, part of the way through the measurement run the sounder suffered a catastrophic loss of sensitivity. The measurement data file was truncated at the point at which this malfunction occurred.

With the 12 dB threshold a second component could be seen for some of the time. The PDP (figure 8.39) clearly shows two distinct peaks, the second of which exceeds the 12 dB threshold for some of the time. The strongest component will have been from the line of sight path between transmitter and receiver. The second component was probably reflected from the tall buildings around Oxford Road railway station and will have interacted with the motor vehicles moving along Whitworth Street. As might be expected there is very little difference between the first and second half of the measurement run with the 6 dB threshold showing the single line of sight component. With the 12 dB threshold there is a small difference caused by the traffic but the number of vehicles in Whitworth was nearly constant so the difference is small.

8.6.3 Summary

The tables below show the number of components exceeded for 10% of the time, the mean number of components and the median number of components.

Measurement	first half	second half
Traffic lights, Durham, 2 Jul 2004, 6dB	2	8
Traffic lights, Durham, 2 Jul 2004, 12dB	7	18
Roundabout, Durham, 26 Jul 2004, 6dB	4	4
Roundabout, Durham, 26 Jul 2004, 12dB	9	10
Roundabout, Durham, 28 Jul 2004, 6dB	2	2
Roundabout, Durham, 28 jul 2004, 12dB	5	5
Hallgarth St, Durham, 2 Aug 2004, 6dB	10	8
Hallgarth St, Durham, 2 Aug 2004, 12dB	20	20
Chorlton St, Manchester, 2 Apr 2003, 6dB	3	3
Chorlton St, Manchester, 2 Apr 2003, 12dB	8	8
Chorlton St, Manchester, 13 Feb 2003, 6dB	5	5
Chorlton St, Manchester, 13 Feb 2003, 12dB	11	11
Chorlton St, Manchester, 17 Dec 2002, 6dB, lower band	4	4
Chorlton St, Manchester, 17 Dec 2002, 12dB, lower band	8	9
Chorlton St, Manchester, 17 Dec 2002, 6dB, upper band	10	8
Chorlton St, Manchester, 17 Dec 2002, 12dB, upper band	28	25

Table 8.1 Number of components exceeded for 10% of the time.

Measurement	First half	Second half
Whitworth St Manchester, 4 Apr 2003, 6dB	1	1
Whitworth St, Manchester, 4 Apr 2003, 12dB	2	2

Table 8.1 (continued) Number of components exceeded for 10% of the time.

The figures in Table 8.1 correspond to the 0.9 probability level of the CDFs. The number of components varies from location to location and clearly shows the differences between locations a few metres apart as in Chorlton Street car park. There were significant differences between the first and second halves of the measurement run only at the traffic lights in Durham where the receiver was exposed to more moving traffic than in other locations.

Measurement	first half	second half
Traffic lights, Durham, 2 Jul 2004, 6dB	1.6	2.9
Traffic lights, Durham, 2 Jul 2004, 12dB	5.2	8.7
Roundabout, Durham, 26 Jul 2004, 6dB	3.2	2.8
Roundabout, Durham, 26 Jul 2004, 12dB	7.3	7.9
Roundabout, Durham, 28 Jul 2004, 6dB	2.1	2.0
Roundabout, Durham, 28 Jul 2004, 12dB	4.2	3.8
Hallgarth St, Durham, 2 Aug 2004, 6dB	8.8	7.8
Hallgarth St, Durham, 2 Aug 2004, 12dB	18.3	18.7
Chorlton St, Manchester, 2 Apr 2003, 6dB	3.0	2.6
Chorlton St, Manchester, 2 Apr 2003, 12dB	7.5	7.3
Chorlton St, Manchester, 13 Feb 2003, 6dB	3.8	4.4
Chorlton St, Manchester, 13 Feb 2003, 12dB	9.9	10.0
Chorlton St, Manchester, 17 Dec 2002, 6dB, lower band	3.6	3.7
Chorlton St, Manchester, 17 Dec 2002, 12dB, lower band	7.8	7.8
Chorlton St, Manchester, 17 Dec 2002, 6dB, upper band	8.4	7.4
Chorlton St, Manchester, 17 Dec 2002, 12dB, upper band	23.9	20.6
Whitworth St, Manchester, 4 Apr 2003, 6dB	1.0	1.0
Whitworth St, Manchester, 4 Apr 2003, 12dB	1.9	2.0

Table 8.2 Mean number of Multipath Components.

Measurement	first half	second half
Traffic lights, Durham, 2 Jul 2004, 6dB	1	1
Traffic lights, Durham, 2 Jul 2004, 12dB	5	6
Roundabout, Durham, 26 Jul 2004, 6dB	3	3
Roundabout, Durham, 26 Jul 2004, 12dB	7	8
Roundabout, Durham, 28 Jul 2004, 6dB	2	2
Roundabout, Durham, 28 Jul 2004, 12dB	4	4
Hallgarth St, Durham, 2 Aug 2004, 6dB	9	8
Hallgarth St, Durham, 2 Aug 2004, 12dB	18	19
Chorlton St, Manchester, 2 Apr 2003, 6dB	3	3
Chorlton St, Manchester, 2 Apr 2003, 12dB	7	7
Chorlton St, Manchester, 13 Feb 2003, 6dB	4	4
Chorlton St, Manchester, 13 Feb 2003, 12dB	10	10
Chorlton St, Manchester, 17 Dec 2002, 6dB, lower band	4	4
Chorlton St, Manchester, 17 Dec 2002, 12dB, lower band	8	8
Chorlton St, Manchester, 17 Dec 2002, 6dB, upper band	8	7
Chorlton St, Manchester, 17 Dec 2002, 12dB, upper band	24	21
Whitworth St, Manchester, 4 Apr 2003, 6dB	1	1
Whitworth St, Manchester, 4 Apr 2003, 12dB	2	2

Table 8.3 Median Number of Multipath Components.

There were differences between the mean number of multipath components detected in the two halves of the measurement run in all locations except Whitworth Street in Manchester where there was a line of sight path to the transmitter. Since the mean number of components involves fractions which are a difficult concept when considering effects which can only be counted in integers the median number of components was also extracted from the data. The median showed far less difference between first and second halves of the measurement run however the differences in mean and median indicated that there was variation with time.

The greatest difference was seen at the traffic lights in Durham where the variation was caused by interactions with motor traffic moving along the two roads crossing at the traffic lights. There were differences between locations which were separated by 5 m or less as in Chorlton Street car park and these differences were greater than those between the two halves. The largest number of multipath components was seen in Hallgarth Street in

Durham. This was due to the arrangement of the buildings and their orientation relative to the transmitter and receiver.

8.7 VARIATION OF MEAN DELAY

Associated with the temporal variation in the number of multipath components were variations in the mean delay of the radio channel. As for the number of multipath components thresholds of 6 dB and 12 dB were used. The mean delays are presented as CDFs since this is the most compact way of representing the variations in a large volume of data. Two ensembles of data have been extracted from the measurement data as the first and second halves of the measurement run. It should be noted that the individual delays and hence the mean delay are relative to an arbitrary datum since with the present sounder configuration it not possible to measure absolute delay.

In addition to a visual inspection of the data a Kolmogorov-Smirnof test was performed on each data set to determine the probability that the first half and second half ensembles belonged to the same population. The Kolmogorov-Smirnof test is a simple way of comparing two ensembles of measurements to see if they could have come from the same population. For this test the Null hypothesis is that the two ensembles do come from the same population. The Kolmogorov-Smirnov test is independent of the distribution of the data unlike other more sensitive tests. This test yields a Difference statistic and a Probability statistic. The Difference statistic is the greatest difference in probabilities found when comparing the CDFs of the two ensembles. A large difference indicates that the probability distributions of the mean delays in the two ensembles are significantly different. The Probability statistic gives a measure of the probability that the two ensembles come from the same population. A Probability of unity tends to confirm the Null hypothesis indicating that the two ensembles definitely come from the same population, a Probability of zero indicates that it is very unlikely that the two ensembles are from the same population and that the Null hypothesis should be rejected.

8.7.1 Durham

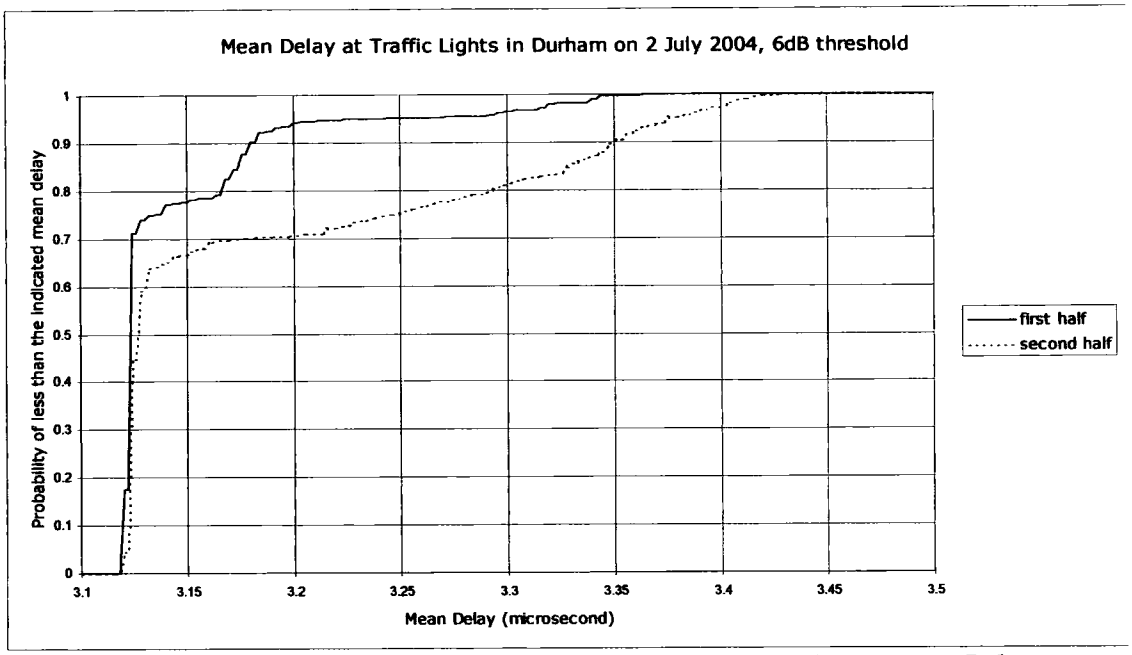

Figure 8.40 Mean Delay by the traffic lights in Durham on 2 July 2004 with a 6 dB threshold.

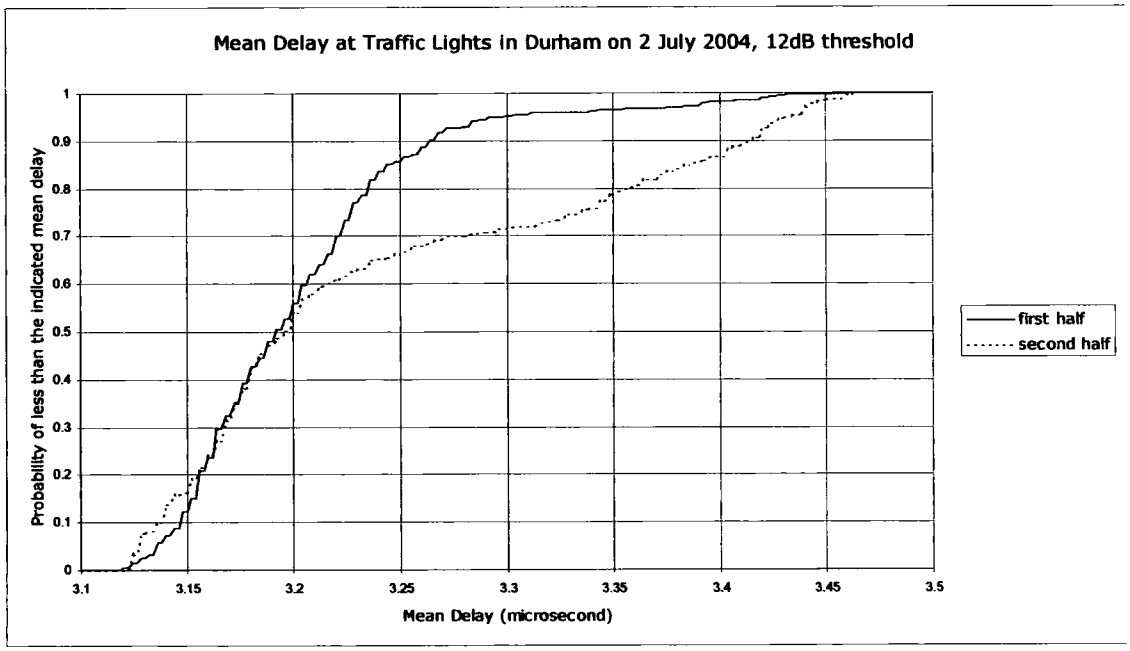

Figure 8.41 Mean Delay by the traffic lights in Durham on 2 July 2004 with a 12 dB threshold.

Figure 8.40 shows a very rapid increase in probability between 3.12 μsec and 3.13 μsec with a more gradual rise in probability for mean delay values greater than this. Reference to figure 8.12 shows that there was a high probability of a single component and smaller incremental probabilities of more than one component. As there was a direct line of sight path to

Durham Cathedral (a large building) it was to be expected that components reflected from this edifice would have a major influence on the mean delay. Since the cathedral does not move its influence did not vary with time whereas the delays from moving vehicles and vegetation did. There was a marked difference between the first and second half of the measurement run, probably due to uneven traffic flow across the cross-roads. Figure 8.41 shows a more continuous variation in the mean delay as with the 12 dB threshold more of the weaker components were captured and these will have been interactions with moving vehicles and local clutter.

The following CDFs are from measurements made on 26 July 2004 and 28 July 2004 on the Western approach island of the roundabout near the Science Laboratories main entrance. The receive antenna was as near to the same location as could be arranged on the two days. On 26 July there was more road traffic than on 28 July.

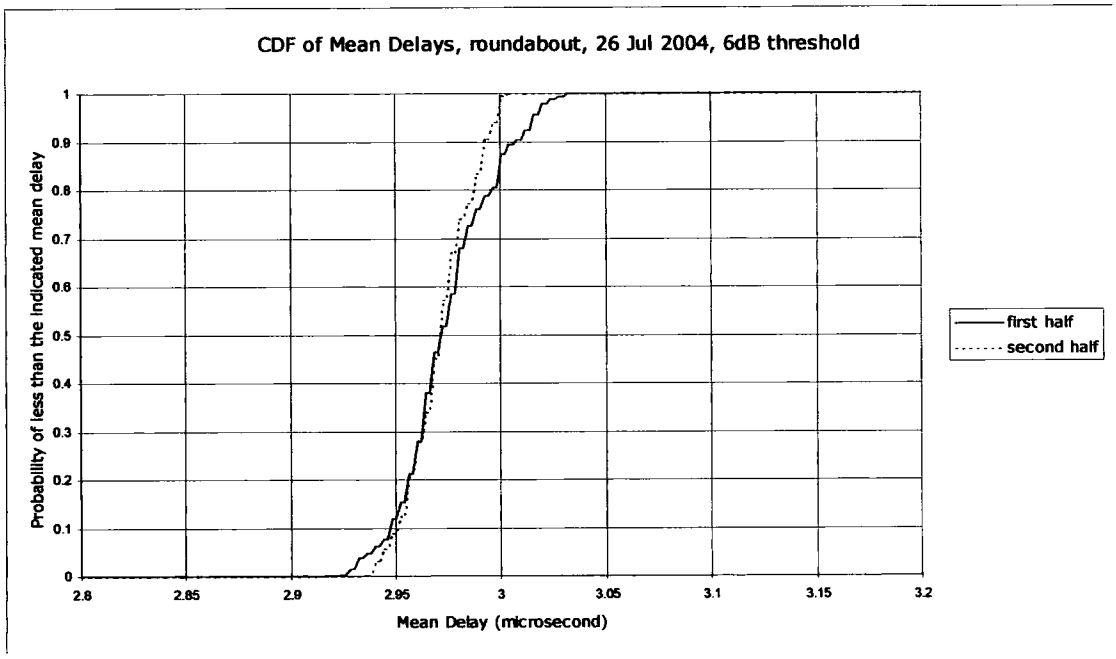

Figure 8.42 CDF of the mean delays at the roundabout on 26 July 2004 with a 6 dB threshold.

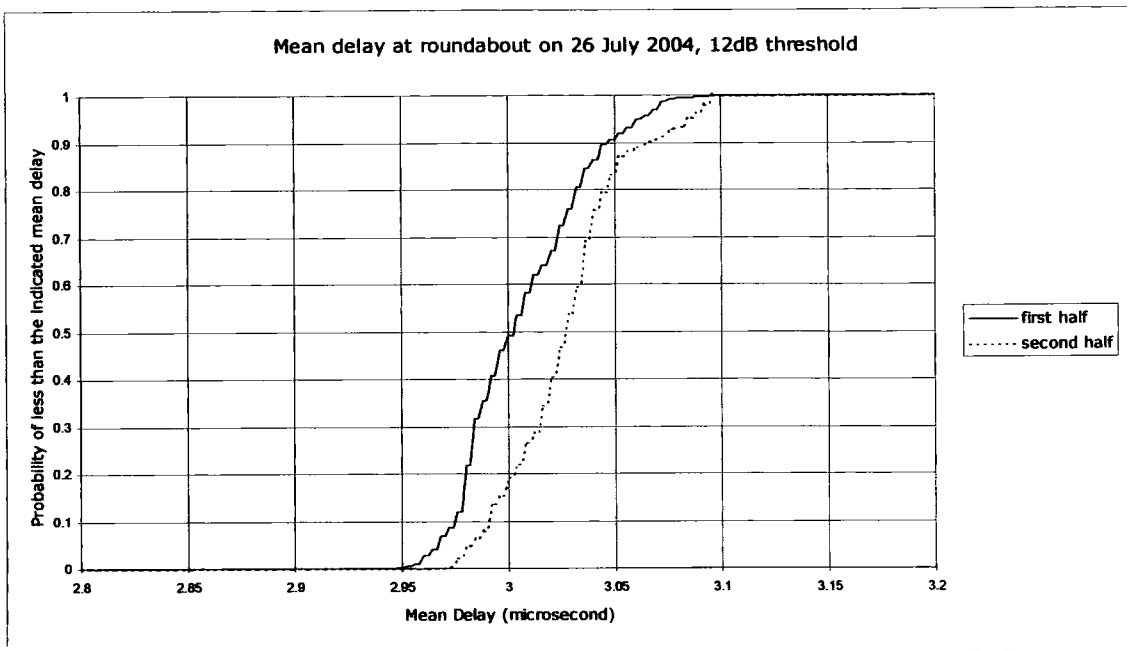

Figure 8.43 CDF of the mean delays at the roundabout on 26 July 2004 with a 12 dB threshold.

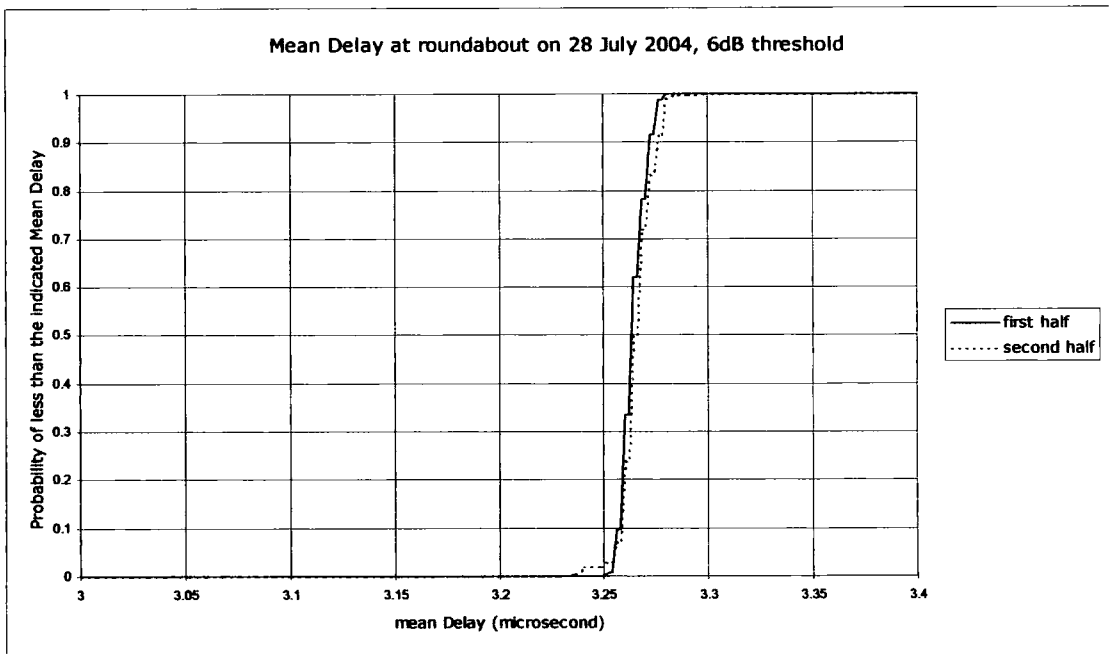

Figure 8.44 CDF of the mean delays at the roundabout on 28 July 2004 with a 6 dB threshold.

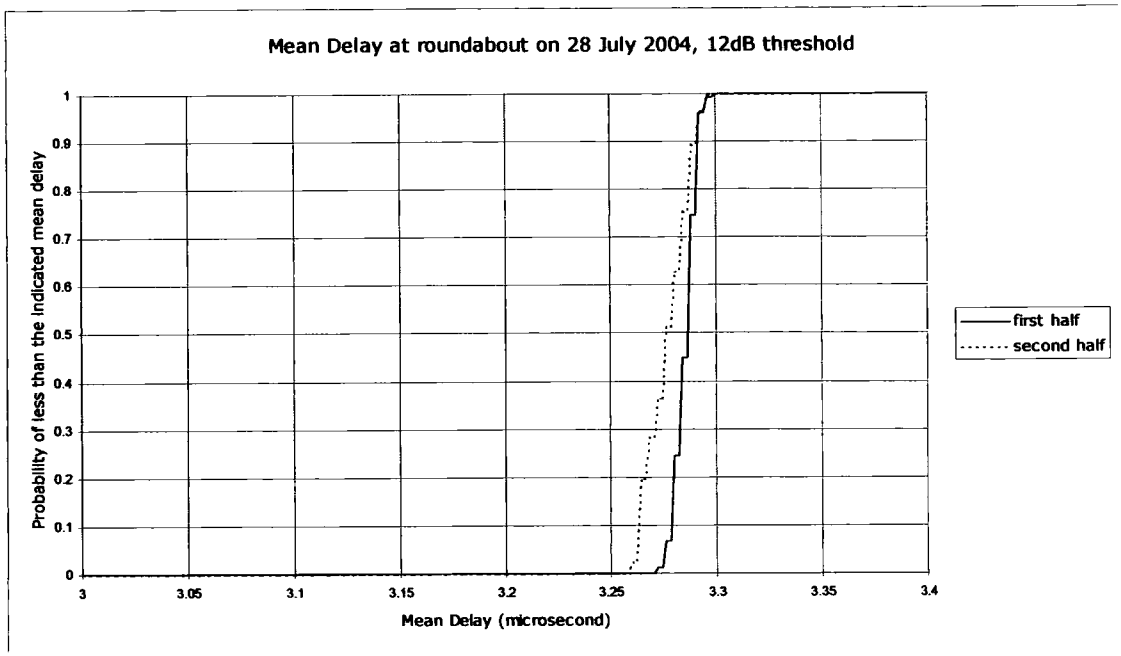

Figure 8.45 CDF of the mean delays at the roundabout on 28 July 2004 with a 12 dB threshold.

Figures 8.42, 8.43, 8.44 and 8.45 show CDFs of the mean delays at the roundabout on 26 July 2004 and 28 July 2004. The measurements were taken at the same place on both days but there could have been a significant fraction of a wavelength difference between the antenna locations. The mean delay scales are different because of the way the sounder was synchronised. In this location there was no line of sight to Durham Cathedral or to the transmitter. The numbers of multipath components (figures 8.16, 8.17, 8.19 and 8.20) was different on the two days but similar between the first and second halves of the measurement run. The measurements were made at different times of day and since the traffic density changes with time of day the difference in the numbers of multipath components and distribution of mean delay was not unexpected.

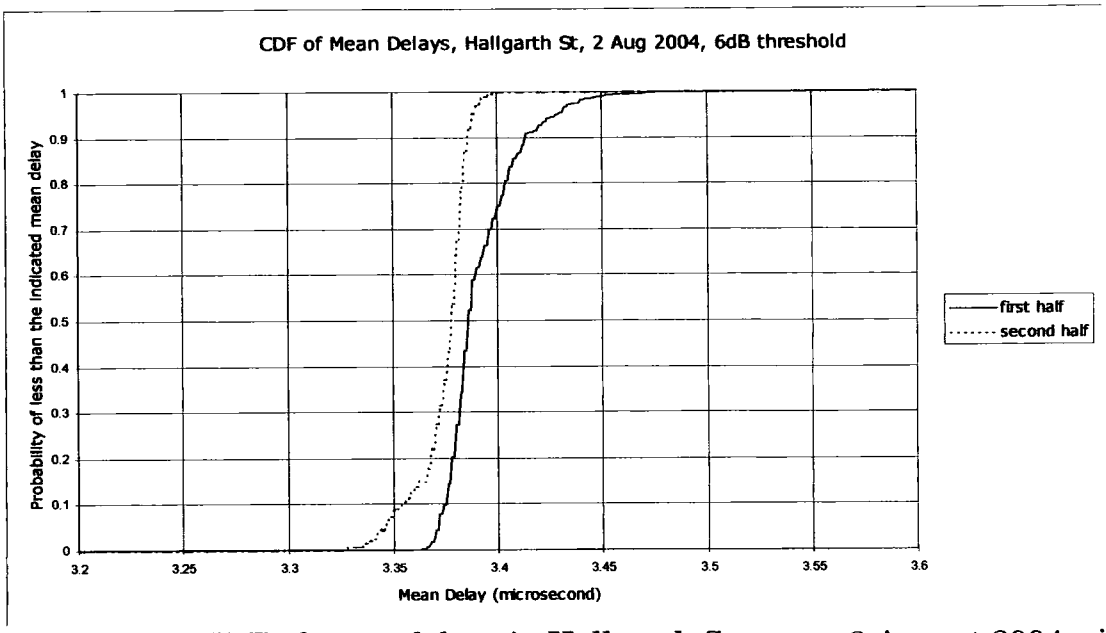

Figure 8.46 CDF of mean delays in Hallgarth Street on 2 August 2004 with a 6 dB threshold.

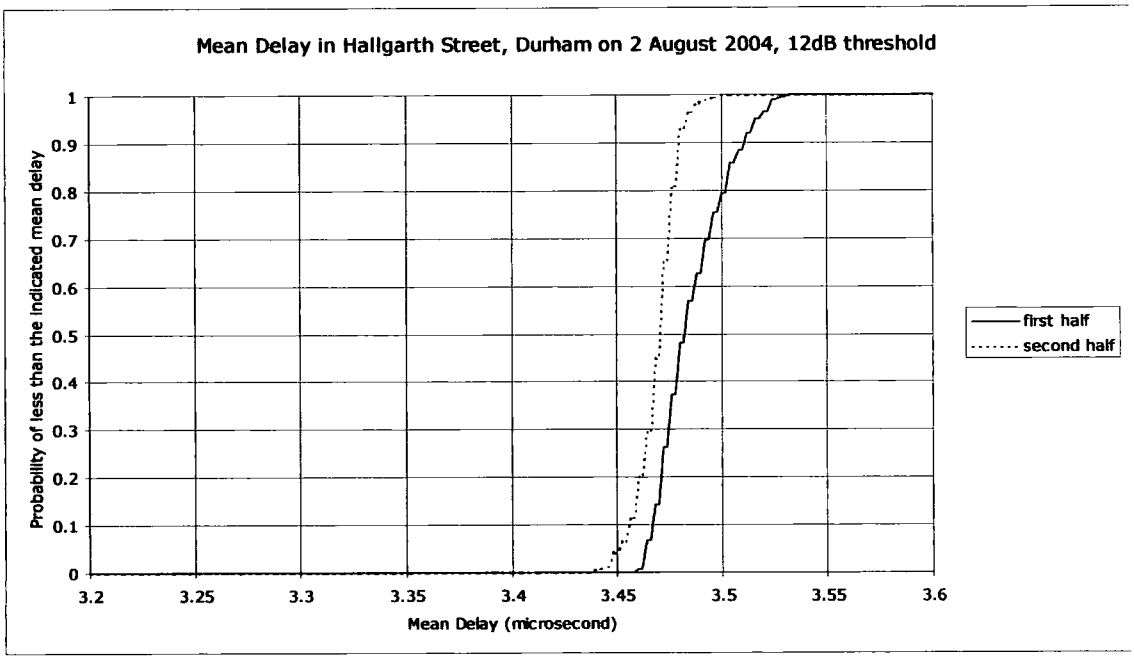

Figure 8.47 CDF of mean delays in Hallgarth Street on 2 August 2004 with a 12 dB threshold.

Figures 8.46 and 8.47 show CDFs of the mean delays in Hallgart Street on 2 August 2004. Figures 8.22 and 8.23 show that there were more multipath components than in other locations. Also, there was no line of sight path to Durham Cathedral or the transmitter and there was little traffic in the street.

8.7.2 Manchester

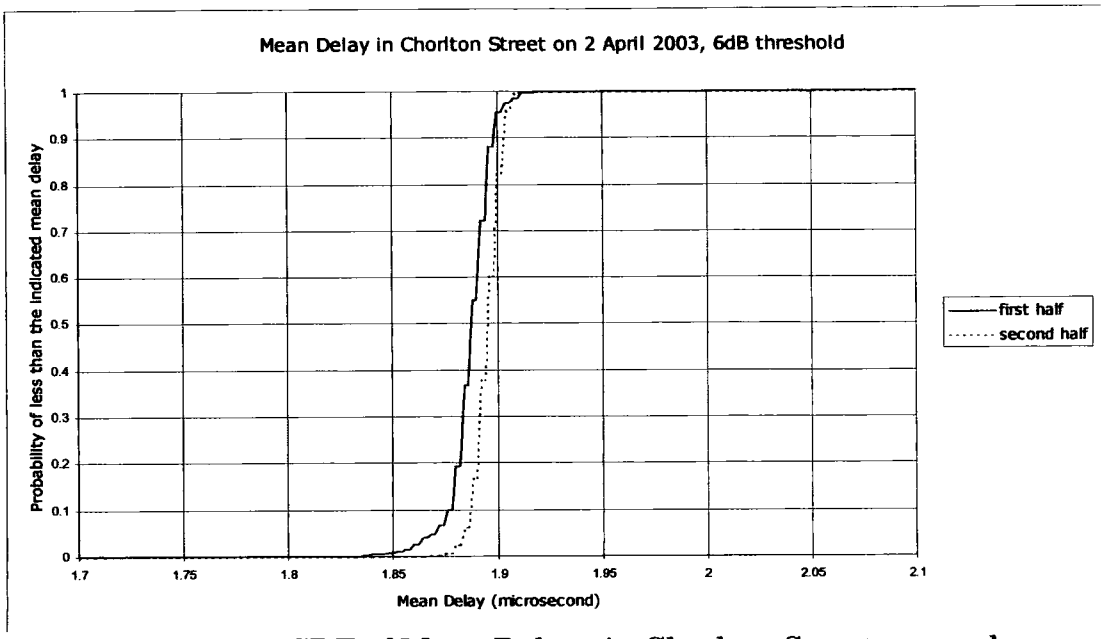

Figure 8.48 CDF of Mean Delays in Chorlton Street car park on 2 April 2003 with 6 dB threshold

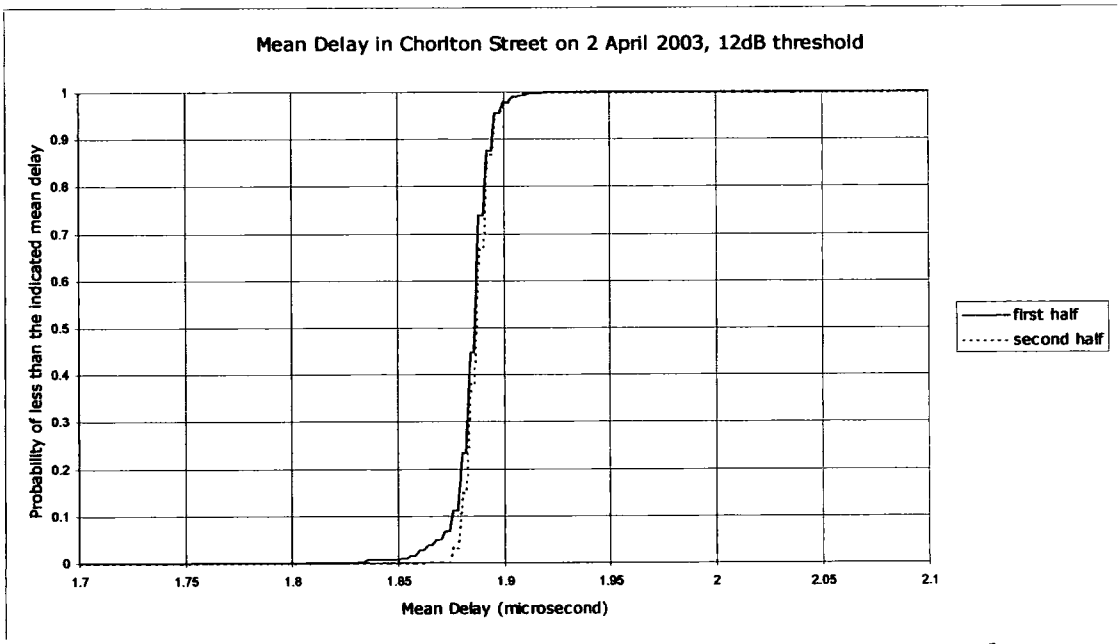

Figure 8.49 CDF of Mean Delays in Chorlton Street car park on 2 April 2003 with 12 dB threshold.

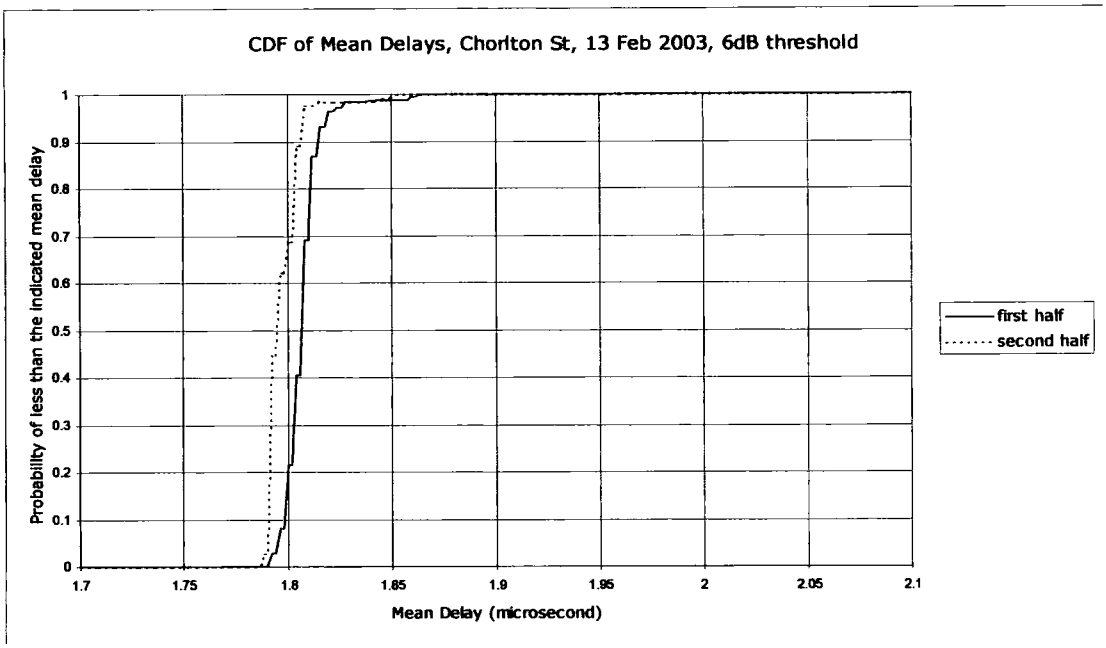

Figure 8.50 CDF of Mean Delays in Chorlton Street car park on 13 February 2003 with 6 dB threshold.

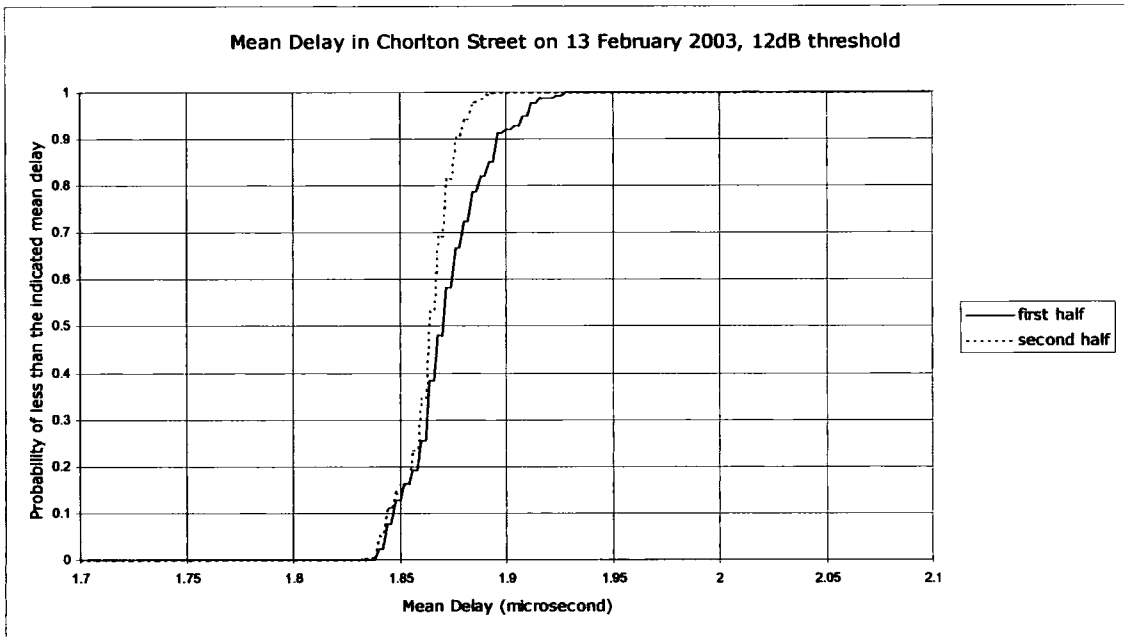

Figure 8.51 CDF of Mean Delays in Chorlton Street car park on 13 Feb 2003 with 12 dB threshold.

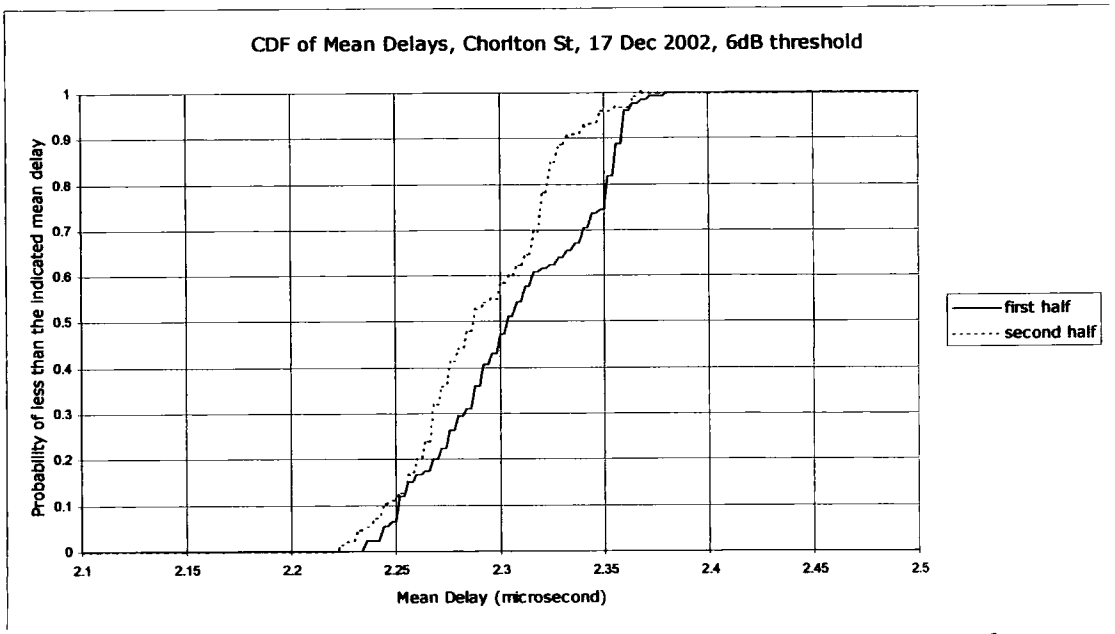

Figure 8.52 CDF of Mean Delays in Chorlton Street car park on 17 December 2002 with 6 dB threshold, measurement in the lower band.

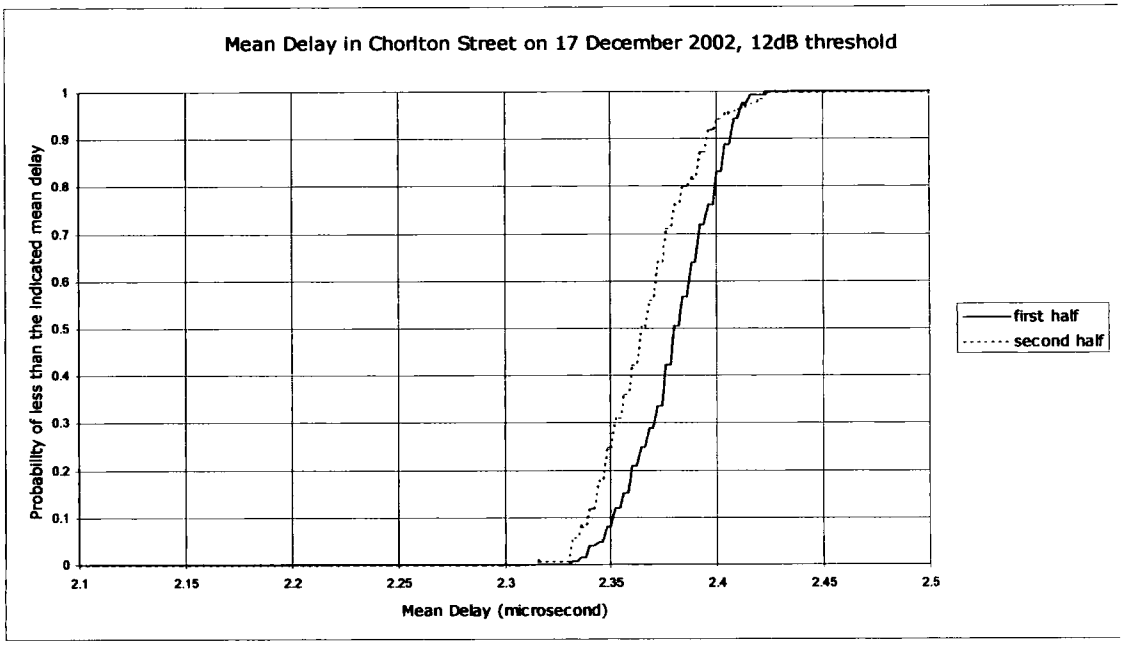

Figure 8.53 CDF of Mean Delays in Chorlton Street car park on 17 December 2002 with 12 dB threshold, measurement in the lower band.

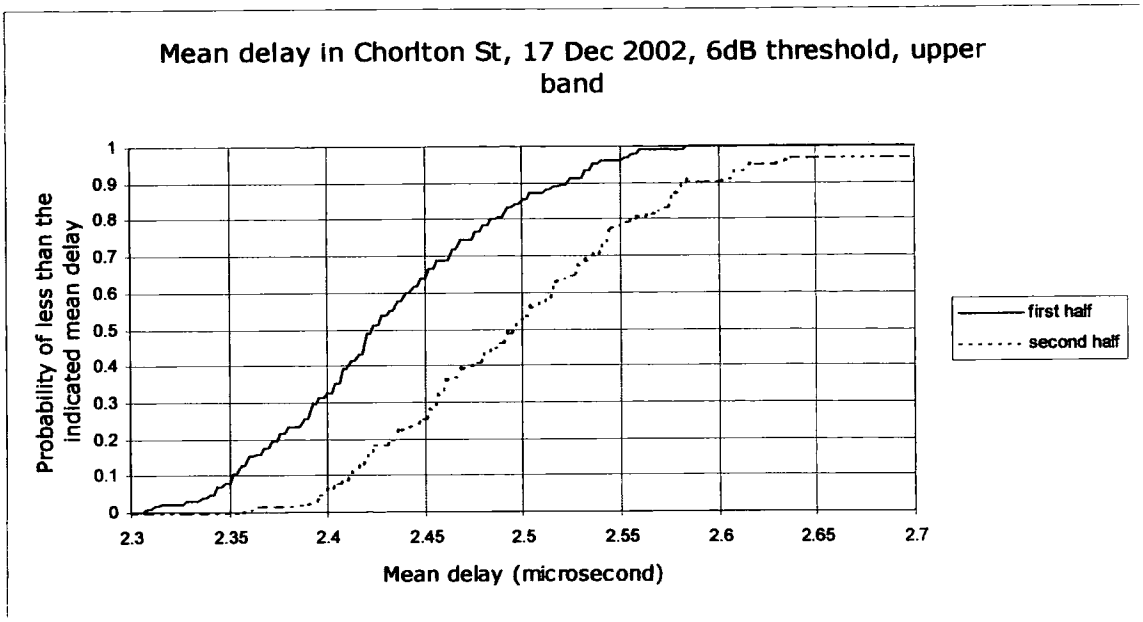

Figure 8.54 CDF of Mean Delays in Chorlton Street car park on 17 December 2002 with 6 dB threshold, measurement in the upper band.

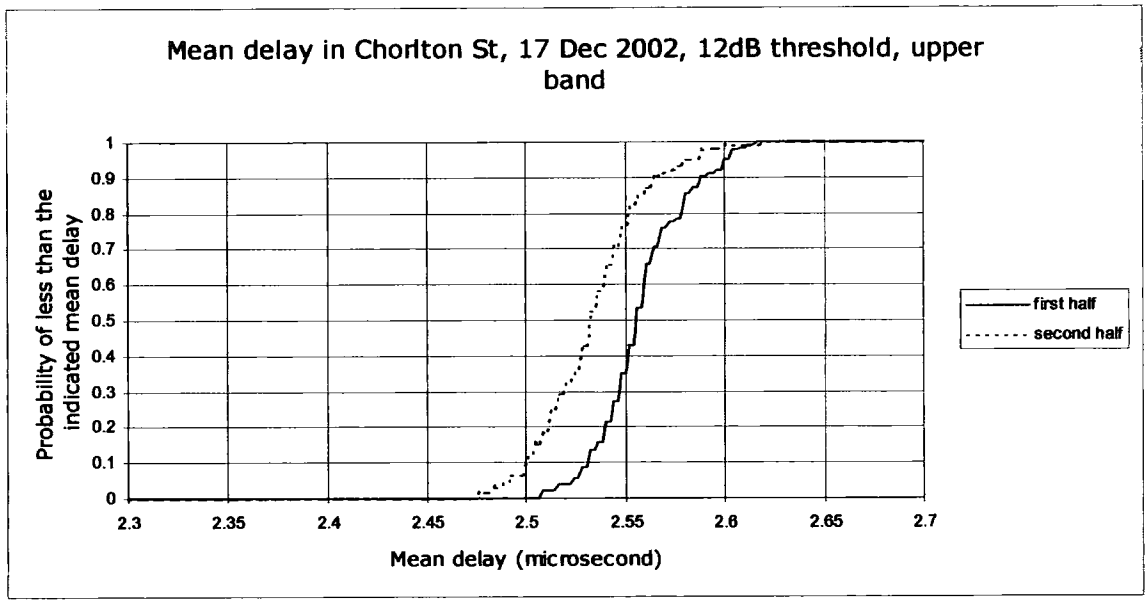

Figure 8.55 CDF of Mean Delays in Chorlton Street car park on 17 December 2002 with 12 dB threshold, measurement in the upper band.

Figures 8.48, 8.49, 8.50, 8.51, 8.52 and 8.53 show CDFs of the mean delays in Chorlton Street car park. The measurements on the three days were in slightly different locations since the parked cars prevented use of the same location. The location used on 17 December 2002 was nearer to Chorlton Street and hence more exposed to the effects of passing vehicles including buses entering and leaving Bloom Street bus station. The locations on the other two days had to be further from the road. In all three locations there

was a difference between the first and second halves of the measurement run. On 17 December there was greater variation during each half of the run, probably due the presence of a number of buses which had a larger RCS than the cars using Chorlton Street.

Figures 8.54 and 8.55 show the variation of the mean delays in the upper band on 17 December 2002. Comparing these figures with figures 8.52 and 8.53 shows more variation in the upper band, particularly when using a 6 dB threshold. The mean delay also appears to be greater in the upper band than in the lower band. A comparison of figures 8.33 and 8.36 shows that there were more multipath components recorded in the upper band than in the lower band and many of these will have been taken into consideration when calculating the mean delays.

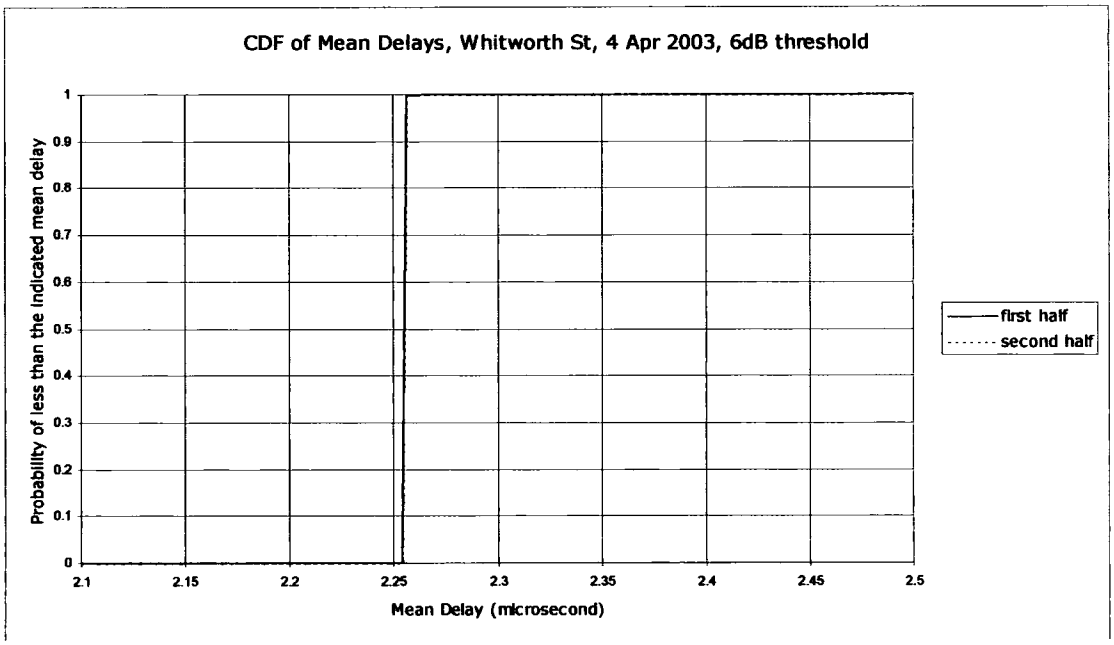

Figure 8.56 CDF of Mean Delays in Whitworth Street on 4 April 2003 with a 6 dB threshold.

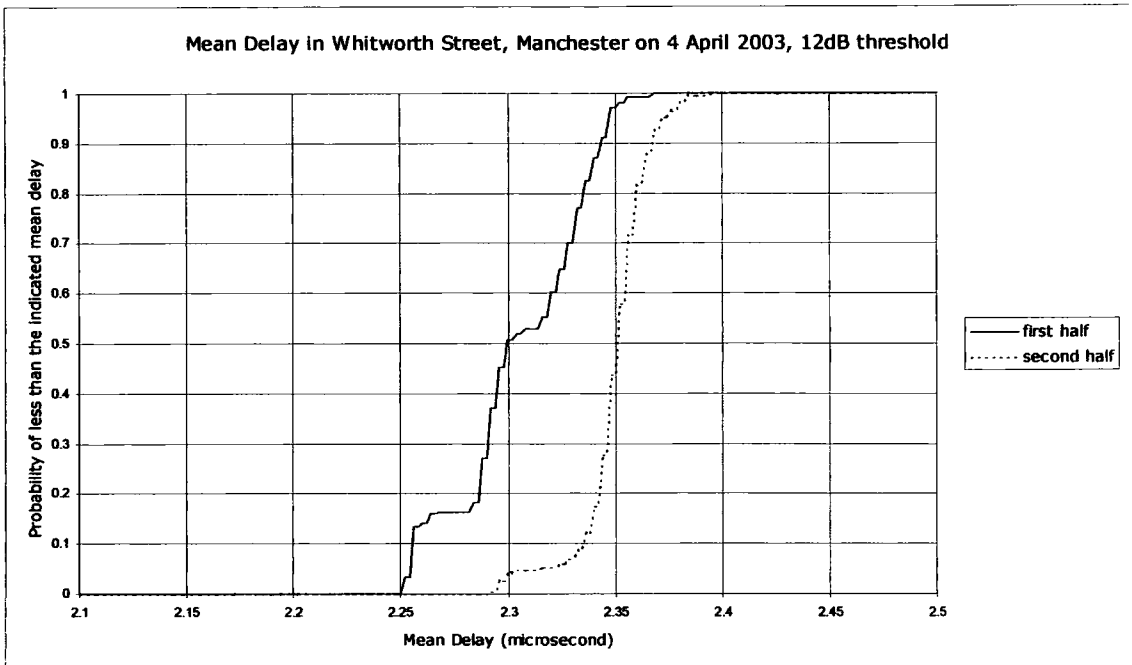

Figure 8.57 CDF of Mean Delays in Whitworth Street on 4 April 2003 with a 12 dB threshold.

At the location in Whitworth Street there was a line of sight path between the transmitter and receiver. The very small variation in mean delay with a 6 dB threshold was not unexpected since for most of the time only a single multipath component was considered. With a 12 dB threshold more multipath components were considered and these were the result of interactions with local clutter and moving vehicles. The difference between the first and second halves of the measurement run are almost certainly due to uneven traffic flow along Whitworth Street and the varying number of multipath components received after reflection from moving vehicles.

8.7.3 Summary of Differences

Table 8.4 below shows the results from Kolmogov-Smirnof tests on the first and second half ensembles for the locations at which measurements were made in Durham. Table 8.5 shows the results for measurement locations in Manchester. All the measurements shown in tables 8.4 and 8.5 were made with omnidirectional antennas.

Measurement	K-S D	K-S P
Traffic lights, 2 Jul 2004, 6dB threshold	0.28	0.000000
Traffic lights, 2 Jul 2004, 12dB threshold	0.24	0.000000
Roundabout, 26 Jul 2004, 6dB threshold	0.14	0.001117
Roundabout, 26 Jul 2004, 12dB threshold	0.34	0.000000
Roundabout, 28 Jul 2004, 6dB threshold	0.16	0.000135
Roundabout, 28 Jul 2004, 12dB threshold	0.45	0.000000
Hallgarth St, 2 Aug 2004, 6dB threshold	0.46	0.000000
Hallgarth St, 2 Aug 2004, 12dB threshold	0.45	0.000000

Table 8.4 Kolmogorov-Smirnof test results for measurement locations in Durham.

Measurement	K-S D	K-S P
Chorlton St, 2 Apr 2003, 6dB threshold	0.42	0.000000
Chorlton St, 2 Apr 2003, 12dB threshold	0.096	0.063109
Chorlton St, 13 Feb 2003, 6dB threshold	0.56	0.000000
Chorlton St, 13 Feb 2003, 12dB threshold	0.26	0.000000
Chorlton St, 17 Dec 2002, 6dB threshold, lower band	0.26	0.000554
Chorlton St, 17 Dec 2002, 12dB threshold, lower band	0.31	0.000010
Chorlton St, 17 Dec 2002, 6dB threshold, upper band	0.39	0.000000
Chorlton St, 17 Dec 2002, 12dB threshold, upper band	0.46	0.000000
Whitworth St, 4 Apr 2003, 6dB threshold	0.089	0.236490
Whitworth St, 4 Apr 2003, 12dB threshold	0.71	0.000000

Table 8.5 Kolmogorov-Smirnof test results for measurement locations in Manchester.

8.7.4 Results from Directional Antennas

All the previous results have been from measurements using omnidirectional antennas. To discover whether a directional antenna changes the temporal variation exhibited by the radio channel the results of measurements using directional antennas were considered. The following tables 8.6 and 8.7 show the Kolmogorov-Smirnof statistics from the measurements in Durham and Manchester respectively.

Measurement	K-S D	K-S P
Traffic lights, 2 Jul 2004, ch 1, 6dB threshold	0.10	0.034636
Traffic lights, 2 Jul 2004, ch1, 12dB threshold	0.20	0.000001
Traffic lights, 2 Jul 2004, ch 2, 6dB threshold	0.17	0.000051
Traffic lights, 2 Jul 2004, ch 2, 12dB threshold	0.14	0.000839
Traffic lights, 2 Jul 2004, ch 3, 6dB threshold	0.23	0.000000
Traffic lights, 2 Jul 2004, ch 3, 12dB threshold	0.24	0.000000
Traffic lights, 2 Jul 2004, ch 4, 6dB threshold	0.38	0.000000
Traffic lights, 2 Jul 2004, ch 4, 12dB threshold	0.41	0.000000
Traffic lights, 2 Jul 2004, ch 5, 6dB threshold	0.16	0.000098
Traffic lights, 2 Jul 2004, ch 5, 12dB threshold	0.24	0.000000
Traffic lights, 2 Jul 2004, ch 6, 6dB threshold	0.13	0.004293
Traffic lights, 2 Jul 2004, ch 6, 12dB threshold	0.18	0.000013
Roundabout, 26 Jul 2004, ch 1, 6dB threshold	0.55	0.000000
Roundabout, 26 Jul 2004, ch 1, 12dB threshold	0.61	0.000000
Roundabout, 26 Jul 2004, ch 2, 6dB threshold	0.62	0.000000
Roundabout, 26 Jul 2004, ch 2, 12dB threshold	0.18	0.000009
Roundabout, 26 Jul 2004, ch 3, 6dB threshold	0.46	0.000000
Roundabout, 26 Jul 2004, ch 3, 12dB threshold	0.21	0.000000
Roundabout, 26 Jul 2004, ch 4, 6dB threshold	0.40	0.000000
Roundabout, 26 Jul 2004, ch 4, 12dB threshold	0.41	0.000000
Roundabout, 26 Jul 2004, ch 5, 6dB threshold	0.31	0.000000
Roundabout, 26 Jul 2004, ch 5, 12dB threshold	0.12	0.009033
Roundabout, 26 Jul 2004, ch 6, 6dB threshold	0.083	0.154127
Roundabout, 26 Jul 2004, ch 6, 12dB threshold	0.34	0.000000
Roundabout, 28 Jul 2004, ch 1, 6dB threshold	0.36	0.000000
Roundabout, 28 Jul 2004, ch 1, 12dB threshold	0.16	0.000135
Roundabout, 28 Jul 2004, ch 2, 6dB threshold	0.24	0.000000
Roundabout, 28 Jul 2004, ch 2, 12dB threshold	0.17	0.000051
Roundabout, 28 Jul 2004, ch 3, 6dB threshold	0.49	0.000000
Roundabout, 28 Jul 2004, ch 3, 12dB threshold	0.82	0.000000
Roundabout, 28 Jul 2004, ch 4, 6dB threshold	0.25	0.000000
Roundabout, 28 Jul 2004, ch 4, 12dB threshold	0.21	0.000000

Table 8.6 Kolmogorov-Smirnof test results for measurement locations in Durham using directional antennas.

Measurement	K-S D	K-S P
Roundabout, 28 Jul 2004, ch 5, 6dB threshold	0.15	0.000345
Roundabout, 28 Jul 2004, ch 5, 12dB threshold	0.31	0.000000
Roundabout, 28 Jul 2004, ch 6, 6dB threshold	0.13	0.004293
Roundabout, 28 Jul 2004, ch 6, 12dB threshold	0.18	0.000018
Hallgarth St, 2 Aug 2004, ch 1, 6dB threshold	0.60	0.000000
Hallgarth St, 2 Aug 2004, ch 1, 12dB threshold	0.10	0.034636
Hallgarth St, 2 Aug 2004, ch 2, 6dB threshold	0.42	0.000000
Hallgarth St, 2 Aug 2004, ch 2, 12dB threshold	0.73	0.000000
Hallgarth St, 2 Aug 2004, ch 3, 6dB threshold	0.92	0.000000
Hallgarth St, 2 Aug 2004, ch 3, 12dB threshold	0.64	0.000000
Hallgarth St, 2 Aug 2004, ch 4, 6dB threshold	0.52	0.000000
Hallgarth St, 2 Aug 2004, ch 4, 12dB threshold	0.45	0.000000
Hallgarth St, 2 Aug 2004, ch 5, 6dB threshold	0.23	0.000000
Hallgarth St, 2 Aug 2004, ch 5, 12dB threshold	0.13	0.003314
Hallgarth St, 2 Aug 2004, ch 6, 6dB threshold	0.52	0.000000
Hallgarth St, 2 Aug 2004, ch 6, 12dB threshold	0.28	0.000000

Table 8.6(continued) Kolmogorov-Smirnof test results for measurement locations in Durham using directional antennas.

Measurement	K-S D	K-S P
Chorlton St, 2 Apr 2003, ch 1, 6dB threshold	0.22	0.000000
Chorlton St, 2 Apr 2003, ch 1, 12dB threshold	0.23	0.000000
Chorlton St, 2 Apr 2003, ch 2, 6dB threshold	0.67	0.000000
Chorlton St, 2 Apr 2003, ch 2, 12dB threshold	0.50	0.000000
Chorlton St, 2 Apr 2003, ch 3, 6dB threshold	0.35	0.000000
Chorlton St, 2 Apr 2003, ch 3, 12dB threshold	0.54	0.000000
Chorlton St, 2 Apr 2003, ch 4, 6dB threshold	0.57	0.000000
Chorlton St, 2 Apr 2003, ch 4, 12dB threshold	0.61	0.000000
Chorlton St, 2 Apr 2003, ch 5, 6dB threshold	0.26	0.000000
Chorlton St, 2 Apr 2003, ch 5, 12dB threshold	0.15	0.000254
Chorlton St, 2 Apr 2003, ch 6, 6dB threshold	0.18	0.000013
Chorlton St, 2 Apr 2003, ch 6, 12dB threshold	0.93	0.000000
Chorlton St, 13 Feb 2003, ch 1, 6dB threshold	0.20	0.000091
Chorlton St, 13 Feb 2003, ch 1, 12dB threshold	0.45	0.000000
Chorlton St, 13 Feb 2003, ch 2, 6dB threshold	0.35	0.000000
Chorlton St, 13 Feb 2003, ch 2, 12dB threshold	0.44	0.000000
Chorlton St, 13 Feb 2003, ch 3, 6dB threshold	0.32	0.000000
Chorlton St, 13 Feb 2003, ch 3, 12dB threshold	0.92	0.000000
Chorlton St, 13 Feb 2003, ch 4, 6dB threshold	0.71	0.000000
Chorlton St, 13 Feb 2003, ch 4, 12dB threshold	0.25	0.000000
Chorlton St, 13 Feb 2003, ch 5, 6dB threshold	0.39	0.000000
Chorlton St, 13 Feb 2003, ch 5, 12dB threshold	0.59	0.000000
Chorlton St, 13 Feb 2003, ch 6, 6dB threshold	0.23	0.000003
Chorlton St, 13 Feb 2003, ch 6, 12dB threshold	0.32	0.000000

Table 8.7 Results from Kolmogorov-Smirnof test for measurement locations in Manchester using directional antennas.

Measurement	K-S D	K-S P
Chorlton St, 17 Dec 2002, ch 1, 6dB threshold, lower band	0.25	0.000917
Chorlton St, 17 Dec 2002, ch 1, 12dB threshold, lower band	0.39	0.000000
Chorlton St, 17 Dec 2002, ch1, 6dB threshold, upper band	0.168	0.058726
Chorlton St, 17 Dec 2002, ch1, 12dB threshold, upper band	0.192	0.0199943
Chorlton St, 17 Dec 2002, ch 2, 6dB threshold, lower band	0.73	0.000000
Chorlton St, 17 Dec 2002, ch 2, 12dB threshold, lower band	0.36	0.000000
Chorlton St, 17 Dec 2002, ch 2, 6dB threshold, upper band	0.12	0.329105
Chorlton St, 17 Dec 2002, ch 2, 12dB threshold, upper band	0.44	0.000000
Chorlton St, 17 Dec 2002, ch 3, 6dB threshold, lower band	0.71	0.000000
Chorlton St, 17 Dec 2002, ch 3, 12dB threshold, lower band	0.74	0.000000
Chorlton St, 17 Dec 2002, ch 3, 6dB threshold, upper band	0.416	0.000000
Chorlton St, 17 Dec 2002, ch 3, 12dB threshold, upper band	0.248	0.000917
Chorlton St, 17 Dec 2002, ch 4, 6dB threshold, lower band	0.44	0.000000
Chorlton St, 17 Dec 2002, ch 4, 12dB threshold, lower band	0.52	0.000000
Chorlton St, 17 Dec 2002, ch 4, 6dB threshold, upper band	0.288	0.000063
Chorlton St, 17 Dec 2002, ch 4, 12dB threshold, upper band	0.16	0.081519
Chorlton St, 17 Dec 2002, ch 5, 6dB threshold, lower band	0.17	0.058726
Chorlton St, 17 Dec 2002, ch 5, 12dB threshold, lower band	0.17	0.058726
Chorlton St, 17 Dec 2002, ch 5, 6dB threshold, upper band	0.272	0.000193
Chorlton St, 17 Dec 2002, ch 5, 12dB threshold, upper band	0.376	0.000000

Table 8.7(continued) Results from Kolmogorov-Smirnof test for measurement locations in Manchester using directional antennas

Measurement	K-S D	K-S P
Chorlton St, 17 Dec 2002, ch 6, 6dB threshold, lower band	0.24	0.001493
Chorlton St, 17 Dec 2002, ch 6, 12dB threshold, lower band	0.32	0.000006
Chorlton St, 17 Dec 2002, ch 6, 6dB threshold, upper band	0.408	0.000000
Chorlton St, 17 Dec 2002, ch 6, 12dB threshold, upper band	0.536	0.000000
Whitworth St, 4 Apr 2003, ch 1, 6dB threshold	0.28	0.000000
Whitworth St, 4 Apr 2003, ch 1, 12dB threshold	0.28	0.000000
Whitworth St, 4 Apr 2003, ch 2, 6dB threshold	0.55	0.000000
Whitworth St, 4 Apr 2003, ch 2, 12dB threshold	0.47	0.000000
Whitworth St, 4 Apr 2003, ch 3, 6dB threshold	0.40	0.000000
Whitworth St, 4 Apr 2003, ch 3, 12dB threshold	0.71	0.000000
Whitworth St, 4 Apr 2003, ch 4, 6dB threshold	0.21	0.000008
Whitworth St, 4 Apr 2003, ch 4, 12dB threshold	0.40	0.000000
Whitworth St, 4 Apr 2003, ch 5, 6dB threshold	0.45	0.000000
Whitworth St, 4 Apr 2003, ch 5, 12dB threshold	0.49	0.000000
Whitworth St, 4 Apr 2003, ch 6, 6dB threshold	0.27	0.000000
Whitworth St, 4 Apr 2003, ch 6, 12dB threshold	0.32	0.000000

Table 8.7(continued) Results from Kolmogorov-Smirnof test for measurement locations in Manchester using directional antennas

From tables 8.4, 8.5, 8.6 and 8.7 it can be seen that there are significant differences between the first half and second half ensembles. Only in the case of Whitworth Street when using an omnidirectional antenna was there more than a very small probability that the first half and second half ensembles came from the same population. In this location there was a line of sight path between transmitter and receiver so the signal received via this direct path would have been much stronger than any signal received after interaction with the environment. The direction of the transmitter was midway between the boresight directions of the antennas on channels 1 and 6 when using directional antennas. The signal from the direct path was not as strong compared with the signals from other paths as in the case of an omnidirectional antenna.

Based on the results shown in tables 8.4, 8.5, 8.6 and 8.7 the hypothesis that the data from the ensembles from the first and second halves of the measurement run belong to the same population must be rejected for all the

measurements. The measurements of mean delay therefore indicate that there is temporal variation in the radio channel.

The differences between the mean delays when using directional antennas were no more and no less than when using omnidirectional antennas. This suggests that the use of moderately directional antennas does not protect a radio system from temporal variations in the radio environment.

8.8 RMS DELAY SPREAD

In this section are presented the results of calculating the RMS delay spread for each 5 sweeps of the measurements in Durham and Manchester. For each measurement the data have been divided into two ensembles, one for the first half of the measurement run and one for the second half, so that any temporal variation may be detected. The results are presented as CDFs as for the mean delay results. The RMS delay spread is calculated as described in chapter 4, paragraph 4.9.3.

8.8.1 Durham

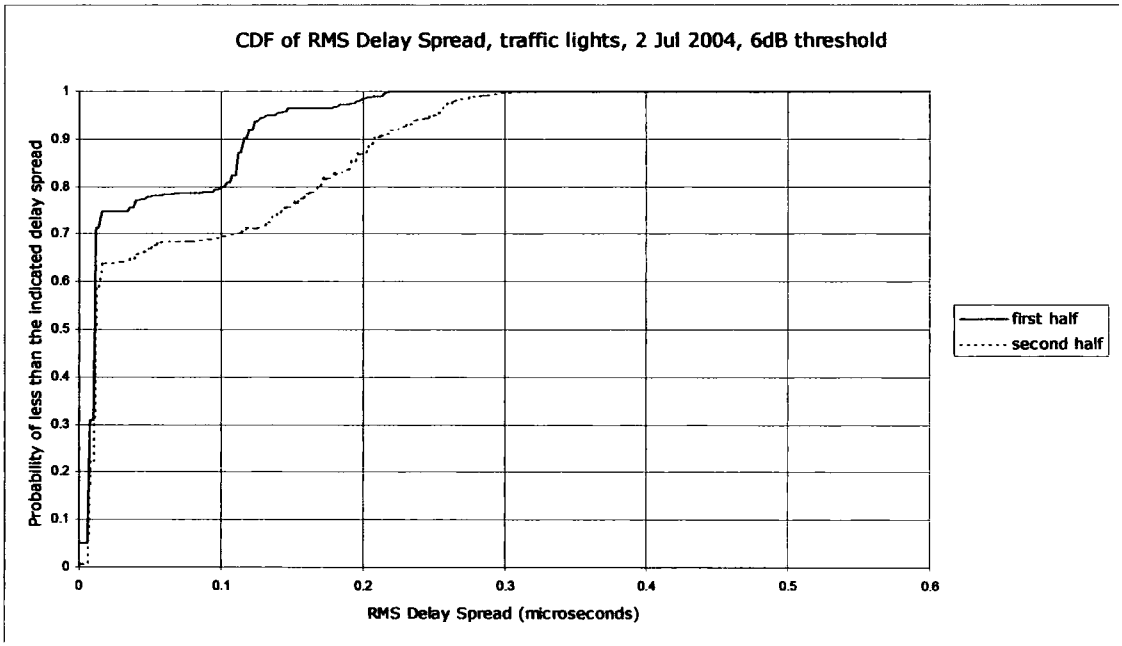

Figure 8.58 CDF of RMS Delay Spread at the traffic lights on 2 July 2004 with a 6 dB threshold.

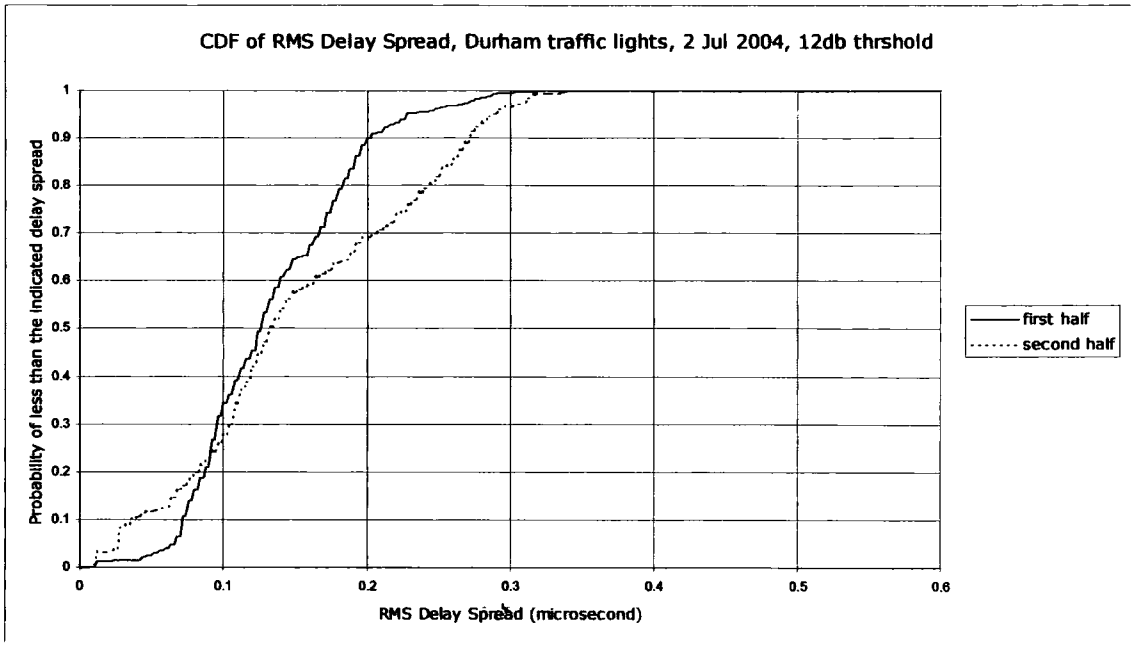

Figure 8.59 CDF of RMS Delay Spread at the traffic lights on 2 July 2004 with a 12 dB threshold.

With a 6 dB threshold the distribution shows a large probability of small delay spreads and a long tail. This was due to the dominant effect of the cathedral and a lesser effect of the local clutter and variable number of large vehicles on the road in the vicinity of the receiver. With a 12 dB threshold the cathedral had a lesser effect and more of the local clutter produced components which exceeded the threshold. The PDFs shown at figures 8.60 and 8.61 confirm this.

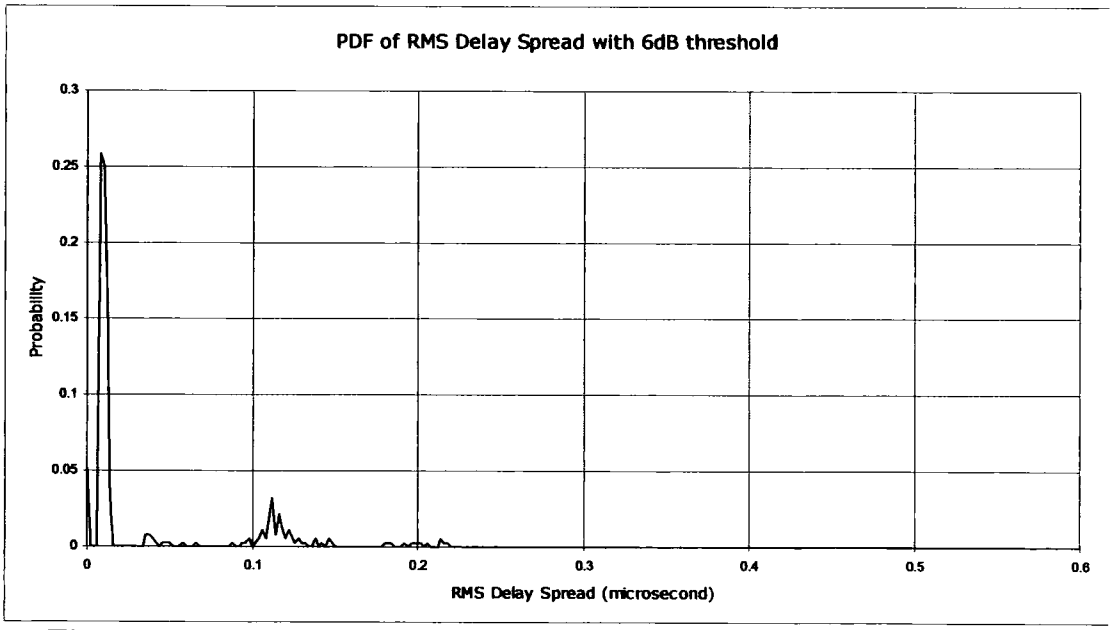

Figure 8.60 PDF of RMS Delay Spread at Traffic Lights in Durham on 2 July 2004 with a 6 dB threshold.

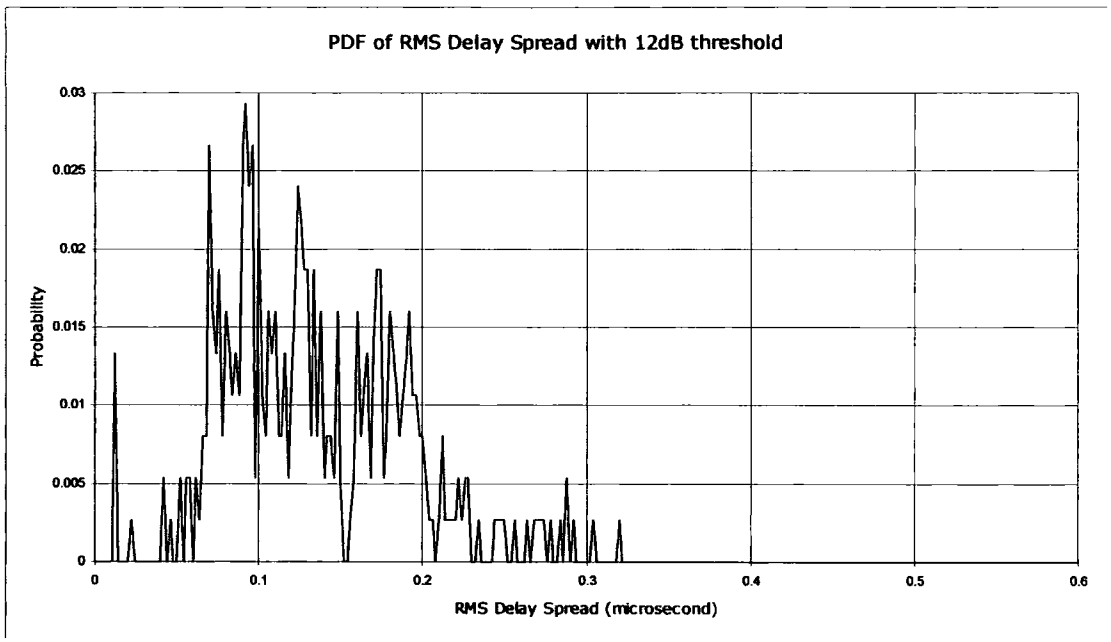

Figure 8.61 PDF of RMS Delay Spread at Traffic Lights in Durham on 2 July 2004 with a12 dB threshold.

There was a significant difference in the delay spread between the first and second halves of the measurement run. This indicates that some of the multipath components came from interactions with motor traffic moving along South Road and the Stockton Road.

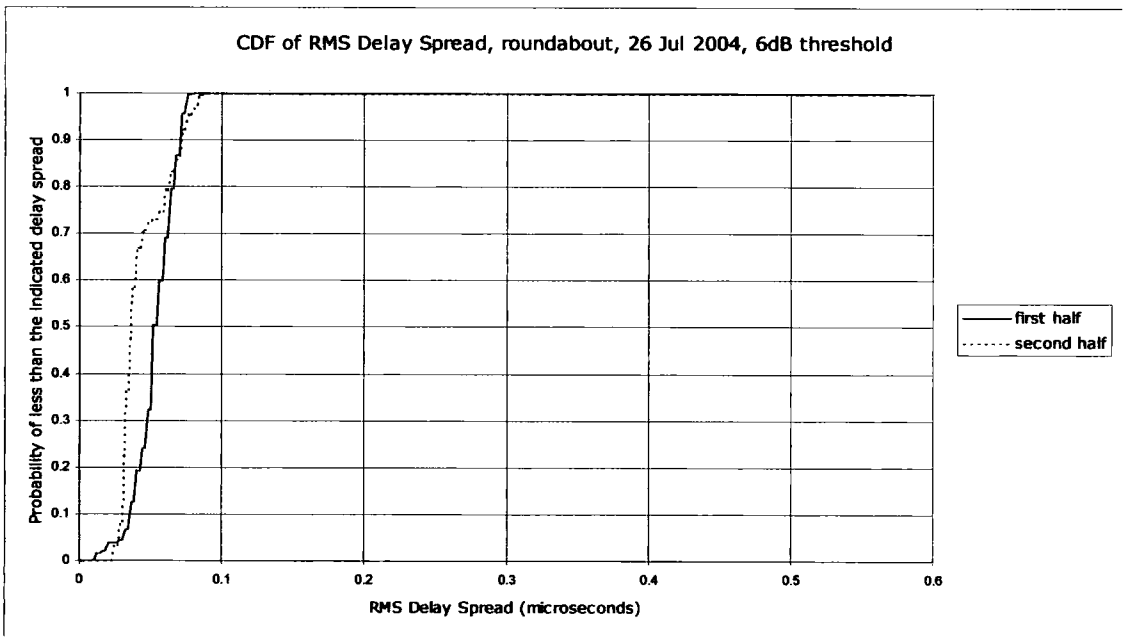

Figure 8.62 CDF of RMS delay Spread at the roundabout on 26 July 2004 with a 6 dB threshold.

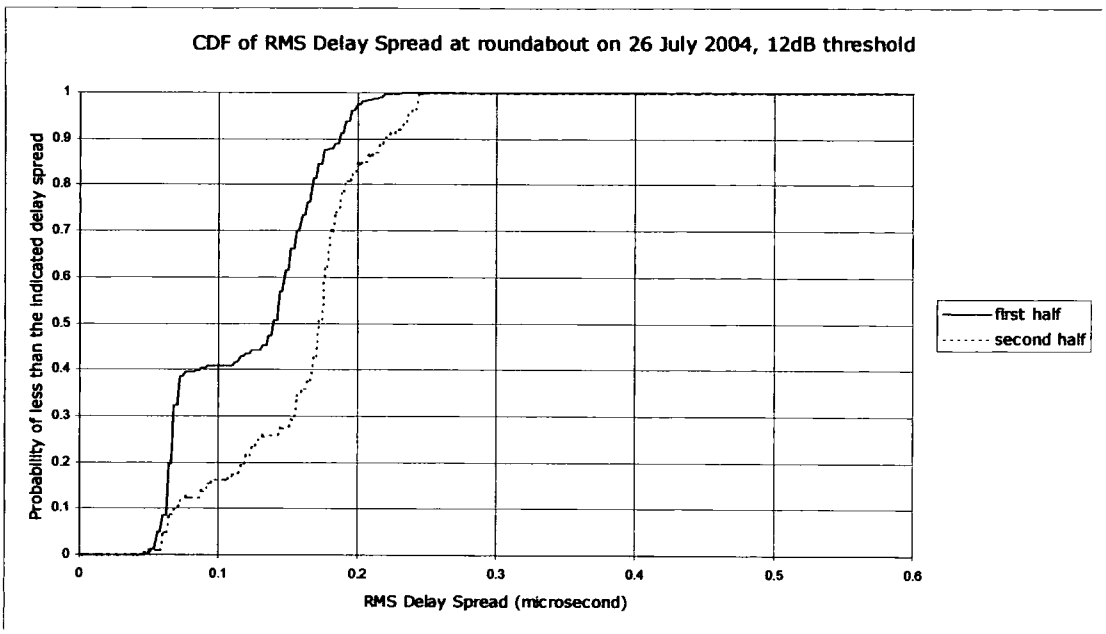

Figure 8.63 CDF of RMS Delay Spread at the roundabout on 26 July 2004 with a 6 dB threshold.

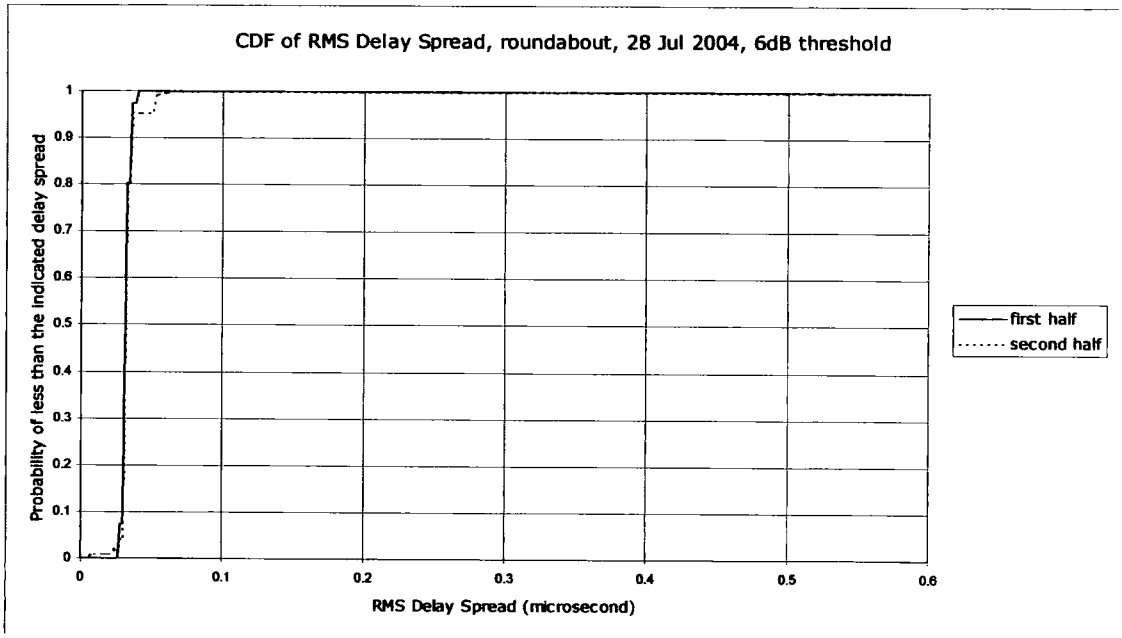

Figure 8.64 CDF of RMS Delay Spread at the roundabout on 28 July 2004 with a 6 dB threshold.

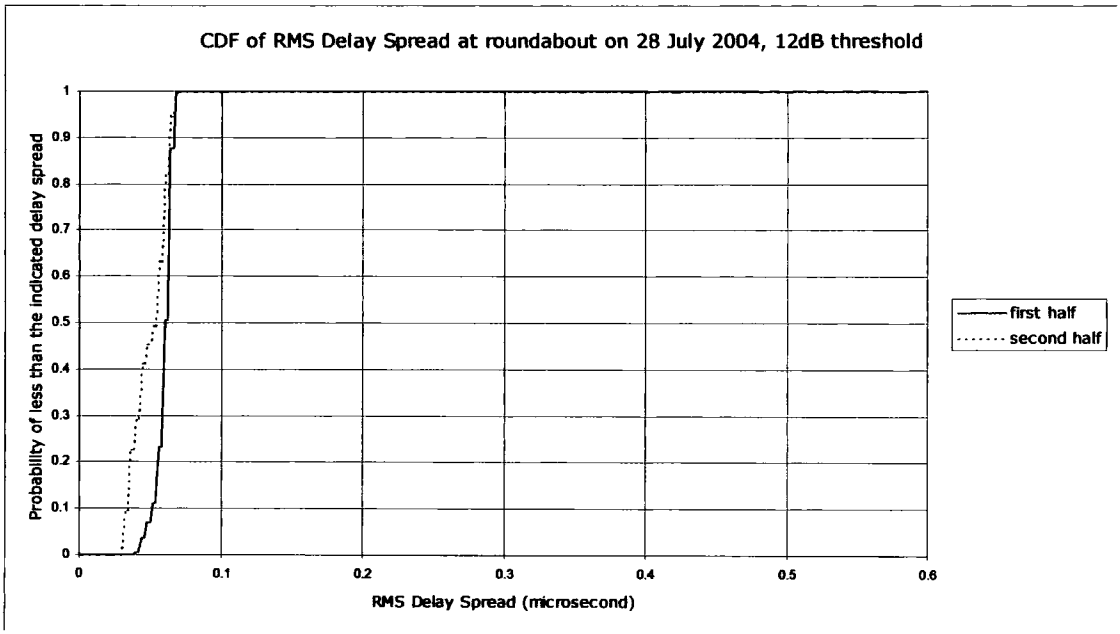

Figure 8.65 CDF of RMS Delay Spread at the roundabout on 28 July 2004 with a 12 dB threshold.

At the roundabout the distribution of delay spread shows similar characteristic to those of the mean delay. On 26 July when there was a moderate amount of traffic higher delay spreads were recorded than on 28 July when there was little traffic. Also the differences between the first and second halves of the measurement run were significant on 26 July but very small on 28 July. The delay spreads were larger than at the traffic lights because the dominating influence of the cathedral was absent and more components from the local clutter exceeded the threshold.

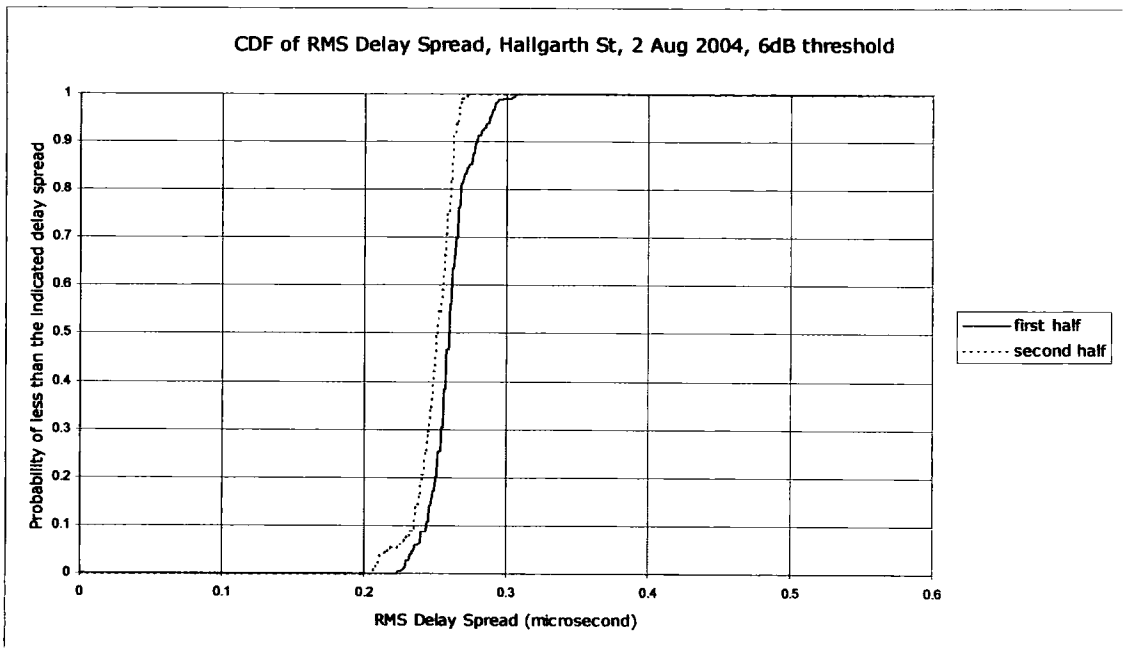

Figure 8.66 CDF of RMS Delay Spread in Hallgarth Street on 2 August 2004 with a 6 dB threshold.

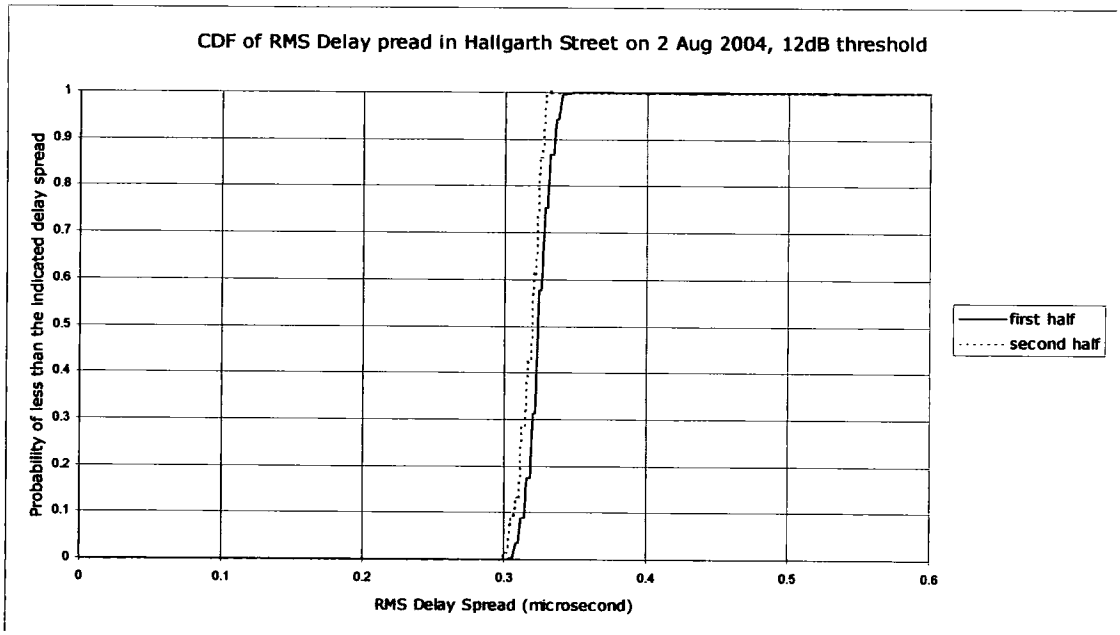

Figure 8.67 CDF of RMS Delay Spread in Hallgarth Street on 2 August 2004 with a 12 dB threshold.

In Hallgarth Street the gable ends of many of the buildings would have had a line of sight path to the transmitter giving rise to many multipath components. Due to the orientation of the street, buildings at many different distances from the receiver reflected multipath components and the large range of distances resulted in a relatively large delay spread. There was a small difference between the first and second halves of the

obstructing the Southern end of the street rather than traffic in the street itself.

8.8.2 Manchester

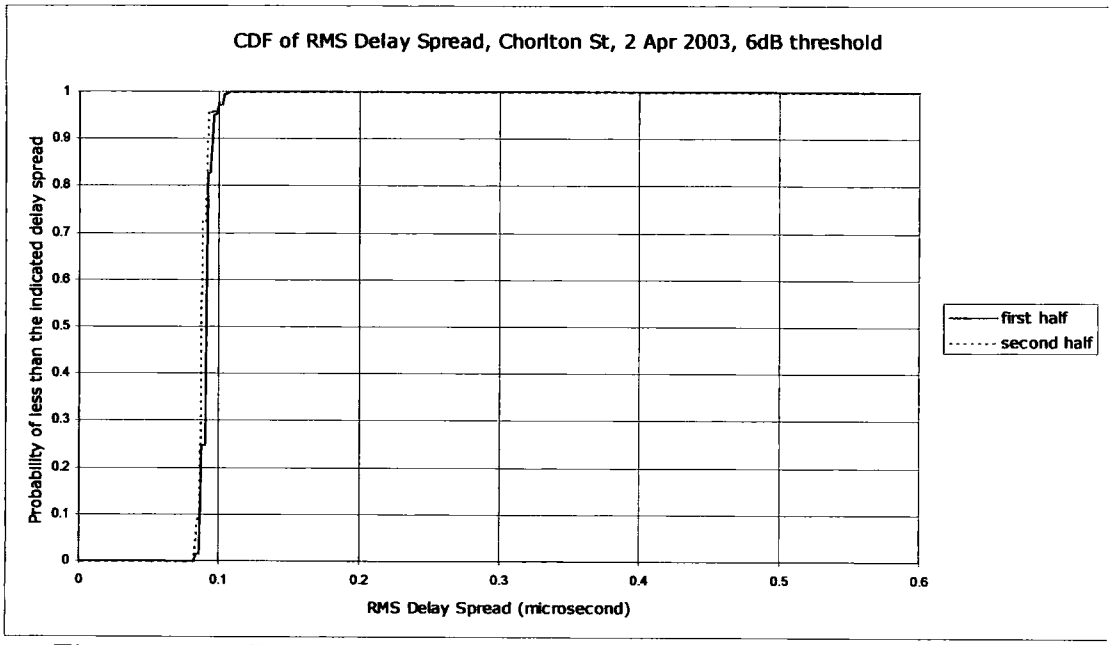

Figure 8.68 CDF of RMS Delay Spread in Chorlton Street car park on 2 April 2003 with a 6 dB threshold.

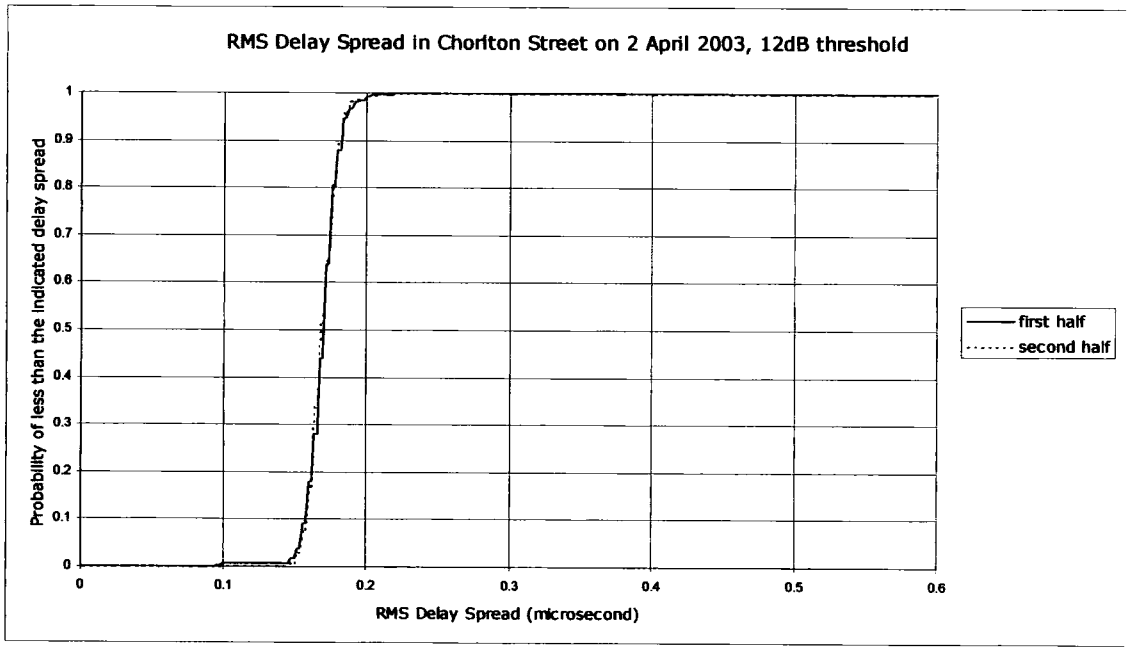

Figure 8.69 CDF of RMS Delay Spread in Chorlton Street car park on 2 April 2003 with a 12 dB threshold.

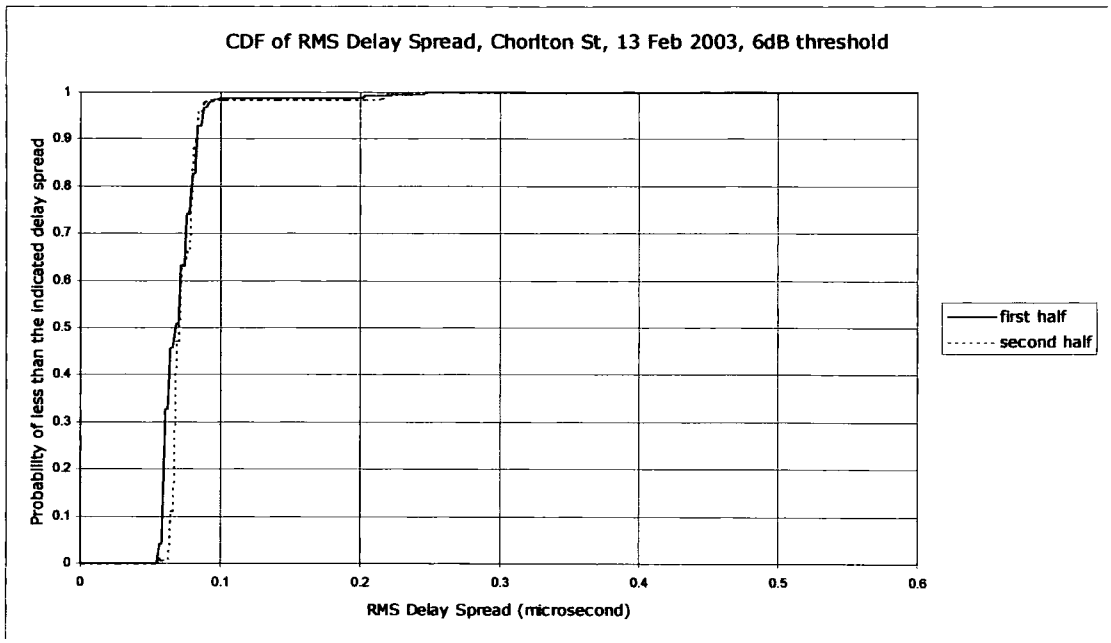

Figure 8.70 CDF of RMS Delay Spread in Chorlton Street car park on 13 February 2003 with a 6 dB threshold.

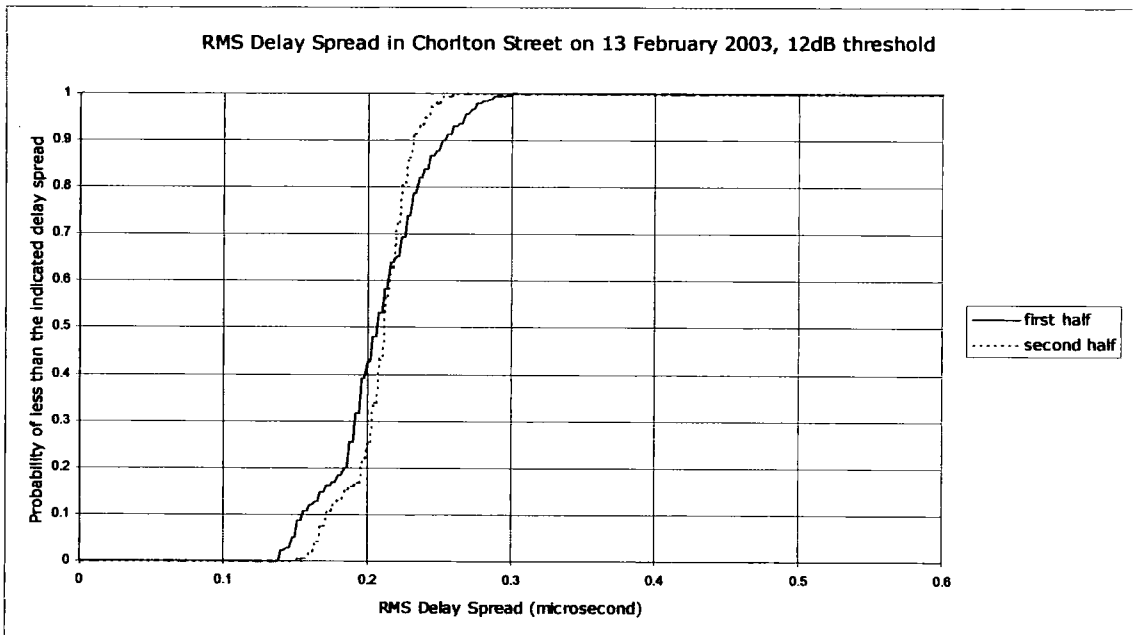

Figure 8.71 CDF of RMS Delay Spread in Chorlton Street car park on 13 February 2003 with a 12 dB threshold.

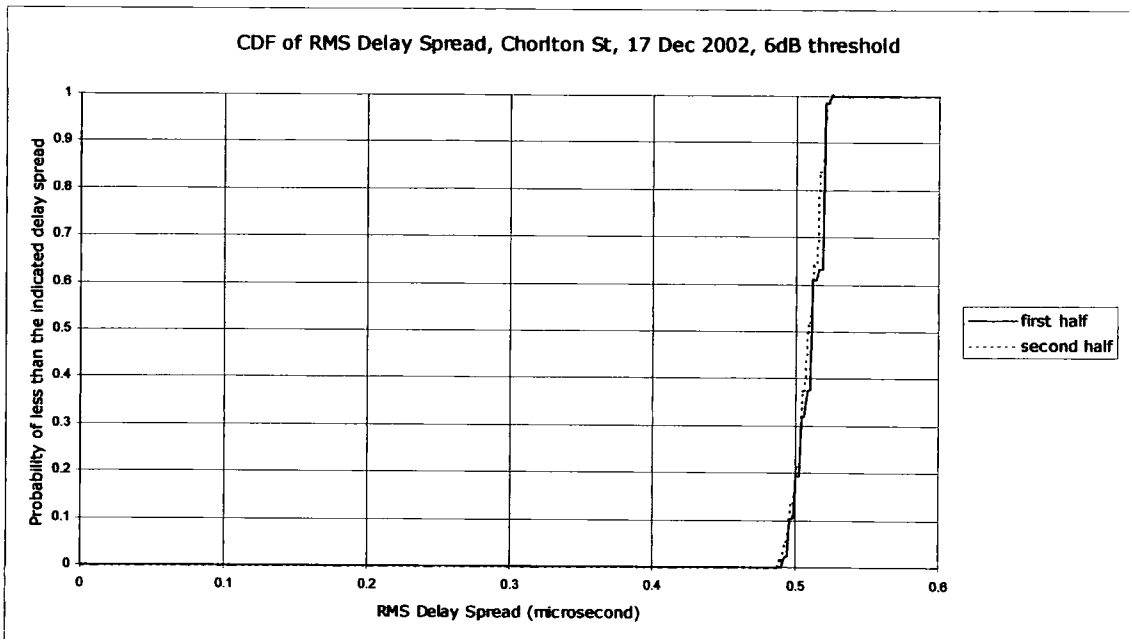

Figure 8.72 CDF of RMS Delay Spread in Chorlton Street car park on 17 December 2002 with a 6 dB threshold, measurement in the lower band.

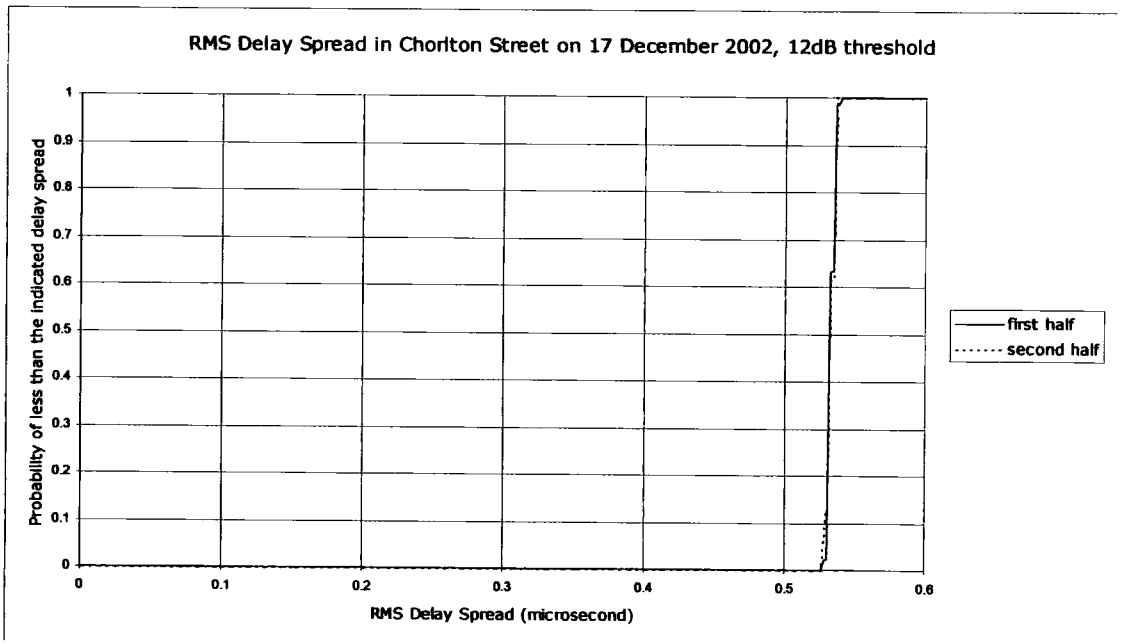

Figure 8.73 CDF of RMS Delay Spread in Chorlton Street car park on 17 December 2002 with a 12 dB threshold, measurement in the lower band.

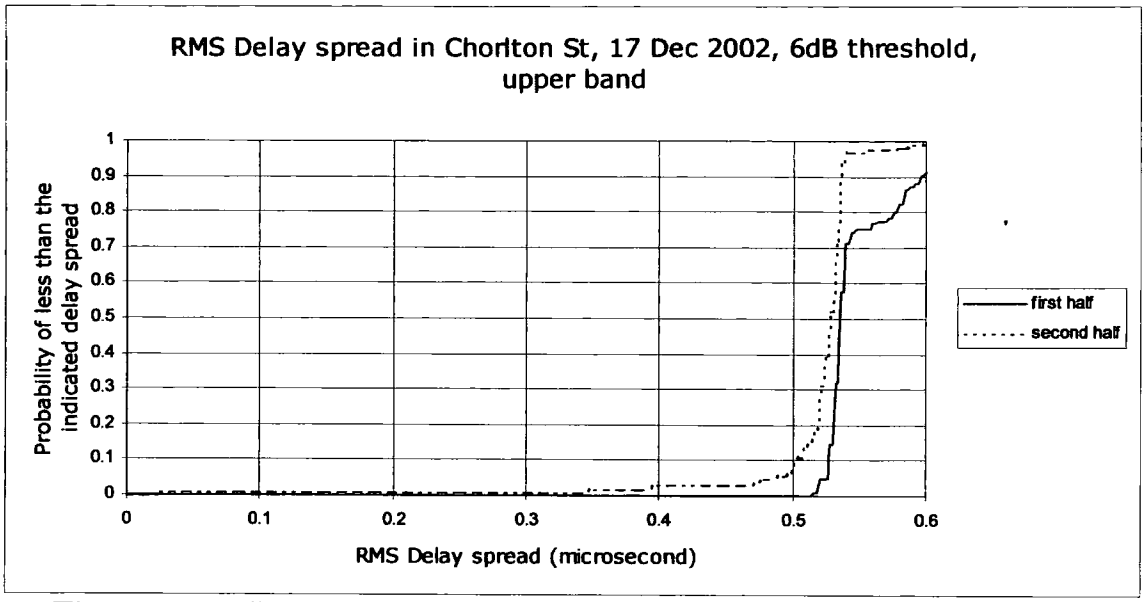

Figure 8.74 CDF of RMS Delay Spread in Chorlton Street car park on 17 December 2002 with a 6 dB threshold, measurement in the upper band.

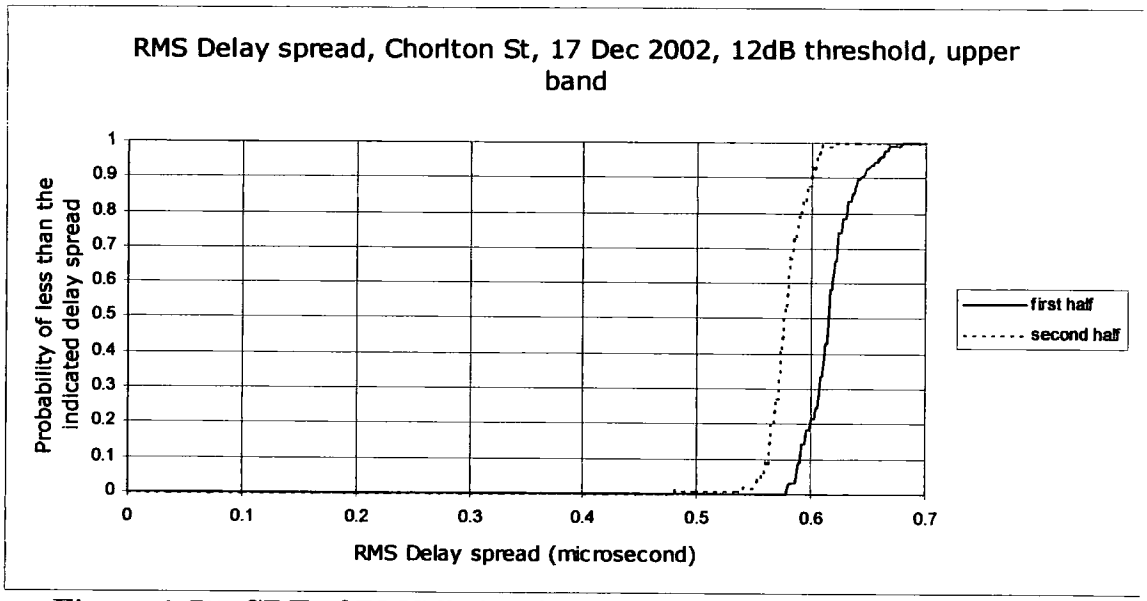

Figure 8.75 CDF of RMS Delay Spread in Chorlton Street car park on 17 December 2002 with a 12 dB threshold, measurement in the upper band.

The delay spread seen in Chorlton Street car park was very dependent on the location of the receiver. On 17 December when the receiver was close to the street and also had visibility of the bus traffic into and from Bloom Street the delay spread was much larger than on the other days. On 13 February and 2 April the receiver had to be located further from the road and so saw less traffic. The number of vehicles in Chorlton Street did not vary much during the day and this accounts for the small differences in delay-spread between the first and second halves of the measurement run.

There were differences in the two bands. In the upper band the delay spread was greater than in the lower band and there was a larger difference between the first and second halves of the measurement run. Since this was the only occasion on which it was possible to make measurements in both bands it is not possible to say whether or not there is a general difference between the two bands. Another series of dual band measurements will be necessary before any conclusions can be drawn.

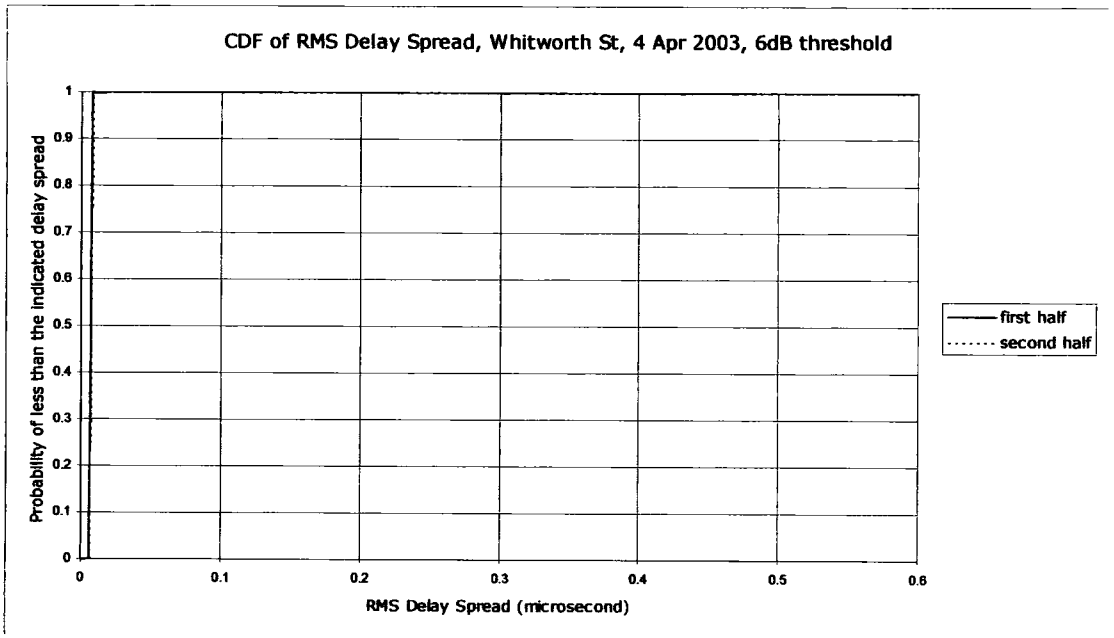

Figure 8.76 CDF of RMS Delay Spread in Whitworth Street on 4 April 2003 with a 6 dB threshold.

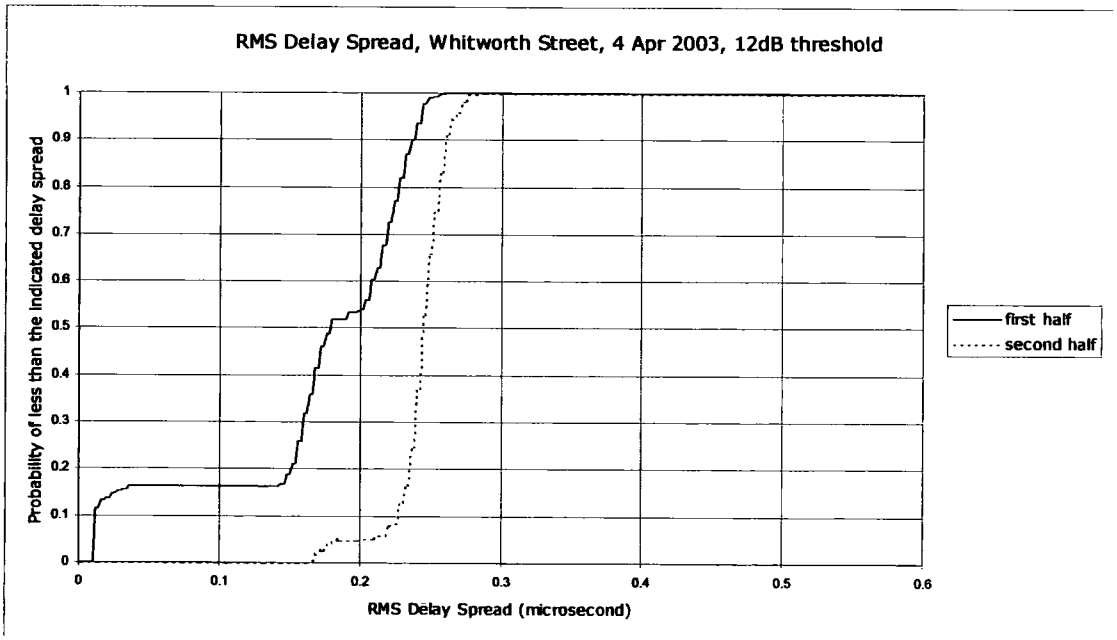

Figure 8.77 CDF of RMS Delay Spread in Whitworth Street on 4 April 2003 with a 12 dB threshold.

The line of sight between the transmitter and the receiver in Whitworth Street ensured a small and nearly constant delay spread when a threshold of 6 dB is used. With the 12 dB threshold components from the motor traffic and buildings along the street exceeded the threshold giving rise to greater delay spreads and some temporal variation. Examination of the PDF in figure 8.66 shows a relatively high probability of small delay spread which will have occurred when there was little traffic along the street. The irregular rate of traffic flow gave rise to the other peaks as a variety of components were received after interaction with vehicles at different ranges.

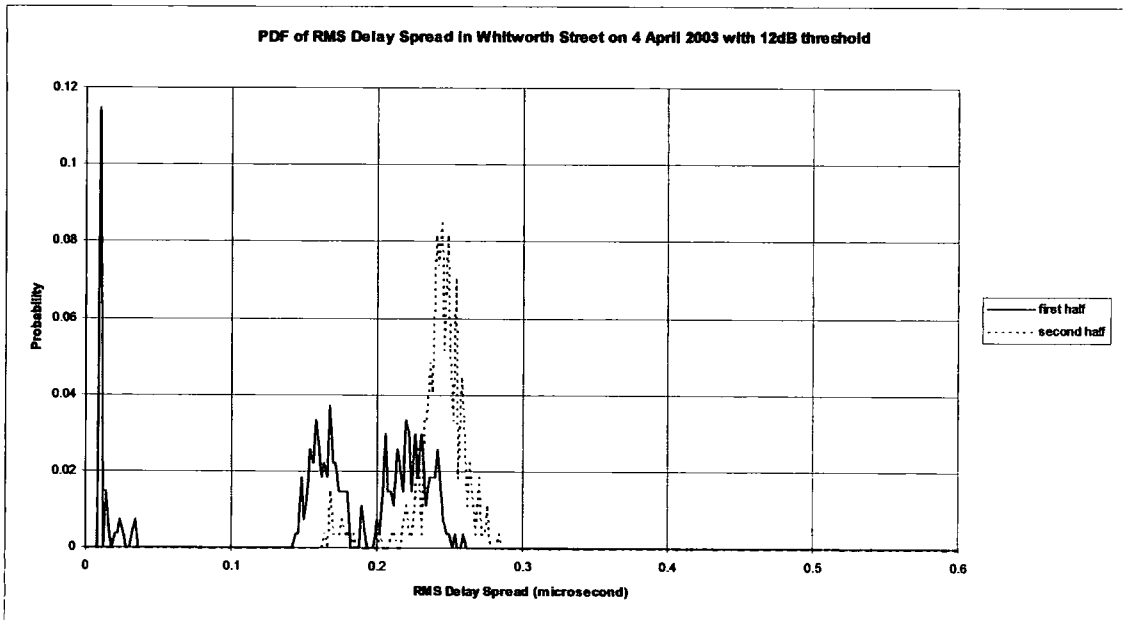

Figure 8.78 PDF of RMS Delay Spread in Whitworth Street on 4 April 2003 using a 12 dB threshold.

8.8.3 Summary

The differences between the first half and second half ensembles from each measurement run are demonstrated by the Kolmogorov-Smirnof test results shown in tables 8.9, 8.10, 8.11 and 8.12 below. Tables 8.9 and 8.10 show results from measurements using omnidirectional antennas and the results using directional antennas are in tables 8.11 and 8.12.

Measurement	K-S D	K-S P
Traffic lights, 2 Jul 2004, 6dB threshold	0.23	0.000000
Traffic lights, 2 Jul 2004, 12dB threshold	0.21	0.000000
Roundabout, 26 Jul 2004, 6dB threshold	0.49	0.000000
Roundabout, 26 Jul 2004, 12dB threshold	0.40	0.000000
Roundabout, 28 Jul 2004, 6dB threshold	0.15	0.000467
Roundabout, 28 jul 2004, 12dB threshold	0.42	0.000000
Hallgarth St, 2 Aug 2004, 6dB threshold	0.31	0.000000
Hallgarth St, 2 Sug 2004, 12dB threshold	0.31	0.000000

Table 8.9 Results from Kolmogorov-Smirnhof tests on measurements in Durham using omnidirectional antennas.

Measurement	K-S D	K-S P
Chorlton St, 2 Apr 2003, 6dB threshold	0.56	0.000000
Chorlton St, 2 Apr 2003, 12dB threshold	0.077	0.212096
Chorlton St, 13 Feb 2003, 6dB threshold	0.42	0.000000
Chorlton St, 13 Feb 2003, 12dB threshold	0.19	0.000199
Chorlton St, 17 Dec 2002, 6dB threshold, lower band	0.24	0.001493
Chorlton St, 17 Dec 2002, 12dB threshold, lower band	0.19	0.019943
Chorlton St, 17 Dec 2002, 6dB threshold, upper band	0.456	0.000000
Chorlton St, 17 Dec 2002, 12dB threshold, upper band	0.736	0.000000
Whitworth St, 4 Apr 2003, 6dB threshold	0.089	0.236490
Whitworth St, 4 Apr 2003, 12dB threshold	0.72	0.000000

Table 8.10 Results from Kolmogorov-Smirnof tests on measurements in Manchester using omnidirectional antennas.

Measurement	K-S D	K-S P
Traffic lights, 2 Jul 2004, ch 1, 6dB threshold	0.12	0.009033
Traffic lights, 2 Jul 2004, ch 1, 12dB threshold	0.14	0.000839
Traffic lights, 2 Jul 2004, ch 2, 6dB threshold	0.13	0.004293
Traffic lights, 2 Jul 2004, ch 2, 12dB threshold	0.20	0.000001
Traffic lights, 2 Jul 2004, ch 3, 6dB threshold	0.29	0.000000
Traffic lights, 2 Jul 2004, ch 3, 12dB threshold	0.29	0.000000
Traffic lights, 2 Jul 2004, ch 4, 6dB threshold	0.18	0.000006
Traffic lights, 2 Jul 2004, ch 4, 12dB threshold	0.35	0.000000
Traffic lights, 2 Jul 2004, ch 5, 6dB threshold	0.39	0.000000
Traffic lights, 2 Jul 2004, ch 5, 12dB threshold	0.29	0.000000
Traffic lights, 2 Jul 2004, ch 6, 6dB threshold	0.31	0.000000
Traffic lights, 2 Jul 2004, ch 6, 12dB threshold	0.18	0.000009

Table 8.11 Results from Kolmogorov-Smirnof tests on measurements in Durham using directional antennas.

Measurement	K-S D	K-S P
Roundabout, 26 Jul 2004, ch 1, 6dB threshold	0.34	0.000000
Roundabout, 26 Jul 2004, ch 1, 12dB threshold	0.49	0.000000
Roundabout, 26 Jul 2004, ch 2, 6dB threshold	0.65	0.000000
Roundabout, 26 Jul 2004, ch 2, 12dB threshold	0.39	0.000000
Roundabout, 26 Jul 2004, ch 3, 6dB threshold	0.38	0.000000
Roundabout, 26 Jul 2004, ch 3, 12dB threshold	0.23	0.000000
Roundabout, 26 Jul 2004, ch 4, 6dB threshold	0.23	0.000000
Roundabout, 26 Jul 2004, ch 4, 12dB threshold	0.30	0.000000
Roundabout, 26 Jul 2004, ch 5, 6dB threshold	0.20	0.000000
Roundabout, 26 Jul 2004, ch 5, 12dB threshold	0.31	0.000000
Roundabout, 26 Jul 2004, ch 6, 6dB threshold	0.11	0.022606
Roundabout, 26 Jul 2004, ch 6, 12dB threshold	0.31	0.000000
Roundabout, 28 Jul 2004, ch 1, 6dB threshold	0.34	0.000000
Roundabout, 28 Jul 2004, ch 1, 12dB threshold	0.31	0.000000
Roundabout, 28 Jul 2004, ch 2, 6dB threshold	0.16	0.000135
Roundabout, 28 Jul 2004, ch 2, 12dB threshold	0.49	0.000000
Roundabout, 28 Jul 2004, ch 3, 6dB threshold	0.93	0.000000
Roundabout, 28 Jul 2004, ch 3, 12dB threshold	0.82	0.000000
Roundabout, 28 Jul 2004, ch 4, 6dB threshold	0.25	0.000000
Roundabout, 28 Jul 2004, ch 4, 12dB threshold	0.33	0.000000
Roundabout, 28 Jul 2004, ch 5, 6dB threshold	0.22	0.000000
Roundabout, 28 Jul 2004, ch 5, 12dB threshold	0.26	0.000000
Roundabout, 28 Jul 2004, ch 6, 6dB threshold	0.19	0.000001
Roundabout, 28 Jul 2004, ch 6, 12dB threshold	0.39	0.000000
Hallgarth St, 2 Aug 2004, ch 1, 6dB threshold	0.68	0.000000
Hallgarth St, 2 Aug 2004, ch 1, 12dB threshold	0.62	0.000000
Hallgarth St, 2 Aug 2004, ch 2, 6dB threshold	0.58	0.000000
Hallgarth St, 2 Aug 2004, ch 2, 12dB threshold	0.68	0.000000
Hallgarth St, 2 Aug 2004, ch 3, 6dB threshold	0.90	0.000000
Hallgarth St, 2 Aug 2004, ch 3, 12dB threshold	0.24	0.000000
Hallgarth St, 2 Aug 2004, ch 4, 6dB threshold	0.71	0.000000
Hallgarth St, 2 Aug 2004, ch 4, 12dB threshold	0.61	0.000000
Hallgarth St, 2 Aug 2004, ch 5, 6dB threshold	0.53	0.000000
Hallgarth St, 2 Aug 2004, ch 5, 12dB threshold	0.53	0.000000
Hallgarth St, 2 Aug 2004, ch 6, 6dB threshold	0.52	0.000000
Hallgarth St, 2 Aug 2004, ch 6, 12dB threshold	0.18	0.000009

Table 8.11 (continued) Results from Kolmogorov-Smirnof tests on measurements in Durham using directional antennas.

Measurement	K-S D	K-S P
Chorlton St, 2 Apr 2003, ch 1, 6dB threshold	0.37	0.000000
Chorlton St, 2 Apr 2003, ch 1, 12dB threshold	0.19	0.000002
Chorlton St, 2 Apr 2003, ch 2, 6dB threshold	0.57	0.000000
Chorlton St, 2 Apr 2003, ch 2, 12dB threshold	0.48	0.000000
Chorlton St, 2 Apr 2003, ch 3, 6dB threshold	0.31	0.000000
Chorlton St, 2 Apr 2003, ch 3, 12dB threshold	0.47	0.000000
Chorlton St, 2 Apr 2003, ch 4, 6dB threshold	0.56	0.000000
Chorlton St, 2 Apr 2003, ch 4, 12dB threshold	0.083	0.154127
Chorlton St, 2 Apr 2003, ch 5, 6dB threshold	0.25	0.000000
Chorlton St, 2 Apr 2003, ch 5, 12dB threshold	0.33	0.000000
Chorlton St, 2 Apr 2003, ch 6, 6dB threshold	0.31	0.000000
Chorlton St, 2 Apr 2003, ch 6, 12dB threshold	0.91	0.000000
Chorlton St, 13 Feb 2003, ch 1, 6dB threshold	0.10	0.164079
Chorlton St, 13 Feb 2003, ch 1, 12dB threshold	0.36	0.000000
Chorlton St, 13 Feb 2003, ch 2, 6dB threshold	0.30	0.000000
Chorlton St, 13 Feb 2003, ch 2, 12dB threshold	0.30	0.000000
Chorlton St, 13 Feb 2003, ch 3, 6dB threshold	0.24	0.000001
Chorlton St, 13 Feb 2003, ch 3, 12dB threshold	0.96	0.000000
Chorlton St, 13 Feb 2003, ch 4, 6dB threshold	0.82	0.000000
Chorlton St, 13 Feb 2003, ch 4, 12dB threshold	0.84	0.000000
Chorlton St, 13 Feb 2003, ch 5, 6dB threshold	0.38	0.000000
Chorlton St, 13 Feb 2003, ch 5, 12dB threshold	0.65	0.000000
Chorlton St, 13 Feb 2003, ch 6, 6dB threshold	0.23	0.000003
Chorlton St, 13 feb 2003, ch 6, 12dB threshold	0.40	0.000000
Chorlton St, 17 Dec 2002, ch 1, 6dB threshold, lower band	0.14	0.197933
Chorlton St, 17 Dec 2002, ch 1, 12dB threshold, lower band	0.19	0.019943
Chorlton St, 17 Dec 2002, ch 1, 6dB threshold, upper band	0.104	0.508494
Chorlton St, 17 Dec 2002, ch 1, 12dB threshold, upper band	0.160	0.081519
Chorlton St, 17 Dec 2002, ch 2, 6dB threshold, lower band	0.73	0.000000
Chorlton St, 17 Dec 2002, ch 2, 12dB threshold, lower band	0.34	0.000000
Chorlton St, 17 Dec 2002, ch 2, 6dB threshold, upper band	0.240	0.001493
Chorlton St, 17 Dec 2002, ch 2, 12dB threshold, upper band	0.480	0.000000

Table 8.12 Results from Kolmogorov-Smirnof tests on measurements in Manchester using directional antennas.

Measurement	K-S D	K-S P
Chorlton St, 17 Dec 2002, ch 3, 6dB threshold, lower band	0.72	0.000000
Chorlton St, 17 Dec 2002, ch 3, 12dB threshold, lower band	0.74	0.000000
Chorlton St, 17 Dec 2002, ch 3, 6dB threshold, upper band	0.344	0.000001
Chorlton St, 17 Dec 2002, ch 3, 12dB threshold, upper band	0.440	0.000000
Chorlton St, 17 Dec 2002, ch 4, 6dB threshold, lower band	0.40	0.000000
Chorlton St, 17 Dec 2002, ch 4, 12dB threshold, lower band	0.42	0.000000
Chorlton St, 17 Dec 2002, ch 4, 6dB threshold, upper band	0.368	0.000000
Chorlton St, 17 Dec 2002, ch 4, 12dB threshold, upper band	0.168	0.058726
Chorlton St, 17 Dec 2002, ch 5, 6dB threshold, lower band	0.42	0.000000
Chorlton St, 17 Dec 2002, ch 5, 12dB threshold, lower band	0.38	0.000000
Chorlton St, 17 Dec 2002, ch 5, 6dB threshold, upper band	0.296	0.000035
Chorlton St, 17 Dec 2002, ch 5, 12dB threshold, upper band	0.416	0.000000
Chorlton St, 17 Dec 2002, ch 6, 6dB threshold, lower band	0.41	0.000000
Chorlton St, 17 Dec 2002, ch 6, 12dB threshold, lower band	0.44	0.000000
Chorlton St, 17 Dec 2002, ch 6, 6dB threshold, upper band	0.368	0.000000
Chorlton St, 17 Dec 2002, ch 6, 12dB threshold, upper band	0.536	0.000000
Whitworth St, 4 Apr 2003, ch 1, 6dB threshold	0.27	0.000000
Whitworth St, 4 Apr 2003, ch 1, 12dB threshold	0.24	0.000000
Whitworth St, 4 Apr 2003, ch 2, 6dB threshold	0.54	0.000000
Whitworth St, 4 Apr 2003, ch 2, 12dB threshold	0.55	0.000000
Whitworth St, 4 Apr 2003, ch 3, 6dB threshold	0.38	0.000000
Whitworth St, 4 Apr 2003, ch 3, 12dB threshold	0.67	0.000000
Whitworth St, 4 Apr 2003, ch 4, 6dB threshold	0.28	0.000000
Whitworth St, 4 Apr 2003, ch 4, 12dB threshold	0.47	0.000000
Whitworth St, 4 Apr 2003, ch 5, 6dB threshold	0.53	0.000000
Whitworth St, 4 Apr 2003, ch 5, 12dB threshold	0.17	0.000790
Whitworth St, 4 Apr 2003, ch 6, 6dB threshold	0.24	0.000001
Whitworth St, 4 Apr 2003, ch 6, 12dB threshold	0.37	0.000000

Table 8.12 (continued) Results from Kolmogorov-Smirnof tests on measurements in Manchester using directional antennas.

The results in tables 8.9, 8.10, 8.11 and 8.12 indicate that, for all measurements except one, there is a very small probability that the data from the first and second halves of the measurement came from the same population. The exception was Whitworth Street where with a 6 dB threshold the line of sight path between transmitter and receiver produced a single component whose temporal variation was much less than in other cases. In this case the small temporal variation was to be expected since any variation over a line of sight path would be caused by clear air effects which only manifest themselves over timescales inexcess of the duration of the measurement (15 seconds) Overall the probabilities that the RMS delay spreads recorded for the first and second halves of the measurements runs came from the same population (had the same distribution) were very small and the null hypothesis had to be rejected.

8.9 MODELLING DELAY SPREAD

8.9.1 General Idea

A system designer or installer will not usually wish to extract system parameters from large quantities of measurement data. A function which expresses the probability of occurrence of a particular parameter would be a useful design tool. In the case where the parameters of the probability distribution are unknown the best that can be achieved is a function which fits the statistics derived from the measurements.

RMS delay spread is a parameter of interest to system designers since it is one indicator of the extent to which a wideband signal will be degraded by the radio channel. Attempts have been made to fit two standard probability distributions to the statistics of the measurements acquired during this project. Since many stochastic processes exhibit a Normal (Gaussian) distribution of their parameters this was the first distribution function to be tried. The second function was a Weibull distribution function since this might better fit statistics which were skewed.

A relaxation method was used to determine the parameters of each distribution which gave the best fit to the measurement statistics. Only the RMS delay spread was considered and the measurements with 6 dB and 12 dB thresholds for the first and second halves of each measurement run were used separately.

8.9.2 The Relaxation Method

The CDFs of the measurements were used as the distribution to which the function needed to be fitted. A generator function for the Normal distribution[39] was used to generate a CDF from a Normal distribution with known mean and standard deviation. For the Weibull distribution a function[47,48] to generate the CDF direct with known shape and scale parameters was used. In both cases the delay spread values from the measurement statistics were used as the independent variable.

Having generated the CDF from the known distribution, for each delay spread value the known distribution was compared with the distribution derived from the measurements. For each comparison the difference

between the known distribution and the measurement distribution was squared to produce an error value which was always positive.
The search for the best parameters of the known distribution was conducted by alternately searching for one of the parameters and then the other until the sum of the error values reached a minimum. In the case of the Normal distribution a value was chosen as a starting point for the mean and a search started for the best standard deviation. This standard deviation was used and a search started for the best value for the mean. Two programs were written, one to search for the best standard deviation and the other to search for the best mean. In each of these a starting value was assigned to the parameter being searched for and an increment value to be added to the starting value at program cycle. If after any cycle the sum of the error values was greater than for the previous cycle the increment was halved and its sign changed, otherwise it was left unchanged. Since points on two CDFs were being compared the maximum difference was ±1.0 and the maximum squared difference (the error) was +1.0. Over the 2000 points in each CDF the maximum sum of the errors was 2000. Each of the parameter searching programs terminated when the sum of errors after the current cycle was less than 0.001 different from the sum of errors after the previous cycle. The program which searched for the mean wrote to a file the Normal distribution which most closely fitted the measurement data. To gauge how closely the CDF from the measurements fitted a Normal CDF a Kolmogorov-Smirnof test was applied.

8.9.3 Fit to Normal Distribution

Tables 8.12 and 8.13 below show the results of the attempts to find a Normal distribution which fitted the measurement data. The Mean and Standard Deviation columns show the parameters for the Normal CDF which best fitted the measurement data. The Error Sum column indicates how well the search process converged. The K-S D and K-S P columns show the results of the Kolmogorov-Smirnof test.

Measurement	Mean	Standard Deviation	Error Sum	K-S D	K-S P
Durham					
2 Jul 2004, 6dB					
first half	-0.06525	0.0515625	1.594	0.09550	0.000000
second half	-0.11875	0.1125	3.241	0.169	0.000000
2 Jul 2004,12dB					
first half	0.13125	0.059375	0.131	0.1705	0.000000
second half	0.125	0.1078125	0.209	0.222	0.000000
26 Jul 2004, 6dB					
first half	0.0429688	0.0421875	1.405	0.072	0.000063
second half	0.0417969	0.0164063	0.366	0.0485	0.018109
26 Jul 2004,12dB					
first half	0.1101562	0.081250	0.946	0.165	0.000000
second half	0.1125	0.140625	3.904	0.229	0.000000
28 Jul 2004, 6dB					
first half	-0.1875	0.0515625	3.904	0.059	0.002131
second half	-0.3	0.1125	3.112	0.0835	0.000002
28 Jul 2004,12dB					
first half	0.0609375	0.0095	0.234	0.0425	0.053968
second half	0.0390625	0.0406250	1.475	0.0665	0.000288
2 Aug 2004, 6dB					
first half	0.2613281	0.021875	0.336	0.1635	0.000000
second half	0.2519531	0.0121094	0.054	0.143	0.000000
2 Aug 2004,12dB					
first half	0.325	0.0078125	0.024	0.176	0.000000
second half	0.31875	0.0097656	0.082	0.172	0.000000

Table 8.12 Results of fitting a Normal distribution to the measurements made in Durham.

Measurement	Mean	Standard Deviation	Error	K-S D	K-S P
Manchester					
2 Apr 2003, 6dB					
first half	0.0916016	0.0027344	0.060	0.0525	0.008072
second half	0.0890625	0.0046875	0.164	0.053	0.007264
2 Apr 2003,12dB					
first half	0.1710938	0.009375	0.0222	0.106	0.000000
second half	0.1703125	0.009375	0.0199	0.1065	0.000000
13 Feb 2003, 6dB					
first half	0.0699219	0.0109375	0.095	0.09	0.000000
second half	0.0726563	0.0076	0.109	0.0815	0.000003

Table 8.13 Results of fitting a Normal distribution to the measurements made in Manchester.

Measurement	Mean	Standard Deviation	Error Sum	K-S D	K-S P
13 Feb 2003,12dB					
first half	0.2085938	0.0338	0.034	0.16	0.000000
second half	0.2113281	0.0203125	0.087	0.1375	0.000000
17 Dec 2002, 6dB, lower band					
first half	0.5113281	0.0097656	0.098	0.2685	0.000000
second half	0.509375	0.009375	0.037	0.2675	0.000000
17 Dec 2002,12dB lower band					
first half	0.5333984	0.0025391	0.074	0.2705	0.000000
second half	0.5332031	0.0027344	0.057	0.27	0.000000
17 Dec 2002, 6dB upper band					
first half	0.5425781	0.0195313	0.750	0.3145	0.000000
second half	0.5273438	0.0109375	0.206	0.2925	0.000000
17 Dec 2002,12dB upper band					
first half	0.6164062	0.0187500	0.050	0.3425	0.000000
second half	0.5773438	0.0144531	0.037	0.3135	0.000000
4 Apr 2003, 6dB					
first half	-0.075	0.0289063	0.998	0.0225	0.691995
second half	-0.08125	0.0296875	1.010	0.02	0.818621
4 Apr 2003,12dB					
first half	0.1820313	0.059375	1.220	0.1685	0.000000
second half	0.2457031	0.0132813	0.074	0.1455	0.000000

Table 8.13 (continued) Results of fitting a Normal distribution to the measurements made in Manchester

8.9.4 Fit to Weibull Distribution

The Weibull distribution was chosen as the second known distribution because it is capable of adopting a range of shapes, some skewed, from the Exponential to the Normal. The Weibull distribution has two parameters and searches for the best value of these were made in the same manner as for the Normal distribution. Tables 8.14 and 8.15 show the results of attempting to fit a Weibull distribution to the measured data.

Measurement	Weibull Shape	Weibull Scale	Error Sum	K-S D	K-S P
Durham					
2 Jul 2004, 6dB					
first half	0.41562	0.01875	0.748	0.44500	0.000000
second half	0.50000	0.03437	1.385	0.50000	0.000000
2 Jul 2004, 12dB					
first half	2.52500	0.15625	0.185	0.17700	0.000000
second half	1.85000	0.18125	0.239	0.23900	0.000000
26 Jul 2004, 6dB					
first half	4.30000	0.06250	0.162	0.04700	0.024117
second half	2.40000	0.05000	0.402	0.05450	0.005261
26 Jul 2004, 12dB					
first half	2.37500	0.14375	0.720	0.15200	0.000000
second half	4.10000	0.18750	0.526	0.14450	0.000000
28 Jul 2004, 6dB					
first half	14.10000	0.03200	0.115	0.01950	0.841507
second half	14.70000	0.03200	0.145	0.02550	0.533797
28 Jul 2004, 12dB					
first half	10.80000	0.06406	0.126	0.03800	0.111356
second half	4.50000	0.05469	0.086	0.04000	0.081519
2 Aug 2004, 6dB					
first half	23.80000	0.26250	0.127	0.14950	0.000000
second half	23.00000	0.25312	0.098	0.13800	0.000000
2 Aug 2004, 12dB					
first half	36.70000	0.32812	0.095	0.17450	0.000000
second half	37.00000	0.32187	0.088	0.16900	0.000000

Table 8.14 Results of fitting a Weibull distribution to the measurements made in Durham.

Measurement	Weibull Shape	Weibull Scale	Error Sum	K-S D	K-S P
Durham					
2 Jul 2004, 6dB					
first half	0.41562	0.01875	0.748	0.44500	0.000000
second half	0.50000	0.03437	1.385	0.50000	0.000000
2 Jul 2004, 12dB					
first half	2.52500	0.15625	0.185	0.17700	0.000000
second half	1.85000	0.18125	0.239	0.23900	0.000000
26 Jul 2004, 6dB					
first half	4.30000	0.06250	0.162	0.04700	0.024117
second half	2.40000	0.05000	0.402	0.05450	0.005261
26 Jul 2004, 12dB					
first half	2.37500	0.14375	0.720	0.15200	0.000000
second half	4.10000	0.18750	0.526	0.14450	0.000000
28 Jul 2004, 6dB					
first half	14.10000	0.03200	0.115	0.01950	0.841507
second half	14.70000	0.03200	0.145	0.02550	0.533797
28 Jul 2004, 12dB					
first half	10.80000	0.06406	0.126	0.03800	0.111356
second half	4.50000	0.05469	0.086	0.04000	0.081519
2 Aug 2004, 6dB					
first half	23.80000	0.26250	0.127	0.14950	0.000000
second half	23.00000	0.25312	0.098	0.13800	0.000000
2 Aug 2004, 12dB					
first half	36.70000	0.32812	0.095	0.17450	0.000000
second half	37.00000	0.32187	0.088	0.16900	0.000000

Table 8.14 Results of fitting a Weibull distribution to the measurements made in Durham.

Measurement	Weibull shape	Weibull scale	Error Sum	K-S D	K-S P
Manchester					
2 Apr 2003, 6dB					
first half	26.7000	0.09062	0.193	0.05200	0.008961
second half	20.6000	0.09062	0.240	0.05150	0.009938
2 Apr 2003, 12dB					
first half	20.4000	0.17187	0.078	0.10250	0.000000
second half	18.9000	0.17344	0.055	0.10400	0.000000
13 Feb 2003, 6dB					
first half	6.9000	0.07344	0.122	0.08800	0.000000
second half	9.2000	0.07656	0.188	0.08100	0.000000
13 Feb 2003,12dB					
first half	7.5000	0.21562	0.126	0.14850	0.000000
second half	12.7000	0.21562	0.075	0.13000	0.000000
17 Dec 2002, 6dB lower band					
first half	42.3000	0.51875	0.368	0.26800	0.000000
second half	49.3000	0.51250	0.096	0.26550	0.000000
17 Dec 2002,12dB lower band					
first half	82.3000	0.53437	0.475	0.27250	0.000000
second half	72.4000	0.53594	0.502	0.27250	0.000000
17 Dec 2002, 6dB upper band					
first half	28.2	0.55	1.029	0.3095	0.000000
second half	41.3	0.51325	0.198	0.2905	0.000000
17 Dec 2002,12dB upper band					
first half	30.0	0.62812	0.305	0.340	0.000000
second half	39.9	0.58281	0.127	0.3095	0.000000
4 Apr 2003, 6dB					
first half	10.0000	0.00742	0.027	0.00750	1.000000
second half	8.8000	0.00781	0.094	0.00500	1.000000
4 Apr 2003, 12dB					
first half	3.8500	0.20625	1.268	0.15900	0.000000
second half	18.2000	0.25156	0.104	0.14250	0.000000

Table 8.15 Results of fitting a Weibull distribution to the measurements made in Manchester.

8.9.5 Summary

Neither the Normal nor the Weibull distribution fitted the distribution of RMS delay spreads in many cases. In the case of Whitworth Street using a 6 dB threshold it was possible to achieve a partial fit to the Normal distribution and a complete fit to the Weibull distribution. When using a

12 dB threshold for the same measurement it was not possible to achieve a close fit at all. For the measurement at the roundabout in Durham on 28 July 2004 it was possible to achieve a partial fit to both distributions. A closer fit was achieved to the Weibull distribution than to the Normal distribution. In both of these locations there was little variation due to interaction with moving road vehicles and a small number of multipath components. Even without the temporal variation caused by moving traffic a location such as Hallgarth Street with many multipath components was not susceptible to modelling with either the Normal or Weibull distribution.

The parameters of both the Normal and the Weibull distributions varied widely from one measurement location to another. It is unlikely that it is possible to model all locations with a single distribution without taking into account the terrain and surface clutter.

An examination of the PDFs of the RMS delay spread revealed that the distribution was multimodal. Since the duration of measurement in each location was limited this was not unexpected. The 15 seconds of measurement allowed by the sounder was not enough to completely characterise the channel so further measurements are desirable.

CHAPTER 9. CONCLUSIONS AND FURTHER WORK

9.1 Conclusions

It has been possible to use the UMIST 8 channel sounder to make wideband measurements continuously over periods of up to 15 seconds.

Testing of the sounder before embarking on a measurement campaign revealed a fault and a number of limitations. The fault (in the signal conditioning unit) was rectified and a number of limitations mitigated by implementing a number of modifications. The noise contribution of the signal conditioning circuits was reduced by including a roofing filter between the signal conditioning inputs and the outputs of the preceding mixers. Other circuit modifications reduced a tendency to instability at high gain settings. One modification which was not implemented, due to lack of time, was to gate out the spike which occurrs at start of sweep. During postprocessing the first 100 samples of the time series data were ignored thus gating out the spike in software.

Overall the sounder has been demonstrated to be robust and capable of operating for 2 hours continuously when the receiver was battery powered.

The predicted resolution of the sounder was confirmed during testing and calibration as a path length difference of 6.5 m.

The limit on the length of a measurement run of 15 seconds was imposed by the data acquisition system and it was impossible to remove this limitation using the existing hardware and software. The existing software needed 90 minutes to save the data from a 15 second measurement to disk. With a battery life of 2 hours it was impossible to make more than one 15 second measurement before returning to the university for a battery change.
It has been possible to develop a new data acquisition system using commercial data acquisition cards. The software for the new data acquisition system needs some more development before it can be used as a matter of routine. It has been demonstrated to work but has not been comprehensively tested for function and robustness. The new data

acquisition software saves the data from a 15 second measurement in less than 3 minutes. This software has been developed for a 32 bit Windows environment and does not rely on the use of the PC parallel port.

It has been possible to develop an inexpensive eight channel antenna characterisation rig. This was developed so that an existing antenna system could be characterised. It has subsequently been used during development of antenna systems on other projects and has eliminated the need to hire an antenna test range.

Measurements were made at 12 locations in Durham and 6 locations in Manchester. Some of these measurements were made with only directional antennas since this was required by the other students with whom the sounder had to be shared. Examination of the measurement data showed interference or sounder malfunction in some files and these were rejected. Of the measurements which survived this examination only those made with an omnidirectional antenna were selected for analysis. There were three locations in Durham and two locations in Manchester. At one location in Durham measurements were made on two days. At one of the locations in Manchester measurements were made on three days.

The first statistic to be extracted from the measurement data was the number of delay bins containing multipath components. The data from each 15 second measurement run was divided to produce one ensemble from the first half of the run and another ensemble from the second half. Thresholds were set at 6 dB and 12 dB below the strongest component as described in chapter 8, section 8.2. A comparison of the number of components in each ensemble revealed differences. The mean and median number of components recorded in each of the ensembles were compared and showed that there were differences of up to 44% with a 6 dB threshold and up to 40% with a 12 dB threshold. These differences were between measurements made at different times and indicate a temporal variation in the number of multipath components. The temporal variation was different between different locations.

Although it was not possible to extract absolute delay information from the measurements it was possible to estimate the differences in mean delay between the ensembles. In addition to a visual examination of the CDFs of the mean delays, a Kolmogorov-Smirnof test was applied to the two ensembles from each measurement location. Taking the Null hypothesis that the two ensembles of data came from the same population the Kolmogorov-Smirnof test indicates whether the Null hypothesis should be accepted or rejected. This test was also applied to data collected using directional antennas at the same locations as the omnidirectional antennas. In all cases the results suggested that the Null hypothesis should be rejected and that there is temporal variation of the mean delay.

The third statistic extracted from the measurement data was the RMS delay spread. Kolmogorov-Smirnof test results indicate that the data from the first and second half ensembles did not come from the same population. Attempts to model the RMS delay spread by fitting known distributions to the data failed in all but two cases. As figure 8.78 shows the PDF of the RMS delay spread was multimodal and this suggests that not enough data was considered. Since the limitations of the sounder and data acquisition system precluded measurements over periods exceeding 15 seconds some more development work will necessary before further measurements are made.

Overall the three statistics examined show that there is temporal variation in the radio environment but further measurements will be needed before this variation can be characterised. The temporal variation observed was mainly due to movement of motor vehicles in the street in which the sounder receiver was located or in adjacent streets.

Measurements in two bands separated by 190 MHz suggest that there are differences in the statistics for the two bands. It was only possible to make one measurement in two bands so it is not possible to conclude that there will be differences between bands with similar separation. Some more dual band measurements should allow a conclusion to be drawn.

9.2 Further Work

Limitations in the data acquisition system prevented the recording of data for periods exceeding 15 seconds. This is due to the limited amount of memory on the data acquisition card and the slow rate of writing data to disk by the software. The new data acquisition system developed during this project should allow faster saving of data to disk and this would allow several measurement runs to be made at each location without having to move back to the university for a battery change. Further work is necessary to test the software so far developed and to extend its functionality.

The dynamic range of the sounder is impaired by the spike which appears at the output of the mixers at start of sweep and an inability to change the RF attenuation on individual channels. Both of these limitations could be alleviated by hardware changes.

A further series of measurements should be conducted. With the new data acquisition it should be possible to record measurements for longer periods and to make measurements at more locations in different environments. Longer measurement periods will allow the radio channel to be better characterised for each measurement location. Measurements in more locations will allow characterisation of different radio channels leading to a more complete understanding of the temporal variations.

BIBLIOGRAPHY

This bibliography contains details of all of the works to which reference is made in the text of the thesis. It also contains details of other works which were useful in the project but which are not refered to in the text. Each item is numbered and the citation of a reference from within the text is indicated thus: [n], where n is the number of the item in the bibliography.

1. Donald C. Livingstone, The Physics of Microwave Propagation, Prentice Hall, 1970.
2. Abramowitz and Stegun, Handbook of Mathematical Functions, Dover, 1970.
3. J. Deygout, Multiple Knife Edge Diffraction of Microwaves, IEEE Transactions on Antennas and Propagation, Vol AP14, pp 480-489, July 1966.
4. J. Epstein and D. W. Peterson, An Experimental Study of Wave Propagation at 850 Mc/s, Proc IEEE, Vol 41, pp 595-611, May 1953.
5. Carlos Lopez Giovaneli, An Analysis of Simplified Solutions for Multiple Knife Edge Diffraction, IEEE Transactions on Antennas and Propagation, Vol AP32, pp 297-301, March 1984.
6. R. G. Lewenz, Pathloss Variation Due to Vegetation Movement, NCAP99.
7. Alfred H. LaGrone, Paul E. Martin and Caroll W. Chapman, Height Gain Measurements at VHF and UHF behind a Grove of Trees, IRE Transactions, Vol BC9, pp 37-54, 1963.
8. R. G. Lewenz, unpublished on the Long Term Variation of Path Loss over Short Paths in the 2 GHz band.
9. Roland King, Radio Channel: Living with Real-world Propagation Effects; Elektrobit AG, CH-8608 Bubikon, Switzerland.
10. P. Sharma, K. Chandra and C. Thompson, Interference in Indoor Wireless Channels; Centre for Advanced Computation and Telecommunications, University of Massachusets Lowell, Lowell, MA 01854.

11. Ben Allen, Julian Webber, Peter Karlsson and Mark Beach, UMTS Spatio-temporal Propagation Trial Results; Proceedings of IEE ICAP 2001 publication No 480 pp 497-501.

12. Philip A. Bello, Characterization of Randomly Time-Variant Linear Channels; IRE Transactions on Communications Systems, vol CS-11, Dec 1963.

13. E. Zollinger, Measured Inhouse Radiowave Propagation Characteristics for Wideband Communication Systems; Proceedings of IEEE EUROCON88

14. Theodore S. Rappaport, Characterization of UHF Multipath Radio Channels in Factory Buildings; IEEE Transactions on Antennas and Propagation, vol 37, No 8, August 1989.

15. Theodore S. Rappaport, Scott Y. Seidel and Koichiro Takamizawa, Statistical Channel Impulse Response Models for Factory and Open Plan Building Radio Communication Systems Design; IEEE Transactions on Communications, vol 39, No 5, May 1991.

16. A. M. D. Turkmani, D. A. Demery and J. D. Parsons, Measurement and Modelling of Wideband Mobile Radio Channels at 900MHz; IEE Proceedings-1, vol 138, No 5, October 1991.

17. Adel A. M. Saleh and Reinaldo A. Valenzuela, A Statistical Model for Indoor Multipath Propagation; IEEE Journal on Selected Areas in Communication, vol SAC-5, No 2, February 1987.

18. J. D. Parsons and A. S. Bajwa, Wideband Characteristics of Fading Mobile Radio Channels; IEE Proceedings vol 129 part F No 2, April 1982.

19. Robert J. C. Bultitude and G. Keith Bedal, Propagation Characteristics on Microcellular Urban Mobile Radio Channels at 910MHz; IEEE Journal on Selected Areas in Communications vol 7 No 1, January 1989.

20. J. G. O. Moss, A. M. Street, M. P. Fitton, K. M. Brown, C. C. Constantinou and D. J. Edwards, Broadband Physical Layer Investigation;

21. Scott Y. Seidel, Theodore S. Rappaport, Sanjiv Jain, Michael L. Lord and Rajendra Singh, Pathloss, Scattering and Multipath Delay Statistics in Four European Cities for Digital Cellular and Microcellular Radiotelephone; IEEE Transactions on Vehicular Technology, vol 40 No 4, November 1991.

22. Paul Marinier, Gilles Y. Delisle and Charles L. Despins, Temporal Variations of the Indoor Wireless Millimeter-Wave Channel; IEEE Transactions on Antennas and Propagation vol 46 No 6, June 1998.

23. Robert J. C. Bultitude, Samy A. Mahmoud and William A. Sullivan, A Comparison of Indoor Radio Propagation Characteristics at 910MHz and 1.75GHz; IEEE Journal on Selected Areas in Communications, vol 7 No 1, January 1989.

24. Gerard J. M. Janssen, Patrick A. Stigter and Ramjee Prasad; Wideband Indoor Channel Measurements and BER Analysis of Frequency Selective Multipath Channels at 2.4, 4.75 and 11.5 GHz, IEEE Transactions on Communications, vol 44 No 10, October 1993.

25. Achmad Affandi, Ghais El Zain and Jaques Citerne; Investigation on Frequency Dependence of Indoor Radio Propagation Parameters; IEEE, 1999.

26. D. P. McNamara, M. A. Beach, P. N. Fletcher and P. Karlsson; Temporal Variation of Multiple-Input Multiple-Output MIMO Channels in Indoor environments; IEE ICAP 2001, April 2001.

27. Hulya Gokalp; Characterisation of UMTS FDD Channels, PhD Thesis, UMIST 2001.

28. Jarmo Kivinen, Xiongwen Zhao and Pertti Vainikainen; Empirical Characterization of Wideband IndoorRadio Channel at 5.3 GHz, IEEE Transactions on Antennas and Propagation, Vol 49, No 8, August 2001, pp1192-1203.

29. R. Bultitude, P. Hou, R. Hahn, G. Hendrantoro, D. Falconer and R. Berube; Radio Propagation Data Pertinent to the Design of LMCS Systems at 28 GHz, Proc ANTEM, Ottawa, August 1998.

30. R. S. Thoma, D. Hampicke, A. Richter, G. Sommerkorn, A. Schneider and U. Trautwein; Identification of Time-Variant Directional Mobile Radio Channels, 16th IEEE Instrumentation and Measurement Technology Conference, IMTC/99, Venice, Italy, May 14-26 1999.

31. Jean Philippe Kermoal, Laurent Schumacher, Klaus Ingermann Pedersen, Preben Elgaard Mogensen and Frank Frederiksen; A Stichastic MIMO Radio Channel Model with Experimental Validation, IEEE Journal on Selected Areas in Communications, Vol 20, No 6, August 2002.

32. D. Hampicke, Ch. Schneider, M. Landmann, A. Richter, G. Sommerkorn and R. S. Thoma; Measurement-Based simulation of mobile radio channels with multiple antennas using a directional parametric data

model, Proceedings 54th Vehicular Technology Conference (VTC Fall 2001), Atlantic City, NJ, USA, October 2001.

33. J. D. Behm, T. J. Endres, P. Schniter, M. L. Alberi, C. Prettie, C. R. Johnson Jr and I. Fijalkow; Characterization of an Empirically-Derived Database of Time-Varying Microwave Channel Responses, Applied Signal Technology and Blind Equalization Research Group at Cornell University, website: http://spib.rice.edu/spib.html (database) and http://backhoe.ee.cornell.edu/BERG (notification of database use).

34. Byoung-Jo Kim, N. K. Shankaranaryanan, Paul S. Henry, Kevin Schlosser and Thomas K. Fong; The AT&T Labs Broadband Fixed Wireless Field Experiment, IEEE Communications Magazine, October 1999.

35. David Brunt, M.A. (Cantab), B.Sc (Wales); The Combination of Observations; Cambridge at the University Press, 1917.

36. W. M. Harper, A.C.W.A; Statistics (The M&E Handbook Series); MacDonald and Evans, London, 1965.

37. G. Udny Yule and M. G. Kendal; An Introduction to the Theory of Statistics; Griffin, London; Fourteenth Edition 1950.

38. Russell Langley; Practical Statistics Simply Explained, second edition; Pan Books.

39. J. Halcombe Laning Jr and Richard H. Batin; Random Processes in Automatic Control; McGraw-Hill Book Company Inc, 1956.

40. Perry R. Hinton; Statistics Explained, 2nd Edition; Routledge, 2004.

41. Pantelis Filippidis; Multi-Channel Sounder for Directional Measurements; PhD Thesis, UMIST, 2002.

42. Hulya Gokalp; Characterisation of UMTS FDD Channels; PhD Thesis, UMIST 2001.

43. Mustafa Abdalla; PhD Thesis, UMIST, 2005.

44. Frederic J Harris, On the Use of Windows for Harmonic Analysis with the Discrete Fourier Transform, Proceedings of the IEEE Vol 66 No 1, January 1978.

45. Electronic Filter Design Handbook, Arthur B. Williams, 1981, McGraw Hill Inc.

46. Handbook of Filter Synthesis, Anatol I. Zverev, 1967, John Wiley and Son Inc.

47. NIST Engineering Statistics Handbook paragraph 1.3.6.6.8. http://www.itl.nist.gov/div898/handbook/eda/section3/eda3668.htm.

48. Online Free Encyclopedia. http://en.wikipedia.org/wiki/Probability_distribution.

49. Professor David Jenn, US Naval Postgraduate School, Lecture Notes Volume V, Electromagnetic Wave Propagation.

APPENDIX 1. FORMAT OF THE MEASURED DATA FILE

A1.1 INTRODUCTION

This appendix describes the format of the measured data file since this does not appear to be documented elsewhere. This appendix describes the format output by the data acquisition software which was written by P. Filippidis in 2001 and 2002.

A1.2 FORMAT

The data file resulting from a field measurement is a character file consisting of a header describing the sounder parameters and the measurement data. The header consists of four lines with the following data items.

Line 1 has two fields separated by a comma. The first field is the number of sweeps recorded as an integer. The second field is the number of samples per sweep as an integer.

Note: If the 500 ksamples/sec rate is selected then the number of sweeps in the file header is half the number of sweeps actually recorded and the number of samples per sweep is double that actually recorded. This is due to an error in the data acquisition software.

Line 2 has a single field which is the RF attenuation in dB as an integer.

Line 3 records the gains of the eight channels as eight integers separated by commas.

Line 4 has a single field which is the accumulated distance recorded by the distance transducer in metres as a fixed point real number.

The remaining lines in the file record the output values from the channel analogue to digital converters as integers. There are eight fields on each line seperated by commas, one for each channel. There will be one line for each sample (all channels are sampled simultaneously). If the number of

samples per sweep is **nsamples** and the number of sweeps recorded in the file is **nsweeps** the first sweep will occupy lines 5 to 5 + **nsamples**. There will be **nsweeps** * **nsamples** lines of data in the file.

The last line in the file is identical to line 4.

A1.3 EXAMPLE

The following is a truncated example of a measurement data file with some annotations.

```
10,4000                          number of sweeps, samples per sweep
0                                    RF attenuation in dB
39,40,42,42,43,41,47,33          channel signal conditioning gains
1310.7                           distance
203,95,60,130,71,229,63,17       sweep 1, sample 1, channels 1 to 8
204,107,73,114,87,232,57,14      sweep 1, sample 2, channels 1 to 8
195,119,106,107,114,215,65,37
176,125,163,123,146,164,96,97
169,121,205,147,158,125,120,138
198,114,197,140,144,149,101,108
.
.many lines removed
.
240,113,173,108,131,199,60,52
247,126,179,85,145,203,44,44
228,145,204,80,172,172,58,73
208,162,219,73,191,149,68,88
199,172,224,63,202,137,73,92
184,179,230,63,215,119,85,109
164,187,237,71,228,98,102,130
145,192,240,80,233,81,117,147    sweep 10, sample 4000, channels 1 - 8
1310.7                           distance
```

APPENDIX 2. COMMUNICATIONS BETWEEN DATA ACQUISITION PC AND SOUNDER

A2.1 INTRODUCTION

Communications between the data acquisition PC and the sounder are via the PC parallel port. This document describes the communications protocols and the command set used.

A2.2 HARDWARE BLOCK DIAGRAM

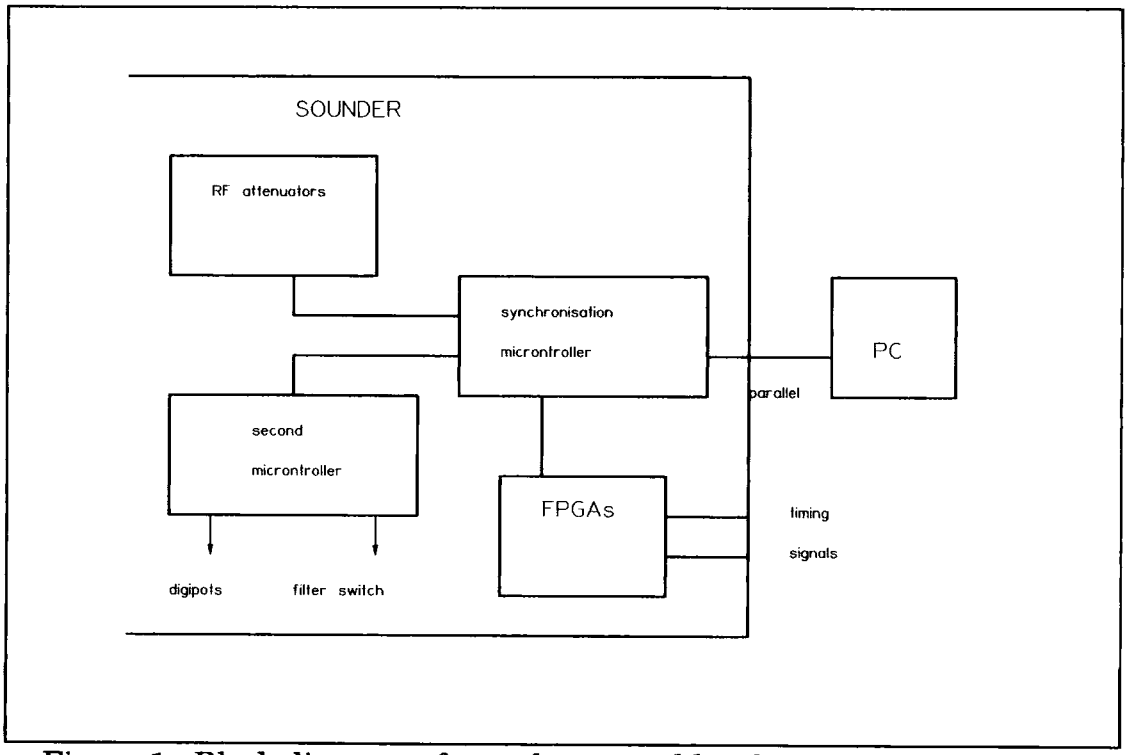

Figure 1. Block diagram of sounder control hardware and connection to data acquisition PC.

A2.3 PROTOCOLS

The protocols used by the PC to communicate with the Synchronisation Board in the sounder allows data to be sent to and received from either of the two FPGAs or the microntroller. These can be regarded as a set of 8 bit registers which may be written to or read from.

The control port in the PC parallel port is used to set the address of the sounder register to be accessed and to set the direction of the data transfer. The data port is used to set the value of data to be sent or to accept the value of data received.

A2.3.1 Physical Layer

The 8 pins of the parallel port connected to the data register is used to transfer an 8 bit value at TTL levels.

The lower 4 bits of the control port are used to set the address of the sounder register to be accessed and these are connected to parallel port pins assigned as Strobe, Autofeed, Init and Select. It should be noted that the Strobe, Autofeed and Select pins are active low. They are inverted in the parallel port hardware and this must be taken into account in the software which sets these pins.

The direction of the data transfer is indicated by the Direction pin which is connected to bit 5 of the control register. This pin is held high for a read operation and held low for a write operation.

The data acquisition software written by P Filippidis addresses the parallel port hardware via an OCX control routine. This places a limitation on the development environment which may be used to change the program and the operating system used on the data acquisition PC. The development environment must be Microsoft Visual Basic 5 since this is the latest version which supports OCX controls. The program was developed under Microsoft Windows 95. It is unlikely to work under Windows NT and would require Windows 2000 to operate in compatibility mode.

A2.3.2 Logical Layer

To transfer a byte to the sounder the following sequence of operations is required:

- The data byte is written to the parallel port data register.
- The address to which the data is to be sent is written to the lower 4 bits of the control port with the higher 4 bits set to zeroes (remembering to invert bits 0, 1 and 3).
- After a short delay decimal value 4 (NOP) is written to the control port.

To receive a byte from the sounder the following sequence of operations is required:

- Decimal value 4 is written to the control port.
- Decimal value 255 is written to the data port.

- The address (with bits 0, 1 and 3 inverted) and bit 5 set to 1 is written to the control port.
- After a short delay decimal 36 is written to the control port.
- The byte value is read from the data port.
- There must be a short delay before repeating the procedure to read another byte.

A2.3.3 Addresses

The following table shows the addresses of the sounder registers and the purpose of each. Both read and write addresses are decimal and have the necessary bits inverted. The table also shows the mnemonic names assigned to the addresses.

Address	Write Value	Read Value	Effect of operation
0 Wsreset	11	n/a	Reset wheel sensor
1 Wsread	n/a	42	Read wheel sensor. Needs 3 reads in succession
2 Sigcond			Allows data and addresses to be sent to the second microntroller

Address	Write Value	Read Value	Effect of operation
3 clockdiv	8	n/a	Set clock divider (0 - 255)
4 SRF_L	15	n/a	Set number of sweeps low byte
5 SRF_M	14	n/a	Set number of sweeps middle byte
6 SRF_H	13	n/a	Set number of sweeps high byte
7 Rfatten	12	n/a	Set the RF attenuators
8 CLK_L	n/a	35	Read clock pulses per sweep low byte
9 CLK_M	n/a	34	Read clock pulses per sweep middle byte
10 CLK_H	n/a	33	Read clocks per sweep high byte
11 Realclock	0	n/a	Start real clock
12 reserved1	7	39	reserved for future use
13 reserved2	6	38	reserved for future use
14 reserved3	5	37	reserved for future use
15 NOP	4	36	No operation. Sets all control bus lines high thus deselecting all sounder registers.

Table 1. Sounder addresses and Operations.

A2.4 PROTOCOL DETAILS

The following paragraphs describe the protocol operations in detail. This is necessary because some operations need to reset the sounder register before or after data transfer. Also the delays required vary from operation to operation.

A2.4.1 Address 0 - Reset Wheel Sensor

This operation resets to zero the counter which accumulates the wheel sensor pulses.

- Decimal 11 is written to the control register.
- There is a delay of 0.1 seconds.
- Decimal 4 is written to the control register.

A2.4.2 Address 1 - Read the wheel sensor

Reads 2 bytes from the wheel sensor counter.

- Write decimal 4 to the control register.
- Write decimal 255 to the data register.
- Write decimal 42 to the control register.
- Delay for 0.1 seconds.
- Write decimal 36 to the control port.
- Read the lower byte from the data register.
- Delay for 0.001 seconds.
- Write decimal 255 to the data register.
- Write decimal 42 to the control port.
- Delay 0.1 seconds.
- Write decimal 36 to the control port.
- Read the higher byte from the data register.
- Delay 0.001 seconds.
- Write decimal 255 to the data port.
- Write decimal 42 to the control port.
- Delay 0.1 seconds.
- Write decimal 4 to the control port.

digital potentiometers. Code 2 is always sent to the control port and the byte sent to the data port contains both address and data. The 2 most significant bits indicate which signal conditioning function is to be performed while the 6 least significant bits are the data to be used. The functions available are:

- Switch the filter bandwidth to 165 kHz or to 250 kHz.
- Send a value to the the digital potentiometers which control the signal conditioning gain.
- Send the address of the digital potentiometer to be set.

Setting the digital potentiometers, and hence the signal conditioning gain, is a two stage process. First the potentiometer value is sent then the address of the potentiometer is sent. There are 16 digital potentiometers, 2 for each of the 8 channels. Both potentiometers must be set to achieve a particular gain. The values to be set are stored in a disk file which is read by the data acquisition program at startup.

A2.4.3.1 Setting the Filter Bandwidth

- Write decimal 192 to the data port.
- Write decimal 2 to the control port.
- Delay.
- Write decimal 80 to the data port for 250kHz bandwidth or decimal 96 to the data port for 165kHz bandwidth.
- Delay.
- Write decimal 192 to the data port.
- Delay.
- Write decimal 4 (NOP) to the control port.
- Write decimal 255 to the data port.

A2.4.3.2 Setting the Signal Conditioning Gain

The value to which the digital potentiometer (digipot) is to be set is sent first as follows:

- Write decimal 192 to the data port.
- Write decimal 2 to the control port.
- Delay.

- Write the digipot value + decimal 128 to the data port.
- Delay
- Write decimal 192 to the data port.
- Delay.
- Write decimal 4 (NOP) to the control port.
- Delay.
- Write decimal 255 to the data port.

The address of the digipot to be set is then sent as follows:

- Write decimal 192 to the data port.
- Write decimal 2 to the control port.
- Delay
- Write the digipot address + decimal 64 to the data port.
- Delay.
- Write decimal 192 to the data port.
- Delay
- Write decimal 4 (NOP) to the control port.
- Delay.
- Write decimal 255 to the data port.

A2.4.4 Address 3 - Set the Clock Divider

This sets the clock division ratio. Actually the value sent is 1 less than the required division ratio.

- Write the required division ratio (minus 1) to the data register.
- Write decimal 8 to the control register.
- Delay 0.1 seconds.
- Write decimal 4 (NOP) to the control register.

A2.4.5 Addresses 4, 5 and 6 - Set the number of sweeps

The number of sweeps may be between 1 and 262143. This requires the transfer of 3 bytes. The least significant byte is sent to address 4, the middle byte to address 5 and the most significant byte to address 6.

- Write the least significant byte to the data register.
- Write decimal 15 to the control port.
- Delay 0.5 seconds.

- Write decimal 4 to the control port.
- Write the middle byte to the data register.
- Write decimal 14 to the control port.
- Delay 0.5 seconds.
- Write decimal 4 to the control port.
- Write the most significant byte to the data register.
- Write decimal 13 to the control port.
- Delay 0.5 seconds.
- Write decimal 4 to the control port.

A2.4.6 Address 7 - Set RF Attenuators

Sounder register 7 programs the RF attenuators. At present all attenuators are set to have the same attenuation value. The attenuation required is used as index into a lookup table containing the values to be sent to the data register.

- The attenuation value is subtracted from 31 and the resultant used as index to the lookup table.
- The value from the lookup table is sent to the data register.
- Decimal 12 is written to the control register.
- Delay 0.1 seconds.
- Decimal 4 is written to the control register.

A2.4.7 Addresses 8, 9 and 10 - Read the number of clock pulses per sweep

This operation reads the actual number of clock pulses per sweep. It is usually performed immediately after setting the clock divider.

- Write decimal 255 to the data port.
- Write decimal 35 to the control port.
- Delay for 0.5 seconds.
- Read the least significant byte from the data register.
- Write decimal 4 (NOP) to the control register.
- Write decimal 255 to the data register.
- Write decimal 34 to the control port.
- Delay for 0.5 seconds.
- Read the middle byte from the data register.

- Write decimal 4 (NOP) to the control port.
- Write decimal 255 to the data port.
- Write decimal 33 to the control port.
- Delay for 0.5 seconds.
- Read the most significant byte from the data port.
- Write decimal 4 to the control port.

A2.4.8 Address 11 - Start Real Clock

The Real Clock output from the sounder consists of timing pulses which are intended to trigger a data acuisition card. Exactly the right number of pulses are output to sample the requested number of sweeps. Writing decimal 255 to address 11 starts the Real Clock.

- Write decimal zero to the control port.
- Write decimal 255 to the data port.

NOTE: The data acquisition card constructed at UMIST and used by Pantelis' data acquisition software does not use the Real Clock. It uses the 10 MHz reference clock direct. Real Clock is not suitable for use with the new 4 channel data acquisition cards since they divide the clock by 2 and hence require the clock to be at twice the required sample rate. The number of samples collected by these new cards is set by the software.

A2.4.9 Addresses 12, 13 and 14

These addresses are not used at present.

A2.4.10 Address 15 - NOP

The contents of the sixteenth element of the address table is a No-Operation which is decimal 4. The sounder has no register at address 15 so sending a NOP effectively deselects all sounder registers.

A2.5 AN ALTERNATIVE TO USING THE PARALLEL PORT

If a data acquisition card with some digital I/O ports is used then the parallel port could be replaced by some of the digital I/O ports. This would have a number of advantages.

- The data acquisition software could operate under the more recent Windows operating systems which do not allow direct access to the machine hardware as is required to use the parallel port.

- Any confusion arising from the need to invert some bits when using the parallel port would be removed.
- Since most data acquisition cards have 24 digital I/O lines there would be scope for simplifying the communications protocol by eliminating the need to send data to the signal conditioning circuits via both microntrollers. They could each have dedicated I/O lines.
- Since most modern printers are connected to a PC using a Universal Serial Bus (USB) connection the PC parallel port will become redundant and will not be implemented. This alternative to using the parallel port would provide some "futureproofing" of sounder operations.

A2.6 PARALLEL PORT PIN CONNECTIONS

Pin number	Function	Direction
1	Strobe (active low)	PC to printer
2	data 0	PC to printer
3	data 1	PC to printer
4	data 2	PC to printer
5	data 3	PC to printer
6	data 4	PC to printer

Pin number	Function	Direction
7	data 5	PC to printer
8	data 6	PC to printer
9	data 7	PC to printer
10	ACK (active low)	printer to PC
11	Busy	printer to PC
12	Paper empty	printer to PC
13	Select	printer to PC
14	Autofeed (active low)	PC to printer
15	Error (active low)	printer to PC
16	Initialise	PC to printer
17	Select In (active low)	PC to printer
18 to 25	ground	

A2.7 CONNECTIONS TO PARALLEL PORT REGISTERS

Logically the parallel port is divided into a Data Register, a Status Register and a Control Register. The connections between the registers and the printer connector lines are shown in figure 2 below.

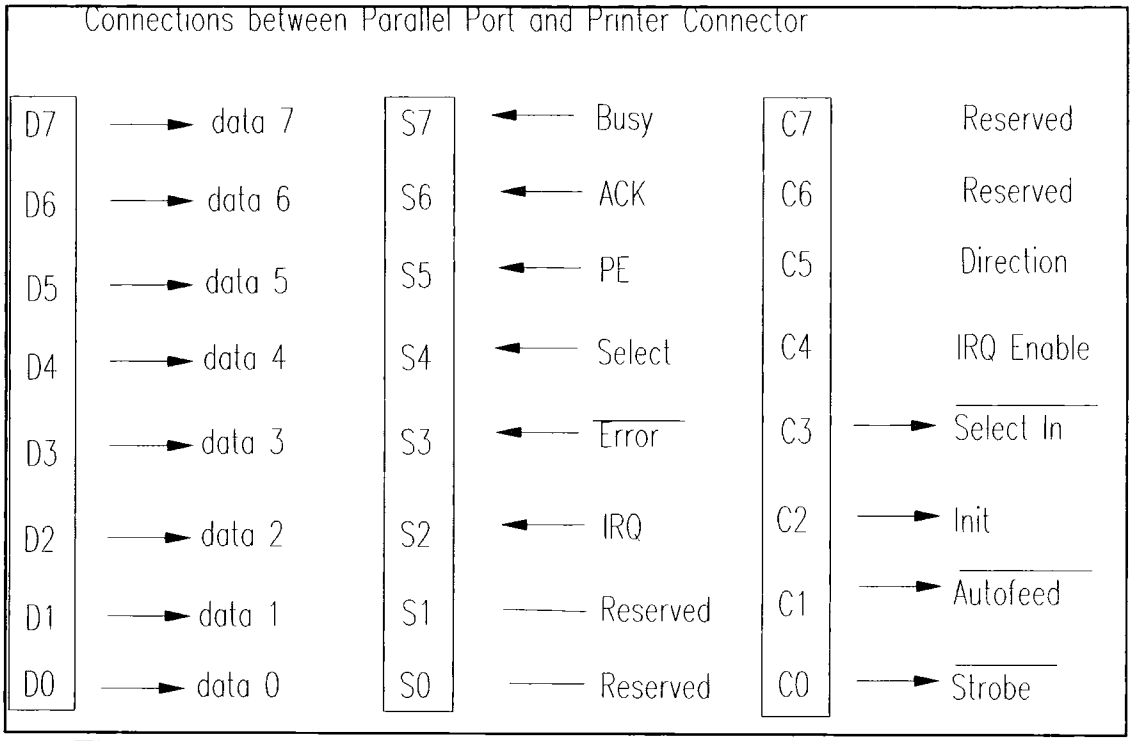

Figure 2. Connections between Parallel Port Registers and Printer Connector.

Parallel port addresses on most PCs are fixed at 3bch, 378h or 278h. On AT class machines the first parallel port is usually found at address 378h (decimal 888). The port address is the address of the data register. The status register is found at the succeeding address and the control register at the address after that. Hence the first parallel port probably has addresses:

Data register: 378h (decimal 888).

Status register: 379h (decimal 889).

Control register: 37Ah (decimal 890).

APPENDIX 3. SOUNDER RESOLUTION

The sounder transmits a signal which sweeps linearly over a bandwidth B in a time T_S as shown in figure 1 below by the solid line. At the receiver the transmitted signal arrives after a short delay as shown by the dotted line in figure 1.

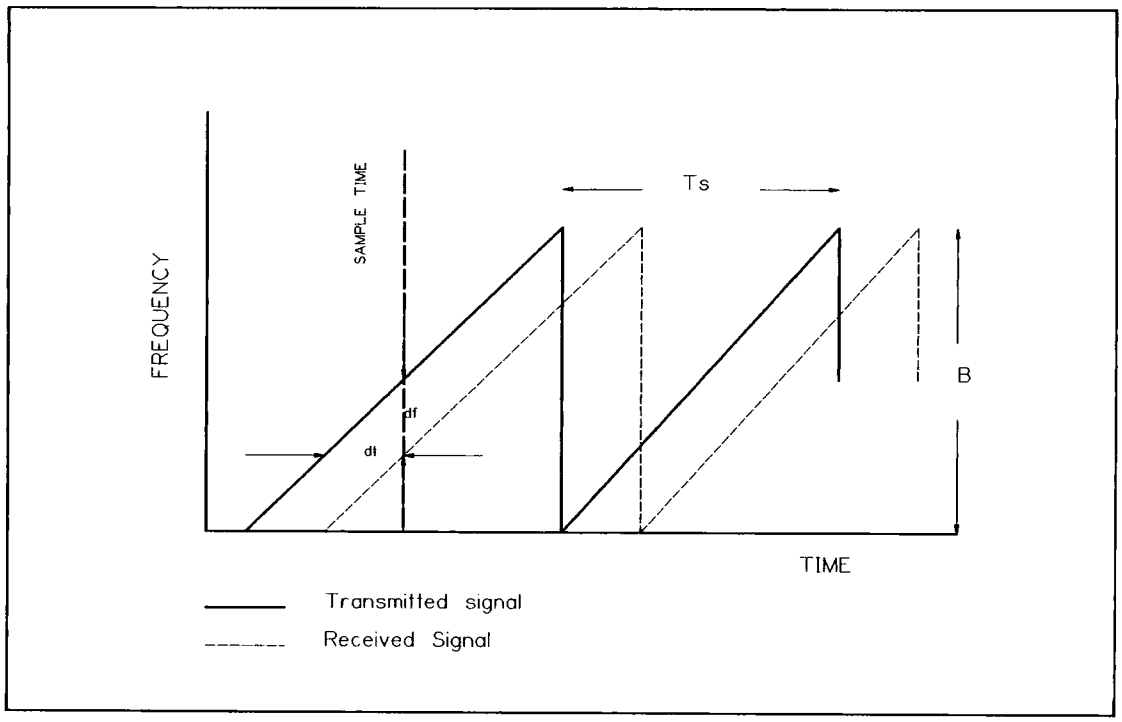

Figure 1. Sounder transmitted and received signals

The received signal is mixed with an exact copy of the transmitted signal and the difference frequencies captured for analysis.

The received signal will be delayed relative to the transmitted signal because is takes a finite time to propagate from the transmitter location to the receiver location. This delay is indicated by dt in figure 1. During the delay time dt the local copy of the transmitted signal will have increased in frequency relative to the received signal by df. This frequency difference gives rise to a beat frequency df in the mixing process and it is this beat frequency that is captured. In the case where there is multipath propagation there will be more than one received signal and each of these signals will be delayed by a different time and give rise to a different beat frequency in the mixing process. The output from the mixing process will

contain a number of beat frequencies, each corresponding to one of the multipath components of the received signal. Spectral analysis identifies the beat frequencies and hence the multipath component delay times.

The signal is captured by digitising it with an analogue to digital converter which takes 1 Msample/sec. The sweep period Ts is 4 msec so 4000 samples are captured during one sweep. The 4000 samples are submitted to a Fourier transform using one of the Discrete Fourier Transforms which yields 4000 bins containing samples in the frequency domain. The first 2000 of the 4000 bins cover the frequencies from zero to the maximum in the captured samples. The second 2000 bins are a mirror image of the first 2000 and represent negative frequencies.

With a sampling rate of 1 Msample/sec the maximum frequency component that can be faithfully reproduced from the samples is 500kHz (sampling theorem). The frequency difference between two adjacent bins after the Fourier Transform is therefore 500000 / 2000 = 250 Hz.

When the sounder is set to sweep over 60 MHz with a sweep repetition frequency of 250 Hz the frequency changes by 60 MHz in 4 msec or 15 Hz in 1 nsec. Since the minimum resolvable frequency is the difference between two bins, 250 Hz, the minimum resolvable delay time is the time taken for the frequency to change by 250 Hz. This is 250 / 15 = 16.67 nsec.

The figure of 16.67 nsec assumes a perfect transformation from the time domain to the frequency domain during the analysis of the data captured at the sounder receiver. Perfect transformation is only possible on an infinitely long series of data. Where the data is a series of finite length the discontinuities at the ends of the series cause spurious components to appear in the frequency domain (sidelobes). To reduce the effect of the discontinuities it is usual to apply a window to the time series data before transformation. This window effectively applies a weighting factor to each sample with least weight given to those samples at either end of the series.

frequency domain bin the those on either side, effectively increasing the frequency spacing between bins, and degrading the resolution in the frequency domain.

There are a number of window functions which are commonly used and each has different properties. We have been using a Hamming window which increases the effective frequency difference between bins by a factor of 1.30 [44]. The practical delay resolution of the sounder when sweeping over a 60 MHz bandwidth is therefore 1.30 * 16.67 = 21.67 nsec. The minimum resolvable difference in path lengths between multipath components is therefore 21.67 / 3.33 = 6.5 m.

APPENDIX 4. REENGINEERING THE SIGNAL CONDITIONING UNIT

A4.1 INTRODUCTION

In the eight channel sounder the signal conditioning unit takes the IF output of the mixers, amplifies it, filters it and passes it to the data acquisition card. The unit has been designed to have eight channels, programmable gain for each channel and two programmable filter bandwidths. The unit has been constructed as a plug-in unit to fit a 3U high rack from which power is acquired via backplane wiring. All signal connections are via front panel connectors.

During testing of part of the next generation of data acquisition software spurious signals were detected at the outputs of all eight of the signal conditioning channels. This document describes the re-engineering work performed to minimise the spurious signals.

A4.2 ORIGINAL CONFIGURATION

Each signal conditioning channel consists of two stages of amplification, each with programmable gain, followed by a three stage six pole active filter with unity gain. The filter acts as an anti-aliasing filter before the analogue to digital converters in the data acquisition card. The A/D converters are capable of sampling the input at a maximum rate of 1000000 samples per second. The sampling rate is programmable by the data acquisition software and may be set to 1Msample/sec or 500ksample/sec.

There are two signal conditioning filters, one with a bandwidth of 250kHz and the other with a bandwidth of 165kHz. The method of selecting the filter bandwidth is to feed both in parallel from the output of the programmable gain amplifier and to switch the output of one of them to the signal conditioning channel output.

The programmable gain amplifier consists of two voltage feedback operational amplifiers each with a digitally controlled potentiometer in the feedback path. This arrangement allows the gain of each stage to be programmed from less than unity to a maximum of approximately 30. The digitally programmed potentiometers are controlled by a microcontroller

within the signal conditioning unit. This microntroller receives commands from the data acquisition PC via the synchronisation microntroller. Physically the signal conditioning unit consists of four printed circuit boards(PCBs) mounted on two metal panels and a front panel with connectors for all signal connections and control circuits. Two of the PCBs are identical and each carries the amplifiers and filters of four signal channels. Of the remaining two PCBs, one carries the switches which connect the filter outputs to the signal conditioning channel outputs while the other carries the microntroller which programs the digital potentiometers and controls the switches.

The signal conditioning unit was designed and built by P Filippidis and is fully described in his PhD thesis. A simplified functional drawing is shown in figure 1 below.

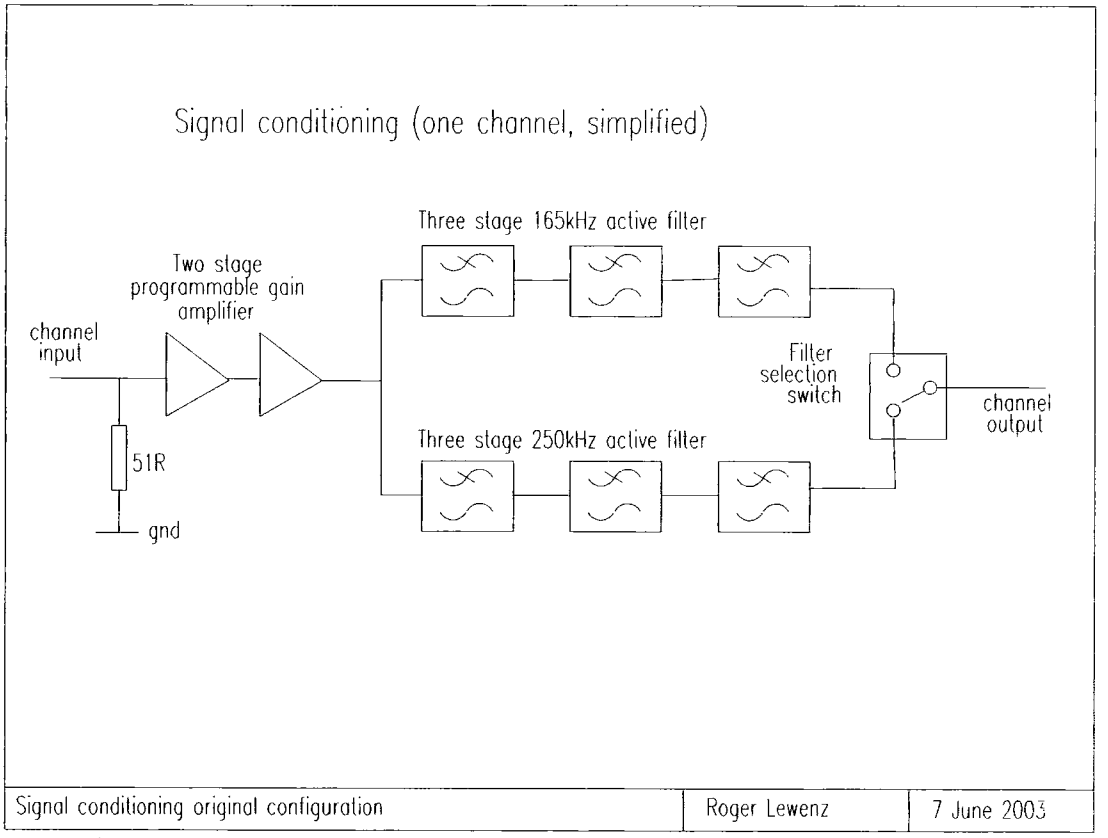

Figure 1. Original signal conditioning configuration, one channel simplified.

A4.3 MODIFICATIONS FOUND

Having discovered the spurious signals a thorough examination of the signal conditioning unit was conducted. It was found that the switches (to

permanently connected the outputs of the 250kHz filters to the channel outputs. Since the eight channel sounder is used for outdoor measurements with a 60MHz sweep width the loss of the 165kHz filter functionality is not considered important.

A4.4 SPURIOUS SIGNALS FOUND

While testing the next generation data acquisition software to check that it properly programmed the digital potentiometers a high frequency spurious signal superimposed on the channel outputs was noticed. For this test a low level signal (20mV) at a frequency within the passband of the filters(50kHz) was injected into the input of each channel from a signal generator. The output from the channel under test was observed with an oscilloscope. The spurious signal was approximately 10mV in amplitude and at a frequency much higher than the filter passband. Further testing with the signal conditioning unit withdrawn from the sounder and supplied with power via an extender card showed that the frequency and amplitude of the spurious signal varied as a hand approached the signal conditioning unit. Using a spectrum analyser it was determined that the frequency of the spurious signal was approximately 1.8MHz reducing as a hand moved nearer to the circuitry.

Two possibilities were investigated. The first possible source of the spurious signal was the unused 165kHz filter which was unterminated at the output. The second possibility was instability due the the operational amplifier in the last stage of the filter being required to drive the large capacitance of the coaxial cables connecting it to the data acquisition card.

A4.5 MECHANICAL RE-ENGINEERING

The original configuration made it impossible to gain access to one of the PCBs carrying four channel amplifiers and filters. The unit has therefore been split into two separate units with an interconnecting cable for control purposes. Since the switch is no longer used the switch PCB was removed entirely and this allowed a major simplification of the signal wiring. It is now possible to gain access to all the components of the channel amplifiers and filters while they are operating if the unit is removed from the sounder and powered via an extension card.

The original configuration had two options for output connectors. One was a ribbon cable header to match the input cable of the in-house data acquisition card and the second was BNC sockets to match the inputs of the next generation data acquisition system. The re-engineered units have only BNC sockets and an external BNC to ribbon cable transition has been added. The front panel layout and assignment of connectors to channels is shown in figure 2 below. The front panel and connector assignments of the BNC to ribbon cable transition are shown in figure 3.

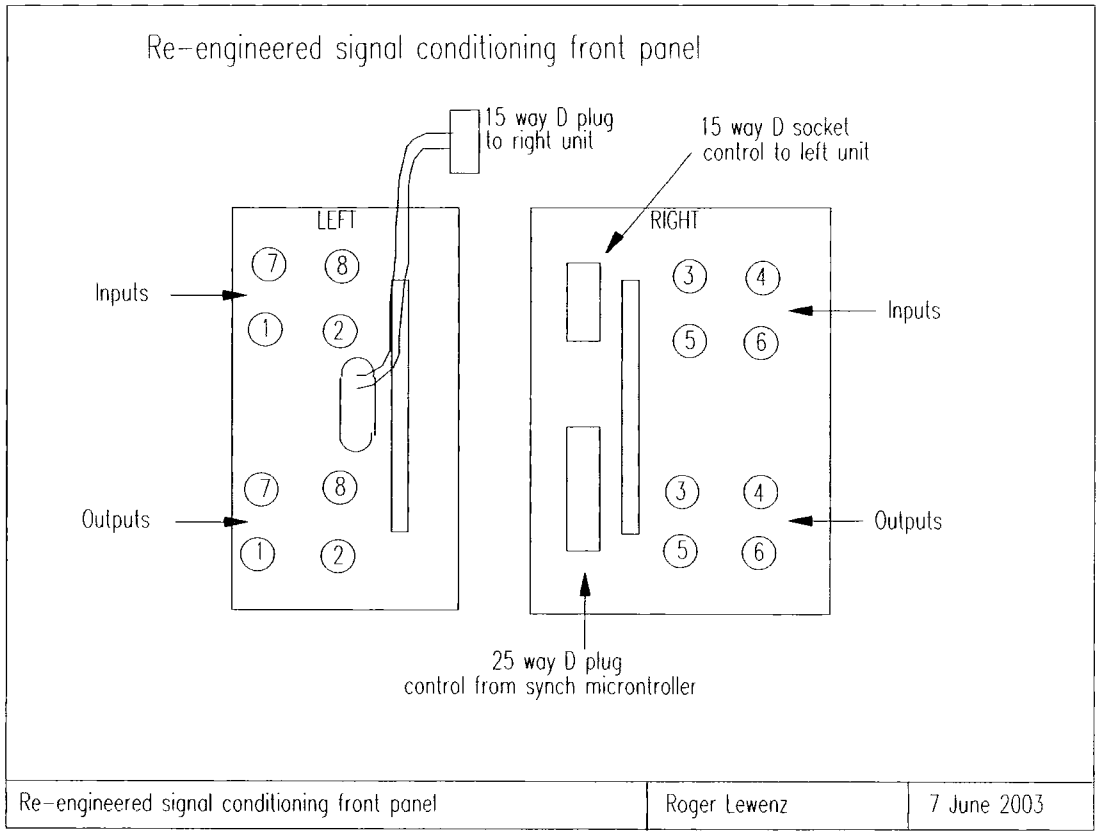

Figure 2. Front panel and connector assignments of re-engineered signal conditioning.

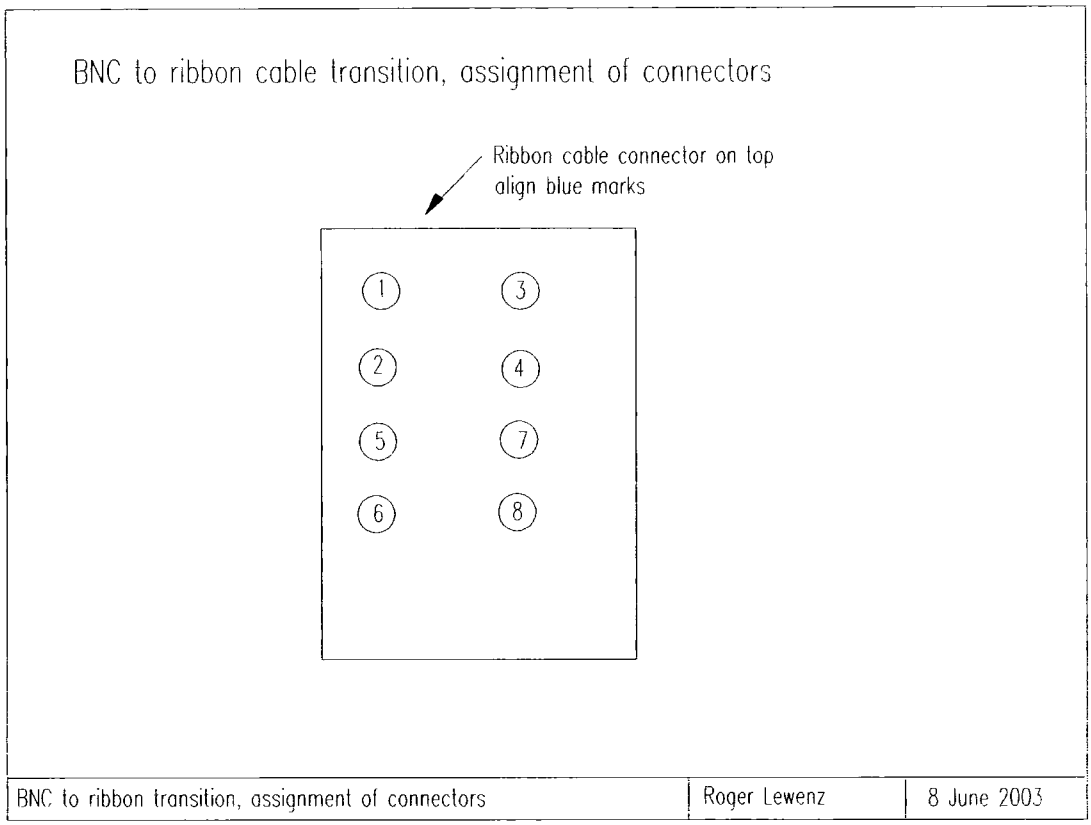

Figure 3. BNC to ribbon cable transition, assignment of connectors to channels.

A4.6 ELECTRICAL RE-ENGINEERING

To ensure that the unused filter sections did not produce oscillations or other spurious signals all the frequency determining capacitors were removed and the inputs to the first and third stages grounded.

To ensure that the capacitive load presented by the coaxial cables did not lead to instability in the final stages of the remaining filters a series resistor of 150Ω was connected between the stage output and the output connector.

A4.7 RESULTS

The 1.8MHz spurious is now absent and the added 150Ω resistor at the output of each final stage amplifier removes the possibility of instability due to the operational amplifiers driving the capacitive loads presented by the coaxial cables. These resistors introduce an additional filter pole which is much higher than the cutoff frequency of the active filters and so should not affect the frequency response of the signal conditioning.

A4.8 ADDITIONAL FILTERING

The noise floor of the frequency domain plots during back to back tests was still higher than desirable and this could be because of the wideband signal

from the mixer causing overloading or intermodulation distortion in the programmable gain amplifiers. Placing a passive low pass filter between the output of the mixer and the input of the programmable gain amplifier improved the situation by lowering the noise floor. This filter, which was of elliptic characteristic characteristic with cutoff frequency of 600kHz, acted as a roofing filter, reducing the noise bandwidth of the input to the programmable amplifier. Since this filter improved the sounder performance eight of them were constructed and built into the signal conditioning unit.

The roofing filter was designed with elliptic characteristic since this gave a rapid rolloff outside the passband with only a few sections. The cutoff frequency is 600kHz with 60dB of attenuation at 800kHz and no less than 40dB of attenuation elsewhere in the stopband. The amplitude and group delay characteristics are flat to 300kHz and therefore do not affect the overall frequency response of the signal conditioning unit. The circuit diagram of the filter is shown in figure 4 below.

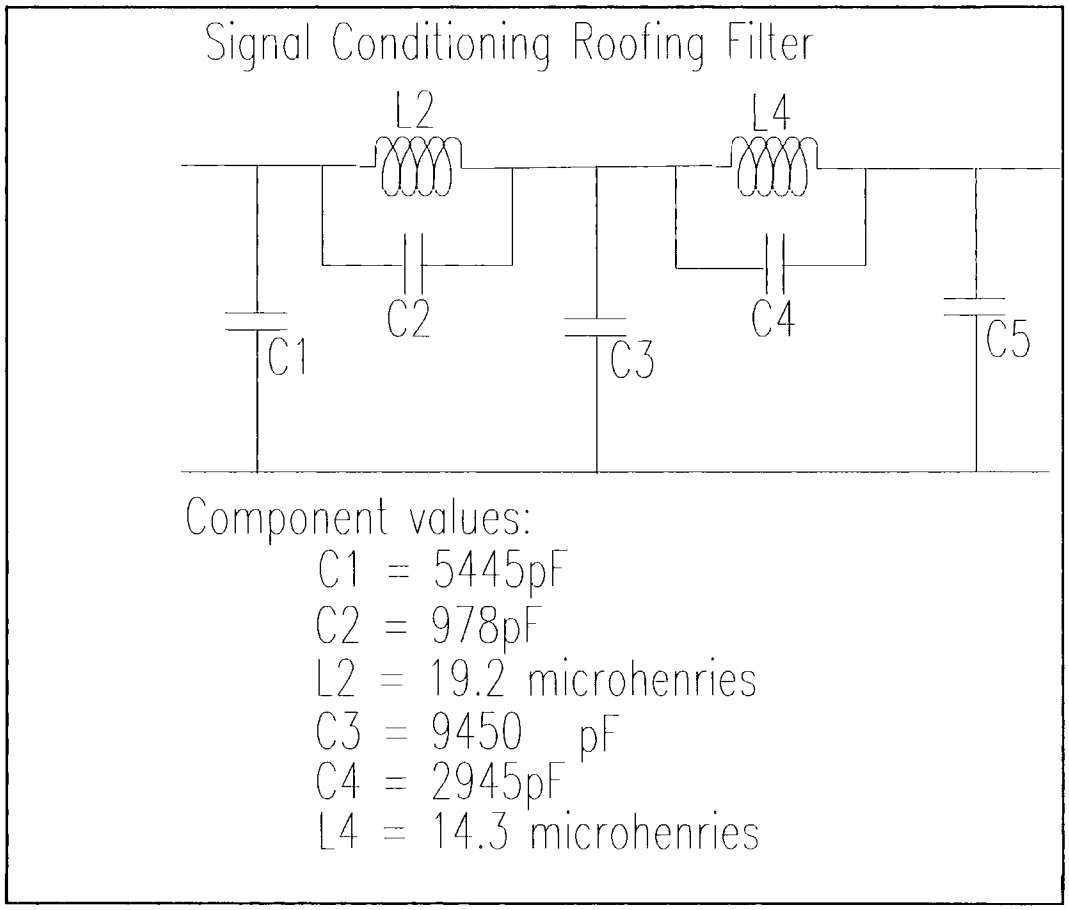

Figure 4. Roofing Filter for Signal Conditioning.

Figure 5 shows the power delay profile plotted from a back to back test with 10 sweeps averaged. Apart from the spurious component at approximately 8.5 microseconds the response is as expected from a back to back test.

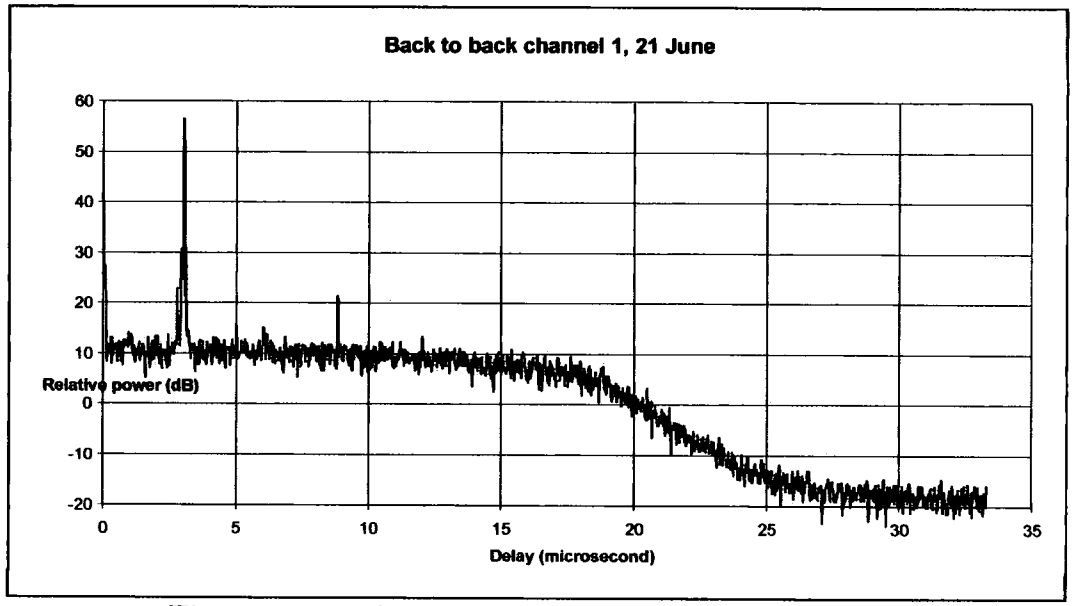

Figure 5. Back to back delay profile with roofing filter.

A4.9 THINGS TO DO

While investigating the spurious responses it was noticed that there is a relatively large transient from the output of the mixer at the start of each sweep. This can be larger than the dynamic range at the input of the programmable amplifier and can cause paralysis of the amplifier. This effect is illustrated in figures 6 and 7 and is well known in radar systems. A possible method of protecting against these transients would be to gate the input of the programmable amplifiers so that the mixer output is disconnected from the amplifiers for a short time at the beginning of each sweep. Time has not permitted any trial of this gating scheme.

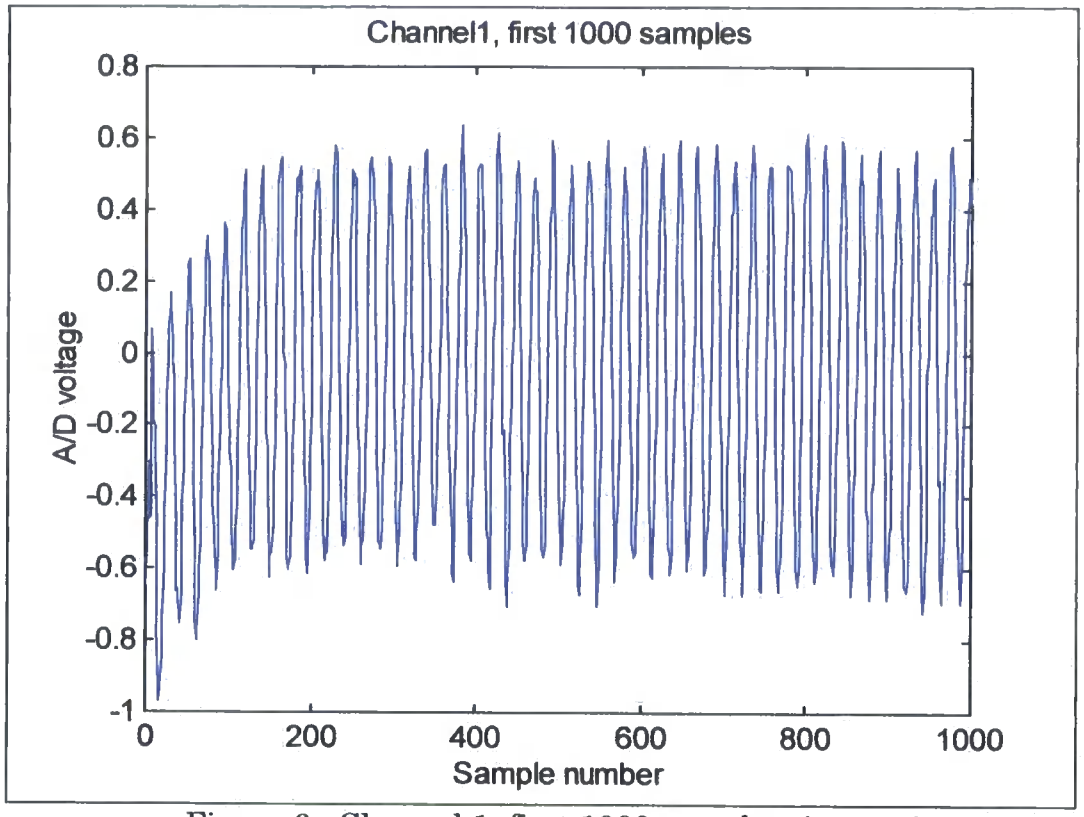

Figure 6.. Channel 1, first 1000 samples time series.

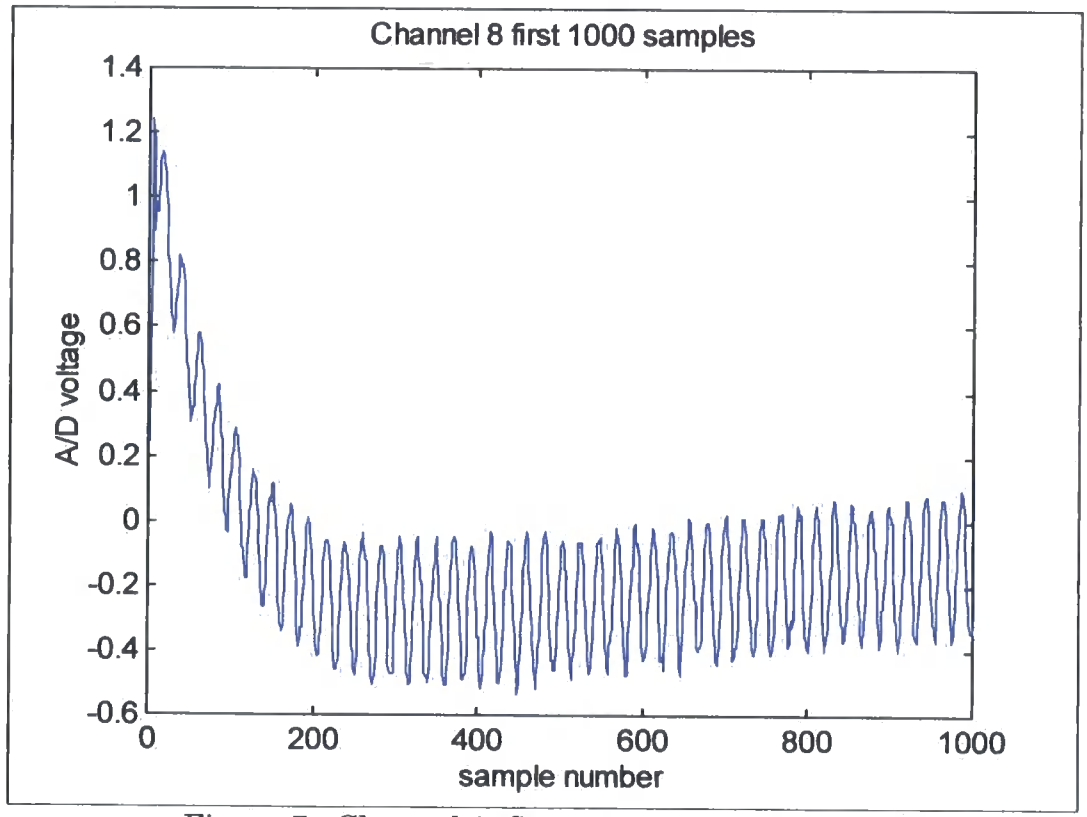

Figure 7. Channel 8, first 1000 samples, time series.

necessary to know the relative gain of the sounder channels. To characterise these relative gains a number of experiments have been conducted as discussed below.

A4.10.1 Variation with time

Two CW sources were constructed with frequencies in the upper band in which the sounder operated. The frequencies of these sources differed by 70kHz which is well within the passband of the signal conditioning filters. One source was used as the local oscillator for the RF front end circuits, driving the amplifier/splitter chain to provide +10dBm to each mixer. The other source was used as a signal, attenuated and split 8 ways and fed to the antenna ports.

With a constant input and all channels set to the same gain the data acquisition was used to measure the voltage output from the signal conditioning over 10 sweep durations.

Measurements were made after the sounder had been switched on for a half hour and at half hourly intervals for a further 3 hours. The peak to peak envelope voltage was calculated and plotted against time.

The output voltage from channels 1 to 7 did not change significantly with time. There were changes in the output from channel 8 when the input was small and the gain high. It is possible that this variation is due to noise or instability. Further investigation is necessary.

A4.11 DIFFERENCE BETWEEN CHANNELS

The plots of output voltage against time showed a difference in gain between the channels. The differences between the channels appeared to depend on the gain set.

After reading the data acquisition software it became apparent that the increments between the settable gains are not constant and that it is impossible to set some gain values. Where the gain required to be set is not available the next lower possible gain is set. It is therefore impossible to predict the differences in gain between the channels and these differences must be measured after the field measurements have been completed.

It may be possible to develop a new architecture for the signal conditioning unit in which any gain may be set at will. This would take time and effort which, at present, are is short supply.

APPENDIX 5. CONTENTS OF CDROM

A5.1 INTRODUCTION

This appendix lists the contents of the CDROM included with this thesis. The programs which have been used for processing the measurement data are included with a brief description of the purpose and method of building and using each of them. For each program the source code, executable and ancillary files have been written on the CDROM. All of the programs have been written in the C programming language using the Kernigan and Ritchie dialect rather than the ANSI dialect. This ensures that simple compilers may be used and the programs may be built an run on a variety of computers. The programs have been run on 486 and Pentium class PCs and on Hewlett Packard 9000 series machines. The programs have been built using the Zortech V3 compiler with 32 bit extender (-mx compiler switch), the GNU C compiler and the Hewlett Packard compiler provided as part of the HP-UX 10.20 operating system. On a PC the programs may be built and run under MS-DOS and in a command window under Windows NT 4.0. The programs are unlikely to run under Windows 2000 since this operating system appears to have an aversion to running programs not developed by Microsoft.

There are Delphi versions of some of the programs. These have been developed with Borland Delphi 5 and provide a Windows interface. These programs will run under Windows 95, Windows 98 and Windows NT 4.0.

The programs used with the Antenna Characterisation rig were intially written in C to run on 16 bit systems. They have been translated into Delphi to provide a Windows interface but because the programs address the hardware direct they were built with Borland Delphi 1 (16 bit).

A5.2 pk2pk4

When using the sounder with an array of directional antennas it was necessary to determine the relative gains of the eight channels. The method of doing this is described in Chapter 6 paragraph 6.2 and the result is a

10 sweep measurement file. The program **pk2pk4** converts the 10 sweep measurement file into a file containing the relative gains.

If the measurement yield the file `example.dac` then by convention the 10 sweep file from relative gain measurement is called `examplex.dac`. This is converted into a file called `example.ini` using **pk2pk4**. `example.ini` is read by the channel splitting program **splitchi**. The following command line is used to effect the conversion

```
pk2pk4 examplex.dac example.ini
```

The files for the C version are:
\pk2pk4\C\pk2pk4.c
\pk2pk4\C\posmean.c
\pk2pk4\C\negmean.c
\pk2pk4\C\pk2pk4.exe

The file for the Delphi version are:
\pk2pk4\delphi\pk2pk.cfg
\pk2pk4\delphi\pk2pk.dof
\pk2pk4\delphi\pk2pk.dpr
\pk2pk4\delphi\pk2pk.exe
\pk2pk4\delphi\pk2pk.res
\pk2pk4\delphi\unit1.dcu
\pk2pk4\delphi\unit1.dfm
\pk2pk4\delphi\unit1.pas

A5.3 splitchi

The **splitchi** program is used to split a measurement file from the sounder into individual channel files and split the upper and lower bands if both band were used. This program silently reads a file with relative gains output by pk2pk4 if it exists in the same directory as the input file. The following command line was used to invoke the program:

```
splitchi input_filename output_file_basename s_flag
```

where

`input_filename` is the name of the measurement file to be split e.g. `example.dac`.

output_file_basename is the part of the names of the output files before the dot. The program will add filename extensions `l1, l2, l3, l4, l5, l6, l7, l8` and `u1, u2, u3, u4, u5, u6, u7, u8` for the single channel files containing the lower band and upper band data.

s_flag is a single letter indicating whether band splitting is required and which band is first in the input file. 'L' indicates that the bands are to be split with the lower band occuring first in the input file. 'U' indicates that band splitting is required and the upper band data is first in the input file. 'N' indicates that band splitting is not required.

The files for the C version are:
\splitchi\C\splitchi.c
\splitchi\C\splitchi.exe

The files for the Delphi version are:
\splitchi\delphi\splitchn.dpr
\splitchi\delphi\splitchn.exe
\splitchi\delphi\splitchn.opt
\splitchi\delphi\splitchn.res
\splitchi\delphi\unit1.dcu
\splitchi\delphi\unit1.dfm
\splitchi\delphi\unit1.pas

A5.4 delay

The **delay** program reads a single channel file from the **splitchi** program and writes a file containing a power delay profile averaged over all the sweeps in the input file. There are three variants, **delay** has an independent axis scaled for delay, **fdelay** has an independent axis scaled for beat frequency and **bdelay** has an independent axis scaled for bin number. All three programs produce an output file which is a text file suitable for reading and plotting with Microsoft Excel. These programs use the FFTW Fourier transform routines from MIT which will be found in the `\fftw` directory. Any of the programs may be invoked with two command line arguments thus:

```
delay input_file output_file
```

The files are:

\delay\C\delay.c
\delay\C\delay.exe
\delay\C\fdelay.c
\delay\C\fdelay.exe
\delay\C\bdelay.c
\delay\C\bdelay.exe.

A5.5 FFTW

This is the FFTW Fourier transform package from MIT. The `\fftw` directory contains the source code and makefiles in `\fftw\src`, the header file in `\fftw\include`, documentation in `\fftw\doc` and compiled library files in `\fftw\lib`. Two library files are included: `fftw.lib` for use with the Zortech compiler and `libfftw.a` for use with the GNU compiler, both for machines with Intel X86 processors.

A5.6 delrun2

This program reads a single channel file from splitchi and writes a file containing the mean delay and RMS delay spread for each 5 sweeps in the input file. The program allows a threshold to be set and only components with more than the threshold power are considered. The output file is a text file which may be read by Microsoft Excel. The program in invoked with the command line:

```
delrun2 input_file output_file threshold
```

The threshold is expressed in dB and uses the power in the strongest component as datum.

There is only a C version of this program. The files are:

```
delrun2.c
delspred.c
makefile
```

This program needs FFTW.

A5.7 pdfcdf

This directory contains four programs which read the output of **delrun2**. **meanpdf** produces a PDF of the mean delays in a file which may be plotted with Microsoft Excel.

rmspdf produces a PDF of the RMS delay spread in a file which may be plotted with Microsoft Excel.

rmscdf produces a CDF of the RMS delay spread in a file which may be plotted with Microsoft Excel.

The programs are called from a command line with two arguments, the first is the name of the input file, the second is the name of the output file.

e.g.

```
meanpdf  input_file  Output_file
```

All of the programs need the subroutine contained in `meanset.c` and expect in initialisation file `meanset.ini` to exist in the current working directory. An example of `meanset.ini` is included in the directory. This file specifies the start point and the increment of the delay axis.

The files are:

```
meanpdf.c
meancdf.c
rmspdf.c
rmscdf.c
meanset.c.
```

A5.8 findcom4

This program reads a file of time series data for a single channel output by the **splitchi** program and writes a file with:

Time from start of measurement run

Number of multipath components

Minimum delay

Maximum delay

for each 5 sweeps of the input data The output file is a text file which may be examined with Microsoft Excel or Notepad. This file is usually input to the **compcdf** program which produces a CDF of the number of components. The program has four command line arguments: the name of the input file, the name of the output file, the threshold to be set, the leakage value to be set.

The files are:

```
findcom4.c
findcmp.c
makefile
```

This program needs FFTW.

A5.9 compcdf

This program reads the output from the findcom4 program and produces a CDF of the number of components. The median and mean number of components are also output on the standard output. The program has two command line arguments: the name of the input file, the name of the output file.

The files are:
`compcdf.c`
`bubble.c`

A5.10 kolmogor

This program reads two files output from **delrun2** and calculates the Kolmogorov-Smirnof difference and probability statistics. The directory contains all the files needed to build a Delphi version of the program.

A5.11 gaussian

This directory contains three programs: **optmean**, **optmean2** and **optsigma**. These programs search for the best mean and standard deviation parameters of a Normal distribution to fit the measurement data. The input file is the output from **delrun2**. The **optmean2** program outputs a file containing the CDF of the Normal distribution which best fits the data from the measurement.

A5.12 weibull

This directory contains three programs: **optshape**, **optshape2** and **optscale**. These programs search for the shape and scale parameters of a Weibull distribution which best fits the measurement data. The **optshape2** program outputs a file containing a CDF of the Weibull distribution which best fits the measurement data. All the programs read a file output from the **delrun2** program.

A5.13 pdelay3

The **tseries** directory contains all the files needed to build the **pdelay3** program. This is a Delphi program which may be used to examine a single channel time series file from the **splitchi** program, 5 sweeps at a time. This program was used to detect faults in the recorded data such as occured

during the measurement on 4 April 2003 in Whitworth Street in Manchester.

A5.14 newdac10

The **newdac10** directory contains all the files needed to build the new simple data acquisition program **sounder1**. This is a Delphi program which acquires 3 channels of data using a single PCI-DAS4020/12 data acquisition card.

A5.15 antcalib

The antcalib directory contains files from which may be built a number of programs for antenna characterisation. These programs control the antenna characterisation rig and record the output of the various receivers. Some of the programs were written in C with assembler subroutines to run in a 16 bit environment. They were build with the Zortech version 1 C compiler and the Microsoft assembler MASM version 4. These programs will run under MS-DOS or in a DOS box under Windows 95. The remainder of the programs were written in Delphi to run in a 16 bit environment. They were built with Borland Delphi version 1 and should run under Windows 3.1 or Windows 95. They will not run under Windows NT. These programs should be described in M. Abdalla's thesis[43].

APPENDIX 6 PAPERS

The following papers were published during the project. The last page of the second paper is missing having been lost due to a disk crash and a partly unreadable backup.

Antenna Arrays for Channel Sounding with Direction of Arrival Estimation and their Calibration

Roger Lewenz, Pantelis Filippidis, Moustafa Abdallah and Dr S Salous
Dept of EE&E, Main Building,
UMIST, PO Box 88, MANCHESTER M60 1QD
England

ABSTRACT

Communication systems which offer high bitrates will need to use greater bandwidths than present systems. This will increase susceptibility to multipath propagation and will require greater frequency resuse compared with present moderate bandwidth systems. One of the possible measures to counteract the effects of multipath propagation and cochannel interference is to use adaptive antennas with intelligent basestations. The basestation will be able to steer the antenna beams to minimise the multipath and interference. A necessary input to the development of these adaptive antennas will be radio channel characteristics including direction of arrival information. UMIST has been conducting a programme of channel characterisation over a number of years. The work described in this paper concerns antenna arrays for use with the UMIST 8 channel sounder and the calibration of these antenna arrays.

Keywords: Antenna array, Calibration

1. INTRODUCTION

Intelligent basestations employing smart antennas are expected to allow fixed and mobile operators to enhance the capacity of present and future radio communications networks. These basestations will steer the antenna beam(s) so as to minimise interference between cochannel basestations and outstations thus facilitating increased frequency reuse. This will allow the number of basestations to be increased thus providing more capacity to users without the need for more radio spectrum. Smart antennas can also be used to combat the effects of multipath interference thus facilitating the use of wideband systems in cluttered environments.

To design intelligent basestations for current and future radio network technologies will require a knowledge of the environment sufficient to allow sensible beam steering. A basestation may be designed to learn about its environment but some rules must be built in to allow decisions to be taken based on what has been learned. These rules can only be determined from an in depth study of the radio environment. For third generation systems using a high symbol rate the effects of multipath propagation are important. A knowledge of the multipath environment is necessary not only for the design of RAKE receivers and equalisers but also for deciding how to track multipath components arriving from different directions and what to do about them.

For several years UMIST has been conducting a programme of measurements to determine the characteristics of the radio channel at frequencies around 2GHz. These measurements have shown significant multipath propagation in both built-up areas and in rural areas. A chirp channel sounder has been constructed with to make the measurements. The sounder can operate on two channel frequencies so simultaneous

measurements may be made in the UMTS uplink and downlink bands. The sounder has a time resolution of 18nSec. Recently the sounder has been enhanced by increasing the number of receiver channels to eight. By connecting an eight element array of antennas to these channels it is possible to deduce the direction of arrival of each multipath component detected. This will require a precise knowledge of the characteristics of the antenna array. At present an array of commercially made patch antennas is used but the absence of any design information has made it impossible to predict the array characteristics. An eight channel calibration rig has been constructed so that the characteristics can be measured. Present work also includes the design of an improved antenna array.

This paper describes the antenna arrays and.the method used to calibrate them.

2. CONSTRAINTS

Since this work formed a part of a PhD project development time was strictly limited. Minimal research funds were available and this has led to the use of readily available inexpensive components in the first instance.

3. THE UMIST SOUNDER

The UMIST sounder uses the chirp technique in which the transmitter emits a signal which is continuously swept in frequency between programmed limits. At the receiver a signal identical to that transmitted is mixed with the signal received from the antenna. The start of the frequency sweep in the transmitter and receiver is synchronised and maintained in synchronism by a pair of accurate and stable clocks.

The output from the receiver mixer is the difference frequency between the signal received from the transmitter and the locally maintained copy. Since there will be a propagation delay, a received signal will produce a beat frequency at the output of the receiver mixer and this beat frequency will be proportional to the propagation delay. Signals arriving at the receiver via reflections off buildings will have a longer propagation delay than that arriving by a line of sight route. The beat notes from the receiver mixer may therefore be spectrally analysed to show the various multipath components arriving at the receiver. This analysis resolves the arrival times of the various multipath components.

By using two channels in the transmitter and receiver, each with a different carrier frequency it is possible to capture the multipath characteristics of the UMTS uplink and downlink bands simultaneously. The sounder is capable of sweeping over 90MHz giving a time resolution of 18nSec but for current studies this is limited to 60MHz for the UMTS bands.

4. DIRECTION OF ARRIVAL MEASUREMENT

To measure the directions of arrival of the various multipath components the sounder must be capable of angle measurement in the spatial domain. For the UMIST sounder this will be achieved using an array of antennas each with its own receiver channel. Each channel will resolve the time delay of the multipath components received at the associated antenna.

The UMIST sounder has eight channels in its receiver. At present an array of six antennas is used to resolve angles in azimuth only. When development work is completed an improved antenna array with eight elements should be available. It should also be possible to take the phase of the incoming multipath components into account and use superresolution techniques to estimate the direction of arrival with greater resolution than at present.

5. THE PRESENT ANTENNA ARRAY

The antenna array has been constructed from commercially available patch

antennas. Each antenna has a 60 degree beamwidth in both azimuth and elevation. These antennas are fixed to a frame so that their boresight directions span a complete circle in 60 degree increments. The spacing between the antennas is the minimum compatible with the mechanical arrangement. It is expected that there will be significant coupling between the antennas so characterising the array must be done for the whole array rather than superimposing the individual antenna characteristics.

6. ANTENNA ARRAY DEVELOPMENT

A number of antenna array configurations have been considered with a view to constructing an antenna array in house. Linear, circular and other forms of array have been examined and simulations have been perdormed to predict their characteristics. It was decided to limit the direction of arrival estimation to the azimuth plane for the present.
It would be possible to mechanically steer an array in order to enhance angular resolution. This technique would not allow antenna beams to move fast enough to synchronise with the sweep of the sounder so the rate of capture of channel impulse responsed would be reduced.
Two alternatives are to steer the beams by changing the relative phases of the energy fed to the driven elements of the array or to induce phase shifts by switching the nodal points of the parasitic elements.
Since direction of arrival with 360 degree coverage is required many of the array configurations were rejected as being unable to provide this facility. Current work is concentrated on simulating a circular array with 8 sets of elements arranged with boresights covering 360 degrees at 45 degree intervals. Each set of elements will be a broadband structure capable of being steered electronically ofer a limited arc. It should be possible to realise each set of elements in stripline and thus construct a compact and robust array. To confirm the accuracy of the predicted performance the antenna array will be calibrated using the rig described in this paper.

7. CHARACTERISING THE ARRAY

Since UMIST does not have an antenna test range or an anechoic chamber large enough to accommodate the antenna array it was decided to construct a portable calibration rig and to find an uncluttered area in which to perform the measurements. Houghend Playing Fields, in Manchester, covers an area approximately 500m by 700m and this is thought to be suitable. This area is surrounded on three sides by further open areas extending to a distange of 500m. An alternative has been to conduct the measurements on the roof of the UMIST Main Building. This is 45m above the ground, well above the surrounding buildings except for an office block approximately 100m away. Measurements have been made on the roof already. Measurements will be performed on Houghend Playing Fields and the results compared with those from the roof measurements.

The frequency at which the antenna array is to be characterised is 2GHz. At this frequency the wavelength (λ) is 0.15m so to ensure that there are only far field interractions between the antenna array and the illuminating antenna the two should be placed at least 3m apart. At this separation the free space transmission loss will be 48dB. If we assume that the worst case for interference is a large perfect reflector 200m away then the receiving antenna will see an image of the illuminating antenna at an apparent distance of 400m. The free space transmission loss over this distance will be 90.5dB which is 42.5dB greater than the loss in the direct path. The dynamic range of the measurement system will therefore be greater than 40dB which is acceptable for antenna measurements.

8. THE CALIBRATION RIG

The antenna calibration rig consists of a turntable on which the test antenna is

mounted and a test transmitter which is used to illuminate the test antenna. The turntable is rotated by a stepper motor via a gearbox. The stepper motor is controlled by a PC which has a data acquisition card fitted. The outputs from the elements of the test antenna are amplified and detected by an eight channel logarithmic receiver. The outputs from the eight receiver channels are digitised by the data acquisition card in the PC and the results recorded on disc.

The turntable assembly, with the antenna array, is mounted on a light metal frame so that the centres of the antena elements is 2m above the. The mechanical arrangement of the turntable is shown in figure 1.

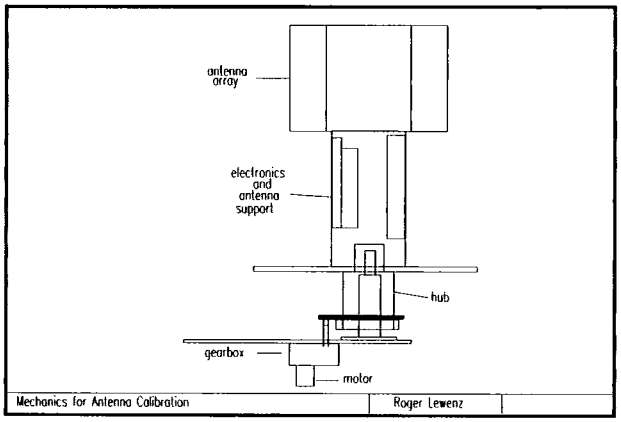

Figure 1. Mechanical arrangement of the calibration turntable.

The test transmitter consists of an oscillator phase locked to a 10MHz crystal oscillator, a power amplifier and a patch antenna similar to those of the antenna array. The test transmitter is mounted on a tripod so that the antenna is at the same height as the antenna array under test..

9. CALIBRATION METHOD

Before attempting to calibrate the antenna the receivers are calibrated. The test transmitter is used as a calibration source. An eight way splitter is used to connect the receiver inputs to the test transmitter. Between the test transmitter and the splitter a variable attenuator with 1dB steps is inserted so that attenuation up to 100dB can be inserted.
The power output from the test transmitter is measured with a calibrated spectrum analyser at each of the frequencies at which the calibration is performed. The receiver outputs are measured using the PC and data acquisition card for input powers to the antenna sockets from -74dBm to -6dBm. These results are formed into a calibration table which is used to convert the receiver outputs into dBm when calibrating the antenna.

Having calibrated the receivers, the test rig is taken to an uncluttered area. The test transmitter is placed 5m away from the antenna array under test. The array is then rotated through 360 degrees in 5 degree increments and at each position the output from the receivers is measured and recorded on disc. It is possible to rotate the turntable in smaller increments than 5 degrees if it is necessary to characterise the fine detail of any sidelobes.

10. RESULTS

The data from the calibration has been converted to dBm using the receiver calibration tables and normalised relative to the element with the maximum boresight gain. The combined radiation pattern for the present 6 element array is shown in figure 2.

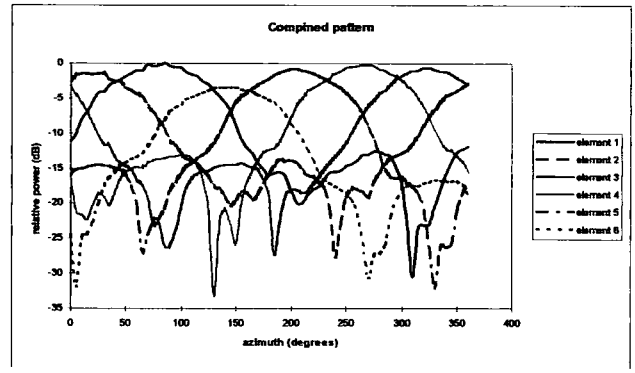

Figure 2. Combined radiation pattern of 6 element array.

11 DISCUSSION

The results show that it is possible to characterise an array antenna using relatively simple equipment and get meaningful results. The result shown is from measurements on the roof of a high building. There was another tall building approximately 100m away and this may have distorted the result. Further measurements on a large field with no obstacles will help to confirm or deny that the roof of a tall building is a suitable site for such measurements. One advantage of the tall building is that there are unlikely to be any ground reflections. This may not be the case in the field. An advantage of the field is that having characterised the antenna array and developed the direction of arrival estimation algorithm it will be possible to place a transmitter at various azimuths and gauge the effectiveness of the algorithm.

12. CONCLUSIONS

TEMPORAL VARIATION IN THE RADIO CHANNEL

R. G. Lewenz and S. Salous

School of Engineering
University of Durham
Science Laboratories
South Road
DURHAM DH1 3LE
England
rlewenz@btinternet.com
sana.salous@dur.ac.uk

Abstract
This paper describes measurements to determine the extent of the variation of RMS delay spread in the radio channel with time. Results from measurements at two locations in Durham over durations of 15 seconds have been analysed. CDFs have been constructed. The mean delay spread and the range between 10^{th} and 90^{th} percentile extracted. It has been found that a single large scatterer (in this case Durham Cathedral) can dominate the multipath characteristics over a significant fraction of the city. It has also been found that moving traffic is a cause of the variation of the channel characteristics with time and that directional antennas give some protection against multipath propagation as compared with omnidirectional antennas.
keywords: **temporal variation, radio propagation, measurement**

1 INTRODUCTION

Current and future radio communications systems need to adapt to the environment. The radio channel through the environment will usually degrade any transmitted signal and various techniques need to be used in the receiver to reconstruct the information sent. Fading will cause variation in received signal level and multipath propagation will cause a number of copies of the transmitted signal with different time delays to be received. Both the signal level and the time delays will vary with time if either one or both of the terminals move with respect to the environment or if the environment moves relative to fixed terminals. A receiver needs to adapt to the environment and smart antenna systems may be used at one or both terminals. The degree to which systems will need to adapt and the speed of the adaption will depend on the variations in the radio channel. Although the results of some measurements have been published, most of the measurements have had durations on the order of 100 ms. This paper reports on work in progress to estimate some channel characteristics from wideband measurements with durations of up to 15 seconds.

2 CHANNEL SOUNDER

The measurements were made using a chirp channel sounder which is illustrated in the following paragraph and Figure 1. Details of the sounder and its use are in [1, 2, 3].

The sounder transmits a signal which sweeps linearly over a bandwidth B Hz in a time T_S sec (solid line in figure 1). At the receiver the transmitted signal arrives after a short delay (dotted line in figure 1). The received signal is mixed with an exact copy of the transmitted signal and the difference frequencies are captured for analysis.

The received signal will be delayed relative to the transmitted signal because is takes a finite time to propagate from the transmitter to the receiver. This delay is indicated by dt in figure 1. During the delay time dt the local copy of the transmitted signal will have increased in frequency relative to the received signal by df. This frequency difference gives rise to a beat frequency df in the mixing process and it is this beat frequency that is captured. In the case where there is multipath propagation there will be more than one received signal and each of these signals will be delayed by a different time and give rise to a different beat frequency. The output from the mixing process will contain a number of beat frequencies, each corresponding to one of the multipath components of the received signal. Spectral analysis identifies the beat frequencies and hence the multipath component delay times.

The data from the sounder are captured using a PC based data acquisition system specially designed for the purposes of the study. This system has 8 channels, 8 bit resolution and a 1 Msample/sec throughput on each channel. Data are stored on disk for offline analysis.

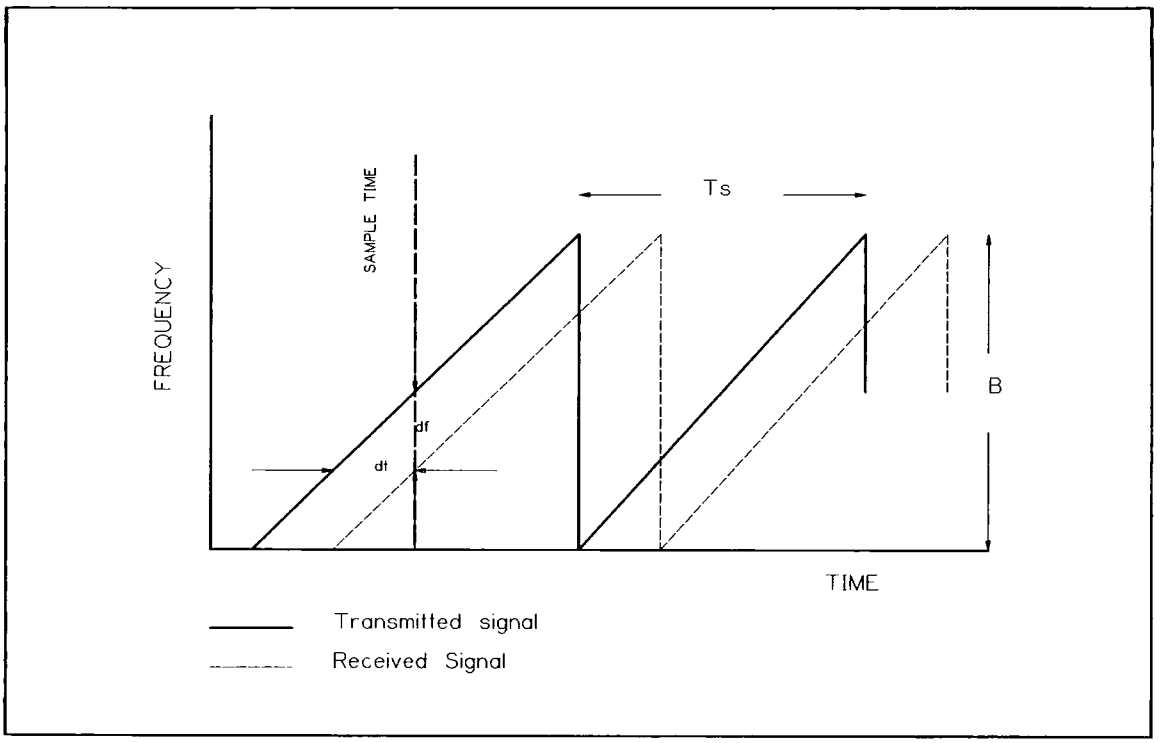

Figure 1. Sounder transmitted and received signals

The channel sounder has been configured to sweep over 60 MHz, centred on 1950 MHz every 4 msec. This gives a delay resolution of 19 nsec (6 m path length difference). The sounder can capture one channel impulse response every 4 msec and it is possible to detect Doppler shifts up to 125 Hz in either direction. The sounder has an eight channel receiver and is used with an antenna system consisting of up to eight elements. With a suitably characterised antenna array it will be possible to extract direction of arrival information from the sounder data. Outdoor measurements with ranges up to 2 km in urban environments and 5 km in rural environments are possible.

3 CHANNEL CHARACTERISTICS

A channel characteristic of interest to both operators and equipment designers is the RMS Delay Spread. This is a measure of the dispersion in the radio channel. From the designer's

point of view channels with large dispersion need complex systems to provide a reliable service. From the operator's point of view channels with large dispersion have less capacity than those with small dispersion. A knowledge of the range of RMS delay spreads in various types of channel can aid the decisions as to what types of service to offer and what type of equipment will be necessary to support the service.

4 MEASUREMENTS

Measurements have been made at locations near the University in Durham with each measurement run lasting 15 seconds. Durham has been built on seven hills. Most buildings have two or three floors and the city is dominated by a large cathedral.

Spectral analysis of the data from the sounder identifies the multipath components. The time series data are processed using the FFT to extract a mean power delay profile. The mean is taken over a number of sweeps so that noise is averaged out. Two examples of power delay profiles are shown in figure 2 below.

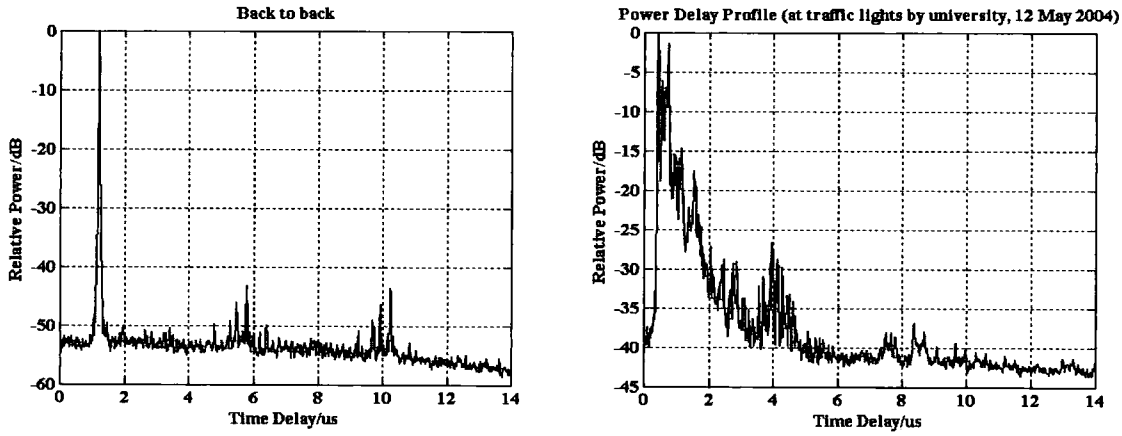

Figure 2a (left) and 2b (right) - Power Delay Profiles

Figure 2a shows a power delay profile when the sounder transmitter is connected to the sounder receiver by a cable and attenuator pads. There are no multipath components (the signals at low level with delays of approximately 7 and 11 microseconds are artefacts of the sounder produced by odd harmonics of the principal beat frequency). The principal component appears with a finite delay because of the way the start of sweep at transmitter and receiver are synchronised. This is intended.

Figure 2b shows the power delay profile from a measurement at a crossroads 400 m from the transmitter. This profile was recorded from a different channel from figure 2a and on a different location hence the difference in the noise floor of the two plots. In addition to multipath components there is some noise which could confuse the estimation of channel characteristics. The breadth of the main peak indicates that the delay spread must be significant.

5 ESTIMATING DELAY SPREAD

To estimate the range of delay spreads which might be encountered at a particular location over a period of time a measurement lasting 15 seconds was made. The data from the measurement covered 3750 sweeps. Power delay profiles were calculated from each 5 sweeps and RMS delay spread estimated for each group of 5 sweeps.

First the mean delay is found. For each component the difference between the component delay and the mean delay is squared and multiplied by the power in the component. This quantity is summed over all components and the resultant divided by the sum of the powers in the components. This gives the mean squared delay spread and the square root yields the RMS delay spread.
i.e. over n components with delays d_i and powers p_i :

$$D_{RMS} = \sqrt{\frac{\sum_{i=1}^{n}\left(d_i - \bar{d}\right)\left(d_i - \bar{d}\right)p_i}{\sum_{i=1}^{n} p_i}} \qquad (1)$$

Each group of 5 sweeps yields one result so there are 750 points from the measurement and a cumulative distribution curve can be plotted. Because operational systems and measurement systems may discover a multiplicity of low level multipath components it is usual to apply a threshold when estimating RMS delay spread. For the measurements described here any component whose power was 20 dB less than that of the strongest component was ignored.

Two measurement locations were selected in Durham. Each is approximately 400 m from the transmitter location. The first was on the approach island to a roundabout near the Science Laboratories main entrance with the cathedral blocked by buildings. The second was by a crossroads near the University library and had a clear view of the cathedral (figure 3). Measurements at the first location were made on two different days and measurements at the second location were made on three different days. The first location was surrounded by buildings of two or three storeys within a range of 100 m with some trees between and in front of the buildings. At the second location the cathedral appeared in a NW direction at a range of 600 m, there were two and three storey buildings to the NE, E (figure 4), SE and S. There was dense woodland to the W and SW directions. To the North was a road to the centre of Durham City.

Figure 3. View from traffic lights looking slightly West of North, the Cathedral is at the left edge of picture

Figure 4. View from traffic lights looking East.

6 RESULTS

At the first location an array of six directional antennas surmounted by a single omnidirectional antenna was used. The directional antennas were arranged with boresight directions covering 360° at 60° intervals. The directional antennas had an azimuth beamwidth of 60° to the 3 dB points. CDFs of the measurements at this location are shown in figure 5 below. The mean of the RMS delay spread and the range between 10th and 90th percentile are shown in table 1. The measurements on 28 July were taken just before midday and there was little road traffic. Those on 26 July were taken at 1630 and there was signifant traffic. The weather was dry on both days. The wind was light on 26 July and moderate on 28 July.

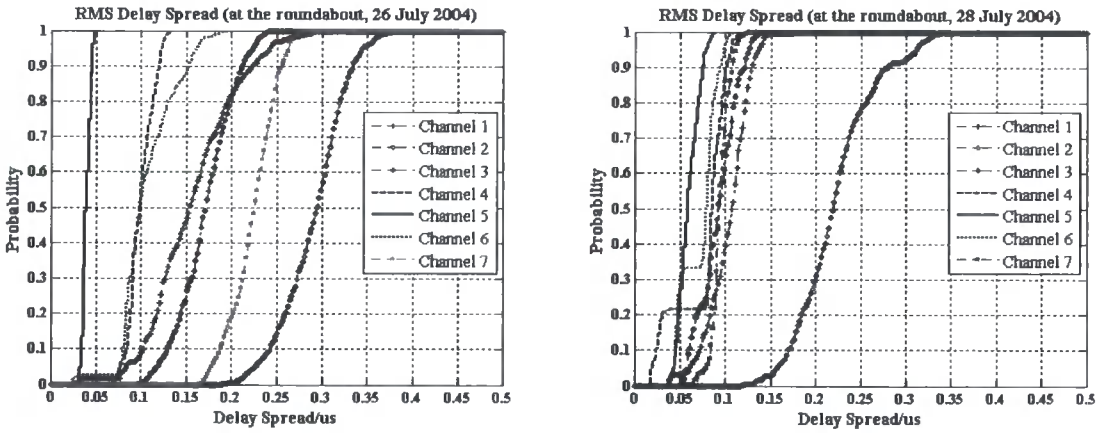

Figures 5a (left) and 5b (right) - CDFs of Delay Spread at location 1.

	26 July 2004		28 July 2004	
channel	mean	10% - 90%	mean	10% - 90%
1	0.154	0.119	0.107	0.058
2	0.294	0.091	0.219	0.108
3	0.171	0.083	0.092	0.060
4	0.098	0.036	0.085	0.077
5	0.039	0.011	0.057	0.028
6	0.099	0.074	0.078	0.049
7	0.226	0.068	0.093	0.024

Table 1. Mean and Range of RMS Delay Spread (microseconds) at Roundabout

The right hand trace in both figures 5a and 5b is from channel 2 which was connected to the antenna that pointed in the direction of the cathedral. The antenna connected to channel 5 pointed away from the cathedral. Channel 7 was connected to the omnidirectional antenna. It can be seen that the presence of the cathedral has a significant effect on the delay spread even when it is masked by buildings. As might be expected an omnidirectional antenna sees more delay spread when in the vicinity of road traffic. This is probably due to the larger number of scatterers visible as compared to a directional antenna. A directional antenna may therefore provide some protection from the effects of multipath propagation. The range between 10th and 90th percentiles indicates the variation in RMS delay spread over the 15 second measurement period. From the results it appears that road traffic increases the variation. It is not possible from these results to determine whether wind, and its effect on vegetation, have any effect on the variation. Another measurement with a detailed description of the environment will be necessary to investigate this.

Measurements at the crossroads by the university library were conducted on 12 May, 13 May and 18 May 2004. For these measurements the antenna system was an array of yagis arranged to cover 360° in azimuth in 45° increments (Figure 6).

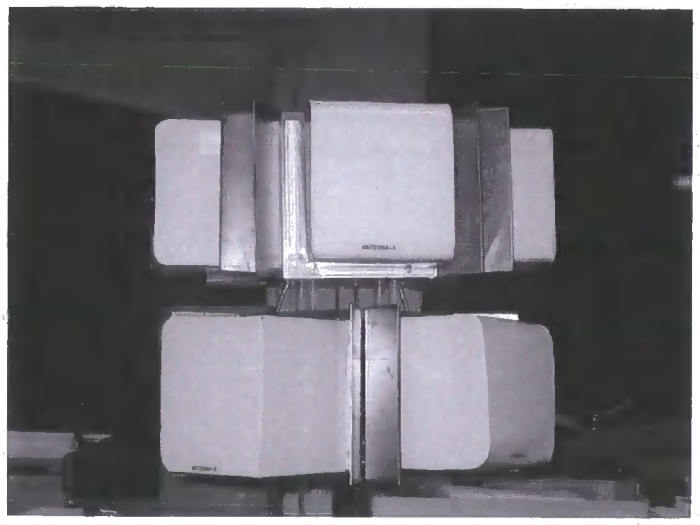

Figure 6. The array of eight directional antennas used at the traffic lights.

Table 2 below shows the results.

	12 May 2004		13 May 2004		18 May 2004	
Direction	mean	10% - 90%	mean	10% - 90%	mean	10% - 90%
N	0.450	0.126	0.128	0.035	0.225	0.158
NE	0.152	0.081	0.118	0.040	0.408	0.156
E	0.193	0.050	0.175	0.028	0.102	0.090
SE	0.207	0.075	0.163	0.026	0.177	0.177
S	0.218	0.129	0.284	0.086	0.227	0.183
SW	0.389	0.218	-	-	0.287	0.130
W	0.689	0.254	0.663	0.484	0.656	0.171
NW	0.578	0.309	0.504	0.338	0.688	0.247

Table 2. Mean and range of RMS Delay Spread (microsecond) at traffic lights.

The dominant effect of the cathedral (NW direction) can clearly be seen from these results. Also the woodland to the SW tends to increase the delay spread as compared with the E direction where there was a road with houses on either side. The two roads which crossed at this location run North-South and East-West. Most of the traffic was along the road running to the North into the city centre. The variable traffic rate may be the cause of the differences in delay spread on the three days.

Considering the variation over the 15 second measurement duration and the differences from day to day it is clear that there are significant variations over short periods of time. Where road traffic contributes to multipath propagation the mean of the RMS delay spread will change from hour to hour.

7 CONCLUSIONS

After a limited measurement campaign, the following results have been demonstrated:

- A single large scatterer (such as the cathedral) can dominate the multipath propagation characteristics over a considerable area.
- Moving road traffic causes significant variation in the delay spread experienced by a radio channel near to a road.
- A directional antenna will provide some protection from multipath propagation when compared to an omnidirectional antenna.
- It is possible that wind induced vegetation movement is responsible for some variation in delay spread. This effect needs to be investigated further using detailed morphological maps of the area in which measurements are made.

8 REFERENCES

1. Salous, S., and Nikandrou, N., 'Architectures for advanced FMCW sounding', Int J Electronics, 1998 Vol 84 No 5, pp 429 – 436.

2. Salous, S., Nikandrou, N, and Bajj, N., 'Digital techniques for mobile radio chirp sounders', IEE Proceedings on Communications, Vol 45, No 3, June 1998, pp 191 – 196.

3. Salous, S., and Gokalp, H., 'Propagation Measurements in FDD UMTS bands', IEE International Conference on Antennas and Propagation, IEE publication 480, April 2001, pp 137 – 141.